



**HAL**  
open science

# Transport and attenuation of pesticides in runoff from agricultural headwater catchments : from field characterisation to modelling

Marie Lefrancq

► **To cite this version:**

Marie Lefrancq. Transport and attenuation of pesticides in runoff from agricultural headwater catchments : from field characterisation to modelling. Earth Sciences. Université de Strasbourg, 2014. English. NNT : 2014STRAH004 . tel-01037928

**HAL Id: tel-01037928**

**<https://theses.hal.science/tel-01037928>**

Submitted on 23 Jul 2014

**HAL** is a multi-disciplinary open access archive for the deposit and dissemination of scientific research documents, whether they are published or not. The documents may come from teaching and research institutions in France or abroad, or from public or private research centers.

L'archive ouverte pluridisciplinaire **HAL**, est destinée au dépôt et à la diffusion de documents scientifiques de niveau recherche, publiés ou non, émanant des établissements d'enseignement et de recherche français ou étrangers, des laboratoires publics ou privés.

**ÉCOLE DOCTORALE DES SCIENCES DE LA TERRE ET DE L'ENVIRONNEMENT (ED 413)**

**Laboratoire d'Hydrologie et de Géo chimie de Strasbourg (LHyGeS) UMR 7517  
(Université de Strasbourg / ENGEES – CNRS)**

# THÈSE

*Présentée par :*

**Marie LEFRANCQ**

**soutenue le : 11 Avril 2014**

pour obtenir le grade de : **Docteur de l'université de Strasbourg**

Discipline/ Spécialité: Science de l'environnement

**Transport and attenuation of pesticides in runoff from  
agricultural headwater catchments:  
from field characterisation to modelling**

**THÈSE dirigée par :**

**M. IMFELD Gwenaël**

Chargé de recherche CNRS, France

**RAPPORTEURS :**

**M. BROWN Colin**

Professeur, Université de York, Royaume-Uni

**M. STAMM Christian**

Directeur de recherche, Eawag, Suisse

**AUTRES MEMBRES DU JURY :**

**Mme GASCUEL-ODOUX Chantal**

Directrice de recherche, INRA Rennes, France

**M. JETTEN Victor**

Professeur, Université de Twente, Pays Bas

**M. PAYRAUDEAU Sylvain**

Maître de conférences, ENGEES, France



“A PhD thesis is like riding a bike, to keep your balance you must keep moving”  
Adapted from Albert Einstein



## Acknowledgements

This Ph.D. thesis was carried out at the Laboratory of Hydrology and Geochemistry of Strasbourg (LHyGeS), France. It was supported by the Interreg IV PhytoRet project (E.U./The Rhin Meuse French national water agency fellowship). I want to thank all persons and institutions who have directly or indirectly contributed to this work.

I had been considering the project of achieving a PhD for a while: The only missing thing was an interesting subject in an exciting context! Sylvain Payraudeau and Gwenaël Imfeld allowed me to get this chance: thanks to both of them for that. I am very grateful to them for their continuous support in the form of discussions, feedbacks and ideas, which definitively contributed to the completion of this project. I also thank them for their help in reviewing this thesis tirelessly and preparing the peer-reviewed publications.

I am grateful to the jury members who kindly accepted to evaluate my work: Pr. Colin Brown, Pr. Victor Jetten, Dr. Chantal Gascuel Odoux and Dr. Christian Stamm.

I particularly wish to thank all the German partners of the 'PhytoRet project'. Herzlichen Dank an Dr. Habil. Jens Lange, Prof. Klaus Kümmerer, Dr. Oliver Olson und Barbara Herbstritt. Ich möchte auch Romy Durst and Brian Sweeney for their great help in the field danken. Thanks as well to the PhD students of the Phytoret project, Matthias Gassmann and Lukasz Gutowski, for the interactive skype sessions, I will remember as well the nice touristic tours of Lüneburg and of the 'Hamburg fish market'. Thanks also to Caroline Grégoire who made possible this Phytoret project.

My heartfelt thanks to Victor Jetten for his precious time and his welcoming to the Faculty of Geo-Information Science and Earth Observation (ITC) in Twente for two stays. Heel hartelijk bedankt! I have really appreciated the teachings, the tips and the secrets on OpenLisem and Qt creator you provided me. Thanks as well to Paul Van Dijk for his invaluable advice on all the parameters of LISEM and his advices in agronomical aspect.

I am immensely grateful to Eric Pernin, Nicolas Tissot and Benoit Guyot for their daily help in the field experiment setting up, the sample collection and their analytical support in the lab. I am very grateful to René Boutin, Sophie Gangloff, Carole Lutz and Marie-Pierre Ottermatte for their precious advice, and analytical support in the lab work. I specially acknowledge Martine Trauttmann for her dedication to the soil laboratory and analyses! I would like to thank as well all the bachelor and master students who contributed to this work: Maxime, Jeanne, Thomas, Célia, Antonio, Diogo, Arthur and Matthieu. Thank you for your deep involvement in these field and modelling experiments.

I would like to warmly thank the farmers who responded to the surveys and made these experimental studies possible; especially for their allowance for the experimental plot study and, for their invaluable help in filling or digging using their agricultural machines when building the experiment sites in the field.

Thanks as well to all my colleagues at the LHyGeS. I want to especially name Sylvain Weill, "my hydrological father", Marie Claire Pierret for her interest in studying rare earth elements transport in the arable crop catchment, Anne Véronique Auzet for her help in understanding agricultural erosion, Raphaël Di Chiara for his motivation in solving numerical problems, Cyrielle Regazonni for the usefull advices in GIS, Alain Clement for solving all kinds of informatic bugs, the colleagues from IMFS for their advice on the Doppler installation or hydraulic calculations, Lauriane and Fanilo for their advices in maths, Joëlle for all her special touches and naturally,

Maurice Millet for his great help in pesticides quantification and for teaching me the bases of chemistry that I had completely forgotten.

I also benefited from the precious help of Philippe Ackerer who provided invaluable advices for resolving my mass balance errors and finding alternative ways to implement the mixing layer concept! Thanks for your permanent good mood, patience and encouragements.

Many thanks to Richard Coupe for proof-reading my manuscript.

A special thanks to Roger Moussa for having the good words at the right time. "The day will come for the firework".

But... These 3 years have also been so nice for many non-academic reasons: My deepest thanks go to all the Ph.D students from the LHyGeS, and especially to my colleagues and friends Elodie, Benoit, Nicolas and Omniea for the coffee and beer times. They greatly contributed to the nice atmosphere which has been prevailed throughout those three years. Thanks as well to the 'third floor' PhD students: Adrien (the golden Palm), Izabella (the Hungarian dancer), the Italian team including Ivan, Eleonora and Clio, Thieb' (the best "pétanque" player), Nicolas (for the crazy Tuesday), Philippe (for the numerous croissants) and the new PhD students Marion (from Arzviller ☺) and Bastien !

Thanks to Marianne for sharing the flat for so long! Thanks to the Strasbourg team for the weekly meetings at the "Grincheux" or the "Marché bar", and also for the soccer games in the Orangerie park. Thanks as well to the "2009 Cemagref wedding agency" from Lyon. Enfin, merci à toute ma famille, surtout aux petiots qui ont grandi ou sont nés pendant ces trois dernières années ... Sans oublier Damien pour m'avoir soutenue jusque-là! De nombreux cols à passer nous attendent encore ...

## Table of Contents

Table of Figures .....	10
Table of Tables .....	13
Abbreviations .....	15
Abstract .....	17
<b>Chapter I. Introduction &amp; context .....</b>	<b>37</b>
1. Pesticides in the environment .....	37
1.1. Impact and diversity .....	37
1.2. Environmental distribution of pesticides .....	39
2. Pesticide transport from agro-ecosystems to surface waters.....	41
2.1. Agro-ecosystems, definition and specificity .....	41
2.2. Pesticide transport and attenuation from agricultural sources to sinks .....	42
2.2.1 Processes affecting pesticides amount at the source area ( $A_{source}$ ) .....	43
2.2.2 Processes affecting pesticide transport in agro-ecosystems ( $A_{active}$ and $A_{connected}$ ) .....	47
2.2.3 Relevance of combining emerging analytical tools for assessing pesticide degradation .....	49
2.2.4 Usefulness and complementarity of modelling following a characterisation phase .....	50
3. Relevance of headwater catchments for pesticide transport in surface water .....	56
3.1. Definition and role of headwater catchments in downstream water quality .....	56
3.2. Importance of combining plot- and catchment-scale observations.....	57
3.3. Models for predicting pesticide transport in headwater catchments.....	58
<b>Chapter II. Research focus and objectives .....</b>	<b>59</b>
1. Research focus .....	59
2. Thesis objectives.....	60
3. Thesis layout.....	63
4. References .....	65
<b>Chapter III. Fungicides drift and mobilisation via runoff and erosion in vineyard.....</b>	<b>76</b>
<b>Section 1. Kresoxim methyl deposition, drift and runoff in a vineyard catchment .....</b>	<b>78</b>
1. Abstract.....	78
2. Introduction.....	80
3. Material and methods.....	81
3.1. Description of the vineyard catchment .....	81
3.2. KM properties and application.....	82
3.3. Sampling procedure .....	83
3.4. KM analysis .....	84
3.5. Data analysis.....	85
4. Results and discussion .....	86
4.1. KM deposition .....	86
4.2. KM drift .....	88
4.3. Runoff-associated KM.....	90
5. Conclusion .....	91
6. References .....	92
<b>Section 2. Fungicides transport in runoff from vineyard plot and catchment: contribution of non-target areas .....</b>	<b>94</b>
1. Abstract.....	94
2. Introduction.....	95
3. Material and methods.....	96
3.1. Chemicals .....	96
3.2. Description of the vineyard catchment .....	97
3.3. Description of the experimental plot.....	98

3.4.	Pesticide applications and soil deposition .....	101
3.5.	Runoff discharge measurement and water sampling procedure.....	101
3.6.	Soil sampling and characterization .....	102
3.7.	Chemical analysis .....	102
3.8.	Data analysis and calculation .....	103
4.	Results .....	104
4.1.	Hydrology.....	104
4.2.	Hydrochemistry .....	104
4.3.	Deposition of KM and CY on soil.....	105
4.4.	KM and CY mobilisation in the runoff dissolved phase (< 0.7 µm) .....	105
4.5.	Partitioning of KM and CY in runoff .....	109
5.	Discussion.....	110
6.	Conclusion .....	112
7.	References .....	113

**Chapter IV. Herbicides transport and attenuation via runoff and erosion in arable crop catchment .....117**

**Section 1. Transport and attenuation of chloroacetanilides in an agricultural headwater catchment .....119**

1.	Abstract.....	119
2.	Introduction.....	120
3.	Material and methods.....	121
3.1.	Description of the study site.....	121
3.2.	Herbicides characteristics and applications.....	123
3.3.	Hydrological measurements and sampling procedure.....	124
3.4.	Hydrochemical and soil analysis .....	125
3.5.	Chloroacetanilide analysis.....	125
3.5.1	Chemicals .....	125
3.5.2	Extraction.....	125
3.5.3	Quantification of the chloroacetanilides and their degradation products .....	126
3.5.4	Enantiomer analysis of S-metolachlor .....	127
3.5.5	Data analysis.....	127
4.	Results and discussion .....	128
4.1.	Chloroacetanilide attenuation in the plot soil .....	128
4.2.	Influence of hydrology and hydrochemistry on chloroacetanilide export and partitioning .....	130
4.2.1	Hydrochemical and chloroacetanilide load variations.....	130
4.2.2	Chloroacetanilide partitioning.....	135
4.3.	ESA and OXA degradation products dynamics.....	136
4.4.	S-metolachlor enantiomeric signatures as indicator of in-situ degradation .....	137
5.	Conclusion .....	140
6.	Acknowledgement .....	141
7.	References .....	142

**Chapter V. Modelling pesticide runoff at the headwater catchment scale.....146**

**Section 1. Agronomical insights for improving runoff prediction in headwater agricultural catchments .....148**

1.	Abstract.....	148
2.	Introduction.....	150
3.	Material and methods.....	152
3.1.	Model description.....	152
3.2.	Continuous agronomical model: I <sub>DR</sub> .....	153
3.3.	Study case .....	154
3.3.1	Description of the study site .....	154
3.3.2	Hydrological procedure and experimental results .....	155
3.3.3	Erosion characterisation.....	158

3.4.	Input parameters.....	159
3.5.	Calibration strategy.....	161
3.6.	Model calibration and sensitivity analysis.....	162
3.7.	Evaluation criteria and data analysis.....	162
4.	Results.....	163
4.1.	Basic calibration method (BCM).....	163
4.2.	Constraint calibration method (CCM).....	166
4.3.	Sensitivity analysis of input parameters.....	168
4.4.	Erosion characterisation and prediction: focus on May 21.....	169
5.	Discussion and conclusion.....	170
6.	Acknowledgements.....	172
7.	References.....	172
<b>Section 2.</b>	<b>A comprehensive mathematical model for mobilisation and transport of dissolved pesticide from the soil surface to runoff: the mixing layer approach.....</b>	<b>177</b>
1.	Introduction.....	177
2.	Mathematical theory and approach.....	180
2.1.	Openlsem.....	180
2.2.	Mixing model.....	182
2.3.	Numerical resolution with operator splitting (LISEM-psni).....	183
2.4.	Pseudo-analytical resolution (LISEM-pa).....	185
2.5.	Mass balance errors calculations.....	187
2.6.	Case study scenarios.....	188
3.	Results and discussion.....	189
3.1.	Steady test case.....	189
3.2.	Dynamic test case: an experimental plot.....	191
3.3.	A study case in an agricultural headwater catchment: Alteckendorf.....	194
4.	Conclusion.....	197
5.	Acknowledgement.....	198
6.	References.....	199
<b>Chapter VI.</b>	<b>General conclusions and perspectives.....</b>	<b>201</b>
<b>1.</b>	<b>Summary and conclusion.....</b>	<b>201</b>
1.1.	The spatial variability of pesticides deposition during application impacts pesticide runoff.....	203
1.2.	Combining plot and catchment scales observations is critical for assessing off-site exports of pesticides.....	205
1.3.	Predicting pesticide transport processes in the agricultural catchments.....	207
1.4.	Pesticides partitioning is crucial for pesticide export under field condition.....	208
1.5.	Combining analytical approaches helps the evaluation of pesticide degradation within agricultural headwater catchment.....	210
<b>2.</b>	<b>Implications and perspectives.....</b>	<b>212</b>
2.1.	How to address the variability of pesticides deposition during application in pesticides runoff studies?.....	213
2.2.	How to improve the evaluation the pesticides partitioning in runoff water?.....	213
2.3.	How to evaluate the degradation of chiral pesticides under field conditions?.....	214
<b>3.</b>	<b>References.....</b>	<b>216</b>
<b>Chapter VII.</b>	<b>Appendices.....</b>	<b>222</b>

# Table of Figures

## Chapter I

Figure I-1. Structures of the four stereoisomers of metolachlor (Kabler and Chen, 2006).....	38
Figure I-2. Pesticide movement in the hydrological system (Barbash, 2014).....	40
Figure I-3. Bio-physical-chemical processes related to pesticide transport and attenuation in agro-ecosystems.....	45
Figure I-4. Degradation pathways of acetochlor in soil (Roberts et al., 1999). Acetochlor was metabolised in soil mainly by two primary pathways. The first pathway involved the hydrolytic/oxidative displacement of chlorine to form the alcohol 2 and the oxidation of the alcohol 2 to oxanilic acid 3. N-dealkylation of 3 yielded oxanilic acid 4. The second pathway involved the displacement of chlorine by glutathione and the further secondary catabolism of the glutathione conjugate 5 to the various sulfynylactic and sulfonic acid products (6-9).....	46
Figure I-5. Processes for transferring pesticides from the soil surface to runoff water.....	48
Figure I-6. Existing physically based pesticide transport models according to their spatial and temporal discretisations.....	51
Figure I-7. Relationship between catchment size and aqueous non-point sources of insecticide contamination detected in samples of surface waters (Schultz, 2004).....	57

## Chapter II

Figure II-1. Locations and schemes of the study catchments (Alsace, France).....	62
Figure II-2. Graphical outline of the PhD thesis.....	64

## Chapter III

Figure III-1. Graphical outline of the PhD thesis (Chapter III).....	77
Figure III-2. Graphical abstract.....	79
Figure III-3. Location of the kresoxim methyl collectors in the vineyard catchment (Rouffach, Alsace, France) on May 24, 2011.....	82
Figure III-4. Kresoxim methyl soil deposition of the nine collectors normalised by corresponding Thiessen area in the vineyard catchment (Rouffach, Alsace, France) during the three periods P1, P2 and P3 on May 24, 2011.....	87
Figure III-5. Scheme of the catchment (A) and the experimental plot (B) (Rouffach, Alsace, France). The geographical coordinates of the meteorological station are 47°57'9N, 07°17'3E.....	99
Figure III-6. Temporal changes in the hydrological conditions (A and B), the fungicides application (green bars for KM, orange bars for CY) and the concentrations in runoff water (C and D), the specific loads (green bars for KM, orange bars for CY) in runoff water (E and and F), with the cumulated amount (markers) and fungicides concentrations in soil (G) at the catchment scale (left) and at the plot scale (right) from May 24 to August 31 2011. ▲ = KM and ● = CY. Figure III-6C and III-6D: error bars show the analytical uncertainty of pesticides measurements. Figure III-6E and III-6F: error bars show the total uncertainty associated with the pesticides measurement and the discharge measurement.....	108
Figure III-7. Load distribution between the dissolved and particulate phases in runoff water at the catchment and plot scales (Rouffach, France). The total loads exported are reported at the top of the barplots.....	109

## Chapter IV

Figure IV-1. Graphical outline of the PhD thesis (Chapter IV).....	118
Figure IV-2. Scheme of the catchment (Alteckendorf, Alsace, France).....	122
Figure IV-3. Chemical structure of S-metolachlor, acetochlor and their degradation products: ethane sulfonic (ESA) and oxanilic acids (OXA) metabolites of metolachlor (MESA and MOXA) and acetochlor (AcESA and AcOXA).....	123

Figure IV- 4. Temporal changes of <i>S</i> -metolachlor concentration in soil and dissolved runoff water samples at the plot scale .....	129
Figure IV-5. Temporal changes of rainfall (A), the chloroacetanilide application (B), the dissolved exported loads (< 0.7 $\mu\text{m}$ ) of the parent compound (C), those of the degradation products (D) and the particulate loads (> 0.7 $\mu\text{m}$ ) of the parent compounds (E) at the catchment outlet (Alteckendorf, Alsace, France) with red bars for acetochlor and purple bars for <i>S</i> -metolachlor. For chloroacetanilide and metabolite loads, error bars were calculated via error propagation, incorporating analytical uncertainties as well as the uncertainty of suspended solids and water volume measurements.....	131
Figure IV-6. Distribution of enantiomeric excess of <i>S</i> -metolachlor in dissolved and solid bound surface water samples from the drain (DW), plot (PW) and catchment (CW) outlets and in soil (plot) and sediment (catchment) samples.....	138
Figure IV- 7. Temporal changes of the enantiomeric excess of metolachlor at the plot outlet (A) and at the catchment outlet (B) in different environmental compartments.....	139

## Chapter V

Figure V-1. Graphical outline of the PhD thesis (Chapter V) .....	147
Figure V-2. Graphical abstract.....	149
Figure V-3. Scheme of the study catchment (Alteckendorf, Alsace, France).....	154
Figure V-4. Temporal changes of calibrated initial water content, saturated hydraulic conductivity and manning coefficient related to the daily rainfall from May 2 to July 10 2012. ....	167
Figure V-5. Relative sensitivity of total discharge [%] for 20% variation of each input parameter separately. Only parameters for which total discharge sensitivity exceeded 1% were represented. Abbreviations for the input parameters are explained in the nomenclature. Plus or minus symbol indicates 20% increase or decrease respectively. Errors bars represent the temporal variability of the sensitivity within the 9 runoff events. ....	168
Figure V-6. Conceptual mixing layer model for pesticides mobilisation .....	183
Figure V-7. Schemes of the three case study scenarios .....	188
Figure V-8. Influence of $Q_{lim}$ value (left) and time step (right) on the pesticide concentration in runoff water during the transient period.....	190
Figure V-9. Observed and simulated runoff on the experimental plot (A) and associated pesticides concentration in runoff water (B) .....	193
Figure V-10. Simulated pesticides concentration in soil water ( $C_M$ ). ....	194
Figure V-11. Measured and simulated runoff and associated pesticides concentration in runoff water at the catchment outlet .....	196
Figure V- 12. Spatial pattern of pesticides runoff in the study catchment on May 21 .....	197

## Chapter VII

Figure VII-1. 3D orthophotography (A) and topography and water pathways (B) which drained at least 0.5 ha of the vineyard catchment.....	232
Figure VII-2. Four Metolachlor stereoisomers (2 diastereomers and 2 enantiomers) (Kabler and Chen, 2006).....	233
Figure VII-3. Examples of GC-MS/MS chromatograms showing the enantiomeric separation for racemic metolachlor (A) and <i>S</i> -metolachlor (B). The stereoisomer elution was aS1'S; aS1'R; aR1'S; aR1'R.....	234
Figure VII-4. Relative loads of solid-bound (> 0.7 $\mu\text{m}$ ) and dissolved (< 0.7 $\mu\text{m}$ ) for <i>S</i> -metolachlor and acetochlor at the catchment outlet from March 12 and August 14. ....	238
Figure VII-5. Temporal changes of the percentage of total loads of chloroacetanilides and their metabolites expressed in molar load equivalent for <i>S</i> -metolachlor at the plot (A) and catchment outlet (B) and for acetochlor at the catchment outlet (C) from March 12 to July 10 2012.....	239
Figure VII- 6. Soil map of the catchment.....	245
Figure VII- 7. Example of deposition pattern with topography change (A), in headlands (B), behind a vegetal barrier (C) and example of rills erosion (D) and diffusive erosion (E).....	247
Figure VII-8. Total discharge as a function of $K_{sat}$ and $\Psi$ for the event June 7 2012.....	247
Figure VII-9. Accumulated runoff pathways and predicted hydrograph for two different parameters set for the event June 7 2012. For configuration A, $K_{sat\ corn}$ and $K_{sat\ wheat}$ were set to 18 and 60 $\text{mm h}^{-1}$ respectively and for configuration B, 55 and 7 $\text{mm h}^{-1}$ .....	248

Figure VII-10. Rainfall, discharge and drain water height together with predicted discharge according to the both calibration methods for the nine runoff events within the headwater catchment. ....	254
Figure VII-11. Comparison of the predicted runoff pathways for May 21 with the pictures of that day within the headwater catchment. ....	255
Figure VII-12. Predicted and observed erosion rates for each plot within the agricultural catchment. ....	255

# Table of Tables

## Chapter I

Table I-1. Summary of catchment-scale hydrological and pesticide transport models in surface water; “dynamic” may represent different erosion equations for erosion splash, rill erosion and/or transport capacity.....	53
-------------------------------------------------------------------------------------------------------------------------------------------------------------------------------------------------------------------------	----

## Chapter III

Table II-1. Physical-chemical properties of the four study compounds (PPDB, 2009).....	61
Table II-2. Main characteristics of both study catchments (Alsace, France).....	62

## Chapter III

Table III-1. KM, application and meteorological characteristics of May 24 2011 in Rouffach.....	83
Table III-2. Kresoxim methyl deposition along the transect at the vineyard catchment (Rouffach, Alsace, France) the May 24 2011. ....	89
Table III-3. Physico-chemical properties of kresoxim-methyl and cyazofamid. Data were obtained from PPDB (2011).....	97
Table III-4. Geomorphology and land use, hydrology and hydrochemistry from May 24 to August 31 2011 in the experimental plot and the vineyard catchment (Rouffach, France).....	100
Table III-5. Kresoxim methyl and cyazofamid application and transport from May 24 to August 31 2011 in the experimental plot and the vineyard catchment (Rouffach, France). Values are provided as the mean and ranges. ....	107

## Chapter IV

Table IV-1. Hydrological characteristics from March 12 to August 14 2012 in the catchment (Alsace, France). Values are provided as the mean and ranges. ....	130
Table IV-2. Hydrochemistry characteristics from March 12 to August 14 2012 in the plot, drain and catchment's outlet (Alsace, France). Values are provided as the mean and ranges. Bold number corresponds to May 21. ....	133
Table IV-3. Chloroacetanilides concentrations and occurrences from March 12 to August 14 2012 in the plot, drain and catchment's outlet (Alsace, France). Values are provided as the mean and ranges. Bold number corresponds to May 21.....	134

## Chapter V

Table V-1. Meteorological and hydrological characteristics of the 9 runoff events yielding at least 10 m <sup>3</sup> at the outlet of the catchment and occurring from May 2 to August 15 2012. ....	157
Table V-2. Description of the LISEM input parameters and their spatial and temporal discretisation for the both calibration methods: BCM and CCM. "Spatialised" indicates that input parameters are discretised for each cell, "crop" that input parameters are homogeneous according to each 11 landuses and "homogeneous" that the input parameters were lumped for the catchment. "Fixed" indicates that input parameters are fixed over time, "temporally" that input parameters were fixed but may vary over time and "calibrated" indicates that the input parameters were calibrated. ....	160
Table V-3. LISEM erosion parameters related to each crop for May 21.....	161
Table V-4. Comparisons of measured and predicted runoff events in terms of total discharge [m <sup>3</sup> ], peak time discharge [min], peak discharge [L s <sup>-1</sup> ] and performance criteria for each runoff events. ....	165
Table V-5. Measured and predicted total erosion and deposition [ton] within the catchment and the total soil loss at the outlet of the catchment. ....	170
Table V-6. Parameters involved in the pesticides mobilisation and transport resolution and their physical range. ....	187
Table V-7. Description of the input parameters of LISEM-psni and LISEM-pa in the three different study scenarios .....	189

## Chapter VII

Table VII-1. Interpolation methods for estimating the total KM deposition at the catchment scale. ....	223
Table VII-2. Kresoxim methyl soil deposition as a percentage of the applied dose for each integrative petri dish. ....	225
Table VII-3. Meteorological data for each transect and kresoxim methyl soil deposition as a percentage of the applied dose. ....	226
Table VII-4. Deposition loads on plot margins in the catchment according to the distances. Values are provided as a range. ....	227
Table VII-5. Commercial products composition (Stroby DF © and Mildicut ©). ....	228
Table VII-6. Application dose and frequency of all the synthetic active substances applied in the catchment during the wine growing season of 2011 (substances representing > 2% of the total pesticide mass applied). Values for the catchment are provided as mean of plots values ± standard deviation according to the plots. The substances marked in grey were used on the study plot. ....	229
Table VII-7. Number of applications and pesticides use in the catchment during the 2011 wine growing season. Values for the catchment are provided as mean of plots values ± standard deviation. ....	230
Table VII-8. Methods and standards for pedological analysis. ....	230
Table VII-9. Hydrochemical comparison of runoff water outflowing from the plot and the catchment using the Wilcoxon Signed Rank test. ....	231
Table VII-10. Methods and standards for soil hydrodynamic properties analysis. ....	235
Table VII-11. Analytical data of the GC-MS/MS quantification of metolachlor and acetochlor and the LC-MS/MS quantification of their degradation products metolachlor ESA (MESA), metolachlor OXA (MOXA), acetochlor ESA(AcESA) and acetochlor OXA (AcOXA). ....	236
Table VII-12. Hydrochemical comparison of water outflowing from the drain, the plot and the catchment using the Wilcoxon Signed Rank test. ....	237

## Abbreviations

$A_{\text{active}}$ : Hydrologically active area  
 $AcESA$ : Ethane sulfonic degradates of acetochlor  
 $AcOXA$ : Oxanilic acids degradates of acetochlor  
 $A_{\text{connected}}$ : Area that is hydrological connected to a stream  
 $AM$ : Arithmetic Mean  
 $ARAA$ : Association for agronomic advances in Alsace  
 $A_{\text{source}}$ : Area where pesticides are applied and/or deposit  
 $BCM$ : Basic calibration method  
 $BIAS$ : Bias indicator  
 $CCM$ : Constraint calibration method  
 $COFRAC$ : French national accreditation authority  
 $CSA$ : Critical source areas  
 $CSIA$ : Compound specific isotope analysis  
 $CY$ : Cyazofamid  
 $DAA$ : Days after application  
 $DE$ : Diastereoisomer excess  
 $DIC$ : Dissolved inorganic carbon  
 $DOC$ : Dissolved organic carbon  
 $DT_{50}$ : half-life time  
 $EE$ : enantiomeric excess  
 $ESA$ : Ethane sulfonic acid  
 $GC-MS$ : Gas chromatography-mass spectrometry  
 $GML$ : Gauss-Marquardt-Levenberg algorithm  
 $HESI$ : Heated electrospray ionisation  
 $HRUs$ : Hydrological responses units  
 $I_{DR}$ : Agronomical continuous model  
 $IDW$ : Inverse distance squared weighting  
 $LC-MS$ : Liquid chromatography-mass spectrometry  
 $K_d$ : Soil water partition coefficient  
 $KGE$ : Kling-Gupta efficiency  
 $KM$ : Kresoxim methyl  
 $K_{oc}$ : Soil organic carbon water partitioning coefficient  
 $K_{ow}$ : Octanol-water partition coefficient  
 $K_{sat}$ : Saturated hydraulic conductivity

$K_{sat2}$ : Saturated hydraulic conductivity for the second layer  
LISEM: Limbourg Soil Erosion Model  
LOQ: Limit of quantification  
 $MEL_P$ : Mass equivalent load of the parent compound  
MESA: Ethane sulfonic degradates of metolachlor  
MOXA: Oxanilic acids degradates of metolachlor  
MS: Mass spectrometer  
 $MW_p$ : Molecular weight  
 $n$ : Manning's coefficient  
NSE: Nash Suttcliff efficiency  
OKri: Ordinary kriging  
OXA: Oxanilic acid  
POC: Particulate organic carbon  
PPDB: Pesticide properties data base  
RMSE: Root mean square errors  
RR: Random roughness  
SEC: Seasonal export coefficient  
 $soildep_{1,2}$ : Soil depth for layer 1 or 2  
SPE: Solid phase extraction  
SRM: Selected reaction monitoring  
TCRP: Tillage-controlled runoff pattern model  
TIC: Total inorganic carbon  
TOC: Total organic carbon  
TM: Thiessen method  
TSS: Total suspended solids  
USLE: Universal soil loss equation  
 $\theta_{i,2}$ : Initial water content for layer 1 or 2  
 $\theta_{sat1,2}$ : Saturated water content for layer 1 or 2  
 $\Psi_{1,2}$ : Wetting front for layer 1 or 2

## Abstract

Understanding the transport and attenuation of pesticides in agricultural areas is crucial to evaluate their ecological impact on non-target ecosystems. Intensive agricultural headwater catchments (0 – 1 km<sup>2</sup>) play a dominant role in pesticide transport and thus, can have major impacts on downstream water quality. However, surface pesticide transport in headwater catchments has received little attention. In-depth experimental knowledge on off-site pesticide transport is required for the prediction of pesticide transport grounded on physically-based models. In particular, current knowledge at the catchment scale on (i) the spatial variability of pesticide deposition during application, (ii) the impact of erosion on pesticide export, and (iii) the extent of pesticide attenuation in both soil and runoff is very limited.

In this context, this thesis aimed at gaining knowledge about pesticide transport and attenuation in agricultural headwater catchments. Interlocked scales and analytical approaches were combined to evaluate the pesticide transport and degradation from the plot application area to the catchment's outlet in contrasting agricultural catchments (vineyard versus arable crops), representative of temperate agro-ecosystems. The results show that (i) non-target areas within catchment may largely contribute (> 40%) to the overall load of runoff-associated fungicides depending on the hydrological forcing. (ii) For both sites, pesticide partitioning between suspended solids and runoff water largely varied over time and according to the molecules and was shown to be linked to suspended solid concentrations. More than 40% of the total export in the runoff water occurred in the particulate phase (> 0.7 µm) for both chloroacetanilides in the arable crop catchment, suggesting that erosion may represent a primary mode of mobilisation and transport of pesticides in runoff. Runoff and erosion are largely influenced by drastic changes in the soil surface states and the hydrodynamic parameters during the growing season in agro-ecosystems. (iii) The need for an event based, spatially distributed pesticides transport model at the catchment scale which integrate temporal changes in soil surface characteristics and soil hydrodynamic parameters has been underlined. A mathematical formalism was therefore developed to predict pesticide mobilisation and transport in runoff, in the dissolved phase, assuming a thin layer of soil-runoff interaction. The developed formalism was integrated in a hydrological and erosion model LISEM (Limbourg Soil Erosion Model), which was designed to explicitly describe the soil surface structures including crusted and compacted zones. The promising preliminary results of the model can be anticipated as a starting point for better predicting pesticide export in runoff during rainfall-runoff events in agricultural catchments. (iv) Based on molar equivalent load calculations, an export coefficient of two chloroacetanilides

degradation products loads of 7% of their total mass applied was estimated underscoring the importance of degradation processes, which may be reflected in enantiomer analyses. Enantiomeric excess of the *S*-enantiomer negatively correlated with *S*-metolachlor concentrations in soil, suspended solids and runoff water samples suggesting enantioselective biodegradation in the different environmental compartments. These results demonstrated that enantiomer analyses may be relevant for assessing biodegradation of chiral pesticides at catchment scale.

Overall, the results provide quantitative field data and insights coupled with a physically-based model on pesticide transport and attenuation processes in runoff at the catchment scale, with further implications for the delineation of critical sources areas that most contribute to pesticide runoff export and for the ecotoxicological risks associated with chiral compounds. The work carried out in this thesis demonstrated that combining different approaches at the catchment scale enables a better understanding of pesticide transport and attenuation.

**Atténuation et transport par ruissellement des pesticides dans les têtes de bassins  
versants agricoles:  
De la caractérisation sur le terrain à la modélisation**

*Résumé étendu en Français*

**Introduction**

De nombreuses études scientifiques soulignent les problèmes sanitaires et écologiques générés par plus de 50 ans d'utilisation de pesticides (Kohler and Triebkorn, 2013; Schwarzenbach et al., 2006). Les pesticides sont intentionnellement et massivement appliqués dans le monde entier et sont donc considérés comme une source importante de pollution de l'environnement (Mostafalou and Abdollahi, 2013). L'utilisation de pesticides est connue pour avoir des effets néfastes sur tous les compartiments environnementaux: atmosphère, sol, eau, flore et faune (Andresen et al., 2012; Aufauvre et al., 2012; Bunemann et al., 2006; Imfeld and Vuilleumier, 2012; Miguens et al., 2007). Malgré leurs impacts écotoxicologiques, les pesticides sont de plus en plus utilisés dans le monde entier (EPA, 2011). La recherche de traitements plus rapides et plus efficaces et l'augmentation des coûts des pesticides ont stimulé le développement de nouvelles technologies conduisant à l'arrivée sur le marché de molécules aux structures de plus en plus complexe (Ye et al., 2010). Vingt-cinq pour cent des pesticides sont chiraux, c'est à dire qu'ils présentent deux (ou plusieurs) isomères, appelés énantiomères, qui sont des images non superposables l'une de l'autre (Kurt-Karakus et al., 2010). Par exemple, la Figure 1 montre les énantiomères du métolachlore. Les énantiomères d'un même pesticide possèdent des propriétés physico-chimiques identiques mais peuvent se comporter différemment dans l'environnement. Les énantiomères peuvent en effet subir des processus, dits énantioselectifs, conduisant par exemple à la biodégradation préférentielle d'un énantiomère par rapport à l'autre (Ye et al., 2010).

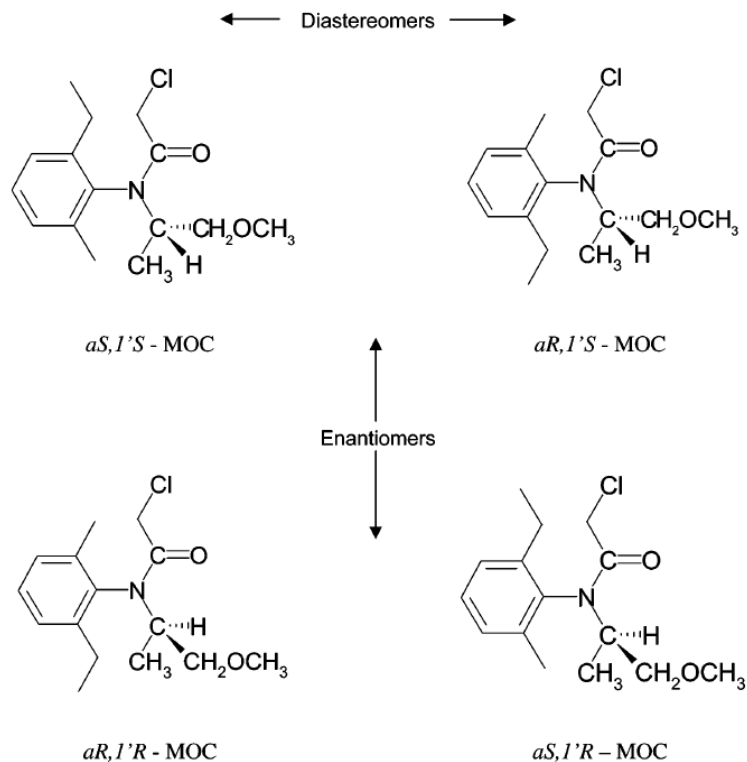


**Figure 1. Structures des quatre stéréoisomères du métolachlore (Kabler and Chen, 2006)**

L'exportation des pesticides dans les eaux de surface, i.e., les cours d'eau, rivières et lacs, représente de 1 à 10% de la masse totale appliquée (Schulz, 2004), ce qui est d'intérêt majeur étant donné que les masses d'eau de surface représentent une source d'eau potable importante dans le monde entier (Arnold et al., 2013). Les eaux de surface sont particulièrement vulnérables à la contamination par les pesticides en raison de leur proximité avec les zones contaminées et la mobilisation rapide des pesticides lors d'événements pluvieux (Botta et al., 2012; Tang et al., 2012). Par conséquent, les zones d'agriculture intensive présentent souvent des niveaux élevés de pollution des eaux de surface par les pesticides (Blann et al., 2009; Vorosmarty et al., 2010).

Comprendre le transport par ruissellement et l'atténuation des pesticides dans les agroécosystèmes est donc primordial pour évaluer leurs impacts écologiques sur les écosystèmes aquatiques. Les têtes de bassin versant (0 - 1 km<sup>2</sup>) correspondent aux surfaces drainées par les premiers cours d'eau des réseaux hydrographiques. Ces petits bassins assurent de nombreuses fonctionnalités essentielles à l'équilibre dynamique d'un hydrosystème

contribuant de manière significative au volume d'eau et aux flux de nutriments ou de pesticides des zones avales. Les têtes de bassins versants agricoles (0 - 1 km<sup>2</sup>) jouent un rôle dominant sur le transport de pesticides et donc peuvent avoir des impacts importants sur la qualité de l'eau en aval (Salmon-Monviola et al., 2013). Cependant, les processus associés au transport des pesticides dans les eaux de surface restent peu compris. Ainsi, nous disposons de peu d'informations sur la variabilité spatiale du dépôt des pesticides à l'échelle du bassin versant, influençant pourtant significativement leur transport par ruissellement. Les études disponibles portent surtout sur le transport des pesticides dans le ruissellement en phase dissoute. Cependant, le transport des pesticides hydrophobiques s'opère principalement sur la phase particulaire, associés aux colloïdes et/ou au carbone organique dissous. Par conséquent, pour évaluer le transport des pesticides dans le ruissellement agricole, les deux phases, dissoutes et particulaires, doivent être prises en compte. Enfin, il reste difficile de quantifier la dégradation *in situ* des pesticides sur le terrain. En effet, les estimations classiques de vitesse de dégradation des pesticides déterminées en laboratoire dans des conditions statiques peuvent ne pas être appropriées pour des conditions expérimentales de terrain (Fenner et al., 2013). En effet, les équilibres d'adsorption sont rarement atteints sur le terrain du à la grande dynamique des conditions hydrologiques et hydrochimiques.

L'objectif général de cette thèse est donc d'améliorer la compréhension et la prédiction du transport des pesticides par ruissellement dans les phases dissoutes et particulaires au sein des têtes de bassins versants agricoles. Deux échelles élémentaires, i.e. la parcelle et le bassin versant, ont été combinées afin de répondre aux objectifs suivants:

- (i) caractériser la variabilité spatiale des dépôts de fongicides lors de leurs applications à l'échelle du vignoble et l'impact de cette variabilité sur le ruissellement.
- (ii) évaluer et comparer la répartition des pesticides entre les phases particulaires et dissoutes dans le ruissellement dans les deux contextes agricoles différents.
- (iii) évaluer la dégradation *in situ* du *S*-métolachlore en combinant analyses énantiomériques et analyses des produits de dégradation.
- (iv) élaborer et valider un modèle physique pour la prédiction de la mobilisation et du transport des pesticides dans le ruissellement.

L'approche à deux échelles a été appliquée sur deux têtes de bassins versants agricoles de 50 ha représentatifs de la région du Rhin supérieur. Les bassins versants diffèrent en termes de cultures (vigne et grandes cultures), topographie, caractéristiques des sols, forçages hydrologiques et pesticides appliqués. Quatre pesticides différents ont été étudiés en raison de leur large utilisation, de leur toxicité et de leur large gamme de propriétés physico-chimiques: le krésoxim-méthyl (KM) et le cyazofamid (CY) (fongicides), l'acétochlore et une molécule chirale, le S-métolachlore (herbicides).

Le plan de la thèse est décrit ci-dessous et dans la représentation graphique (Figure 2). Il comprend deux articles publiés et deux articles en préparation.

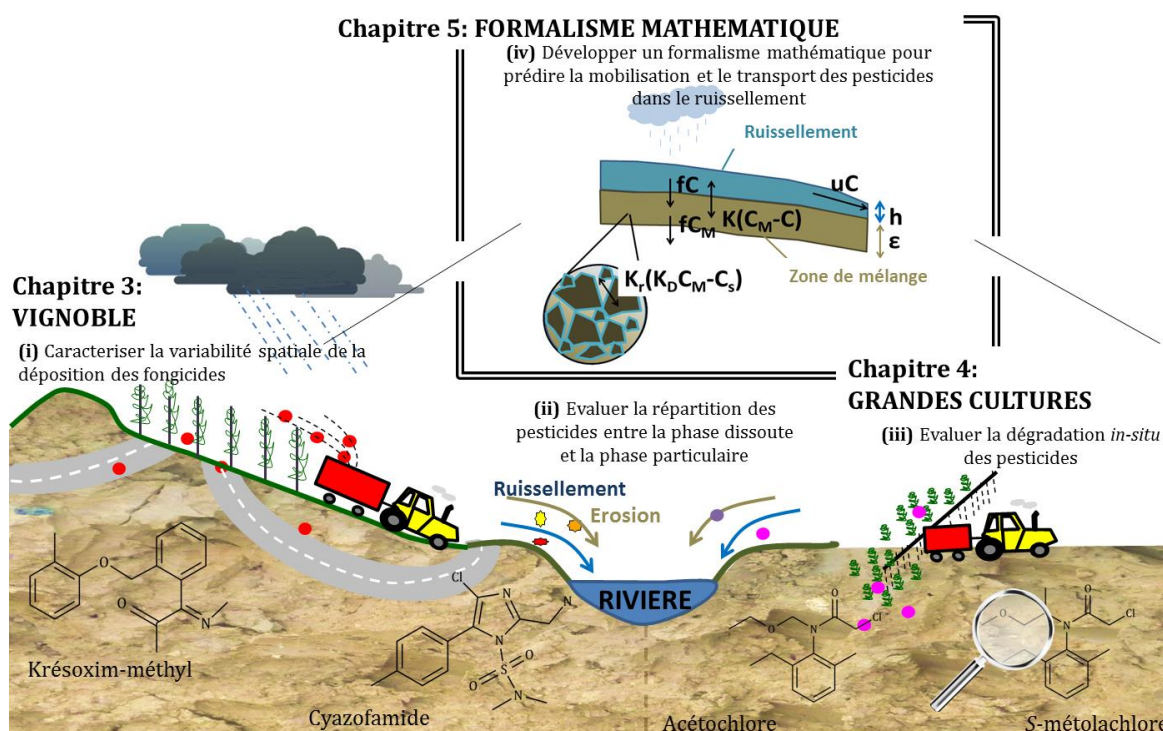


Figure 2. Représentation graphique du plan de la thèse

### Chapitre 3. Dérive et transport des fongicides via le ruissellement et l'érosion dans un vignoble

Les vignobles sont des agrosystèmes fortement anthropisés qui présentent une forte densité de routes et chemins sujets au ruissellement et potentiellement au transport de fongicides. L'application foliaire en vigne est effectuée à 2 m de hauteur et peut donc conduire à une dérive significative des pesticides. Dans un premier chapitre, nous avons donc étudié la dérive et le transport de fongicides *via* le ruissellement dans les vignobles. La dérive et la variabilité spatiale du dépôt de deux fongicides (KM et CY) ont été étudiées dans des conditions d'application réelle dans un bassin versant de 42,7 ha (Rouffach, Alsace, France). Après leur déposition, leur transport par ruissellement et leur répartition entre la phase dissoute et particulaire ont été évalués conjointement à l'échelle du vignoble et d'une parcelle représentative pendant une saison viticole, i.e., de mai à août 2011 (Figure 3).

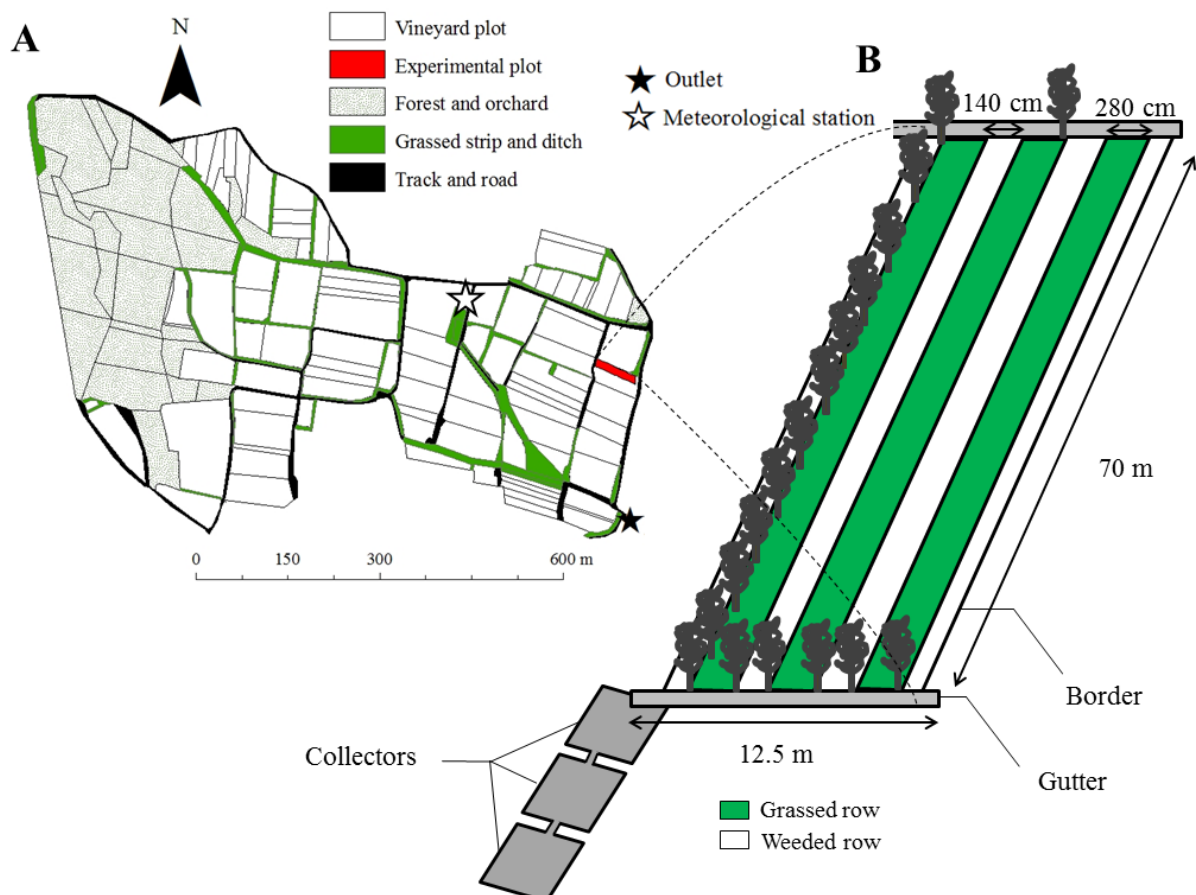


Figure 3. Schéma du bassin versant (A) et de la parcelle expérimentale (B) (Rouffach, Alsace, France).

Les résultats ont montré que le dépôt des fongicides sur le sol varie spatialement et temporellement de manière significative. Le dépôt total de fongicides sur le sol des parcelles à l'échelle du vignoble a été estimé par différentes méthodes d'interpolation et est en moyenne de 60 g (7% de la masse totale appliquée) pour le KM et 18 g (2%) pour le CY. La quantité de fongicides déposée sur les routes était 50 fois supérieure à celle dans les eaux de ruissellement recueillies à l'exutoire du bassin versant. Les observations combinées aux deux échelles montrent que les coefficients d'exportation du KM et du CY étaient plus importants au bassin versant qu'à la parcelle. Les estimations montrent que 85 et 62% des charges mesurées à la sortie du bassin versant ne peuvent pas être expliqués par une contribution des parcelles de vigne. Cela souligne que les éléments inter-parcellaires pourraient largement contribuer à la charge totale de fongicides exportées par ruissellement. La répartition du KM et du CY entre trois fractions, à savoir les matières en suspension ( $> 0,7 \mu\text{m}$ ) et deux fractions dissoutes (i.e.  $< 0,22 \mu\text{m}$  et entre  $0,22$  et  $0,7 \mu\text{m}$ ) dans l'eau de ruissellement étaient similaires aux deux échelles. Le KM a été principalement détecté en dessous de  $0,22 \mu\text{m}$ , alors que le CY a été principalement détecté dans la fraction comprise entre  $0,22$  et  $0,7 \mu\text{m}$ . Bien que le KM et le CY aient des propriétés physico-chimiques similaires et sont supposés se comporter de façon similaire, ces résultats montrent que leur répartition entre les deux fractions au sein de la phase dissoute diffère largement.

Pour une meilleure compréhension du transport des pesticides par l'érosion, nous avons étudié le transport de pesticides dans un bassin versant sujet à l'érosion.

## Chapitre 4. Le transport et l'atténuation des chloroacetanilides dans un bassin versant en grandes cultures

Dans un deuxième chapitre, l'approche de suivi à deux échelles a donc également été appliquée dans un bassin versant en grandes cultures en Alsace (Alteckendorf, Alsace, France), sujet à des coulées d'eaux boueuses fréquentes. L'acétochlore et le *S*-métochlorure, un herbicide chiral sont mondialement utilisés sur la betterave et le maïs. Le *S*-métochlorure dispose de quatre stéréoisomères stables avec un atome de carbone asymétrique et une chiralité axiale. Sa dégradation dans les sols agricoles peut conduire à un enrichissement d'un énantiomère spécifique (Milosevic et al., 2013). Les objectifs de cette étude étaient i) d'évaluer l'exportation de deux herbicides de la famille des chloroacétanilides (le *S*-métochlorure et l'acétochlore) à la fois dans la phase dissoute et particulaire et de quatre produits de dégradation (l'éthane sulfonique acide (ESA) et l'acide oxanilique (OXA), les produits de dégradation du métochlorure (MESA et MOXA) et de l'acétochlore (ACESA et AcOXA)) dans un bassin versant agricole pendant une saison agricole et ii) de tester le potentiel des analyses énantiomériques pour évaluer la biodégradation du *S*-métochlorure. Le bassin versant et l'une de ses parcelles de betteraves à sucre ont été étudiés conjointement en termes de ruissellement, d'érosion, d'hydrochimie et d'exportation de chloroacétanilides au cours d'une saison culturale, i.e. de mars à août 2012.

Nos résultats indiquent que la répartition des chloroacétanilides varie significativement en fonction du temps et des concentrations en matières en suspensions et des caractéristiques des événements ruisselants. La grande variabilité temporelle des coefficients de répartition du *S*-métochlorure et de l'acétochlore peut être reliée à leur grande solubilité par rapport à leur  $\log K_{ow}$  (Boithias et al., 2014) et la nature des adsorbants (taille des particules, aromaticité et polarité), qui peut changer avec le temps et selon différents événements érosifs (Boithias et al., 2014; Si et al., 2009). Un seul épisode ruisselant a été responsable de 53% du volume ruisselé total à l'exutoire, de 92% des matières en suspension totales exportées et de 96% du total des charges du *S*-métochlorure et de l'acétochlore exportées à l'exutoire du bassin versant au cours de la saison culturale (Figure 4). Le taux d'exportation du *S*-métochlorure et de l'acétochlore à l'échelle du bassin versant a été de 3,4% et 5,8% de la masse totale appliquée avec plus de 40% des charges totales sous forme particulaire.

Les produits de dégradation du *S*-métochlorure se sont montrés beaucoup plus persistants dans les eaux de ruissellement que ceux de l'acétochlore. Pour quantifier le transport de la charge totale des chloroacétanilides (composés parents et produits de dégradation) au sein du bassin versant agricole, les charges d'ESA et d'OXA ont été exprimés en équivalent molaire de la masse

du composé parent. La charge équivalent-molaire de la molécule mère (P) ( $MEL_P$ ) a été calculée selon l'équation 1.

$$MEL_P = Load_P + \left\{ Load_{OXA} \left[ \frac{MW_P}{MW_{OXA}} \right] \right\} + \left\{ Load_{ESA} \left[ \frac{MW_P}{MW_{ESA}} \right] \right\} \quad (Eq. 1)$$

Basé sur ce calcul (Eq 1), un coefficient d'exportation de l'ESA et de l'OXA de 7,3% et de 6,7% de la masse totale appliquée pour le S-métolachlore et acétochlore, respectivement, ont été estimés, ce qui indique une contribution majeure des charges des produits de dégradation de l'ESA et OXA (Figure 4).

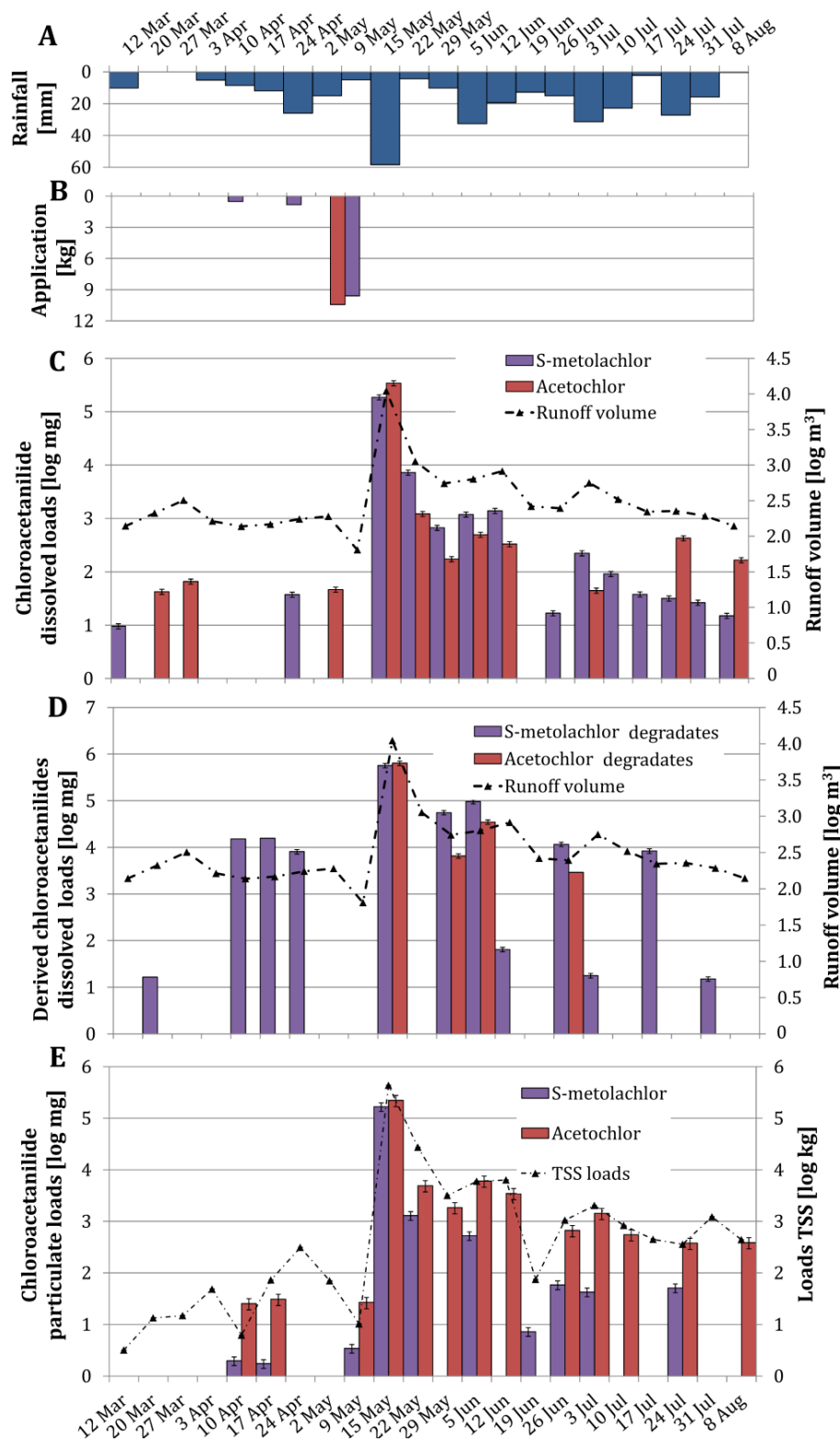


**Figure 4. Variabilit  temporelles des charges du S-m tolachlore, de l'ac tochlore et de leurs produits de d gradation dans la phase dissoute (<0,7  $\mu$ m) et dans la phase particulaire (> 0,7  $\mu$ m)   l'exutoire du bassin versant (Alteckendorf, Alsace, France). L'erreur totale a  t  estim e par propagation d'erreurs bas e sur les incertitudes analytiques, ainsi que sur les incertitudes li es aux mesures des mati res en suspension et des mesures de volume d'eau.**

Les quatre isomères du métolachlore peuvent se regrouper en deux paires d'énantiomères, où aS1'S et aR1'S constitue la première paire, appelée *S*-métolachlore et aS1'R et aR1'R constitue la seconde, appelée *R*-métolachlore. Pour observer la différence de signature chirale au cours du temps, l'excès énantiomérique (EE) a été défini. EE est calculé par l'excédent des 1'S isomères sur les 1'R isomères (Buser et al., 2000) (Eq. 2).

$$EE = \frac{(aS1'S + aR1'S) - (aS1'R + aR1'R)}{(aS1'R + aR1'S + aS1'R + aR1'R)} \quad (\text{Eq. 2})$$

Le produit commercial appliqué, le Mercantor Gold, a une signature énantiomérique comprise entre 0,72 et 0,74. EE a augmenté de 0,6 à 0,75 et de -0,02 à 0,75 dans la phase dissoute à l'échelle de la parcelle et du bassin versant juste après les applications. Dans l'ensemble, pour les échantillons de sol, de matières en suspension et d'eau de ruissellement, une légère corrélation a été montrée entre les valeurs de EE et les concentrations de *S*-métolachlore [ppm] ( $\rho = 0,22$ ,  $p < 0,05$ ,  $n = 94$ ). Ce résultat suggère qu'il y a un enrichissement en *R*-métolachlore pour les échantillons à faible concentration, indiquant une possible dégradation énantiosélective. Il s'agit de la première étude qui combine les analyses de produits de dégradation et des énantiomères du *S*-métolachlore dans différentes matrices environnementales à l'échelle d'un bassin versant agricole. Même si peu d'études ont été menées sur la stéréosélectivité du métolachlore, la dégradation stéréosélective du *S*-métolachlore reste un sujet controversé (Buser et al., 2000; Klein et al., 2006; Kurt-Karakus et al., 2010). Ces résultats représentent donc un point de départ pour une meilleure compréhension et prévision du transport et de la dégradation des chloroacétanilides à l'échelle des bassins versants agricoles.

Dans cette thèse, le ruissellement de pesticides dans deux contextes différents représentatifs des têtes de bassins versants agricoles de la région du Rhin supérieur a été étudié. Cependant, les processus physico-chimiques observés dans un contexte agricole pendant une saison particulière ne peuvent être ni validés, ni extrapolés sans l'aide de la modélisation.

## **Chapitre 5. Modéliser le ruissellement de pesticides à l'échelle de petits bassins versants agricoles**

La première étape pour modéliser le ruissellement des pesticides est de correctement prédire le ruissellement et l'érosion au sein de petits bassins versants agricoles. Les états de surface du sol, principalement la couverture du sol, la structure et l'encroûtement des sols, sont connus pour significativement influencer la répartition des précipitations entre l'infiltration et le ruissellement (Pare et al., 2011; Ulrich et al., 2013). Au cours d'une saison agricole, les changements temporels des paramètres hydrodynamiques du sol et des états de surface des sols peuvent être très rapides et importants (Alaoui et al., 2011; O'Hare et al., 2010). La connaissance des états de surface du sol et des paramètres hydrodynamiques est cruciale pour comprendre et prévoir les processus de transport des pesticides dans les agroécosystèmes. Actuellement, peu de modèles de transport des pesticides prennent en compte les effets des pratiques agricoles sur les paramètres hydrodynamiques et sur les caractéristiques de la surface du sol. Un seul événement pluvieux peut être à l'origine de plus de la moitié du taux d'érosion mesuré dans un bassin versant sur toute la saison culturale. Une compréhension détaillée de la génération du ruissellement et de la dynamique et des voies de transfert du ruissellement est donc essentielle à une échelle événementielle. Or, la plupart des modèles de transport de pesticide sont inappropriés pour étudier à l'échelle de petits bassins versants agricoles le transport des pesticides avec une résolution temporelle très fine ( $\leq 1$  min). En outre, les modèles de transport de pesticides par ruissellement intègrent rarement les processus d'érosion et négligent donc le transport des pesticides sur la phase particulaire. Pour toutes ces raisons, il est nécessaire de développer un modèle de transport de pesticides, (i) qui soit complètement distribué, (ii) soit conçu pour des petits bassins versants agricoles, (iii) qui ait une résolution temporelle fine à échelle événementielle, et (iv) qui soit basé sur une approche dynamique pour évaluer les processus d'érosion et pouvoir prendre en compte le transport des pesticides dans la phase particulaire. Un formalisme mathématique a donc été développé pour prédire la mobilisation des pesticides et le transport par ruissellement dans la phase dissoute dans un premier temps basé sur la théorie de la couche de mélange (Wallender et al., 2008). Les pesticides présents dans la couche superficielle du sol interagissent avec l'eau de ruissellement (Wallender et al., 2008).

La première étape pour prédire le transport des pesticides par ruissellement est de correctement simuler la dynamique et les parcours de l'eau avec un ensemble de paramètres d'entrée physiques et cohérents. Une nouvelle approche de calibration a donc été développée pour prédire les processus de ruissellement et d'érosion avec LISEM afin de prendre en compte

la variabilité temporelle des états de surface du sol et des paramètres hydrodynamiques au long de la saison culturale. Cette méthode, basée sur une expertise agronomique, a été développée pour sélectionner le jeu de paramètres optimaux d'entrée, notamment pour le coefficient de Manning et la conductivité hydraulique à saturation et est représenté Figure 5.

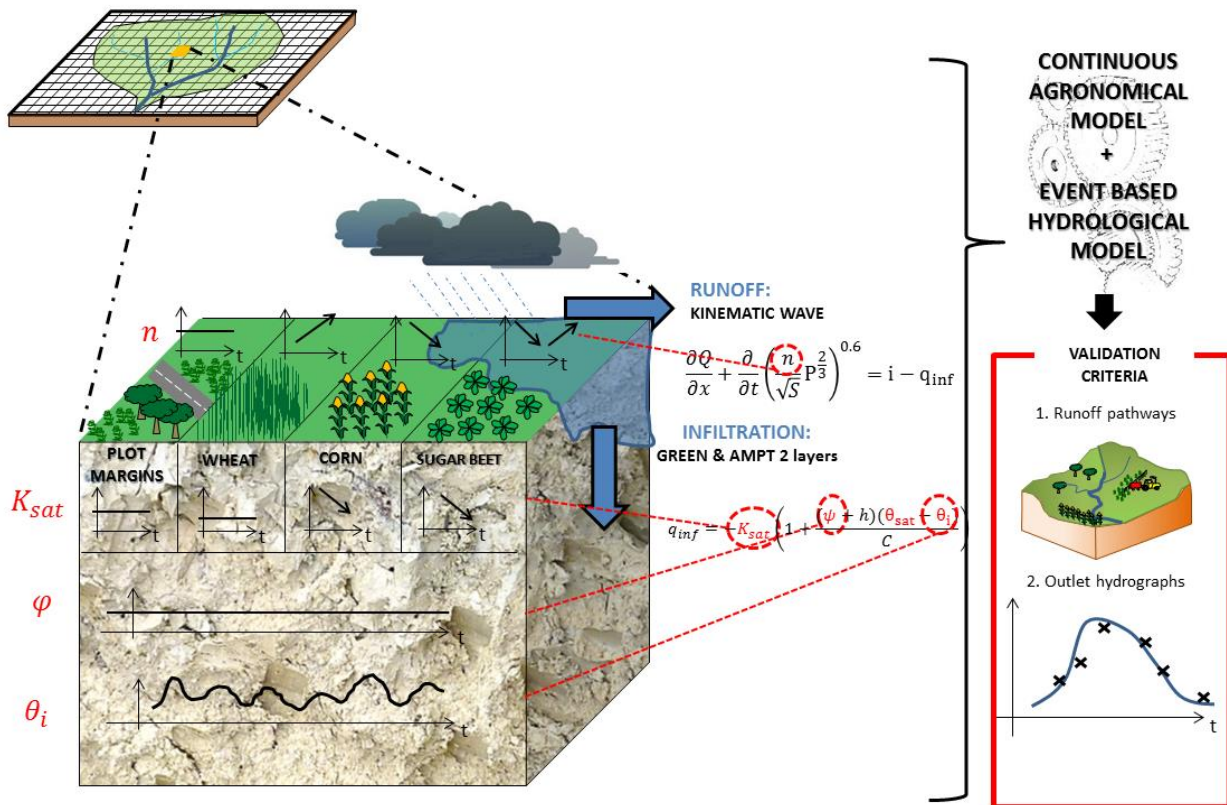


**Figure 5. Schéma de la méthode de calibration**

Cette nouvelle méthode de calibration a été appliquée sur les observations obtenues sur le bassin versant en grandes cultures pendant la saison culturale 2012. Neuf événements ruisselants, de plus de 10 m<sup>3</sup> ont été étudiés. Les résultats montrent que par rapport à une méthode de calibration classique, les prédictions des neuf évènements ruisselants ont été considérablement améliorées basé sur un nombre limité de connaissances supplémentaires.

Deux approches numériques différentes pour prédire la mobilisation et le transport des pesticides par ruissellement ont été développées: une approche dite de séparation d'opérateurs et une approche pseudo-analytique. Les deux résolutions ont été intégrées dans LISEM. La méthode de séparation d'opérateurs basée sur une approche séquentielle non itérative a été testée en raison de sa simplicité pour ajouter un module à un modèle existant et de sa similitude avec la résolution de transport de sédiments déjà existante dans LISEM. L'approche pseudo-

analytique utilisée sur un schéma implicite présente plusieurs avantages. L'intérêt de cette approche est que la conservation de la masse n'est pas altérée et que la sensibilité au pas de temps est négligeable (Jacques et al., 2006).

Ces deux résolutions ont été testées sur 3 niveaux d'échelles: une seule cellule ( $1 \text{ m}^2$ ), une parcelle expérimentale ( $4,5 \text{ m}^2$ ) disposant de données observées et à l'échelle du bassin versant en grandes cultures précédemment présenté ( $470,000 \text{ m}^2$ ) (Figure 6).

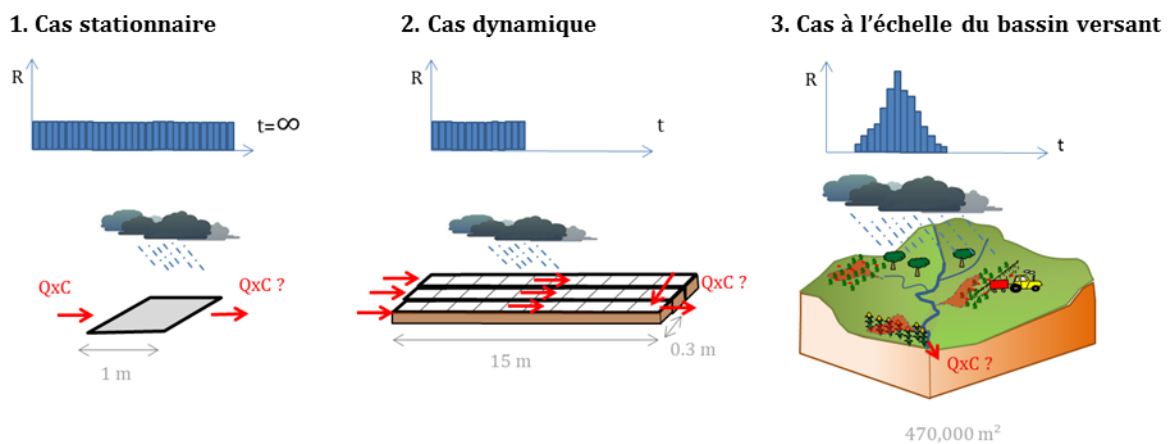


**Figure 6. Schéma des trois différents cas test**

L'instabilité numérique de la méthode de séparation d'opérateurs a été démontrée dès le premier cas test. Cette résolution ne semble donc pas appropriée pour prédire le transport des pesticides à l'échelle de bassins versants agricoles. La résolution pseudo-analytique a été évaluée et validée sur les trois échelles. La dynamique d'exportation de pesticides et les bilans de masses ont été validés à l'échelle de la parcelle expérimentale. Ce formalisme s'est montré robuste à la fois en fonction de différents pas de temps et conditions de déclenchement de ruissellement et en fournissant des ordres de grandeur raisonnables à l'échelle du bassin versant. Ces résultats préliminaires sont donc encourageants mais nécessitent des études supplémentaires, notamment avec (i) une validation dynamique des concentrations de pesticides à l'exutoire d'un bassin versant disposant d'une discrétisation temporelle fine des concentration en pesticides, (ii) une validation spatiale des concentrations de pesticides en utilisant des points de contrôle interne de mesures, (iii) une réflexion sur l'évaluation des concentrations initiales spatiales des pesticides dans le sol et l'eau du sol, et (iv) l'évaluation de l'influence des paramètres d'entrées. La prédiction des pesticides sur la phase particulière fera l'objet d'une étude future.

## Conclusion

Cette thèse vise à améliorer les connaissances sur le transport des pesticides par ruissellement dans deux contextes agricoles différents: vignoble et grandes cultures, et se concentre plus particulièrement sur la répartition des pesticides dans la phase dissoute et particulaire dans les eaux de ruissellement. Les observations combinées des pesticides transportés *via* le ruissellement à la fois à l'échelle du bassin versant et de la parcelle ont permis d'identifier les zones à l'origine d'une exportation de pesticides. Le travail effectué dans cette thèse a souligné l'importance de la dérive des pesticides sur des surfaces imperméables. Cette dérive devrait être prise en compte dans le futur dans les modèles de transport des pesticides *via* le ruissellement pour les bassins versants fortement anthropisés. La répartition des pesticides dans la phase dissoute et particulaire diffère significativement sur les deux bassins versants selon les molécules, même si leurs propriétés physico-chimiques sont similaires. Ceci souligne la complexité de prédire la répartition « dissous-particulaire » des pesticides dans des conditions dynamiques de terrain. En effet, l'équilibre d'adsorption des pesticides est rarement atteint sur le terrain et l'affinité des pesticides avec des particules dépend fortement de la nature des adsorbants. L'étude de terrain a aussi démontré que les analyses énantiomériques peuvent être pertinentes pour évaluer les processus de dégradation des pesticides chiraux in situ dans les eaux de surface à l'échelle des bassins versants. Il est maintenant crucial de quantifier les conditions et l'étendue de cette dégradation énantioselective du *S*-métolachlore en laboratoire pour pouvoir comparer les données de terrain avec des études de référence qui sont actuellement manquantes. D'autre part, il est essentiel d'interpréter ces données de terrain plus profondément avec des modèles physiques qui prennent en compte l'énantioselectivité.

Cette étude a démontré que la combinaison de différentes approches à l'échelle du bassin versant permet une meilleure compréhension du transport des pesticides et de leur atténuation.

## Références

- Alaoui, A., Lipiec, J., Gerke, H.H., 2011. A review of the changes in the soil pore system due to soil deformation: A hydrodynamic perspective. *Soil & Tillage Research*. 115, 1-15.
- Andresen, L.C., Nothlev, J., Kristensen, K., Navntoft, S., Johnsen, I., 2012. The wild flora biodiversity in pesticide free bufferzones along old hedgerows. *Journal of Environmental Biology*. 33, 565-572.
- Arnold, S.M., Clark, K.E., Staples, C.A., Klecka, G.M., Dimond, S.S., Caspers, N., Hentges, S.G., 2013. Relevance of drinking water as a source of human exposure to bisphenol A. *Journal of Exposure Science and Environmental Epidemiology*. 23, 137-144.
- Aufauvre, J., Biron, D.G., Vidau, C., Fontbonne, R., Roudel, M., Diogon, M., Vignes, B., Belzunces, L.P., Delbac, F., Blot, N., 2012. Parasite-insecticide interactions: a case study of *Nosema ceranae* and fipronil synergy on honeybee. *Scientific Reports*. 2.
- Blann, K.L., Anderson, J.L., Sands, G.R., Vondracek, B., 2009. Effects of Agricultural Drainage on Aquatic Ecosystems: A Review. *Critical Reviews in Environmental Science and Technology*. 39, 909-1001.
- Boithias, L., Sauvage, S., Merlina, G., Jean, S., Probst, J.-L., Sánchez Pérez, J.M., 2014. New insight into pesticide partition coefficient  $K_d$  for modelling pesticide fluvial transport: Application to an agricultural catchment in south-western France. *Chemosphere*. 99, 134-142.
- Botta, F., Fauchon, N., Blanchoud, H., Chevreuil, M., Guery, B., 2012. Phyt'Eaux Cites: Application and validation of a programme to reduce surface water contamination with urban pesticides. *Chemosphere*. 86, 166-176.
- Bunemann, E.K., Schwenke, G.D., Van Zwieten, L., 2006. Impact of agricultural inputs on soil organisms - a review. *Australian Journal of Soil Research*. 44, 379-406.
- Buser, H.R., Poiger, T., Muller, M.D., 2000. Changed enantiomer composition of metolachlor in surface water following the introduction of the enantiomerically enriched product to the market. *Environmental Science & Technology*. 34, 2690-2696.
- EPA, 2011. Pesticide Industry Sales and Usage: 2006 and 2007 Market Estimates. US Environmental Protection Agency, Washington (DC).
- Fenner, K., Canonica, S., Wackett, L.P., Elsner, M., 2013. Evaluating Pesticide Degradation in the Environment: Blind Spots and Emerging Opportunities. *Science*. 341, 752-758.
- Imfeld, G., Vuilleumier, S., 2012. Measuring the effects of pesticides on bacterial communities in soil: A critical review. *European Journal of Soil Biology*. 49, 22-30.
- Jacques, D., Simunek, J., Mallants, D., van Genuchten, M.T., 2006. Operator-splitting errors in coupled reactive transport codes for transient variably saturated flow and contaminant transport in layered soil profiles. *Journal of Contaminant Hydrology*. 88, 197-218.
- Kabler, A.K., Chen, S.M., 2006. Determination of the 1' S and 1' R diastereomers of metolachlor and S-metolachlor in water by chiral liquid chromatography - Mass spectrometry/mass spectrometry (LC/MS/MS). *Journal of Agricultural and Food Chemistry*. 54, 6153-6158.
- Klein, C., Schneider, R.J., Meyer, M.T., Aga, D.S., 2006. Enantiomeric separation of metolachlor and its metabolites using LC-MS and CZE. *Chemosphere*. 62, 1591-1599.
- Kohler, H.R., Triebkorn, R., 2013. Wildlife Ecotoxicology of Pesticides: Can We Track Effects to the Population Level and Beyond? *Science*. 341, 759-765.
- Kurt-Karakus, P.B., Bidleman, T.F., Muir, D.C.G., Struger, J., Sverko, E., Cagampan, S.J., Small, J.M., Jantunen, L.M., 2010. Comparison of concentrations and stereoisomer ratios of mecoprop, dichlorprop and metolachlor in Ontario streams, 2006-2007 vs. 2003-2004. *Environmental Pollution*. 158, 1842-1849.
- Miguens, T., Leiros, M.C., Gil-Sotres, F., Trasar-Cepeda, C., 2007. Biochemical properties of vineyard soils in Galicia, Spain. *Science of The Total Environment*. 378, 218-222.
- Mostafalou, S., Abdollahi, M., 2013. Pesticides and human chronic diseases: Evidences, mechanisms, and perspectives. *Toxicology and Applied Pharmacology*. 268, 157-177.
- O'Hare, M.T., McGahey, C., Bissett, N., Cailles, C., Henville, P., Scarlett, P., 2010. Variability in roughness measurements for vegetated rivers near base flow, in England and Scotland. *Journal of Hydrology*. 385, 361-370.
- Pare, N., Andrieux, P., Louchart, X., Biarnes, A., Voltz, M., 2011. Predicting the spatio-temporal dynamic of soil surface characteristics after tillage. *Soil & Tillage Research*. 114, 135-145.
- Salmon-Monviola, J., Moreau, P., Benhamou, C., Durand, P., Merot, P., Oehler, F., Gascuel-Oudou, C., 2013. Effect of climate change and increased atmospheric CO<sub>2</sub> on hydrological and nitrogen cycling in an intensive agricultural headwater catchment in western France. *Climatic Change*. 120, 433-447.

- Schulz, R., 2004. Field studies on exposure, effects, and risk mitigation of aquatic nonpoint-source insecticide pollution: A review. *Journal of Environmental Quality*. 33, 419-448.
- Schwarzenbach, R.P., Escher, B.I., Fenner, K., Hofstetter, T.B., Johnson, C.A., von Gunten, U., Wehrli, B., 2006. The challenge of micropollutants in aquatic systems. *Science*. 313, 1072-1077.
- Si, Y.B., Takagi, K., Iwasaki, A., Zhou, D.M., 2009. Adsorption, desorption and dissipation of metolachlor in surface and subsurface soils. *Pest Management Science*. 65, 956-962.
- Tang, X.Y., Zhu, B., Katou, H., 2012. A review of rapid transport of pesticides from sloping farmland to surface waters: Processes and mitigation strategies. *Journal of Environmental Sciences-China*. 24, 351-361.
- Ulrich, U., Dietrich, A., Fohrer, N., 2013. Herbicide transport via surface runoff during intermittent artificial rainfall: A laboratory plot scale study. *Catena*. 101, 38-49.
- Vorosmarty, C.J., McIntyre, P.B., Gessner, M.O., Dudgeon, D., Prusevich, A., Green, P., Glidden, S., Bunn, S.E., Sullivan, C.A., Liermann, C.R., Davies, P.M., 2010. Global threats to human water security and river biodiversity (vol 467, pg 555, 2010). *Nature*. 468, 334-334.
- Wallender, W.W., Joyce, B.A., Ginn, T.R., 2008. Modeling the Transport of Spray-Applied Pesticides from Fields with Vegetative Cover. *Transactions of the Asabe*. 51, 1963-1976.
- Ye, J., Zhao, M.R., Liu, J., Liu, W.P., 2010. Enantioselectivity in environmental risk assessment of modern chiral pesticides. *Environmental Pollution*. 158, 2371-2383.





# Chapter I. Introduction & context

---

## 1. Pesticides in the environment

### 1.1. Impact and diversity

Multiple scientific reports emphasise the health and ecological problems created by over 50 years of anthropogenic pollutant contamination (Kohler and Triebkorn, 2013; Schwarzenbach et al., 2006). Nearly 80% of the world's population is threatened by water contamination arising from many different stressors (Vörösmarty et al., 2010). Because pesticides are intentionally and massively applied worldwide, pesticides are considered a major source of environmental pollution (Mostafalou and Abdollahi, 2013). Pesticide use is known to have prejudicial impacts in all environmental compartments: atmosphere, soil, water, flora and fauna. For example, pesticide contamination has been reported to affect soil biogeochemical activity (Miguens *et al.*, 2007) and living organisms, such as animals (Aufauvre et al., 2012; Bunemann et al., 2006), bacteria (Imfeld and Vuilleumier, 2012) and plants (Andresen *et al.*, 2012). Ecotoxicological tests are fundamental tools for assessing the toxicity of pesticides to organisms and have demonstrated the acute and/or chronic toxicity of a wide range of pesticides (Alves et al., 2013). The toxicity of a specific pesticide can be assessed by its  $LC_{50}$  value, corresponding to the concentration at which half of the population dies following a given exposure time. For example, the widely used fungicide kresoxim methyl is considered highly toxic to aquatic crustaceans and aquatic invertebrates, with an acute, 96-hour  $LC_{50}$  of  $47 \mu\text{g L}^{-1}$  (PPDB, 2009). Residues of pesticides have been reported to exceed the European Union's maximum residue level in food, causing concern regarding their possible effects on public health; such concerns exist for the fungicide cyazofamid in grapes, for example (Gonzalez-Rodriguez et al., 2011). Several pesticides, such as chlorinated, organophosphate and carbamate insecticides, as well as phenoxy acid and triazine herbicides have demonstrated significant exposure-response associations in human-health studies, such as studies regarding specific human cancers (Alavanja and Bonner, 2012; Bassil et al., 2007) and Parkinson's disease (Fitzmaurice et al., 2013).

Despite their ecotoxicological impacts, numerous pesticides are increasingly used worldwide (EPA, 2011). In general, pesticides comprise three main subgroups, i.e., fungicides, herbicides and insecticides, and more than 20 other types, such as rodenticides, molluscicides, and

algaecides (EPA, 2011). In 2007, 250 different synthetic pesticides were commercialised (Directive 91/414/EEC; EPA, 2011). Since then, every year, 2.4 million tons of pesticides have been sold worldwide, with world pesticide expenditure growing to more than \$39.4 billion in 2007 (EPA, 2011). While herbicides are the most applied pesticide group in the world, comprising 39% of total worldwide pesticide use (EPA, 2011), fungicides are the most used in Europe, constituting an annual amount of approximately 107,574 tons of active ingredient and comprising 49% of European pesticide use (Eurostat, 2007). The worldwide use of pesticides has increased, as have the complexities of molecular structures allowed on the market (Ye et al., 2010). The steadily growing need for more rapid and efficient treatment and the increased cost of pesticides has stimulated development of new technologies, such as nano-pesticides. Nano-pesticides include entities in the nanometer size range that enhance pesticide properties, for instance, increasing apparent solubility (Kah et al., 2013). Twenty-five percent of pesticides are chiral (Kurt-Karakus et al., 2010), i.e. pesticides presenting two (or more) isomers, called enantiomers, which are non-superimposable mirror images of each other; for example, Figure I-2 shows the enantiomers for metolachlor. Enantiomers behave differently in different environments, and bioaccumulation, persistence and/or toxicity may demonstrate enantioselectivity (Ye et al., 2010).

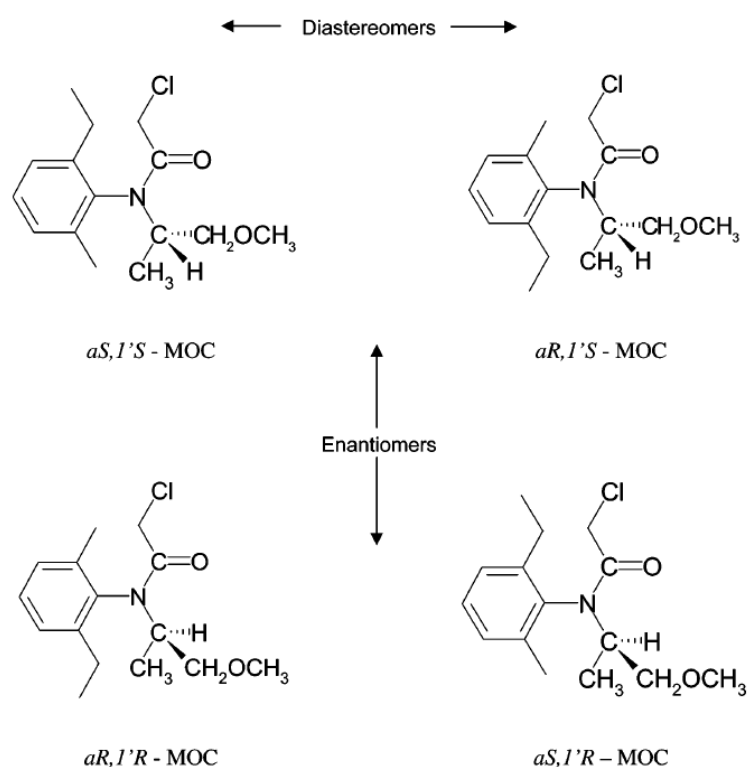


Figure I-2. Structures of the four stereoisomers of metolachlor (Kabler and Chen, 2006)

Apart from the new generation compounds, there are a number of concerns regarding the detrimental effects of pesticides on the environment. Ancient and complex molecules still cause serious water quality issues (Kümmerer, 2010). Despite being banned more than 40 years ago, some pesticides, such as DDT, are still very persistent in soil and groundwater (Kümmerer, 2010). Surfactants are a diverse group of chemicals that are often added to commercial pesticide formulations designed to benefit solubilisation properties (Ying, 2006). The fate of such surfactants, which often constitute the major part of the mass applied, is almost entirely unknown (Oliver-Rodriguez et al., 2013). Pesticide degradation may lead to the formation of unknown metabolites that may be more harmful and/or persistent than the parent compounds. Pesticides, surfactants and their metabolites are among the most relevant environmental contaminants. Understanding pesticide distribution among environmental compartments has therefore become of utmost importance.

## 1.2. Environmental distribution of pesticides

Figure I-3 illustrates the diversity of pathways by which pesticides are dispersed in the various compartments of the environment, including atmosphere, soil, water and vegetation. Pesticides are either released intentionally, through application processes (i.e., diffuse pollution), or unintentionally, occurring during an accident (i.e., point-source pollution). Sprayed pesticide may drift and reach non-target areas during pesticide application. Spray drift may account for 1 to 75% of the total mass of pesticides applied, depending on the meteorological conditions, application methods and pesticide characteristics (Barbash, 2014). Once pesticides are applied, off-site losses through volatilisation may reach 90% (Bedos et al., 2002). Pesticides can be transported and persist over long distances in the atmosphere; such an example is organochlorines, which were detected in the Arctic (Sadiki and Poissant, 2008). Pesticide deposition can be caused by precipitation (wet deposition) or by gaseous and particle deposition (dry deposition) (Coupe et al., 2000; Messing et al., 2013). Following deposition, pesticides may be dispersed within hydrosystems, particularly groundwater systems and surface water bodies.

Losses due to leaching in groundwater may represent a few percent of the total pesticide mass for moderately mobile pesticides such as atrazine (Farlin et al., 2013). Pesticide losses into surface water, which includes streams, rivers and lakes, have been shown to range between 1 to 10% (Schulz, 2004). Due to their close connections with contaminated areas and the fast mobilisation of pesticides during rainfall-runoff events, surface waters are particularly and rapidly vulnerable to contamination (Botta et al., 2012; Tang et al., 2012), which is of serious concern given that surface water bodies represent drinking water sources worldwide (Arnold et

al., 2013). Diffuse input paths by which pesticides contaminate surface waters are as follows: tile drain outflow, baseflow seepage, surface and subsurface runoff and soil erosion from contaminated areas (Reichenberger et al., 2007).

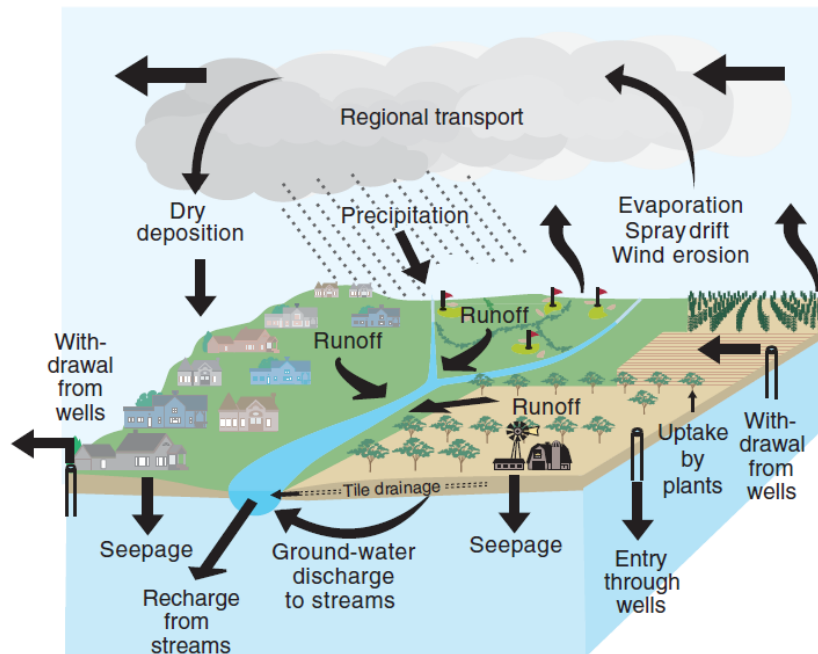


Figure I-3. Pesticide movement in the hydrological system (Barbash, 2014)

The majority of offsite pesticide movements enter streams as a result of their close connections to agricultural areas, where most pesticides are applied. Therefore, areas with intensive agriculture can exhibit high degrees of water pollution (Vörösmarty et al., 2010); for example, 83% of American monitored streams from farmland areas had at least one pesticide for which the concentration exceeded USEPA guidelines for aquatic life (Blann et al., 2009). Agricultural streams may receive highly contaminated water and be incapable of fully attenuating the impacts of concentrated pesticide contamination, underscoring the necessity of limiting threats at their source rather than via costly remediation of symptoms (Vörösmarty et al., 2010). Hence, understanding pesticide transport from agricultural systems to surface water ecosystems represents a major challenge.

## 2. Pesticide transport from agro-ecosystems to surface waters

### 2.1. Agro-ecosystems, definition and specificity

An *ecosystem* is “a functional system of complementary relations between living organisms and their environment, delimited by arbitrarily chosen boundaries, which in space and time appear to maintain a steady yet dynamic equilibrium” (Gliessman, 2007). An *agro-ecosystem* is an ecosystem that integrates agricultural production (e.g., the farm or, on a larger scale, the region impacted by agricultural activity). Due to anthropogenic activities, an agro-ecosystem is often characterised by a reduction of biological diversity and by an alteration in natural energy flow (harvest period) and an alteration of biogeochemical cycles (nutrient saturation) compared to a natural ecosystem (Gliessman, 2007). Nitrogen (N) and phosphorus (P) are the two most important nutrients limiting biological production and are the most extensively applied nutrients in agricultural areas, mainly via soluble inorganic fertilisers (Drinkwater and Snapp, 2007).

An agricultural landscape is divided into arable lands (e.g., cereals, cotton, vegetables), permanent crops (e.g., orchards, vineyards) and permanent pastures (FAO, 2011). Arable land and permanent crops represent 28% and 3%, respectively, of the total agricultural area worldwide. Although vineyards cover a small percentage of agricultural land surfaces, they contribute a major share to European pesticide use (Eurostat, 2007). Vineyards are risky agricultural contamination ‘hotspots’ due to the large quantities and diversity of pesticides applied in addition to the vulnerability of the soil to erosion. Vineyards undergo ten to a thousand tons of soil loss per hectare per year due to shallow soil depth and steep slopes (Gómez et al., 2011; Quiquerez et al., 2014). Vineyards are strongly impacted by anthropogenic forcing, including the planting of vine rows along the fall line or the presence of impermeable tracks, thereby creating favourable conditions for water runoff and concomitant sediment and pesticide losses (Novara et al., 2011).

In arable crop areas, simplified rotations, through the replacement of a variety of spring and winter-sown crops with winter-sown cereals, have been possible through the use of nutrient and carbon inputs. These simplified rotations lead to the prevalence of bare land during some part of the year. Farmers are often advised to apply non-selective herbicides during pre-sowing and/or pre-emergence (Lodovichi et al., 2013). Pre-sowing and/or pre-emergence herbicides are applied to the soil surface and can thus be easily mobilised by runoff and erosion. Vineyard and

arable crops therefore epitomise a situation in which soil and water sustainability is highly threatened.

For all types of crops, the common agricultural practices of leaving bare soil areas (Durán-Zuazo et al., 2013), removing perennial vegetation (Xu et al., 2013) or tilling (Meijer et al., 2013) are the main factors contributing to soil erosion, runoff and subsequent pesticide transport. Soil surface characteristics, primarily soil cover, topsoil structure and soil crusting, are known to largely influence the partition of rainfall between infiltration and runoff (Pare et al., 2011; Ulrich et al., 2013). Cultivated soils are particularly affected by soil deformation due to agricultural practices and specific soil surface characteristics (Alaoui et al., 2011). During a growing season, temporal changes of the soil hydrodynamic parameters can be very rapid and significant (Alaoui et al., 2011; O'Hare et al., 2010). Soil deformation includes compaction, sealing and crusting. Agricultural field operations depend heavily on wheeled tractors, which implies repeated compressive stress leading to the formation of a dense soil layer with low porosity and hydraulic conductivity (Lipiec and Hatano, 2003). Soil structure is significantly affected by mechanical stresses, such as tillage or hydraulic stresses from natural wetting and drying cycles. Air slaking (wind erosion) and raindrops (splash erosion) hit the soil surface and destroy small soil aggregates. The detached material is easily transported and infiltrated into the upper millimetres of the soil, clogging the pores leading to soil surface sealings and crust development (Ulrich et al., 2013). Crust development results in higher runoff velocities and sediment transport and, thus, higher pesticide loss. Knowledge of soil-surface and hydrodynamic characteristics is therefore essential for understanding and predicting pesticide transport processes in agro-ecosystems.

### **2.2. Pesticide transport and attenuation from agricultural sources to sinks**

Pesticides mainly enter agricultural streams during rain events, when they are mobilised and transported via fast runoff. From a hydrological viewpoint, it has been known for decades that only small parts of a catchment contribute to runoff (Dunne and Black, 1970). Consequently, relatively small proportions of an agro-ecosystem can cause the majority of off-site pesticide export and are thus often called the critical source areas (CSA) (Doppler et al., 2012). Identifying these areas of high-risk 'hotspots' may help with focusing management practices on vulnerable areas. For example, wetlands or buffer strips within agro-ecosystems may act as sinks of pesticides and can efficiently attenuate pesticide mixtures associated with agricultural runoff (Maillard et al., 2011; Reichenberger et al., 2007). A CSA may be defined as the intersection of the following three areas: i) an area where pesticides are applied and/or deposited ( $A_{\text{source}}$ ), (ii) a

hydrologically active area ( $A_{active}$ ), i.e., where surface or subsurface runoff has occurred and (iii) an area that is hydrologically connected to a stream ( $A_{connected}$ ) (Doppler et al., 2012). In other words, a CSA can be represented by the following spatial intersection:

$$CSA = A_{source} \cap A_{active} \cap A_{connected} \quad (1)$$

The amount of substance that is available for transport via runoff or erosion may be attenuated by sorption and degradation between two runoff events. Finally, various factors, including farming practices, intrinsic physical-chemical properties of pesticide compounds, soil and vegetation characteristics and hydrological and biogeochemical conditions, govern pesticide transport and attenuation within agro-ecosystems.

### 2.2.1 Processes affecting pesticides amount at the source area ( $A_{source}$ )

When pesticides are applied, some of the spray may move beyond the intended area and reach a non-target ecosystem. Chlorpyrifos and metalaxyl drift, for example, have occurred at distances as great as 24 m in the vineyard (Vischetti et al., 2008). Such pesticide drift largely depends on the equipment, application techniques and farming practices used. Nozzle height, nozzle pressure, droplet size and driving speed are main factors influencing pesticide drift (Arvidsson et al., 2011; Nuyttens et al., 2009). Climatic conditions, such as wind speed, temperature or atmospheric humidity, also play a major role in the spatial variability of pesticide deposition. For example, lower atmospheric humidity results in greater pesticide drift (Nuyttens et al., 2007). Vegetation may act as a barrier and intercept pesticide drift (Ohliger and Schulz, 2010). Finally, chemical factors, i.e., formulation, presence of additives, density, viscosity and volatility, also affect pesticide drift (Nuyttens et al., 2009). However, studies have often focused on the distance that pesticides drift from the spray origin, and very little is known with regard to the spatial variability of pesticide application within and surrounding the application area (Lazzaro et al., 2008). Spatial variability of pesticide deposition within the application area can be observed due to the micro-scale variability in local conditions (Gregorio et al., 2014). It is therefore crucial to investigate the spatial patterns of deposited pesticides to understand and predict which pesticide is available for transport. Given that considerable amounts of impermeable surfaces are present, pesticide deposition via drift in vineyards may be particularly prone to fast runoff.

Once pesticides are deposited, pesticide attenuation in agro-ecosystems involves destructive processes, e.g., photolysis, hydrolysis and biodegradation, and non-destructive processes, e.g., plant uptake and sorption (Figure I-3).

Among the non-destructive processes, plant uptake occurs via the following two major pathways: (i) desorption from the soil followed by root uptake from the soil solution and (ii) deposition on plant surfaces followed by uptake into the inner parts of the plant (Juraska et al., 2009). Root uptake generally increases in relation to the affinity of the pesticide to lipids (Barbash, 2014) and varies considerably between individual plant species and root depths (Fantke et al., 2013). The octanol-water partition coefficient ( $K_{ow}$ ) is often used to estimate the absorptive properties of the rhizodermis. Because of their hydrophilic properties, pesticides with low  $\log K_{ow}$  values (i.e.,  $< 1$ ) will hardly penetrate the lipid-containing root epidermis. On the contrary, pesticides with  $\log K_{ow}$  values  $> 3$  will be increasingly retained by the lipids in the root epidermis and the organic matter surrounding the root (Verkleij et al., 2009).

Sorption/desorption processes govern pesticide leaching into the deeper soil layer and the timing and amount of pesticides mobilised by runoff. Sorption is influenced by soil texture, soil particle size distribution, soil moisture, soil organic carbon content, pH, temperature, and compound characteristics (Wauchope et al., 2002). Increased contact time between pesticides and sorbents may result in the formation of stronger bonds (Gevao et al., 2000). Pesticides can remain strongly sorbed on the soil particles, depending on their affinities with natural organic carbon and/or mineral surfaces. The affinity of a compound with soil is often estimated based on the soil/solution distribution coefficient ( $K_d$ ). The  $K_d$  values vary greatly among soils and sediments and may span an order of magnitude for a single active ingredient (Barbash, 2014). The  $K_d$  values are often strongly correlated with the soil's organic matter content and lead to the development of  $K_{oc}$ , the organic-carbon water partition coefficient that is defined as the ratio of  $K_d$  and the mass fraction of organic carbon (Barbash, 2014). For most pesticides,  $\log K_{oc}$  ranges between 1 and 4 (Calvet, 2005).

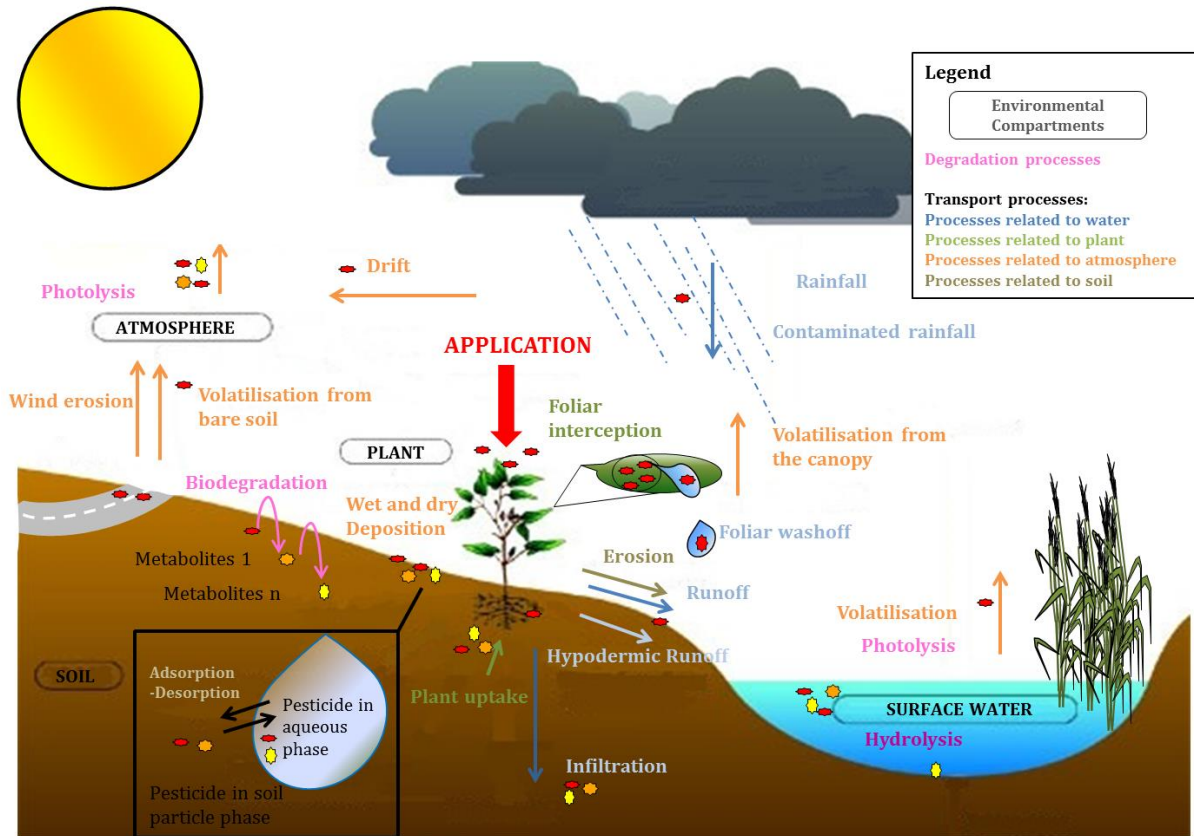


**Figure I-4. Bio-physical-chemical processes related to pesticide transport and attenuation in agro-ecosystems**

Different degradation processes co-exist in the environment and can be classified into two main categories, biotic and abiotic processes (processes in pink in Figure I-3). Abiotic processes involve non-living chemical and physical factors in the environment, such as photolysis, hydrolysis and chemical transformations (e.g., redox reactions). Pesticides may also be transformed by living organisms via biotic processes, as in the case of microbial transformation. The soil ecosystem is inhabited by billions of microorganisms and numerous other organisms, including fungi, algae, insects and plants (Jacobsen and Hjelmsø, 2014). Plants, animals and fungi typically transform pesticides for environmental detoxification purposes, whereas bacteria more commonly metabolise pesticides for assimilation and energy (Fenner et al., 2013). Biodegradation is generally identified as the most important manner, mass-balance-wise, of pesticide degradation (Fenner et al., 2013). It is often impossible to distinguish between biotic and abiotic processes because all of these processes may occur simultaneously or sequentially, making a mechanistic understanding difficult, especially under field conditions. Except for complete mineralisation, transformation processes lead often to the presence of degradation products in the environment, as illustrated by the degradation pathways of acetochlor in soil (Figure I-4) (Roberts et al., 1999). Degradation products may behave differently in the environment compared with the parent compound (la Farre et al., 2008). For example,

enantiomers of chiral pesticides have identical physical-chemical properties and are expected to undergo similar abiotic processes, such as sorption or volatilisation. Conversely, due to their spatial configurations, enantiomers can behave differently during biological processes, such as plant uptake or microbial degradation; the term 'enantioselective process' is used to describe this phenomenon (Celis et al., 2013).

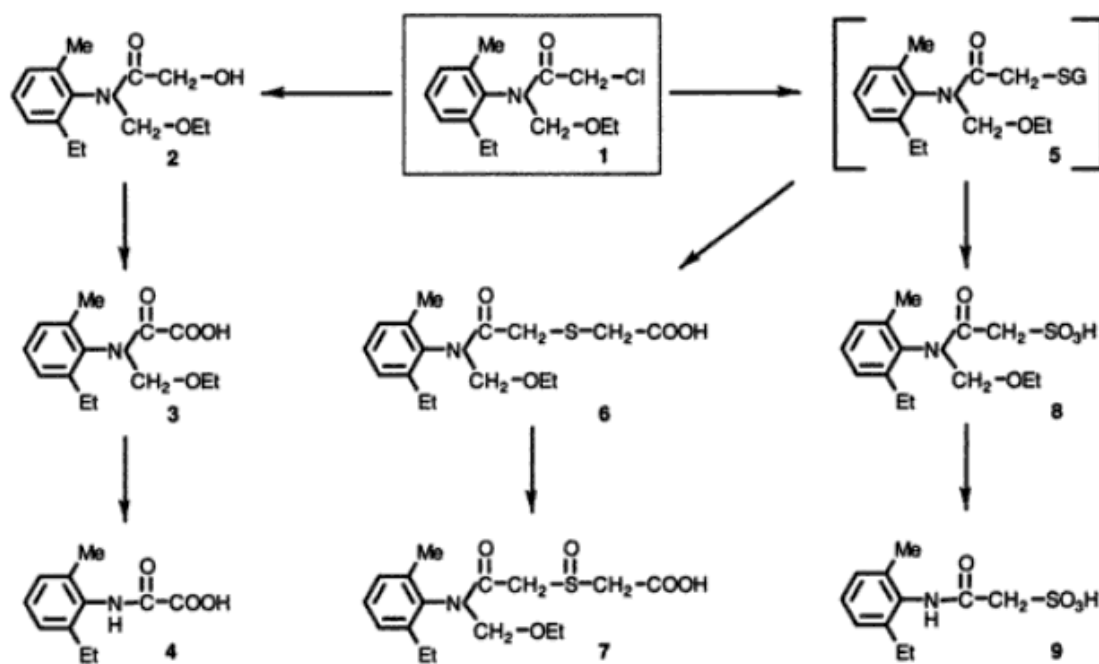


Figure I-5. Degradation pathways of acetochlor in soil (Roberts et al., 1999). Acetochlor was metabolised in soil mainly by two primary pathways. The first pathway involved the hydrolytic/oxidative displacement of chlorine to form the alcohol 2 and the oxidation of the alcohol 2 to oxanilic acid 3. N-dealkylation of 3 yielded oxanilic acid 4. The second pathway involved the displacement of chlorine by glutathione and the further secondary catabolism of the glutathione conjugate 5 to the various sulfanylactonic and sulfonic acid products (6-9)

The half-life time ( $DT_{50}$ ) corresponds to the time required to degrade half of the quantity of a molecule. Pesticide half-life times are widely used to quantify the persistence of a compound in the environment for registration procedures (Farlin et al., 2013). However, classical estimates of pesticide degradation rates determined in the laboratory may not be relevant under the dynamic conditions that exist in the field (Papiernik et al., 2009) and may therefore inaccurately predict pesticide transformation in agro-ecosystems (Gassmann et al., 2014). Thus, approaches capable of measuring the *in situ* extent of degradation at catchment scales must be developed (Turner et al., 2006).

The spatial variability of pesticide deposition during application and processes of degradation and sorption considerably influence pesticide mobilisation and transport via runoff (Barbash, 2014; Doppler et al., 2012; Gascuel-Oudoux et al., 2009).

### 2.2.2 Processes affecting pesticide transport in agro-ecosystems (**A<sub>active</sub>** and **A<sub>connected</sub>**)

Depending on the time that elapses between pesticide application and the next rainfall event, pesticides may be mobilised in the course of a rainfall-runoff event from vegetation or soil surfaces (processes in blue in Figure I-3). Studies of pesticide washoff generally indicate that a large fraction of pesticides deposited on foliage can be mobilised by rain (up to 100% for highly soluble pesticides) (Wauchope et al., 2004).

On soil surfaces, runoff and erosion mobilise pesticides in a thin, near-surface soil layer (McGrath et al., 2008). This soil layer is often called the 'mixing layer' and has been found to be in the millimetre to centimetre range (Ahuja et al., 1981). Erosion may be caused by rainfall or surface runoff and may lead to subsequent transport of sorbed pesticides. Different types of erosion exist, including sheet erosion, rill erosion and gully erosion. Sheet erosion is the uniform removal of soil in thin layers by the forces of raindrops and overland flow. Rill erosion is the removal of soil by concentrated water running through little streams. Gully erosion is an advanced stage of rill erosion (Toy et al., 2002). Pesticide transfer from the soil surface is difficult to predict because various processes occur simultaneously (Shi et al., 2011). These processes include pesticide diffusion induced by the concentration gradient between water runoff and soil water (1 in Figure I-5), ejection of soil water by rainfall (2 in Figure I-5), erosion of contaminated sediment by rainfall and concentrated flow (3 in Figure I-5) and pesticide adsorption-desorption (4 in Figure I-5) (Shi et al., 2011).

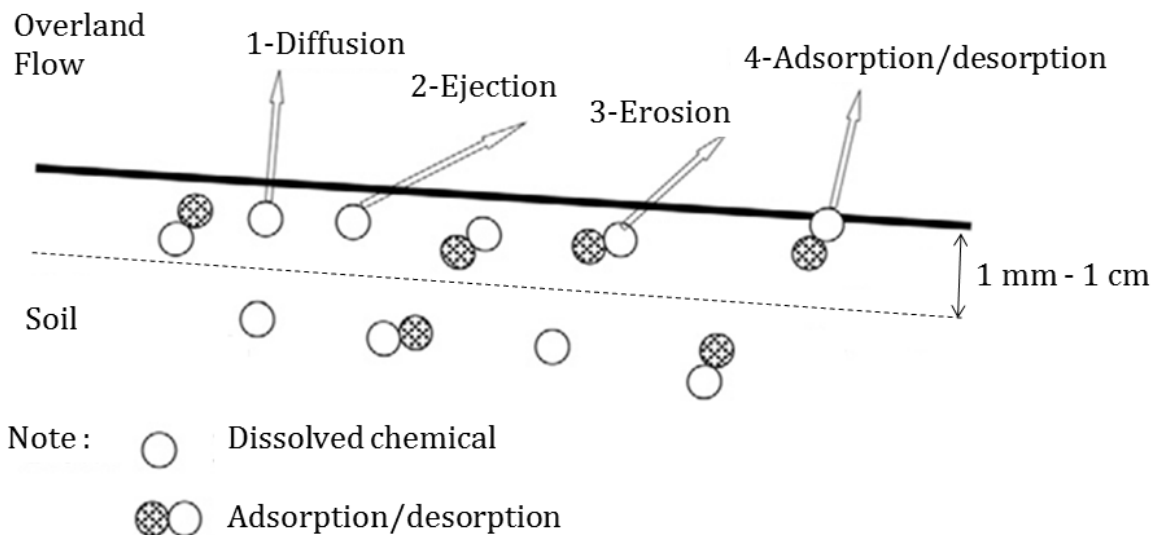


**Figure I-6. Processes for transferring pesticides from the soil surface to runoff water (Shi et al., 2011)**

As previously stated (§2.1), soil surface characteristics and hydrodynamic parameters are essential for triggering runoff, erosion and pesticide transport. Various additional factors affect the mobilisation of pesticides in runoff and erosion, including rainfall intensity, topography, initial water content and pesticide characteristics (Shi et al., 2011). Rainfall variability within a storm event can also have a significant impact on pesticide losses via runoff (McGrath et al., 2008). Pesticide transfer occurs in both soluble and particulate phases and depends primarily on the physical-chemical characteristics of the compound and the nature of the sorbent, e.g., organic matter or mineral surfaces (Rodriguez-Liebana et al., 2011). Erosion processes may therefore contribute to pesticide transport (Bereswill et al., 2013; Taghavi et al., 2011). To date, most studies have focused on dissolved pesticide transport. Hydrophobic pesticides are mainly transported in runoff in association with colloids and dissolved organic carbon (DOC) (Chen et al., 2010; Maillard et al., 2011). Hence, erosion processes and pesticides in particulate phases should be considered when evaluating pesticide transport in agricultural runoff.

### 2.2.3 Relevance of combining emerging analytical tools for assessing pesticide degradation

Approaches capable of measuring *in situ* the extent of pesticide degradation are required for deciphering attenuation processes, such as sorption, dilution or degradation at catchment scales (Turner et al., 2006). Indeed, quantitative chemical analysis of the parent pesticide is not sufficient for distinguishing degradation from sorption and/or dilution. Evidence of *in situ* degradation may be determined via degradation products quantification, enantiomeric analysis or CSIA (Compound Specific Isotope Analysis) methods. These alternative approaches may be combined to gain mechanistic insights into pesticide transformation processes (Milosevic et al., 2013) and can be used to evaluate pesticide transformation under the dynamic conditions that exist in the field.

Degradation product analysis is one of the most used methods for assessing the occurrence of pesticide degradation in the environment. Quantitative chemical analyses of the degradation products are often challenging because they are often unstable compounds (Andreu and Pico, 2004). Furthermore, the degradation products must be known, and standards must be available for developing analytical methods. The absence of one type of degradation-product analysis does not exclude other degradation pathways involving other degradation products.

Chiral pesticide biodegradation may lead to the enrichment of the remaining fraction of non-degraded pesticides in one or another enantiomer. A shift, compared with the initial enantiomeric signature of the commercial product, can indicate preferential degradation of one enantiomer (Celis et al., 2013). Enantiomeric analyses of chiral pesticides have been successfully used to assess pesticide degradation, for instance, for metalaxyl in batch experiments (Celis et al., 2013), phenoxyacid herbicides in a groundwater system (Milosevic et al., 2013), metolachlor in surface water (Buser et al., 2000) or chlordane in soil and vegetation (White et al., 2002). Enantiomeric analyses may fail if both enantiomers are equally degraded by the same enzyme or if enantiomer-preferential enzymes are simultaneously present in the environment.

CSIA analysis, which is based on an approach that is similar to enantiomeric analysis, may provide additional information regarding possible *in-situ* degradation. CSIA measures the isotopic composition, i.e., the ratio between the abundance of the heavy isotope against the light stable isotope of an element like oxygen or carbon in a molecule (Thullner et al., 2012). Compared with the isotopic ratio of the commercial compound, biodegradation may lead to

enrichment in heavy isotopes because molecules with light isotopes tend to degrade more quickly (Elsner, 2010).

So far, degradation product analyses and enantiomer and isotope approaches have not been combined to assess degradation in runoff water in agro-ecosystems. Combining analytical methods can provide advantages that are beyond the reach of any of the methods applied alone. Based on the weaknesses and strengths of each method, combined approaches may complement each other in their assessment of pesticide degradation. Models may then validate mechanistic hypotheses based on field experimentation.

### **2.2.4 Usefulness and complementarity of modelling following a characterisation phase**

A model is “a mathematical description of a simplified conceptual representation of a certain fragment of the real world” (Alvarez-Benedi and Munoz-Carpena, 2004). Because environmental processes are complex and mathematically describing every process is logistically impossible, model conceptualisations are always simplifications. “Essentially, all models are wrong, but some are useful” (Box and Draper, 1987). Once it has been established that a model can reproduce reality with sufficient accuracy, the model may be used to prognosticate the impacts of environmental scenarios under different meteorological or hydrological conditions or agricultural contexts at significantly lower cost and in much less time than experimental field trials require (Alvarez-Benedi and Munoz-Carpena, 2004; Quilbe et al., 2006). Pesticide transport models in agro-ecosystems are therefore crucial to achieving sustainability of current agriculture practices. Predictive models are used to (i) assess the extent of pesticide dispersion, (ii) evaluate possible mitigating management practices and regulatory policies (Payraudeau and Grégoire, 2012) and (iii) prognosticate future potential problems (Alvarez-Benedi and Munoz-Carpena, 2004). Modelling may also confirm or negate a hypothesis regarding physical mechanisms based on a comprehensive field characterisation study (Lutz et al., 2013).

A large number of models describing pesticide transport in agro-ecosystems have been developed over the last 40 years for various scales and contexts and have been already used for intercomparisons and/or in reviews (Borah and Bera, 2003b; Holvoet et al., 2007; Kohne et al., 2009; Payraudeau and Grégoire, 2012; Quilbe et al., 2006). Numerical models, including those that are empirical, stochastic, conceptual and physically based, have been used to describe pesticide transport processes (Payraudeau and Grégoire, 2012). Physically based models can be differentiated based on their ability to decipher the contribution of each physical process and to

estimate pesticide concentrations under different hydrological conditions and with different pesticide characteristics (Berenzen et al., 2005). The existing physically based models designed for predicting pesticide transport in surface water in agro-ecosystems for various spatial and temporal scales are detailed in Table I-1. Obviously, this brief census is not exhaustive and only models for cases in which sufficient information has been obtained were included in this analysis. The 32 selected physically based models for pesticide behaviours in surface water are presented in Figure I-6 according to their spatial and temporal discretisations. Catchment representations, spatial and temporal discretisations and processes are detailed for various existing pesticide-fate models in Table I-1.

### Temporal resolution

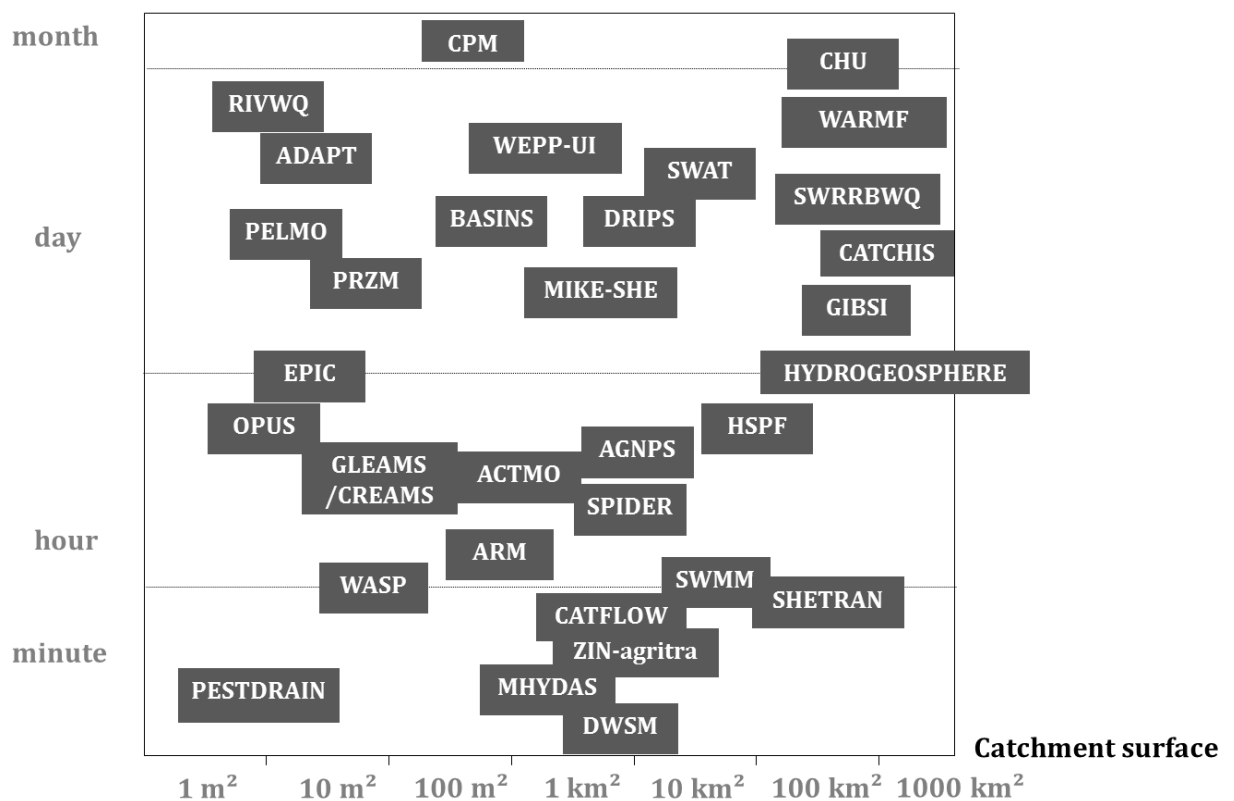


Figure I-7. Existing physically based pesticide transport models according to their spatial and temporal discretisations.

To date, no single pesticide-fate model has proved to be a satisfactory tool for all purposes (Alvarez-Benedi and Munoz-Carpena, 2004). Currently, few models account for the effects of agricultural practices on hydrodynamic parameters and soil surface characteristics (Pare et al., 2011).

Distributed models may consider the variability in contributing areas in catchments and are useful for delineating critical-source areas for pesticide runoff (Frey et al., 2009). Fully distributed models, such as AGNPS (Merritt et al., 2003), describe the landscape on the scale of a grid cell, whereas semi-distributed models define homogeneous elements, such as Hydrological Responses Units (HRUs) for the model SWAT (Boithias et al., 2011) (Table I-1). Fully distributed models may help decipher the contributions of small features, such as roads or buffer strips, in agro-ecosystems.

**Table I-1. Summary of catchment-scale hydrological and pesticide transport models in surface water; “dynamic” may represent different erosion equations for erosion splash, rill erosion and/or transport capacity.**

Model name	References	Time step	Spatial scale	Discretisation	Erosion	Particulate pesticide
ACTMO	(Frere et al., 1975)	hourly	< 100 km <sup>2</sup>	hydrological units	USLE	Yes
ADAPT	(Gowda et al., 2012)	daily	field -100 km <sup>2</sup>	hydrological units	USLE	Yes
(Ann-)AGNPS	(Merritt et al., 2003) (Bingner and Theurer, 2001)	hourly/daily	1- 200 km <sup>2</sup>	square grid cell	RUSLE	Yes
ARM	(Donigian and Crawford, 1976)	hourly/daily	< 5 km <sup>2</sup>	?	dynamic	Yes
BASINS	(Tong and Chen, 2002)	daily	no specific size	hydrological units	dynamic	Yes
CATCHIS/SWATCHCATCH	(Brown et al., 2002)	daily/weekly	> 100 km <sup>2</sup>	subcatchments	No	No
CATFLOW	(Zehe et al., 2001)	< 1 hour	field - 100 km <sup>2</sup>	hillslope elements	dynamic	Yes
CHU model	(Chu and Marino, 2004)	monthly	> 100 km <sup>2</sup>	grid cell	MUSLE	Yes
CPM	(Haith and Loehr, 1979)	monthly	< 100 km <sup>2</sup>	?	USLE	?
DRIPS	(Röpke et al., 2004)	daily	no specific size	grid cell	No	No
DWSM	(Borah et al., 2004)	seconds	no specific size	segments	dynamic	Yes
EPIC-PST	(Sabbagh et al., 1991)	hourly/daily	field - 100 ha	grid cell	MUSLE	?
GIBSI	(Rousseau et al., 2000)	daily	>100 km <sup>2</sup>	hydrological units	RUSLE	Yes
GLEAMS/CREAMS	(Leonard et al., 1991)	hourly/daily	field	grid cell	USLE	No
HSPF	(Borah and Bera, 2003a) (Donigian et al., 1995)	hourly/daily	no specific size	hydrological units	dynamic	Yes
HYDROGEOSPHERE	(Rosenbom et al., 2009)	hourly/daily	> 100 km <sup>2</sup>	grid cell	No	No

Model name	References	Time step	Spatial scale	Discretisation	Erosion	Particulate pesticide
MHYDAS	(Moussa et al., 2002)	seconds	< 100 km <sup>2</sup>	hydrological units	dynamic	Yes
MIKE-SHE	(Fauser et al., 2008)	hourly/daily	< 100 km <sup>2</sup>	square grid cell	dynamic	?
OPUS	(Bogena et al., 2003)	hourly/daily	Field	hillslope elements	MUSLE	No
PELMO	(Huber et al., 2000)	daily	Field	grid cell	No	No
PESTDRAIN	(Branger et al., 2009)	< 1 hour	Field	conceptual	No	No
PRZM	(Centofanti et al., 2008) (Luo and Zhang, 2010)	daily	field/catchment	grid cell	USLE	Yes
RIVWQ	(Karpouzas and Capri, 2006)	daily	field/catchment	grid cell	?	Yes
SHETRAN	(Ewen et al., 2000)	seconds hourly	1 - 2000 km <sup>2</sup>	grid cell	dynamic	Yes
SPIDER	(Renaud et al., 2008)	hourly	0-10 km <sup>2</sup>	stream segment	No	No
SWAT	(Boithias et al., 2011)	daily	30-15000 km <sup>2</sup>	hydrological units	MUSLE	Yes
SWMM	(Park et al., 2008)	< 1 hour	no specific size	subcatchments	?	?
SWRRBWQ	(SWRRBWQ manual, 1993)	daily	> 100 km <sup>2</sup>	subcatchments	MUSLE	?
WARMF	(Dayyani et al., 2010)	daily	> 100 km <sup>2</sup>	compartments	dynamic	?
WASP6/DYNHYD5	(Ekdal et al., 2011)	< 1 hour	river/field	compartments	?	Yes
WEPP-UI	(Singh et al., 2009)	daily	no specific size	hillslope segments	dynamic	Yes
ZIN-AgriTra	(Gassmann et al., 2013)	seconds	Field/catchment	square grid cell	USLE	Yes

In agro-ecosystems, soil surface characteristics and hydrodynamic parameters may change very rapidly due to agricultural practices (§2.1), and rainfall variability within a storm event can have a significant impact on pesticide losses via runoff (§2.2.2). In parallel, a significant short-term pesticide export may occur within one single storm in agricultural catchments (McGrath et al., 2010). Consequently, predicting the generation and dynamics of pesticide transport at the event scale is essential for better understanding fast transport processes, such as contaminated runoff. An event-based model that employs a very small time step ( $\leq 1$  min) and very high resolution rainfall data seems more appropriate when the goal is to better understand the detailed dynamics of pesticide export. In this context, event-based models, such as DWSM, are particularly designed to use fine temporal discretisations (Borah et al., 2004).

In pesticide-fate models, erosion processes are often predicted based on the Universal Soil Loss Equation (USLE) or its revisions, RUSLE and MUSLE (Kinnell, 2010); examples are the cases of ZIN-AgriTra (Gassmann et al., 2013) or CREAMS (Leonard et al., 1991)(Table I-1). Theoretically, USLE was designed to predict long-term (e.g., annual) average soil losses at field scale. Despite numerous revisions to extend these results to the entire catchment at event scale, the USLE equations do not consider runoff explicitly for determining erosion (Kinnell, 2010). Pesticide-fate models rarely integrate erosion processes with dynamic approaches (Table I-1).

Agro-ecosystems provide a foundation for evaluating and understanding the interactions of physical-chemical processes and agricultural practices affecting the transport and fate of pesticides. Combining emerging analytical tools and modelling may be a valuable approach to investigate pesticide transport in agro-ecosystems. Changes in agricultural practices occur locally at farm and agricultural plot levels. In contrast, different measures for water protection are defined on the scale of hydrological areas ( $> 10,000$  km<sup>2</sup>) (Macary et al., 2014). Agricultural regional areas integrate numerous catchments, making difficult a comprehensive understanding of pesticide transport. Among the agro-ecosystems, headwater agricultural catchments (0 - 1 km<sup>2</sup>) represent an intermediary scale between agricultural plot and agricultural regional area, where ongoing processes affecting pesticide transport remain poorly known.

### **3. Relevance of headwater catchments for pesticide transport in surface water**

#### **3.1. Definition and role of headwater catchments in downstream water quality**

Headwater catchments are the initial drainage areas that catch water and direct it into surface water features such as creeks and streams. Headwater streams are often defined as first- and second-order streams according to the Horton-Strahler method (Brutsaert, 2005). In aggregate, headwater streams compose the majority of the total stream length in a river network and often represent small hydrological catchments (0 – 1 km<sup>2</sup>) (Dodds and Oakes, 2008). Because these catchments are not large, headwater streams are easily influenced by small-scale differences in local conditions (Meyer et al., 2007). Headwater streams dominate surface water drainage networks and may have a major impact on downstream water quality (Dodds and Oakes, 2008; Freeman et al., 2007; Salmon-Monviola et al., 2013). This is due to several factors, including (i) the major contribution of headwater streams to the mean water volume and flux in higher-order streams (Alexander et al., 2007), (ii) the greatest capacity of headwater streams for interaction between water and contaminated areas due to their proximity with agricultural land and (iii) the potential for rapid in-stream uptake and retention of pesticides due to riparian vegetation (Dodds and Oakes, 2008). Furthermore, because of their high habitat diversity, headwater streams significantly contribute to the biodiversity of the overall stream system and are essential for the successful dispersal of species among stream networks (Meyer et al., 2007; Rasmussen et al., 2013). Headwater catchments therefore play a dominant role in pesticide transport and the resulting downstream water quality.

Headwater catchments located in agricultural areas are identified as high-risk 'hotspots' of pesticide contamination. For example, small Swiss streams have clearly shown higher pesticide-mixture concentrations (150 compounds) than medium or large rivers and represent more than 70% of Swiss streams (Munz et al., 2012). Reported insecticide concentrations in surface water worldwide have been shown to be negatively correlated with catchment size (Figure I-7) (Schulz, 2004).

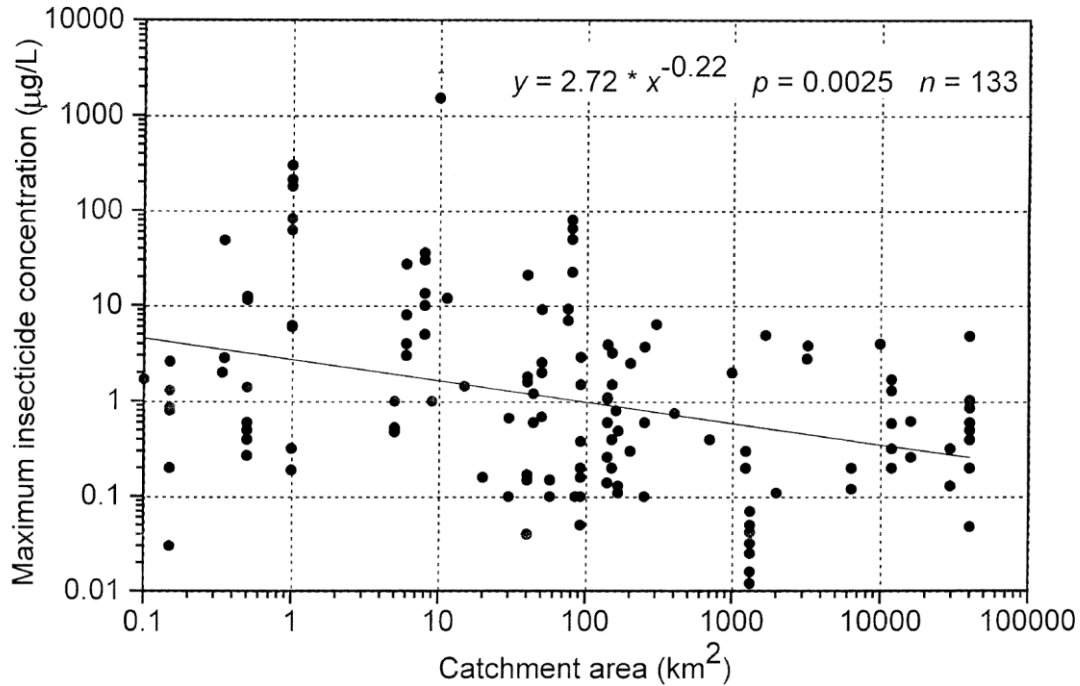


**Figure I-8. Relationship between catchment size and aqueous non-point sources of insecticide contamination detected in samples of surface waters (Schultz, 2004)**

However, due to their small size, hydrological headwater catchments are often not qualified as significant surface water bodies and are generally disregarded and poorly investigated, despite their importance for supporting higher ecological quality in higher order streams (Munz et al., 2012; Rasmussen et al., 2013). For example, implementation of the Water Framework Directive in the European Union encourages member states to obtain “good ecological and chemical status” of surface waters. However, these objectives exclude headwater catchments and only consider larger surface water bodies (Rasmussen et al., 2013). There is, therefore, a lack of knowledge concerning water quality in headwater catchments, which are often less monitored and highly contaminated and may have major impacts on water quality downstream.

### 3.2. Importance of combining plot- and catchment-scale observations

Combining different control points within a study area is useful for the delineation of critical source areas for pesticide runoff (Freitas et al., 2008). Furthermore, considering the complexity of interactions of the processes, several measurement points within a study area are necessary to validate a distributed model (Lee et al., 2012). Pesticide transport is often evaluated on a plot- or catchment-scale (Viglizzo et al., 2011) but has rarely been evaluated with regard to both scales simultaneously. Combining experimental information obtained using different scales within the same catchment is necessary to identify the critical source areas of off-site pesticide transport and to evaluate how pesticide runoff varies for different scales.

### 3.3. Models for predicting pesticide transport in headwater catchments

A previous analysis of existing pesticide-fate models (§2.2.4) emphasized that a fully distributed event-based model that considers erosion processes with a dynamic approach may facilitate our understanding of the generation, dynamics and pathways of pesticide transport in agroecosystems. Based on this analysis, only the following four models have been designed for assessing pesticide transport using very fine temporal resolutions ( $\leq 1$  min) in headwater catchments: CATFLOW (Zehe et al., 2001), ZIN-AgriTra (Gassmann et al., 2013), MHYDAS (Moussa et al., 2002) and DWSM (Borah et al., 2004). None of these models are fully distributed, and use a dynamic approach to evaluate erosion processes (Table I-1).

For all the reasons stated above, there is need for a pesticide transport model that (i) is fully distributed, (ii) is designed for considerations on the agricultural headwater-catchment scale and (iii) the rainfall-runoff event scale, and (iv) is based on a dynamic approach to assess erosion processes to predict pesticide transport in the particulate phase.

The hydrological and erosion model LISEM (Limbourg Soil Erosion Model) (DeRoo et al., 1996) seems to be a good candidate for fulfilling the above four criteria. Admittedly, LISEM does not predict pesticide mobilisation and transport in runoff. However, it is an event-based model that is fully distributed for headwater catchments. Sediment detachment is generated by rainfall splash based on rainfall kinetic energy (Sanchez-Moreno et al., 2012) and/or overland flow. Flow erosion is calculated with a stream-power-based transport capacity (Morgan et al., 1998). LISEM is specifically designed to describe agricultural landscape components containing crusted and compacted zones and soil surface structures. Furthermore, LISEM was validated for various agricultural contexts and hydrological conditions (Baartman et al, 2012; Hessel, 2006; Hessel et al, 2007; Sheikh et al, 2010).

# Chapter II. Research focus and objectives

## 1. Research focus

Several scientific gaps and challenges have been identified in the previous chapter, and these must still be addressed if we are to understand, characterise and predict pesticide transport into surface water in headwater catchments. This PhD thesis attempts to provide evidence that partially addresses these remaining issues.

Vineyard and arable crops epitomise a situation where soil and water sustainability is highly threatened. Headwater catchments located in those areas are identified as high-risk 'hotspots' of pesticide contamination. From a management perspective, the headwater-catchment scale is suitable for more readily implementing remediation actions by local groups. In addition, limiting threats as closely as possible to their source may be more efficient than the costly remediation of symptoms downstream. From a scientific viewpoint, the ongoing processes affecting pesticide transport remain poorly understood with regard to the intermediate scale between agricultural plot and regional-scale catchment. Thus, understanding pesticide transport and attenuation in headwater catchments implies the combination of different approaches (characterisation and modelling), analytical methods (degradation products and enantiomeric analyses) and scales (plot and catchment). Such a comprehensive approach may help us understand the processes of pesticide transport and attenuation in headwater catchments.

During the course of this study, the following several questions have arisen, highlighting major gaps in our current ability to understand, model and predict pesticide transport and attenuation in agricultural headwater catchments:

- What are the spatial patterns of fungicide deposition following a vineyard application, and how does the spatial variability of fungicide deposition influence off-site movement in runoff?

- How are pesticides distributed between the dissolved and particulate phases in runoff water in relation to each compound's characteristics and the hydrological and hydrochemical conditions?
- What is the potential contribution of analytical approaches, such as enantiomer analysis of chiral pesticides, to identifying, characterising and quantifying the *in situ* degradation of pesticides on the headwater-catchment scale?
- Finally, how is it possible to predict the impact of erosion processes and pesticide partitioning between the dissolved and particulate phases on pesticide transport into surface water?

## 2. Thesis objectives

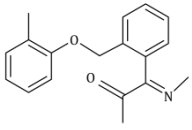
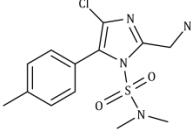
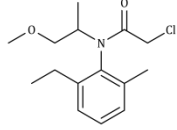
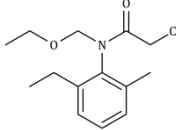
The overall aim of this thesis is to evaluate and predict pesticide transport in runoff water in the dissolved and particulate phases within headwater agricultural catchments. Two contrasting agricultural catchments, one in a vineyard and one in an arable crop, were investigated on two elemental scales, i.e., agricultural-plot and headwater-catchment, to meet the following objectives:

- (i) Characterise the spatial variability of fungicide deposition during application in the vineyard catchment and its impact on subsequent runoff.
- (ii) Evaluate and compare pesticide partitioning of four model compounds between the dissolved and particulate phases in runoff in both model agricultural catchments.
- (iii) Evaluate the *in-situ* degradation of a major pre-emergence herbicide, *S*-metolachlor, in the arable crop catchment by combining analytical approaches.
- (iv) Develop and validate a physically based model for predicting pesticide mobilisation in runoff water that is applicable to both agricultural catchments.

The PhD approach is to combine characterisation and modelling for assessing pesticide transport. Two 50-ha catchments representative of agricultural headwater catchments in temperate areas have been investigated in terms of runoff, erosion, hydrochemistry and pesticide transport. The catchments differ in terms of crops (grape and corn), topography, soils,

hydrological processes and applied pesticides (Table II-2). Both catchments are located in Alsace in the east of France (Figure II-1). Four different model pesticides were selected owing to their wide usage, their toxicity and their large range of physical-chemical properties. Kresoxim-methyl (KM) and cyazofamid (CY) are both fungicides applied in vineyards, and acetochlor and S-metolachlor are both herbicides that are widely used on corn and sugar beet. Their main physical-chemical characteristics are presented in Table II-1. In parallel, a mathematical formalism has been developed to predict dissolved pesticide mobilisation and transport in runoff, which is applicable to both agricultural catchments. This formalism has then been integrated into LISEM (Limbourg Soil Erosion Model) (DeRoo et al., 1996). Extension of the mathematical formalism for assessing pesticide transport in the particulate phase is further discussed below and will be the topic of future investigations.

**Table II-1. Physical-chemical properties of the four study compounds (PPDB, 2009).**

Pesticides groups	Fungicides		Herbicides	
Active substance	Kresoxim - methyl	Cyazofamid	S-metolachlor	Acetochlor
Family	Strobilurin	Cyanoimidazole	Chloroacetamides	Chloroacetamides
Chemical formula	C <sub>18</sub> H <sub>19</sub> NO <sub>4</sub>	C <sub>13</sub> H <sub>13</sub> ClN <sub>4</sub> O <sub>2</sub> S	C <sub>15</sub> H <sub>22</sub> ClNO <sub>2</sub>	C <sub>14</sub> H <sub>20</sub> ClNO <sub>2</sub>
Chemical structure				
Molecular mass [g mol <sup>-1</sup> ]	313.4	324.8	283.8	269.8
Water solubility [g L <sup>-1</sup> ]	2	0.11	480	282
Log K <sub>ow</sub> [-]	3.4	3.2	3.05	4.14
Log K <sub>oc</sub> [-]	2.5 <sup>a</sup>	2.8 – 3.2 <sup>b</sup>	1.8 – 2.6 <sup>c</sup>	2.2
DT50 soil [days]	16	10	15	14
DT50 Hydrolysis in water (20°C, pH 7) [days]	35	25	stable	Stable
Aquatic invertebrates 48 h EC50 [mg L <sup>-1</sup> ]	0.19	0.19	26	8.6

<sup>a</sup>(Fenoll et al., 2010);<sup>b</sup>(<http://toxnet.nlm.nih.gov/>); <sup>c</sup>(Alletto et al., 2013)

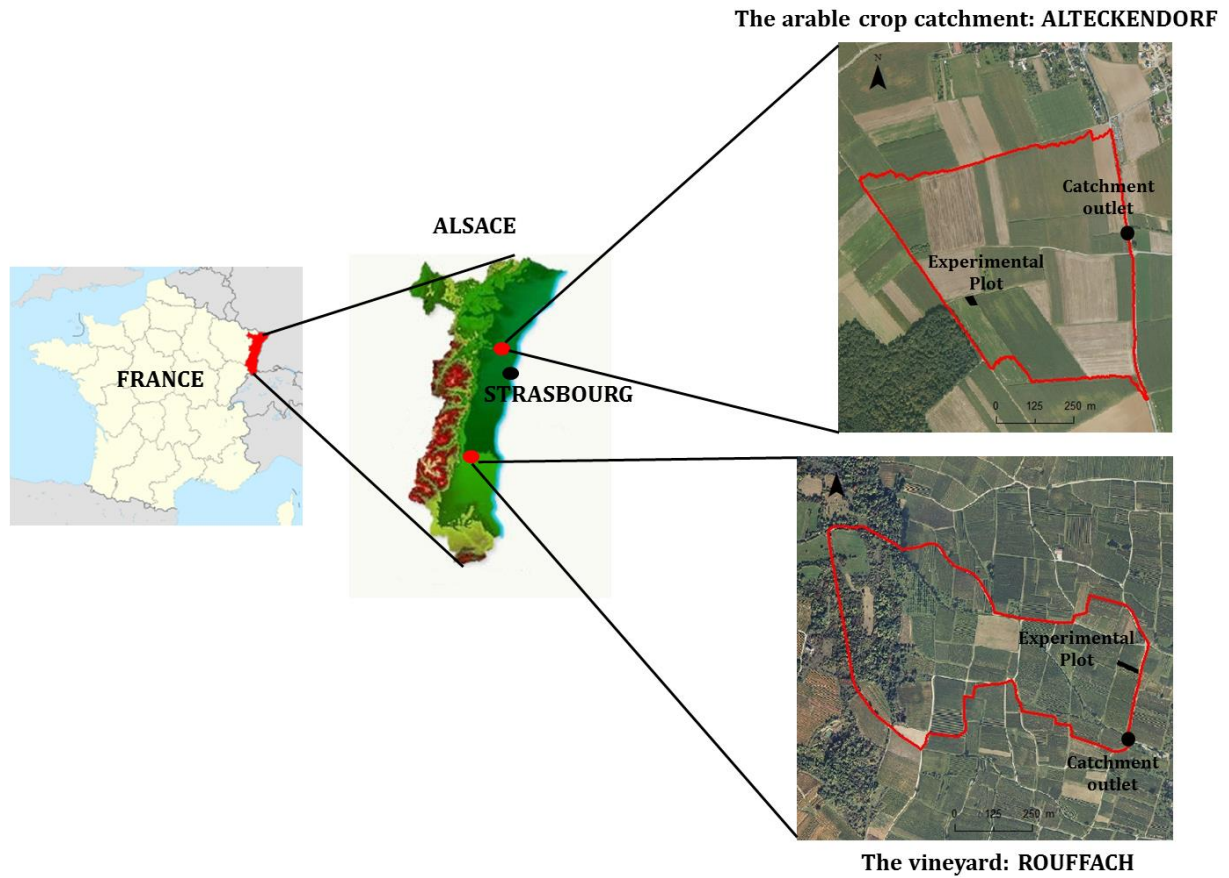


Figure II-1. Locations and schemes of the study catchments (Alsace, France)

Table II-2. Main characteristics of both study catchments (Alsace, France)

	ROUFFACH	ALTECKENDORF
<b>Catchment area [ha]</b>	42.7	47
<b>Elevation [m]</b>	230 – 379	190 - 230
<b>Slope [% ]</b>	15	7
<b>Crops</b>	Vine	Corn, sugar-beet, wheat
<b>Crops ratio [%]</b>	59	88
<b>Studied plot area [m<sup>2</sup>]</b>	880	77.2
<b>Annual precipitation [mm]</b>	563 ± 174	704 ± 151

### 3. Thesis layout

The dissertation outline is described below and in the following diagram outline (Figure II-2). **Chapter 3** investigates fungicide drift and related runoff in vineyards and is divided into two sections. Evaluation of drift and spatial variability in the deposition of two fungicides (KM and CY) as formulated products were first investigated under foliar application conditions in the vineyard catchment (Rouffach, Alsace, France) (Section 1; published in *Science of the Total Environment*, 2013). Following deposition of the fungicides, their transport in runoff water and their partitioning within the dissolved and particulate phases were jointly evaluated for the vineyard catchment and a representative plot during wine-growing season (i.e., May to August 2011) (Section 2; published in *Environmental Science and Pollution Research*, 2013).

To better understand pesticide transport *via* erosion, **Chapter 4** explores pesticide transport in a corn catchment, where erosion may occur much more often compared with the vineyard catchment. The transport of two herbicides, i.e., metolachlor and acetochlor, was evaluated in both the dissolved and particulate phases. An integrative approach combining analyses of the parent compound, degradation products and enantiomers was used to investigate the *in-situ* transformation of *S*-metolachlor and acetochlor in water, suspended solids and soil (publication in prep).

Mobilisation and transport of pesticides observed in one agricultural context during one season could only be confirmed and further extended with the help of modelling. **Chapter 5** focuses on pesticide transport modelling in runoff from headwater catchments and is divided into two sections. The first step for correctly predicting pesticide transport into surface water is to accurately predict runoff and erosion dynamics and pathways. A new approach was developed for choosing a suitable and meaningful set of input parameters for calibrating an event-based model to predict runoff and erosion in the arable crop catchment during a crop-growing season (Section 1; publication in prep). A mathematical formalism was then developed and integrated in LISEM to predict dissolved pesticide mobilisation and transport in runoff. This formalism is applicable to both agricultural catchments (Section 2).

**The final chapter** summarises the main findings and conclusions derived from this research. It concludes by suggesting future research directions to investigate pesticide contamination of surface water in headwater agricultural catchments.

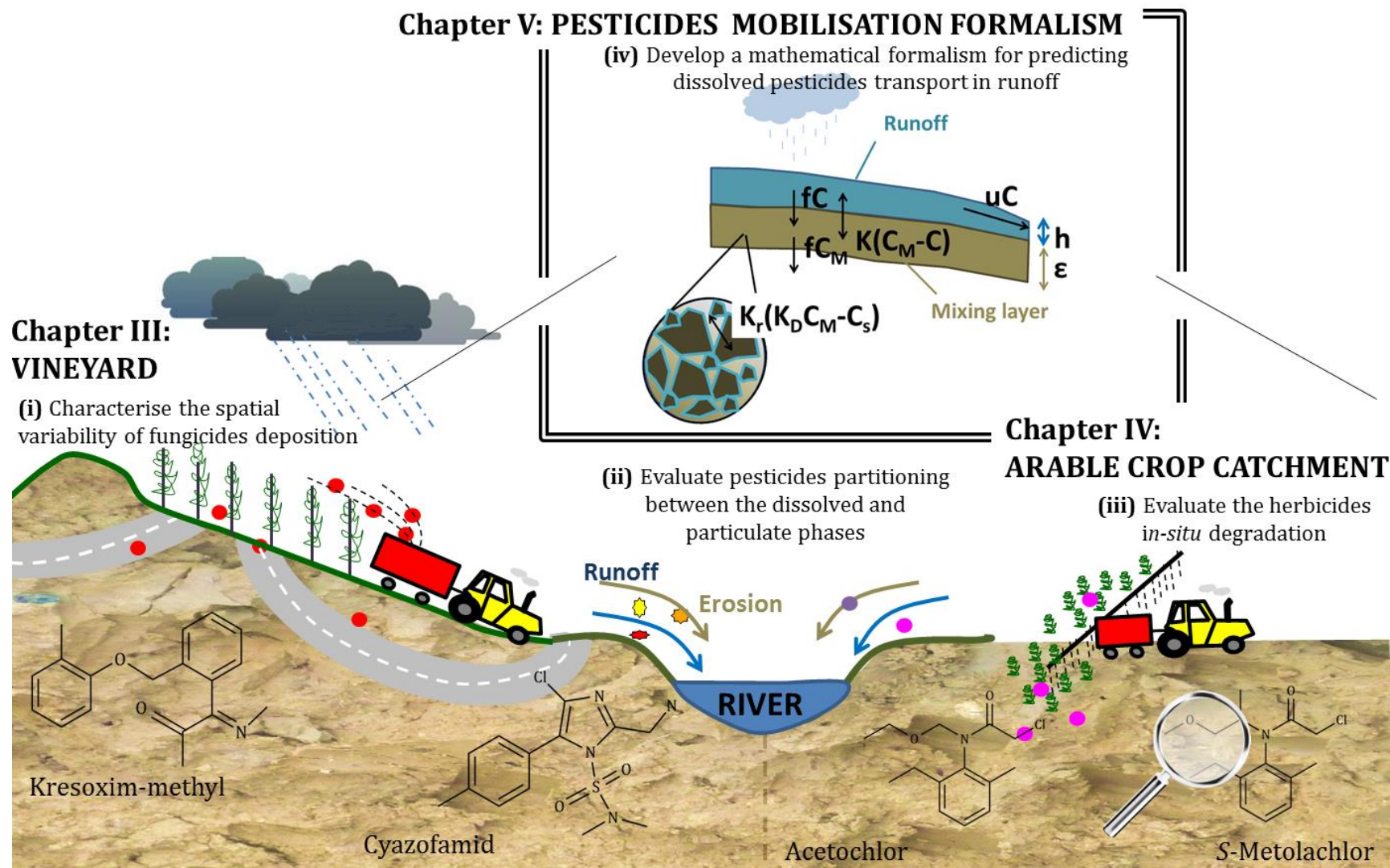


Figure II-2. Graphical outline of the PhD thesis

## 4. References

- Ahuja, L.R., Sharpley, A.N., Yamamoto, M., Menzel, R.G., 1981. The Depth of Rainfall-Runoff-Soil Interaction as Determined by P-32. *Water Resources Research*. 17, 969-974.
- Alaoui, A., Lipiec, J., Gerke, H.H., 2011. A review of the changes in the soil pore system due to soil deformation: A hydrodynamic perspective. *Soil & Tillage Research*. 115, 1-15.
- Alavanja, M.C.R., Bonner, M.R., 2012. Occupational Pesticide Exposures and Cancer Risk: A Review. *Journal of Toxicology and Environmental Health-Part B-Critical Reviews*. 15, 238-263.
- Alexander, R.B., Boyer, E.W., Smith, R.A., Schwarz, G.E., Moore, R.B., 2007. The role of headwater streams in downstream water quality. *Journal of the American Water Resources Association*. 43, 41-59.
- Alletto, L., Benoit, P., Bolognesi, B., Couffignal, M., Bergheaud, V., Dumeny, V., Longueval, C., Barriuso, E., 2013. Sorption and mineralisation of S-metolachlor in soils from fields cultivated with different conservation tillage systems. *Soil & Tillage Research*. 128, 97-103.
- Alvarez-Benedi, J., Munoz-Carpena, R., 2004. *Soil-Water-Solute Process Characterization: An Integrated Approach*, Vol., Taylor & Francis.
- Alves, P.R.L., Cardoso, E.J.B.N., Martines, A.M., Sousa, J.P., Pasini, A., 2013. Earthworm ecotoxicological assessments of pesticides used to treat seeds under tropical conditions. *Chemosphere*. 90, 2674-2682.
- Andresen, L.C., Nothlev, J., Kristensen, K., Navntoft, S., Johnsen, I., 2012. The wild flora biodiversity in pesticide free bufferzones along old hedgerows. *Journal of Environmental Biology*. 33, 565-572.
- Andreu, V., Pico, Y., 2004. Determination of pesticides and their degradation products in soil: critical review and comparison of methods. *Trac-Trends in Analytical Chemistry*. 23, 772-789.
- Arnold, S.M., Clark, K.E., Staples, C.A., Klecka, G.M., Dimond, S.S., Caspers, N., Hentges, S.G., 2013. Relevance of drinking water as a source of human exposure to bisphenol A. *Journal of Exposure Science and Environmental Epidemiology*. 23, 137-144.
- Arvidsson, T., Bergstrom, L., Kreuger, J., 2011. Spray drift as influenced by meteorological and technical factors. *Pest Management Science*. 67, 586-598.
- Aufauvre, J., Biron, D.G., Vidau, C., Fontbonne, R., Roudel, M., Diogon, M., Vignes, B., Belzunces, L.P., Delbac, F., Blot, N., 2012. Parasite-insecticide interactions: a case study of *Nosema ceranae* and fipronil synergy on honeybee. *Scientific Reports*. 2.
- Barbash, J.E., 2014. The Geochemistry of Pesticides. In: *Treatise on Geochemistry (Second Edition)*. Vol., H.D. Holland, K.K. Turekian, eds. Elsevier, Oxford, pp. 535-572.
- Baartman, J.E.M., Jetten, V.G., Ritsema, C.J., de Vente, J., 2012. Exploring effects of rainfall intensity and duration on soil erosion at the catchment scale using openLISEM: Prado catchment, SE Spain. *Hydrological Processes*. 26, 1034-1049.
- Bassil, K.L., Vakil, C., Sanborn, M., Cole, D.C., Kaur, J.S., Kerr, K.J., 2007. Cancer health effects of pesticides - Systematic review. *Canadian Family Physician*. 53, 1705-1711.
- Bedos, C., Cellier, P., Calvet, R., Barriuso, E., Gabrielle, B., 2002. Mass transfer of pesticides into the atmosphere by volatilization from soils and plants: overview. *Agronomie*. 22, 21-33.

- Berenzen, N., Lentzen-Godding, A., Probst, M., Schulz, H., Schulz, R., Liess, M., 2005. A comparison of predicted and measured levels of runoff-related pesticide concentrations in small lowland streams on a landscape level. *Chemosphere*. 58, 683-91.
- Bereswill, R., Golla, B., Streloke, M., Schulz, R., 2013. Entry and toxicity of organic pesticides and copper in vineyard streams: Erosion rills jeopardise the efficiency of riparian buffer strips (vol 146, pg 81, 2012). *Agriculture Ecosystems & Environment*. 172, 49-50.
- Bingner, R.L., Theurer, F.D., 2001. Topographic factors for RUSLE in the continuous-simulation watershed model for predicting agricultural, non-point source pollutants (AnnAGNPS). *Soil Erosion Research for the 21st Century, Proceedings*. 619-622.
- Blann, K.L., Anderson, J.L., Sands, G.R., Vondracek, B., 2009. Effects of Agricultural Drainage on Aquatic Ecosystems: A Review. *Critical Reviews in Environmental Science and Technology*. 39, 909-1001.
- Bogena, H., Diekkruger, B., Klingel, K., Jantos, K., Thein, J., 2003. Analysing and modelling solute and sediment transport in the catchment of the Wahnbach River. *Physics and Chemistry of the Earth*. 28, 227-237.
- Boithias, L., Sauvage, S., Taghavi, L., Merlina, G., Probst, J.L., Perez, J.M.S., 2011. Occurrence of metolachlor and trifluralin losses in the Save river agricultural catchment during floods. *Journal of Hazardous Materials*. 196, 210-219.
- Borah, D.K., Bera, M., 2003a. Watershed scale hydrologic and nonpoint source pollution models for long-term continuous and storm event simulations. *Total Maximum Daily Load (Tmdl): Environmental Regulations Ii, Proceedings*. 161-167.
- Borah, D.K., Bera, M., 2003b. Watershed-scale hydrologic and nonpoint-source pollution models: Review of mathematical bases. *Transactions of the Asae*. 46, 1553-1566.
- Borah, D.K., Bera, M., Xia, R., 2004. Storm event flow and sediment simulations in agricultural watersheds using DWSM. *Transactions of the Asae*. 47, 1539-1559.
- Botta, F., Fauchon, N., Blanchoud, H., Chevreuil, M., Guery, B., 2012. Phyt'Eaux Cites: Application and validation of a programme to reduce surface water contamination with urban pesticides. *Chemosphere*. 86, 166-176.
- Box, G.E.P., Draper, N.R., 1987. *Empirical model-building and response surfaces*, Vol., Wiley.
- Branger, F., Tournebize, J., Carlier, N., Kao, C., Braud, I., Vauclin, M., 2009. A simplified modelling approach for pesticide transport in a tile-drained field: The PESTDRAIN model. *Agricultural Water Management*. 96, 415-428.
- Brown, C.D., Bellamy, P.H., Dubus, I.G., 2002. Prediction of pesticide concentrations found in rivers in the UK. *Pest Management Science*. 58, 363-373.
- Brutsaert, W., 2005. *Hydrology: An Introduction*, Vol., Cambridge University Press.
- Bunemann, E.K., Schwenke, G.D., Van Zwieten, L., 2006. Impact of agricultural inputs on soil organisms - a review. *Australian Journal of Soil Research*. 44, 379-406.
- Buser, H.R., Poiger, T., Muller, M.D., 2000. Changed enantiomer composition of metolachlor in surface water following the introduction of the enantiomerically enriched product to the market. *Environmental Science & Technology*. 34, 2690-2696.

- Calvet, R., 2005. Les pesticides dans le sol: conséquences agronomiques et environnementales, Vol., Editions France Agricole.
- Celis, R., Gamiz, B., Adelino, M.A., Hermosin, M.C., Cornejo, J., 2013. Environmental behavior of the enantiomers of the chiral fungicide metalaxyl in Mediterranean agricultural soils. *Science of The Total Environment*. 444, 288-297.
- Centofanti, T., Hollis, J.M., Blenkinsop, S., Fowler, H.J., Truckell, I., Dubus, I.G., Reichenberyer, S., 2008. Development of agro-environmental scenarios to support pesticide risk assessment in Europe. *Science of The Total Environment*. 407, 574-588.
- Chen, G.A., Lin, C., Chen, L.A., Yang, H., 2010. Effect of size-fractionation dissolved organic matter on the mobility of prometryne in soil. *Chemosphere*. 79, 1046-1055.
- Chu, X.F., Marino, M.A., 2004. Semidiscrete pesticide transport modeling and application. *Journal of Hydrology*. 285, 19-40.
- Coupe, R.H., Manning, M.A., Foreman, W.T., Goolsby, D.A., Majewski, M.S., 2000. Occurrence of pesticides in rain and air in urban and agricultural areas of Mississippi, April-September 1995. *Science of The Total Environment*. 248, 227-240.
- Dayyani, S., Prasher, S.O., Madani, A., Madramootoo, C.A., 2010. Development of DRAIN-WARMF model to simulate flow and nitrogen transport in a tile-drained agricultural watershed in Eastern Canada. *Agricultural Water Management*. 98, 55-68.
- DeRoo, A.P.J., Wesseling, C.G., Ritsema, C.J., 1996. LISEM: A single-event physically based hydrological and soil erosion model for drainage basins .1. Theory, input and output. *Hydrological Processes*. 10, 1107-1117.
- Dodds, W.K., Oakes, R.M., 2008. Headwater influences on downstream water quality. *Environmental Management*. 41, 367-377.
- Donigian, A., Crawford, N., 1976. Modelling pesticides and nutrients on agricultural lands. U.S. Environmental Protection Agency, EPA-600/2-76-043, Athens, Ga.
- Donigian, A., Bicknell, B., Imhoff, J., 1995. Hydrological simulation program – Fortran (HSPF). Computer models of watershed hydrology. Water Resources Publications, Highlands Ranch, Colo., 396-442.
- Doppler, T., Camenzuli, L., Hirzel, G., Krauss, M., Luck, A., Stamm, C., 2012. Spatial variability of herbicide mobilisation and transport at catchment scale: insights from a field experiment. *Hydrology and Earth System Sciences*. 16, 1947-1967.
- Drinkwater, L.E., Snapp, S.S., 2007. Nutrients in agroecosystems: Rethinking the management paradigm. *Advances in Agronomy*, Vol 92. 92, 163-186.
- Dunne, T., Black, R.D., 1970. Partial Area Contributions to Storm Runoff in a Small New England Watershed. *Water Resources Research*. 6, 1296-1311.
- Durán-Zuazo, V.H., Francia-Martínez, J.R., García-Tejero, I., Tavira, S.C., 2013. Implications of land-cover types for soil erosion on semiarid mountain slopes: Towards sustainable land use in problematic landscapes. *Acta Ecologica Sinica*. 33, 272-281.
- Ekdal, A., Gurel, M., Guzel, C., Erturk, A., Tanik, A., Gonenc, I.E., 2011. Application of WASP and SWAT models for a Mediterranean Coastal Lagoon with Limited Seawater Exchange. *Journal of Coastal Research*. 1023-1027.

- Elsner, M., 2010. Stable isotope fractionation to investigate natural transformation mechanisms of organic contaminants: principles, prospects and limitations. *Journal of Environmental Monitoring*. 12, 2005-2031.
- EPA, 2011. Pesticide Industry Sales and Usage: 2006 and 2007 Market Estimates. US Environmental Protection Agency, Washington (DC).
- Eurostat, 2007. The use of plant protection products in the European Union: data 1992–2003. Statistical book. European Communities, Luxembourg.
- Ewen, J., Parkin, G., O'Connell, P.E., 2000. Shetran: Distributed River Basin Flow and Transport Modeling System. *Journal of Hydrologic Engineering*. 5, 250-258.
- Fantke, P., Wieland, P., Wannaz, C., Friedrich, R., Jolliet, O., 2013. Dynamics of pesticide uptake into plants: From system functioning to parsimonious modeling. *Environmental Modelling & Software*. 40, 316-324.
- FAO, 2011. Food and agriculture organization of the united nations. <http://faostat.fao.org>.
- Farlin, J., Galle, T., Bayerle, M., Pittois, D., Braun, C., El Khabbaz, H., Lallement, C., Leopold, U., Vanderborght, J., Weihermueller, L., 2013. Using the long-term memory effect of pesticide and metabolite soil residues to estimate field degradation half-life and test leaching predictions. *Geoderma*. 207, 15-24.
- Fausser, P., Thomsen, M., Sorensen, P.B., Petersen, S., 2008. Predicted concentrations for pesticides in drainage dominated catchments. *Water Air and Soil Pollution*. 187, 149-156.
- Fenner, K., Canonica, S., Wackett, L.P., Elsner, M., 2013. Evaluating Pesticide Degradation in the Environment: Blind Spots and Emerging Opportunities. *Science*. 341, 752-758.
- Fenoll, J., Ruiz, E., Flores, P., Hellin, P., Navarro, S., 2010. Leaching potential of several insecticides and fungicides through disturbed clay-loam soil columns. *International Journal of Environmental Analytical Chemistry*. 90, 276-285.
- Fitzmaurice, A.G., Rhodes, S.L., Lulla, A., Murphy, N.P., Lam, H.A., O'Donnell, K.C., Barnhill, L., Casida, J.E., Cockburn, M., Sagasti, A., Stahl, M.C., Maidment, N.T., Ritz, B., Bronstein, J.M., 2013. Aldehyde dehydrogenase inhibition as a pathogenic mechanism in Parkinson disease. *Proceedings of the National Academy of Sciences of the United States of America*. 110, 636-641.
- Freeman, M.C., Pringle, C.M., Jackson, C.R., 2007. Hydrologic connectivity and the contribution of stream headwaters to ecological integrity at regional scales. *Journal of the American Water Resources Association*. 43, 5-14.
- Freitas, L.G., Singer, H., Muller, S.R., Schwarzenbach, R.P., Stamm, C., 2008. Source area effects on herbicide losses to surface waters - A case study in the Swiss Plateau. *Agriculture Ecosystems & Environment*. 128, 177-184.
- Frere, M.H., Onstad, C.A., Holtan, H.N., 1975. ACTMO, an agricultural chemical transport model. U.S. Dept. of Agr., Agr. Res. Ser. ARS-H-3. U.S. Govt Printing Oft., Washington, D.C. . 54 pp.
- Frey, M.P., Schneider, M.K., Dietzel, A., Reichert, P., Stamm, C., 2009. Predicting critical source areas for diffuse herbicide losses to surface waters: Role of connectivity and boundary conditions. *Journal of Hydrology*. 365, 23-36.

- Gascuel-Oudou, C., Aurousseau, P., Cordier, M.O., Durand, P., Garcia, F., Masson, V., Salmon-Monviola, J., Tortrat, F., Trepos, R., 2009. A decision-oriented model to evaluate the effect of land use and agricultural management on herbicide contamination in stream water. *Environmental Modelling & Software*. 24, 1433-1446.
- Gassmann, M., Stamm, C., Olsson, O., Lange, J., Kümmerer, K., Weiler, M., 2013. Model-based estimation of pesticides and transformation products and their export pathways in a headwater catchment. *Hydrology and Earth System Science*. 17, 5213-5228.
- Gassmann, M., Khodorkovsky, M., Friedler, E., Dubowski, Y., Olsson, O., 2014. Uncertainty in the river export modelling of pesticides and transformation products. *Environmental Modelling & Software*. 51, 35-44.
- Gevao, B., Semple, K.T., Jones, K.C., 2000. Bound pesticide residues in soils: a review. *Environmental Pollution*. 108, 3-14.
- Gliessman, S.R., 2007. *Agroecology: The Ecology of Sustainable Food Systems*, Vol., CRC Press.
- Gómez, J.A., Llewellyn, C., Basch, G., Sutton, P.B., Dyson, J.S., Jones, C.A., 2011. The effects of cover crops and conventional tillage on soil and runoff loss in vineyards and olive groves in several Mediterranean countries. *Soil Use and Management*. 27, 502-514.
- Gonzalez-Rodriguez, R.M., Cancho-Grande, B., Simal-Gandara, J., 2011. Decay of fungicide residues during vinification of white grapes harvested after the application of some new active substances against downy mildew. *Food Chemistry*. 125, 549-560.
- Gowda, P.H., Mulla, D.J., Desmond, E.D., Ward, A.D., Moriasi, D.N., 2012. Adapt: Model Use, Calibration, and Validation. *Transactions of the Asabe*. 55, 1345-1352.
- Gregorio, E., Rosell-Polo, J.R., Sanz, R., Rocadenbosch, F., Solanelles, F., Garcerá, C., Chueca, P., Arnó, J., del Moral, I., Masip, J., Camp, F., Viana, R., Escolà, A., Gràcia, F., Planas, S., Moltó, E., 2014. LIDAR as an alternative to passive collectors to measure pesticide spray drift. *Atmospheric Environment*. 82, 83-93.
- Haith, D., Loehr, R., 1979. Effectiveness of soil and water conservation practices for pollution control. U.S. Environmental Protection Agency, EPA-600/3-82-024, Athens, Ga.
- Hessel, R., van den Bosch, R., Vigiak, O., 2006. Evaluation of the LISEM soil erosion model in two catchments in the East African Highlands. *Earth Surface Processes and Landforms*. 31, 469-486.
- Hessel, R., Jetten, V., 2007. Suitability of transport equations in modelling soil erosion for a small Loess Plateau catchment. *Engineering Geology*. 91, 56-71.
- Holvoet, K.M.A., Seuntjens, P., Vanrolleghem, P.A., 2007. Monitoring and modeling pesticide fate in surface waters at the catchment scale. *Ecological Modelling*. 209, 53-64.
- Huber, A., Bach, M., Frede, H.G., 2000. Pollution of surface waters with pesticides in Germany: modeling non-point source inputs. *Agriculture Ecosystems & Environment*. 80, 191-204.
- Imfeld, G., Vuilleumier, S., 2012. Measuring the effects of pesticides on bacterial communities in soil: A critical review. *European Journal of Soil Biology*. 49, 22-30.
- Jacobsen, C.S., Hjelmsø, M.H., 2014. Agricultural soils, pesticides and microbial diversity. *Current Opinion in Biotechnology*. 27, 15-20.

- Juraske, R., Castells, F., Vijay, A., Munoz, P., Anton, A., 2009. Uptake and persistence of pesticides in plants: Measurements and model estimates for imidacloprid after foliar and soil application. *Journal of Hazardous Materials*. 165, 683-689.
- Kabler, A.K., Chen, S.M., 2006. Determination of the 1'S and 1'R diastereomers of metolachlor and S-metolachlor in water by chiral liquid chromatography - Mass spectrometry/mass spectrometry (LC/MS/MS). *Journal of Agricultural and Food Chemistry*. 54, 6153-6158.
- Kah, M., Beulke, S., Tiede, K., Hofmann, T., 2013. Nanopesticides: State of Knowledge, Environmental Fate, and Exposure Modeling. *Critical Reviews in Environmental Science and Technology*. 43, 1823-1867.
- Karpouzas, D.G., Capri, E., 2006. Risk analysis of pesticides applied to rice paddies using RICEWQ 1.6.2v and RIVWQ 2.02. *Paddy and Water Environment*. 4, 29-38.
- Kinnell, P.I.A., 2010. Event soil loss, runoff and the Universal Soil Loss Equation family of models: A review. *Journal of Hydrology*. 385, 384-397.
- Kohler, H.R., Triebkorn, R., 2013. Wildlife Ecotoxicology of Pesticides: Can We Track Effects to the Population Level and Beyond? *Science*. 341, 759-765.
- Kohne, J.M., Kohne, S., Simunek, J., 2009. A review of model applications for structured soils: b) Pesticide transport. *Journal of Contaminant Hydrology*. 104, 36-60.
- Kümmerer, K., 2010. Emerging contaminants in waters. *Hydrologie und Wasserbewirtschaftung*. 54, 349-359.
- Kurt-Karakus, P.B., Bidleman, T.F., Muir, D.C.G., Struger, J., Sverko, E., Cagampan, S.J., Small, J.M., Jantunen, L.M., 2010. Comparison of concentrations and stereoisomer ratios of mecoprop, dichlorprop and metolachlor in Ontario streams, 2006-2007 vs. 2003-2004. *Environmental Pollution*. 158, 1842-1849.
- la Farre, M., Perez, S., Kantiani, L., Barcelo, D., 2008. Fate and toxicity of emerging pollutants, their metabolites and transformation products in the aquatic environment. *Trac-Trends in Analytical Chemistry*. 27, 991-1007.
- Lazzaro, L., Otto, S., Zanin, G., 2008. Role of hedgerows in intercepting spray drift: Evaluation and modelling of the effects. *Agriculture Ecosystems & Environment*. 123, 317-327.
- Lee, G., Tachikawa, Y., Sayama, T., Takara, K., 2012. Catchment responses to plausible parameters and input data under equifinality in distributed rainfall-runoff modeling. *Hydrological Processes*. 26, 893-906.
- Leonard, R.A., Knisel, W.G., Truman, C.C., Davis, F.M., 1991. The Gleams Model-a Computer Tool for Evaluating Agrochemical Fate. *Abstracts of Papers of the American Chemical Society*. 201, 93-Agro.
- Lipiec, J., Hatano, R., 2003. Quantification of compaction effects on soil physical properties and crop growth. *Geoderma*. 116, 107-136.
- Lodovichi, M.V., Blanco, A.M., Chantre, G.R., Bandoni, J.A., Sabbatini, M.R., Vigna, M., Lopez, R., Gigon, R., 2013. Operational planning of herbicide-based weed management. *Agricultural Systems*. 121, 117-129.

- Luo, Y.Z., Zhang, M.H., 2010. Spatially distributed pesticide exposure assessment in the Central Valley, California, USA. *Environmental Pollution*. 158, 1629-1637.
- Lutz, S.R., van Meerveld, H.J., Waterloo, M.J., Broers, H.P., van Breukelen, B.M., 2013. A model-based assessment of the potential use of compound-specific stable isotope analysis in river monitoring of diffuse pesticide pollution. *Hydrology and Earth System Science*. 17, 4505-4524.
- Macary, F., Morin, S., Probst, J.L., Saudubray, F., 2014. A multi-scale method to assess pesticide contamination risks in agricultural watersheds. *Ecological Indicators*. 36, 624-639.
- Maillard, E., Payraudeau, S., Faivre, E., Grégoire, C., Gangloff, S., Imfeld, G., 2011. Removal of pesticide mixtures in a stormwater wetland collecting runoff from a vineyard catchment. *Science of The Total Environment*. 409, 2317-2324.
- SWRRBWQ manual, S., 1993. SWRRBWQ Window's Interface User's Guide (1993). Office of Science and Technology Standards and Applied Science Division U. S. Environmental Protection Agency.
- McGrath, G.S., Hinz, C., Sivapalan, M., 2008. Modeling the effect of rainfall intermittency on the variability of solute persistence at the soil surface. *Water Resources Research*. 44.
- McGrath, G.S., Hinz, C., Sivapalan, M., Dressel, J., Putz, T., Vereecken, H., 2010. Identifying a rainfall event threshold triggering herbicide leaching by preferential flow. *Water Resources Research*. 46.
- Meijer, A.D., Heitman, J.L., White, J.G., Austin, R.E., 2013. Measuring erosion in long-term tillage plots using ground-based lidar. *Soil & Tillage Research*. 126, 1-10.
- Merritt, W.S., Letcher, R.A., Jakeman, A.J., 2003. A review of erosion and sediment transport models. *Environmental Modelling & Software*. 18, 761-799.
- Messing, P., Farenhorst, A., Waite, D., Sproull, J., 2013. Influence of usage and chemical-physical properties on the atmospheric transport and deposition of pesticides to agricultural regions of Manitoba, Canada. *Chemosphere*. 90, 1997-2003.
- Meyer, J.L., Strayer, D.L., Wallace, J.B., Eggert, S.L., Helfman, G.S., Leonard, N.E., 2007. The contribution of headwater streams to biodiversity in river networks. *Journal of the American Water Resources Association*. 43, 86-103.
- Miguens, T., Leiros, M.C., Gil-Sotres, F., Trasar-Cepeda, C., 2007. Biochemical properties of vineyard soils in Galicia, Spain. *Science of The Total Environment*. 378, 218-222.
- Milosevic, N., Qiu, S., Elsner, M., Einsiedl, F., Maier, M.P., Bensch, H.K.V., Albrechtsen, H.J., Bjerg, P.L., 2013. Combined isotope and enantiomer analysis to assess the fate of phenoxy acids in a heterogeneous geologic setting at an old landfill. *Water Research*. 47, 637-649.
- Morgan, R.P.C., Quinton, J.N., Smith, R.E., Govers, G., Poesen, J.W.A., Chisci, G., Torri, D., 1998. The EUROSEM model. *Modelling Soil Erosion by Water*. 55, 389-398.
- Mostafalou, S., Abdollahi, M., 2013. Pesticides and human chronic diseases: Evidences, mechanisms, and perspectives. *Toxicology and Applied Pharmacology*. 268, 157-177.
- Moussa, R., Voltz, M., Andrieux, P., 2002. Effects of the spatial organization of agricultural management on the hydrological behaviour of a farmed catchment during flood events. *Hydrological Processes*. 16, 393-412.

- Munz, N., Wittmer, I., Leu, C., 2012. Biocide Monitoring in Switzerland. . Workshop on environmental monitoring of biocides in Europe - from prioritisation to measurements. . Berlin (DE), 5-6 November 2012.
- Novara, A., Gristina, L., Saladino, S.S., Santoro, A., Cerda, A., 2011. Soil erosion assessment on tillage and alternative soil managements in a Sicilian vineyard. *Soil & Tillage Research*. 117, 140-147.
- Nuyttens, D., De Schampheleire, M., Baetens, K., Sonck, B., 2007. The influence of operator-controlled variables on spray drift from field crop sprayers. *Transactions of the Asabe*. 50, 1129-1140.
- Nuyttens, D., De Schampheleire, M., Verboven, P., Brusselman, E., Dekeyser, D., 2009. Droplet Size and Velocity Characteristics of Agricultural Sprays. *Transactions of the Asabe*. 52, 1471-1480.
- O'Hare, M.T., McGahey, C., Bissett, N., Cailes, C., Henville, P., Scarlett, P., 2010. Variability in roughness measurements for vegetated rivers near base flow, in England and Scotland. *Journal of Hydrology*. 385, 361-370.
- Ohliger, R., Schulz, R., 2010. Water body and riparian buffer strip characteristics in a vineyard area to support aquatic pesticide exposure assessment. *Science of The Total Environment*. 408, 5405-5413.
- Oliver-Rodriguez, B., Zafra-Gomez, A., Camino-Sanchez, F.J., Conde-Gonzalez, J.E., Perez-Trujillo, J.P., Vilchez, J.L., 2013. Multi-residue method for the analysis of commonly used commercial surfactants, homologues and ethoxymers, in marine sediments by liquid chromatography-electrospray mass spectrometry. *Microchemical Journal*. 110, 158-168.
- Papiernik, S.K., Koskinen, W.C., Yates, S.R., 2009. Solute Transport in Eroded and Rehabilitated Prairie Landforms. 2. Reactive Solute. *Journal of Agricultural and Food Chemistry*. 57, 7434-7439.
- Pare, N., Andrieux, P., Louchart, X., Biarnes, A., Voltz, M., 2011. Predicting the spatio-temporal dynamic of soil surface characteristics after tillage. *Soil & Tillage Research*. 114, 135-145.
- Park, S.Y., Lee, K.W., Park, I.H., Ha, S.R., 2008. Effect of the aggregation level of surface runoff fields and sewer network for a SWMM simulation. *Desalination*. 226, 328-337.
- Payraudeau, S., Grégoire, C., 2012. Modelling pesticides transfer to surface water at the catchment scale: a multi-criteria analysis. *Agronomy for Sustainable Development*. 32, 479-500.
- PPDB, 2009. The Pesticide Properties DataBase (PPDB) developed by the Agriculture & Environment Research Unit (AERU) at the University of Hertfordshire, from the database that originally accompanied the EMA (Environmental Management for Agriculture) software (also developed by AERU), with additional input from the EU-funded FOOTPRINT project (FP6-SSP-022704). <http://www.herts.ac.uk/aeru/footprint>.
- Quilbe, R., Rousseau, A.N., Lafrance, P., Leclerc, J., Amrani, M., 2006. Selecting a pesticide fate model at the watershed scale using a multi-criteria analysis. *Water Quality Research Journal of Canada*. 41, 283-295.
- Quiquerez, A., Chevigny, E., Allemand, P., Curmi, P., Petit, C., Grandjean, P., 2014. Assessing the impact of soil surface characteristics on vineyard erosion from very high spatial resolution aerial images (Côte de Beaune, Burgundy, France). *Catena*. 116, 163-172.

- Rasmussen, J.J., McKnight, U.S., Loinaz, M.C., Thomsen, N.I., Olsson, M.E., Bjerg, P.L., Binning, P.J., Kronvang, B., 2013. A catchment scale evaluation of multiple stressor effects in headwater streams. *Science of The Total Environment*. 442, 420-431.
- Reichenberger, S., Bach, M., Skitschak, A., Frede, H.G., 2007. Mitigation strategies to reduce pesticide inputs into ground- and surface water and their effectiveness; A review. *Science of The Total Environment*. 384, 1-35.
- Renaud, F.G., Bellamy, P.H., Brown, C.D., 2008. Simulating pesticides in ditches to assess ecological risk (SPIDER): I. Model description. *Science of The Total Environment*. 394, 112-123.
- Roberts, T.R., Hutson, D.H., Services, R.S.o.C.I., 1999. *Metabolic Pathways of Agrochemicals: Insecticides and fungicides*, Vol., Royal Society of Chemistry.
- Rodriguez-Liebana, J.A., Mingorance, M.D., Pena, A., 2011. Sorption of hydrophobic pesticides on a Mediterranean soil affected by wastewater, dissolved organic matter and salts. *Journal of Environmental Management*. 92, 650-654.
- Röpke, B., Bach, M., Frede, H.G., 2004. DRIPS - a DSS for estimating the input quantity of pesticides for German river basins. *Environmental Modelling & Software*. 19, 1021-1028.
- Rosenbom, A.E., Therrien, R., Refsgaard, J.C., Jensen, K.H., Ernstsens, V., Klint, K.E.S., 2009. Numerical analysis of water and solute transport in variably-saturated fractured clayey till. *Journal of Contaminant Hydrology*. 104, 137-152.
- Rousseau, A.N., Mailhot, A., Turcotte, R., Duchemin, M., Blanchette, C., Roux, M., Etong, N., Dupont, J., Villeneuve, J.P., 2000. GIBSI - An integrated modelling system prototype for river basin management. *Hydrobiologia*. 422, 465-475.
- Sabbagh, G.J., Geleta, S., Elliott, R.L., Williams, J.R., Griggs, R.H., 1991. Modification of Epic to Simulate Pesticide Activities - Epic-Pst. *Transactions of the Asae*. 34, 1683-1692.
- Sadiki, M., Poissant, L., 2008. Atmospheric concentrations and gas-particle partitions of pesticides: Comparisons between measured and gas-particle partitioning models from source and receptor sites. *Atmospheric Environment*. 42, 8288-8299.
- Salmon-Monviola, J., Moreau, P., Benhamou, C., Durand, P., Merot, P., Oehler, F., Gascuel-Oudou, C., 2013. Effect of climate change and increased atmospheric CO<sub>2</sub> on hydrological and nitrogen cycling in an intensive agricultural headwater catchment in western France. *Climatic Change*. 120, 433-447.
- Sanchez-Moreno, J.F., Mannaerts, C.M., Jetten, V., Löffler-Mang, M., 2012. Rainfall kinetic energy-intensity and rainfall momentum-intensity relationships for Cape Verde. *Journal of Hydrology*. 454, 131-140.
- Schulz, R., 2004. Field studies on exposure, effects, and risk mitigation of aquatic nonpoint-source insecticide pollution: A review. *Journal of Environmental Quality*. 33, 419-448.
- Schwarzenbach, R.P., Escher, B.I., Fenner, K., Hofstetter, T.B., Johnson, C.A., von Gunten, U., Wehrli, B., 2006. The challenge of micropollutants in aquatic systems. *Science*. 313, 1072-1077.
- Sheikh, V., van Loon, E., Hessel, R., Jetten, V., 2010. Sensitivity of LISEM predicted catchment discharge to initial soil moisture content of soil profile. *Journal of Hydrology*. 393, 174-185.

- Shi, X.N., Wu, L.S., Chen, W.P., Wang, Q.J., 2011. Solute Transfer from the Soil Surface to Overland Flow: A Review. *Soil Science Society of America Journal*. 75, 1214-1225.
- Singh, P., Wu, J.Q., McCool, D.K., Dun, S., Lin, C.H., Morse, J.R., 2009. Winter Hydrologic and Erosion Processes in the US Palouse Region: Field Experimentation and WEPP Simulation. *Vadose Zone Journal*. 8, 426-436.
- Taghavi, L., Merlina, G., Probst, J.L., 2011. The role of storm flows in concentration of pesticides associated with particulate and dissolved fractions as a threat to aquatic ecosystems Case study: the agricultural watershed of Save river (Southwest of France). *Knowledge and Management of Aquatic Ecosystems*. 400-06.
- Tang, X.Y., Zhu, B., Katou, H., 2012. A review of rapid transport of pesticides from sloping farmland to surface waters: Processes and mitigation strategies. *Journal of Environmental Sciences-China*. 24, 351-361.
- Thullner, M., Centler, F., Richnow, H.H., Fischer, A., 2012. Quantification of organic pollutant degradation in contaminated aquifers using compound specific stable isotope analysis - Review of recent developments. *Organic Geochemistry*. 42, 1440-1460.
- Tong, S.T.Y., Chen, W.L., 2002. Modeling the relationship between land use and surface water quality. *Journal of Environmental Management*. 66, 377-393.
- Toy, T.J., Foster, G.R., Renard, K.G., 2002. *Soil Erosion: Processes, Prediction, Measurement, and Control*, Vol., Wiley.
- Turner, J., Albrechtsen, H.J., Bonell, M., Duguet, J.P., Harris, B., Meckenstock, R., McGuire, K., Moussa, R., Peters, N., Richnow, H.H., Sherwood-Lollar, B., Uhlenbrook, S., van Lanen, H., 2006. Future trends in transport and fate of diffuse contaminants in catchments, with special emphasis on stable isotope applications. *Hydrological Processes*. 20, 205-213.
- Ulrich, U., Dietrich, A., Fohrer, N., 2013. Herbicide transport via surface runoff during intermittent artificial rainfall: A laboratory plot scale study. *Catena*. 101, 38-49.
- Verkleij, J.A.C., Golan-Goldhirsh, A., Antosiewicz, D.M., Schwitzguebel, J.P., Schroder, P., 2009. Dualities in plant tolerance to pollutants and their uptake and translocation to the upper plant parts. *Environmental and Experimental Botany*. 67, 10-22.
- Viglizzo, E.F., Ricard, M.F., Jobbagy, E.G., Frank, F.C., Carreno, L.V., 2011. Assessing the cross-scale impact of 50 years of agricultural transformation in Argentina. *Field Crops Research*. 124, 186-194.
- Vischetti, C., Cardinali, A., Monaci, E., Nicelli, M., Ferrari, F., Trevisan, M., Capri, E., 2008. Measures to reduce pesticide spray drift in a small aquatic ecosystem in vineyard estate. *Science of The Total Environment*. 389, 497-502.
- Vörösmarty, C.J., McIntyre, P.B., Gessner, M.O., Dudgeon, D., Prusevich, A., Green, P., Glidden, S., Bunn, S.E., Sullivan, C.A., Liermann, C.R., Davies, P.M., 2010. Global threats to human water security and river biodiversity. *Nature*. 467, 555-561.
- Wauchope, R.D., Yeh, S., Linders, J.B.H.J., Kloskowski, R., Tanaka, K., Rubin, B., Katayama, A., Kordel, W., Gerstl, Z., Lane, M., Unsworth, J.B., 2002. Pesticide soil sorption parameters: theory, measurement, uses, limitations and reliability. *Pest Management Science*. 58, 419-445.

- Wauchope, R.D., Johnson, W.C., Sumner, H.R., 2004. Foliar and soil deposition of pesticide sprays in peanuts and their washoff and runoff under simulated worst-case rainfall conditions. *Journal of Agricultural and Food Chemistry*. 52, 7056-7063.
- White, J.C., Mattina, M.J.I., Eitzer, B.D., Iannucci-Berger, W., 2002. Tracking chlordane compositional and chiral profiles in soil and vegetation. *Chemosphere*. 47, 639-646.
- Xu, Q.X., Wang, T.W., Cai, C.F., Li, Z.X., Shi, Z.H., Fang, R.J., 2013. Responses of Runoff and Soil Erosion to Vegetation Removal and Tillage on Steep Lands. *Pedosphere*. 23, 532-541.
- Ye, J., Zhao, M.R., Liu, J., Liu, W.P., 2010. Enantioselectivity in environmental risk assessment of modern chiral pesticides. *Environmental Pollution*. 158, 2371-2383.
- Ying, G.G., 2006. Fate, behavior and effects of surfactants and their degradation products in the environment. *Environment International*. 32, 417-431.
- Zehe, E., Maurer, T., Ihringer, J., Plate, E., 2001. Modeling water flow and mass transport in a loess catchment. *Physics and Chemistry of the Earth Part B-Hydrology Oceans and Atmosphere*. 26, 487-507.

# Chapter III. Fungicides drift and mobilisation via runoff and erosion in vineyard

---

Viticulture represents an important agricultural practice in the world and the long-term use of organic and inorganic pesticides in vineyards leads to contamination of aquatic ecosystems. Vineyards are agro-systems which are strongly impacted by anthropogenic forcing and present impermeable surfaces which are easily prone to fungicides runoff. Moreover, foliar application in vineyards is carried out at 2 m height and can therefore lead to significant pesticide drift. Fungicides represent 80% of the total amount of pesticides used in French vineyards. Farmers are advised to apply different groups of pesticide in sequence in order to avoid fungal resistances, which increase the variety of fungicides used at a single production site. Kresoxim methyl (KM) and cyazofamid (CY) are recent fungicide compounds used in the treatment of downy (*Plasmopara viticola*) and powdery (*Uncinula necator*) mildews. These pesticides directly inhibit essential fungal functions such as respiration (for KM) or energy production (for CY).

The drift and the spatial variability of the deposition of these two fungicides as formulated products were investigated under real application condition in a vineyard (Section 1). Following their deposition, their transport in runoff water and partitioning within the dissolved and particulate phases were jointly evaluated from the vineyard catchment and a representative plot (Section 2).

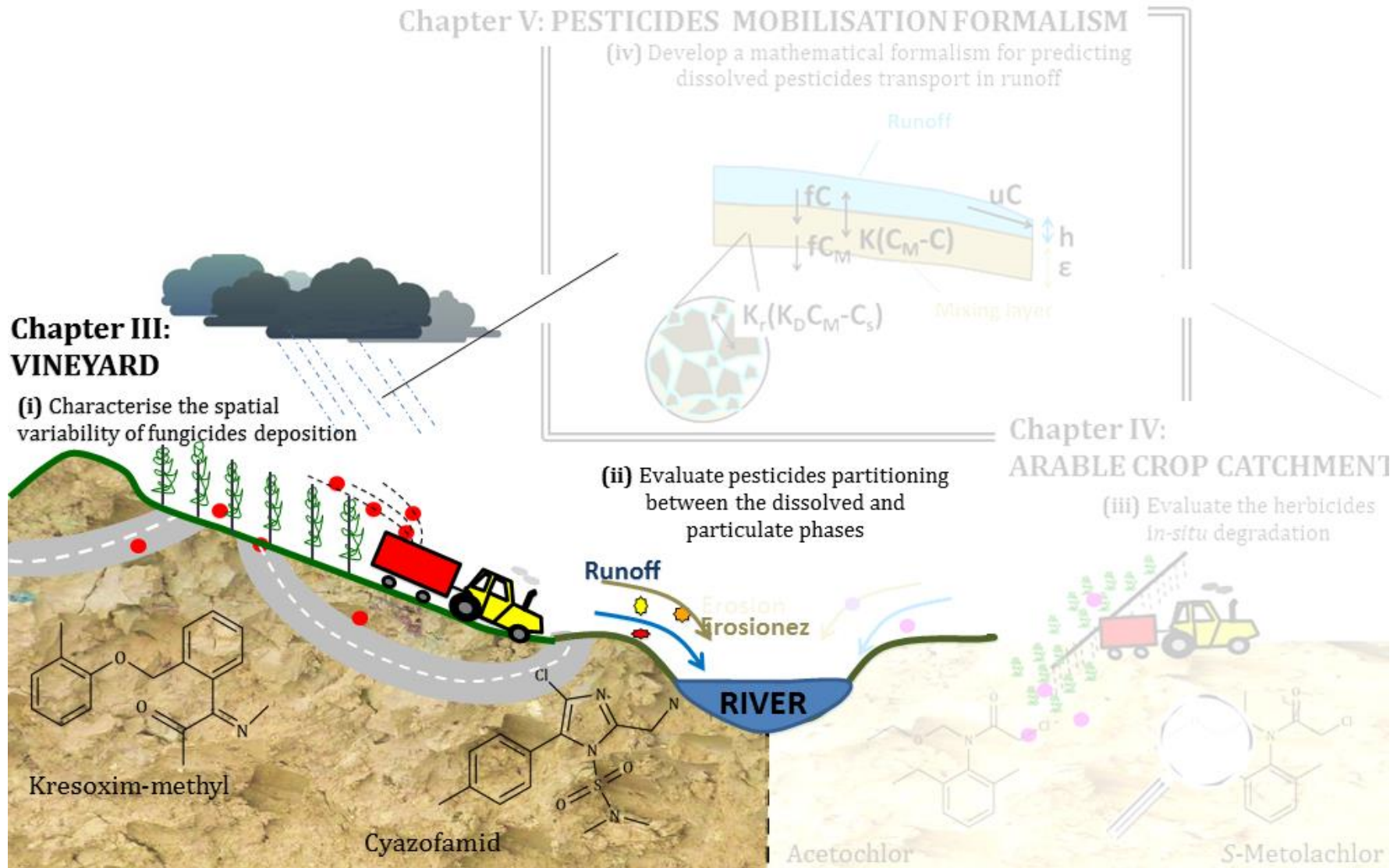


Figure III-1. Graphical outline of the PhD thesis (Chapter III)

## Section 1. Kresoxim methyl deposition, drift and runoff in a vineyard catchment

Marie Lefrancq, Gwenaël Imfeld, Sylvain Payraudeau, Maurice Millet

(Section published in Science of the Total Environment 442: 503-508; Appendices are given in Chapter VII)

### 1. Abstract

Surface runoff and spray drift represent a primary mode of pesticide mobilisation from agricultural land to ecosystem. Though pesticide drift has mainly been studied at small scale (< 1 ha), pesticide transport by drift and runoff have rarely been compared in the same agricultural catchment. Here kresoxim methyl (KM) drift during foliar application was evaluated in a vineyard catchment (Rouffach, Alsace, France), and KM deposition on non-target surfaces was compared to KM runoff. KM was detected on 55% of the collectors and concentration reached 18% of the applied dose (i.e. 1.5 mg m<sup>-2</sup>). Our results indicated that KM soil deposition greatly varied in space and time. The total KM soil deposition in the vineyard plots was estimated by four different interpolation methods (arithmetic mean, Thiessen method, inverse weighting distance and ordinary kriging) and ranged between 53 g and 61 g (5.8 and 6.6% of the total mass applied). The amount of KM drifted on roads was 50 times larger than that in runoff water collected at the outlet of the catchment. Although KM application was carried out under regular operational and climatic conditions, its deposition on non-target surfaces may be significant and lead to pesticide runoff. These results can be anticipated as a starting point for assessing pesticide deposition during spray application and corresponding pesticide runoff in agricultural catchments.

#### Highlights

- We evaluated kresoxim methyl (KM) drift in a vineyard catchment
- KM deposition at the catchment scale widely varied in space and time
- KM concentration represented up to 18% of the applied dose (1.5 mg m<sup>-2</sup>)
- KM soil deposition represented between 5.8 and 6.6% of the total mass applied
- KM road deposition (0.6 to 5.2 g) was 50 times larger than KM in runoff.

**Keywords:** Soil; Catchment; Transport; Pesticide; Vine; Fungicide

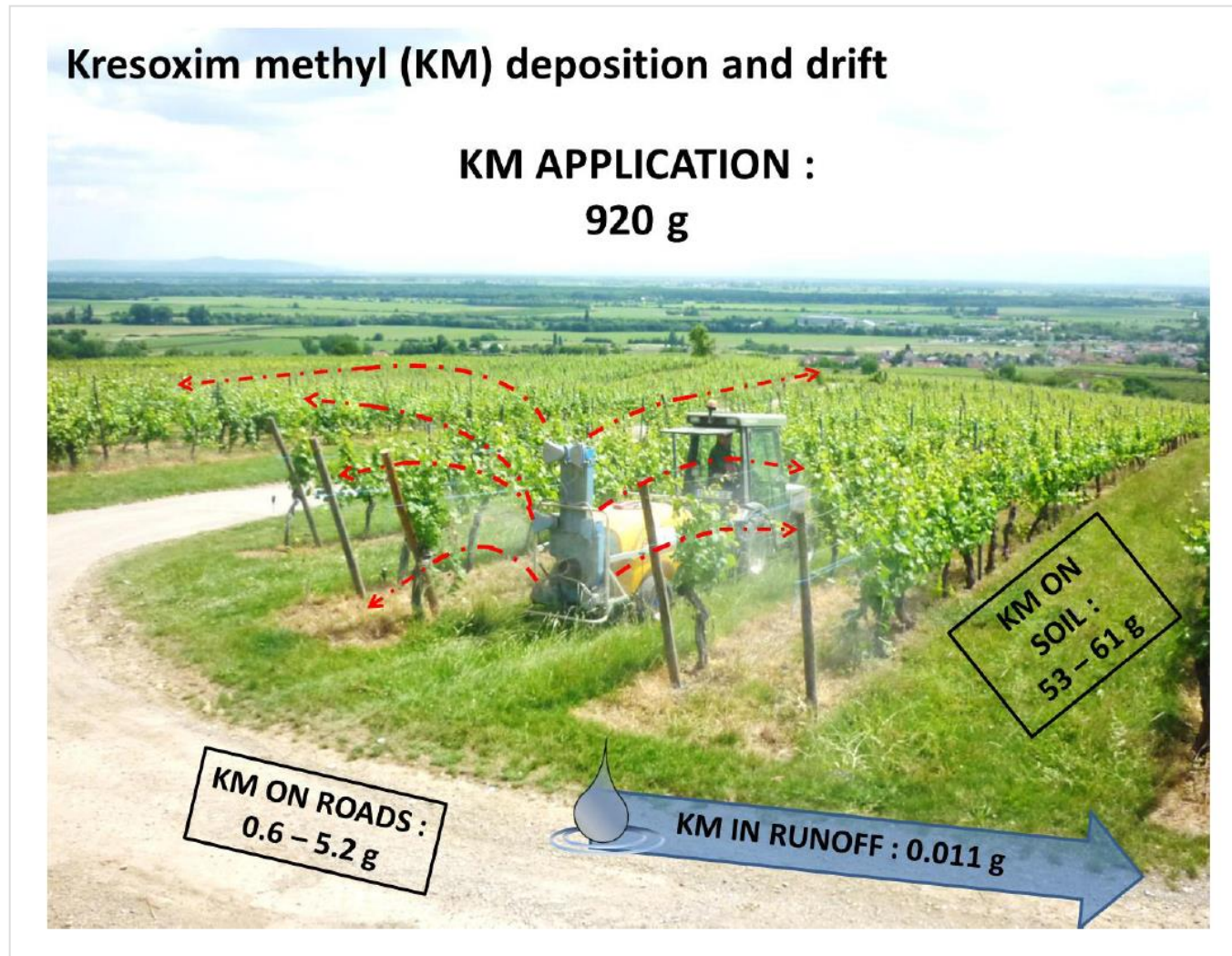


Figure III-2. Graphical abstract

## 2. Introduction

Pesticide loss represents the portion of applied pesticides that does not reach the intended target during or after an application event. Pesticides are directly lost during air spraying, or indirectly, via surface runoff, leaching in soil, drain flow, volatilisation from soil and plants and/or wind erosion (Felsot et al., 2011; McGrath et al., 2010; Oliver et al., 2012). Pesticide drift is defined as droplets, dry particles or vapour sprays moving beyond the target zone during or immediately after an application (Carlsen et al., 2006), and can affect soil or aquatic ecosystems (Vischetti et al., 2008). Following application, surface runoff and the associated transport of suspended solids represent a primary mode of pesticide mobilisation from agricultural land to aquatic ecosystems (Brady et al., 2006). However, quantitative knowledge on pesticide loss by drift and runoff at the catchment scale is scarce. Pesticide loss largely depends on the farming practices, and hydrological and climatic conditions, although the diversity of experimental approaches, agricultural contexts and modes of application render an inter-comparison difficult. During foliar application, 6% of chlorpyrifos and 1.6% of the metalaxyl doses were found on soil 3 m beyond the application zone (Vischetti et al., 2008). For folpet and tebuconazole, loss on soil during spray drift reached 41.1 and 88.8% of the applied dose, respectively (Druart et al., 2011). In another study, loss of ten herbicides by spray drift ranged from 0.1 to 9% of the applied amount close to the sprayed area (up to 2 m) (Carlsen et al., 2006). Though climatic factors, such as wind speed, temperature or atmospheric humidity, influence pesticide drift, the vegetation (i.e. cover, height) (Lazzaro et al., 2008), chemical factors (i.e. formulation, presence of additives, density, viscosity and volatility), the type of application (i.e. sprayer type, nozzle pressure and size, release height) (Arvidsson et al., 2011; Nuyttens et al., 2009) and the topography also play a crucial role (Carlsen et al., 2006; Gil and Sinfort, 2005). However, little is known about the drift of widely used pesticides at the catchment scale.

Fungicides represent 80% of the total amount of pesticides used in vineyards (Provost et al., 2007), and may affect beneficial fungi (Bunemann et al., 2006) and bacteria (Imfeld and Vuilleumier, 2012). The fungicide kresoxim methyl (KM) has been widely used for treating downy (*Plasmopara viticola*) and powdery (*Uncinula necator*) mildews (Abreu et al., 2006). KM is toxic to aquatic crustaceans and aquatic invertebrates, with an acute 96 hour lethal concentration for half of the population (LC50) of 47  $\mu\text{g L}^{-1}$  (PPDB, Pesticide Properties Data Base, 2009). The KM acid, one of the KM degradation products, has a high risk index and is part of the priority list for the source drinking water protection in Great Britain (Sinclair et al., 2006). KM is preventatively applied on vine leaves during the critical period for mildews infections, generally from May to August in Alsace (France). KM deposition on vineyard soil is therefore

considered as a loss. In this study, deposition is defined as KM losses on vineyard soil, and drift is defined as KM losses beyond the application area, i.e. outside the plots. Although KM is increasingly used and potentially toxic, to the best of our knowledge, KM losses by drift, deposition and surface runoff at the agricultural catchment scale have not been quantified yet. Such evaluation is required to better evaluate the source of pesticide losses during and following an application in agricultural catchments. Therefore, this study aims (1) to quantify in a vineyard catchment the KM deposition and drift on non-target areas, and (2) to compare the KM losses with KM runoff collected at the outlet of the catchment.

### **3. Material and methods**

#### **3.1. Description of the vineyard catchment**

The experiment was performed in a 42.7 ha vineyard catchment in Rouffach (Alsace, France, latitude 47°57'9" N; longitude 007°17'3" E). The catchment was described previously (Grégoire et al., 2010) and a scheme with its land use is provided in Figure III-3. Briefly, vineyards cover 59% of the catchment and forest and pasture 29%. The main soil type is calcareous clay loam with medium infiltration capacity. A meteorological station located in the catchment provided air temperature, relative humidity, wind velocity and rainfall data with a resolution of 6 min. The mean annual precipitation is  $605 \pm 115$  mm (period from 1998 to 2011). Rainfall events do not generate a permanent stream at the catchment and runoff events statistically occur every week through the year. The road network is dense and accounts for 4.6% of the catchment area and represents the principal route of water flow (Figure III-3). The vineyard plots are grass covered every two vine rows.

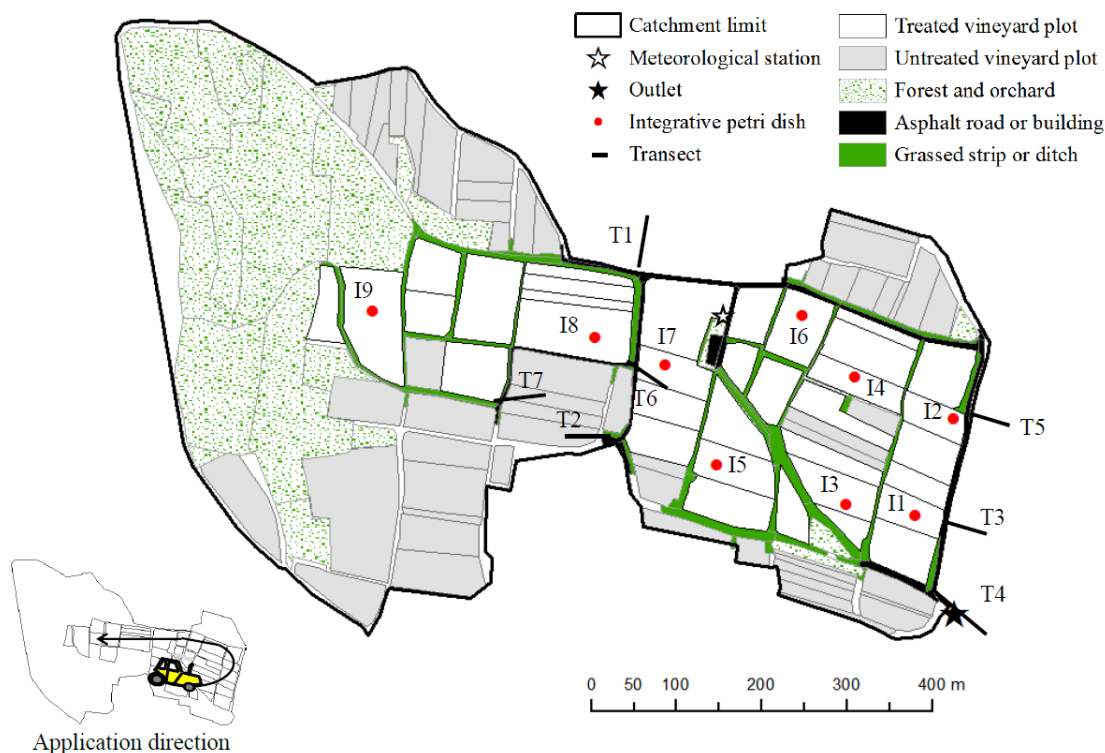
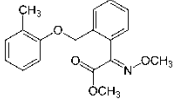


Figure III-3. Location of the kresoxim methyl collectors in the vineyard catchment (Rouffach, Alsace, France) on May 24, 2011.

### 3.2. KM properties and application

Kresoxim-methyl (methyl- $\alpha$ -(methoxyimino)-2-[(2-methylphenoxy)-methyl]phenyl acetate) belongs to the strobilurin family. The physicochemical characteristics of KM are summarised in Table III-1. KM has a  $\log K_{oc}$  of 2.5 (Fenoll et al., 2010), an aqueous hydrolysis half-life of 35 days (20 °C, pH 7) and a half-life in soil of 16 days. The application of KM in the form of STROBY DF® was conducted between 6:10 am and 3:45 pm on May 24, 2011. Detailed meteorological and application characteristics are provided in Table III-1. KM application rate was 0.08 kg ha<sup>-1</sup> sprayed using a broadcast air assisted by a dragged sprayer VICAR (600 L), with a nozzle pressure of 8.5 bars and a maximum nozzle height of 1.8 m. The driving speed ranged between 5 and 6 km h<sup>-1</sup> and the application headed from east to west (Figure III-3). KM is applied only on 11.5 ha of vineyard plots corresponding to a total mass applied of KM of 920 g.

**Table III-1. KM, application and meteorological characteristics of May 24 2011 in Rouffach (Alsace, France). Values are provided as the mean and ranges.**

<b>Kresoxim methyl</b>	
Chemical formula	C <sub>18</sub> H <sub>19</sub> NO <sub>4</sub>
Chemical structure	
Molecular weight [g mol <sup>-1</sup> ] <sup>a</sup>	313.35
Henry constant [Pa m <sup>3</sup> mol <sup>-1</sup> ] (25 °C) <sup>a</sup>	3.60 10 <sup>-7</sup>
Log <i>K<sub>ow</sub></i> <sup>a</sup>	3.40
<b>Application</b>	
Maximum nozzle height [m]	2
Nozzle pressure [bars]	8.5
Application rate of kresoxim methyl [kg ha <sup>-1</sup> ]	0.08
Amount applied [kg]	0.92
Driving speed [km h <sup>-1</sup> ]	5 - 6
<b>Meteorology</b>	
Wind velocity (2m) [m.s <sup>-1</sup> ]	1.9 (0.8 - 3.3)
Mean wind direction (10 m) [°] <sup>b</sup>	187 (20 - 320)
Air temperature (2 m) [°C]	24 (16.7 - 27.2)
Relative humidity (2 m) [%]	39.9 (25 - 73)
Global radiation [kJ m <sup>-2</sup> ]	252.8 (132 - 344)

<sup>a</sup> Obtained from the [PPDB Pesticide Properties DataBase \(2009\)](#).

<sup>b</sup> Data from Mayenheim meteorological station at 8 km from Rouffach.

### 3.3. Sampling procedure

At the vineyard catchment, 51 glass circular Petri dishes (150 ID×25 mm, 176.71 cm<sup>2</sup>) were used to collect surface fungicide droplets to quantify KM deposition and drift, according to Mathers et al. (2000). The dishes were located using a differential global positioning system. Nine dishes, named “integrative”, were distributed within the investigated plots to estimate the direct KM deposition on the vineyard soil (Figure III-3). In the eastern part of the catchment, which is the largest, two dishes were placed at each plot strip (dishes I1, I2, I3, I4, I5 and I6). Only one dish was placed at each plot strip in the western part (dishes I7, I8 and I9) because the covered area was lower. The collector density at the catchment scale was 1.3 ha<sup>-1</sup>. The dishes were replaced three times every 4 h during the application period to limit photolytic degradation. Exposure

time for each Petri dish and for each period were (mean h  $\pm$  SE h; n=9): period 1 (P1): 4.05  $\pm$  0.19; period 2 (P2): 4.04  $\pm$  0.18 and period 3 (P3): 2.01  $\pm$  0.15. In parallel, seven transects outside the vineyard plots, encompassing 42 dishes, were deployed to estimate the drift extent. Dishes were placed along the transect at 0, 1, 5, 10, 25 and 40 m from the vineyard plot in the downwind direction and in other directions to encircle the catchment (Figure III-3). Dishes on each transect were immediately collected after KM application on the plot containing the first dish. KM on the dishes was extracted by three successive washings with ethyl acetate with a recovery rate assumed to be 100%. Samples were transferred in glass flasks, placed on ice during transport to the laboratory and stored in the dark at -20 °C until analysis. At the catchment outlet (Figure III-3), runoff discharges were continuously monitored following the application. Water depth was measured using flow bubbler modules with a precision of 1 mm (Hydrologic, Sainte-Foy, Quebec, Canada) combined with a Venturi channel (ENDRESS+HAUSER, Switzerland). 300 mL of water were collected every 3 m<sup>3</sup> using a 4010 Hydrologic automatic sampler (Sainte-Foy, Quebec, Canada).

The detailed procedure of sample collection and storage ensuring reliable pesticide measurements was previously tested and discussed (Domange and Grégoire, 2006). Briefly, water samples were collected in glass jars, stored in the dark at 4 °C until collection on June 1, 2011, and placed on ice during transportation to the laboratory. Water samples were filtered through 0.7  $\mu$ m glass fibre filters within 1 day and stored in the dark at -20 °C until analysis. Suspended solids were considered as the fraction of runoff solids larger than 0.7  $\mu$ m.

#### 3.4. KM analysis

Eluates of ethyl acetate with KM were concentrated to 1 mL using a rotary evaporator (45 °C, 240 mbar). Before injection, metolachlor D6 was spiked in each sample as an internal standard at 100  $\mu$ g L<sup>-1</sup>. Analysis was carried out using a Focus-ITQ 700 GC-MS/MS (Thermo Scientific les Ulis, France). Pulsed injection (3  $\mu$ L at 3 mL min<sup>-1</sup> for 1 min) was done in splitless mode with an Optima 5MS column (30 m $\times$ 0.25 mm ID, 0.25 mm OD; MN, Hoerdt, France). The GC temperature programme was held to 50 °C (2min), ramped at 30 °C min<sup>-1</sup> until 150 °C, at 5 °C min<sup>-1</sup> until 250 °C and finally increased at 30 °C min<sup>-1</sup> until 300 °C. Helium at 1 mL min<sup>-1</sup> was used as carrier gas. Injector and transfer line temperatures were 280 °C and 300 °C, respectively. Mass spectrometric detection was done in electronic impact ionisation mode with source and the trap temperature set at 210 °C. Quantification was based on the daughter ion 89 and identification on the parent ion 116. KM was never detected in blank samples. Each sample was measured at least three times. Detection limit was 0.1  $\mu$ g L<sup>-1</sup> with an analytical uncertainty of 10%.

KM analysis in water samples was performed according to the NF XPT 90–210 French standards at the Pasteur Institute of Lille (France), which is a service of pesticide residue analysis accredited by the French National Accreditation Authority (COFRAC). The COFRAC calibration certificate is recognized by other European calibration services (EA - European Cooperation for Accreditation). KM in water samples was extracted by solid phase extraction (SPE) and quantified using liquid chromatography coupled to tandem mass spectrometry (LC-MS/MS). Limits of quantification were  $0.1 \mu\text{g L}^{-1}$  with a mean uncertainty of 23% and a recovery rate ranging from 80 to 90%.

### 3.5. Data analysis

Reported concentrations were normalised by the size of the Petri dishes [ $\text{kg ha}^{-1}$ ] and provided as a percent of the KM applied dose. The total amount of KM deposited within the plots during application was estimated using four different spatial interpolation methods to evaluate biases when interpolating deposited concentrations at the catchment scale. Deposition loads were estimated based on (1) an arithmetic mean, (2) the classical Thiessen method (TM) generally applied for rain gauges (Fiedler, 2003), (3) inverse distance squared weighting (IDW), and (4) ordinary kriging (OKri) using a spherical semi variance function which were previously applied for estimating soil contamination (Xie et al., 2011). The interpolations were done using the ArcGIS software (version 10.1). The TM consisted in allocating a portion of the catchment's surface ( $P_i$  [ha]) using TM for each Petri dish  $i$ . The total amount directly deposited on plot soil,  $T$  [kg] is given by:

$$T = \sum_{i=1}^{14} D_i P_i \quad (1)$$

where  $D_i$  is the dose [ $\text{kg ha}^{-1}$ ] of the Petri dishes  $i$ . The IDW and OKri methods provided a mean rate  $R_j$  [ $\text{kg ha}^{-1}$ ] for each plot  $j$  with a surface  $S_j$ . The total amount deposited on plot soil,  $T$  [kg] is given by:

$$T = \sum_{j=1}^n R_j S_j \quad (2)$$

where  $n$  is the number of plots in the application zone. Detailed description and root mean square errors (RMSE) for each method are provided in Table VII-1 in the Appendices. The amount of KM deposited along transects were compared with an empirical decreasing power

function for drift in vineyards (Rautmann et al., 1999). The total amount of KM deposited on plot margins between two distances  $i$  and  $j$  from the plot ( $M_{ij}$ ) was calculated as a range according to the following equation:

$$M_{ij} = S_{ij} \frac{C_i + C_j}{2} \quad (3)$$

where  $M_{ij}$  is the minimum (or maximum respectively) amount of KM deposited on plot margins,  $S_{ij}$  is the surface of roads between  $i$  and  $j$  meters from the plot, and  $C_i$  and  $C_j$  are the minimum (or maximum respectively) deposition concentrations among all transects at the distance  $i$  and  $j$ , respectively.

## 4. Results and discussion

### 4.1. KM deposition

KM soil deposition was defined in this study as the deposition on the vineyard plots, corresponding to losses for the intended target, i.e. vine leaves in our case. Detailed results for the integrative Petri dishes are provided in Table VII-2. KM was detected in at least one of the three dishes at each location. KM was detected in 41% of the 27 integrative Petri dishes within the vineyard plots. The spatial and temporal variability of KM deposition is shown for the three periods P1, P2 and P3 and for the entire day in 0. The daily deposition of KM, i.e. summing KM concentrations on dishes at the same location and changed three times during the day, ranged between 0.09 and 1.20 mg m<sup>-2</sup>, which corresponded maximally to 15% of the applied dose (dish I8, see Figure III-3). Mean deposited load on the catchment soil and standard deviation was 2.91 ± 4.39, 1.17 ± 1.92 and 1.59 ± 4.69% ha<sup>-1</sup> for the period P1, P2 and P3, respectively, and 5.66 ± 5.13% ha<sup>-1</sup> for the entire period.

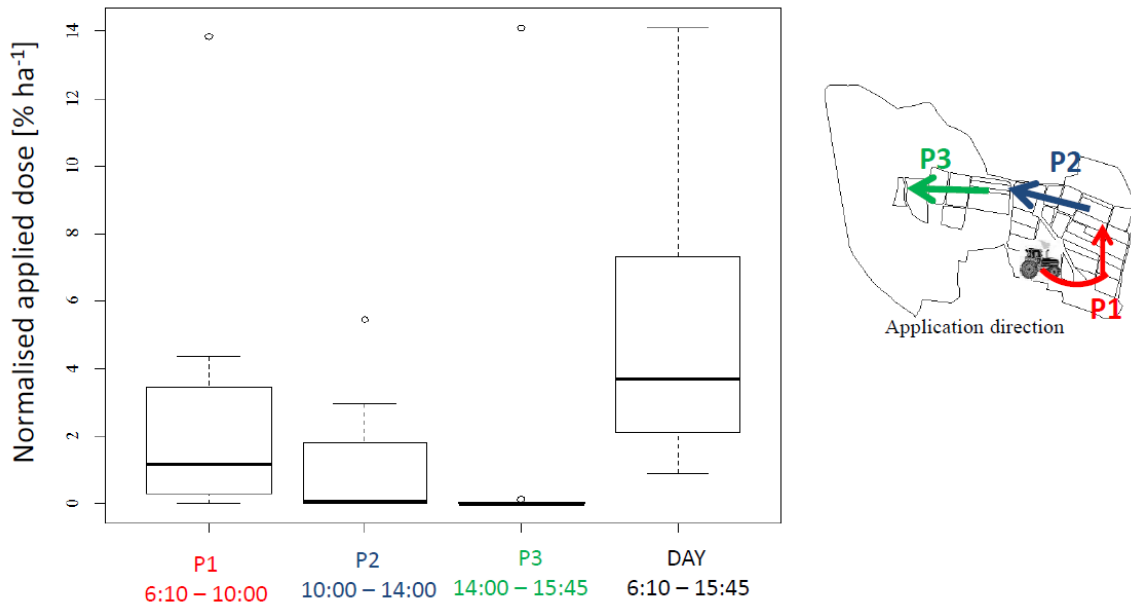


**Figure III-4. Kresoxim methyl soil deposition of the nine collectors normalised by corresponding Thiessen area in the vineyard catchment (Rouffach, Alsace, France) during the three periods P1, P2 and P3 on May 24, 2011.**

These results clearly emphasise that KM depositions on the vineyard soil largely varied in space and time. Spatial variation of KM deposition is to be related to the interception of spray application by the vine plants. Collectors were systematically placed in the middle of the inter-rows, and thus only intercepted the KM fraction that passed through the vine plants during application. The height of vine plants ranged from 35 to 200 cm and the distance between vine rows was 170 cm for 77% of the vineyard area, whereas it varied between 140 or 280 cm in the remaining area. The third period was shorter than the two others, explaining less KM deposition compared to the first two periods. During the third period, application occurred in the western part of the catchment (Figure III-4), which was smaller, thus implying lower frequency of sprayer runs. The mean value of air humidity during the first period was  $51.7 \pm 2.0\%$  whereas it was  $30.2 \pm 0.2\%$  and  $30.4 \pm 0.3\%$  during the two other periods. The lower the absolute humidity, the greater the pesticide drift. This is due to smaller droplet with high drift potential during evaporation (Nuyttens et al., 2007). Consequently, less pesticide drift is expected when humidity is high, explaining larger amounts of KM deposited directly on the vine plots during the first period.

The total amount of KM deposition on the vineyard soil is estimated to be 53 g (5.8% of the total mass applied) using an arithmetic mean (AM), 58 g (6.2%) based on the OKri, 59 g (6.4%) using the IDW and 61 g (6.6%) using the TM. Estimation of total deposited amount is associated with

an uncertainty, which depends on the number of samples, the distance between sampling locations and the choice of interpolation methods (Kravchenko, 2003). In this study, an opportunity sampling approach (i.e. placing dishes in representative plots) was used. This choice was selected because the spatial variability of KM deposition could not be predicted before the application. Cross validation consisted in removing consecutively a sampling point, before interpolating the value based on the remaining observations and comparing the estimated value with the observed one. Cross validation was used for each interpolation method to evaluate at each sampling point the difference between observed and interpolated KM deposition. The root mean square error (RMSE) ranged from 530 (AM) to 847% (TM) (see Table VII-1). The error calculation shows that errors at each sampling site may be large, which emphasises that the accuracy of deposition estimates can largely vary. Nevertheless, these results also show that the four interpolation methods result in similar estimates of total KM deposition. Therefore their combined use may confer a more accurate estimation range of total KM deposition on vineyard soil (Table VII-1).

#### 4.2. KM drift

KM drift was defined in this study as KM deposition in areas located beyond the vineyard plots. The location and characteristics of the transects used for evaluating KM drift are provided in Figure III-3 and Table III-2. Detailed results of KM drift along the transects are provided in Table VII-3. The distance at which KM could not be detected differed among transects and ranged between 1 m and beyond 40 m from the vineyard plots. KM concentrations along the transect 2 (T2) reached  $1.5 \text{ mg m}^{-2}$ , which represents 18.2% of the applied dose between 6:33 and 9:10 am. The maximum drift distance was beyond 40 m for T2, with a concentration representing 0.1% of the applied dose. This is in agreement with previous studies, showing that chlorpyrifos and metalaxyl drift occurred up to 24 m in vineyard (Vischetti et al., 2008). Drift on 40 m surrounding plot margins, such as grass strips, vegetated ditches or road networks ranged, according to the interpolation method used (see Eq. (3)), from 2.4 to 20.0 g, which corresponds to 0.3 to 2.2% of the total mass applied respectively. The detailed results of KM load estimates on plot margins are provided in Table VII-4.

Between 0 and 5 m, KM concentrations were significantly lower than those found using a Rautmann model, which results in RMSE between the observed and the estimated quantities for each transect larger than four orders of magnitude. In contrast, values above 5 m from the plot were closer to the modelled values (RMSE = 20.2%). However, exposure time for each transect varied according to the application time at each plot (mean min  $\pm$  SE min; n = 7: 86 min  $\pm$  37).

Varying exposure time at each plot may have influenced the amount of KM recovered on the dishes, mainly due to different lengths of photolytic period. Moreover, KM concentrations at the plot border of transects 6 and 7 (Figure III-3) were lower than those at 1 m suggesting that dishes were not directly exposed to application owing to partial or total interception of KM by the vine plants. While our results highlight the interest of mitigation measures such as grass strips for intercepting pesticide drift during application, the large variability in KM drift along transects may limit an accurate estimation of the drift distance.

**Table III-2. Kresoxim methyl deposition along the transect at the vineyard catchment (Rouffach, Alsace, France) the May 24 2011.**

	T1	T2	T3	T4	T5	T6	T7
<b>Characteristics</b>							
Opening time	11:54 am	6:33 am	9:05 am	8:41 am	9:10 am	2:22 pm	1:43 pm
Closing time	12:26 pm	9:10 am	10:24 am	10:05 am	10:05 am	3:51 pm	2:50 pm
Orientation [°]	8	125	109	130	109	101	73
<b>Meteorology</b>							
Mean relative humidity [%]	29.3	58.4	35.6	39.1	42.8	28.9	29.5
Mean temperature [°C]	26.7	20.7	25.7	25.2	24.5	24.8	25.4
Mean wind speed [m s <sup>-1</sup> ]	1.8	1.6	1.3	1.3	1.3	2.6	2.8
Mean wind orientation [°]	225	185	225	177	210	165	170
<b>Kresoxim methyl</b>							
Maximum of KM deposit [% <sup>a</sup> ]	2.26	18.24	3.66	10.06	8.12	2.8	17.98
Last KM deposit [% <sup>a</sup> ]	0.06	0.11	0.21	5.16	3.35	0.4	0.15
D50% [m] <sup>b</sup>	2.59	0.88	3.03	1.1	0.85	7.28	3.47
D100% [m] <sup>c</sup>	10-25	> 40	5-10	1-5	1-5	> 25	> 25

<sup>a</sup> in [%] of the application rate. <sup>b</sup> Estimated distance to measure half the largest amount of KM. <sup>c</sup> Distance at which KM was not detected.

**4.3. Runoff-associated KM**

Rainfall events in the week following KM application occurred on May 27 (2.0 mm) and 31 (10.5 mm) yielding a total runoff volume of 66.3 m<sup>3</sup>. KM concentration in runoff water at the catchment outlet was 0.17 µg L<sup>-1</sup>, which corresponded to a KM load of 11 mg and an export coefficient of 0.001%. Even the minimum estimated KM load via drift found on plot margins (i.e. 2.4 g) was 200 times larger than the KM load in runoff water collected at the catchment's outlet. No KM could be detected in suspended solids. Two weeks after KM application, KM was no longer detected in runoff generated by the six successive rainfall events, which, in total, accounted for a rainfall depth of 8.6 mm and a total runoff volume of 51.7 m<sup>3</sup>. This indicates that deposited and drifted KM was mobilised from the catchment over the course of the two rainfall runoff events that directly followed KM application. Two weeks after the first KM application, a new KM application occurred on the vineyard catchment. This new application prevented further estimation of KM export by runoff related to the target application event.

Due to its low sorption potential in soils and its high solubility, KM is expected to be prone to runoff when a significant rainfall event directly follows an application. Since KM drifted on roads may be mobilised during rainfall–runoff events, the portion of KM on roads requires specific consideration. Estimated amount of KM drifted on roads ranged from 0.6 to 5.2 g (Table VII-4), which corresponds to a KM amount 50 times larger than that found in runoff. This suggests that, following drift, various KM attenuation processes can simultaneously act at the catchment scale and control KM transport by runoff. Dissipation of KM following its application on the vineyard can be partly due to photolysis and sorption on both soil particles and road surfaces (Navarro et al., 2009; Ramwell, 2005). KM photolysis and sorption on soil or road surfaces has not been reported yet. This lack of information precludes a compound-specific estimation of attenuation at the catchment scale. Nevertheless, half-life of KM during photolysis in leaching water from lysimeters was estimated to be 0.04 days (Navarro et al., 2009), which suggests that KM drifted onto roads may be degraded rapidly if no rainfall–runoff event occurs in the meanwhile. The fate of pesticides applied on road surfaces also depends on the extent of sorption. KM and the herbicide diuron have similar *K<sub>oc</sub>* values (316 and 334 respectively) suggesting that the sorption behaviour of these two compounds is similar (Ramwell, 2005). A previous study showed that 23% of diuron remained sorbed to the asphalt during 6 days (Ramwell, 2005). Using this value, the contribution of KM sorption on roads estimated for this study would range between 0.49 and 3.98 g, which is still 43 times larger than the KM load measured in runoff at the outlet.

The low export of KM observed in runoff in the present study is to be related to the low runoff coefficient and hydrological connectivity between vineyard plots and the road network during rainfall-runoff events. Hydrological connectivity between vineyard plots and roads was previously observed in the study catchment during two runoff events on June 29, 2005 (18.6 mm; maximum intensity of 8 mm 6 min<sup>-1</sup>) and 2006 (13 mm; maximum intensity of 6.6 mm 6 min<sup>-1</sup>). These observations showed that, despite larger rainfall depths and intensities, only 12% of the catchment effectively contributed to runoff discharge that reaches the catchment outlet. Assuming that only 12% of the catchment was involved in the discharge produced at the catchment outlet, the KM load which can be mobilised from connected roads is estimated to be 36 times larger than the KM load recorded in runoff at the outlet of the catchment (Table VII-4). This suggests that only a small fraction of KM drifted onto roads was exported from the catchment. Our results also highlight that further experiments are required to more accurately quantify and predict under environmental conditions KM sorption, photolysis and mobilisation.

## 5. Conclusion

This study was designed to evaluate and compare in a small vineyard catchment KM deposition and drift during application as well as KM export in runoff following KM application. KM losses were quantified on non-target zones, including vineyard soil and roads. The daily soil deposition of KM on the vineyard plots ranged between 0.09 and 1.20 mg m<sup>-2</sup>, which corresponds to maximally 15% of the applied dose. KM drift on non-target areas ranged between 0 and 1.5 mg m<sup>-2</sup>, i.e. 18% of the applied dose. The results indicated that KM depositions on soil widely varied in space and time, depending on soil and meteorological conditions. The total estimated amount of KM deposition in the study catchment ranged from 53 g (5.8% of the total mass applied) to 61 g (6.6%), depending on the interpolation method used. KM loads on roads represented between 0.07 and 0.57% of the total mass applied, i.e. about 50 times more than the KM load in runoff during the week following the application. Though the KM application was carried out under controlled and climatically favourable conditions, KM deposition and drift on non-target zones, and especially on roads, may lead to significant KM transport by runoff that eventually reaches downstream aquatic ecosystems. We anticipate our results to be a starting point for assessing in agricultural catchments pesticide deposition and drift during pesticide application and following runoff.

## 6. Acknowledgements

This research has been funded by the PhytoRET project (C.21) of the European INTERREG IV program Upper Rhine. Marie Lefrancq is supported by the European INTERREG IV program Upper Rhine and by the water agency of Rhin Meuse. The authors wish to thank the Agricultural and Viticulture College of Rouffach, the City of Rouffach and the farmers of the Hohrain domain, Rouffach, France for their contribution. Special appreciation goes to Thibault Coll, Thomas Dreidemy, Romy Durst, Elodie Maillard, Julien Moronval, Angela Mutschler, Cyrielle Regazzoni and Izabella Babcsányi for their support in sampling, measurement and analysis.

## 7. References

- Abreu SD, Caboni P, Cabras P, Garau VL, Alves A. Validation and global uncertainty of a liquid chromatographic with diode array detection method for the screening of azoxystrobin, kresoxim-methyl, trifloxystrobin, famoxadone, pyraclostrobin and fenamidone in grapes and wine. *Anal Chim Acta* 2006; 573: 291-297.
- Arvidsson T, Bergstrom L, Kreuger J. Spray drift as influenced by meteorological and technical factors. *Pest Manag Sci* 2011; 67: 586-598.
- Brady JA, Wallender WW, Werner I, Fard BM, Zalom FG, Oliver MN, et al. Pesticide runoff from orchard floors in Davis, California, USA: A comparative analysis of diazinon and esfenvalerate. *Agr Ecosyst Environ* 2006; 115: 56-68.
- Bunemann EK, Schwenke GD, Van Zwieten L. Impact of agricultural inputs on soil organisms - a review. *Aust J Soil Res* 2006; 44: 379-406.
- Carlsen SCK, Spliid NH, Svensmark B. Drift of 10 herbicides after tractor spray application. 2. Primary drift (droplet drift). *Chemosphere* 2006; 64: 778-786.
- Domange N, Grégoire C. Quality of in situ data about pollutant concentration. *TrAC* 2006;25:179-89.
- Druart C, Millet M, Scheifler R, Delhomme O, Raeppl C, de Vaufleury A. Snails as indicators of pesticide drift, deposit, transfer and effects in the vineyard. *Sci Total Environ* 2011; 409: 4280-4288.
- Felsot AS, Unsworth JB, Linders JBHJ, Roberts G, Rautman D, Harris C, et al. Agrochemical spray drift; assessment and mitigation - A review. *J Environ Sci Heal B* 2011; 46: 1-23.
- Fenoll J, Ruiz E, Flores P, Hellin P, Navarro S. Leaching potential of several insecticides and fungicides through disturbed clay-loam soil columns. *Int J Environ An Ch* 2010; 90: 276-285.
- Fiedler FR. Simple, practical method for determining station weights using Thiessen polygons and isohyetal maps. *J Hydrol Eng* 2003; 8: 219-221.
- Gil Y, Sinfort C. Emission of pesticides to the air during sprayer application: A bibliographic review. *Atmos Environ* 2005; 39: 5183-5193.

- Grégoire C, Payraudeau S, Domange N. Use and fate of 17 pesticides applied on a vineyard catchment. *Int J Environ An Ch* 2010; 90: 406-420.
- Imfeld G, Vuilleumier S. Measuring the effects of pesticides on bacterial communities in soil: A critical review. *Eur J Soil Biol* 2012; 49: 22-30.
- Kravchenko AN. Influence of spatial structure on accuracy of interpolation methods. *Soil Sci Soc Am J* 2003; 67: 1564-1571.
- Lazzaro L, Otto S, Zanin G. Role of hedgerows in intercepting spray drift: Evaluation and modelling of the effects. *Agr Ecosyst Environ* 2008; 123: 317-327.
- Mathers JJ, Wild, S. A., and Glass, C. R. Comparison of ground deposit collection media in field drift studies. *Aspects appl Biol* 2000; 57: 242-248.
- McGrath GS, Hinz C, Sivapalan M, Dressel J, Putz T, Vereecken H. Identifying a rainfall event threshold triggering herbicide leaching by preferential flow. *Water Resour Res* 2010; 46: W02513.
- Navarro S, Fenoll J, Vela N, Ruiz E, Navarro G. Photocatalytic degradation of eight pesticides in leaching water by use of ZnO under natural sunlight. *J Hazard Mater* 2009; 172: 1303-1310.
- Nuyttens D, De Schampheleire M, Baetens K, Sonck B. The influence of operator-controlled variables on spray drift from field crop sprayers. *T Asabe* 2007; 50: 1129-1140.
- Nuyttens D, De Schampheleire M, Verboven P, Brusselman E, Dekeyser D. Droplet Size and Velocity Characteristics of Agricultural Sprays. *T Asabe* 2009; 52: 1471-1480.
- Oliver DP, Kookana RS, Anderson JS, Cox JW, Waller N, Smith LH. Off-site transport of pesticides in dissolved and particulate forms from two land uses in the Mt. Lofty Ranges, South Australia. *Agr Water Manage* 2012; 106: 78-85.
- PPDB, Pesticide Properties DataBase. Agriculture & Environment Research Unit (AERU) at the University of Hertfordshire. <http://www.herts.ac.uk/aeru/footprint>. 2009.
- Provost D, Cantagrel A, Lebailly P, Jaffre A, Loyant V, Loiseau H, et al. Brain tumours and exposure to pesticides: a case-control study in southwestern France. *Occup Environ Med* 2007; 64: 509-14.
- Ramwell CT. Herbicide sorption to concrete and asphalt. *Pest Manag Sci* 2005; 61: 144-150.
- Rautmann D, Strelake M, Winkler R. New basic drift values in the authorization procedure for plant protection products. In: Forster, R., Strelake, M. (Eds), *Workshop on Risk Assessment and Risk Mitigation Measures in the Context of Authorization of plant protection (WORMM)* organised by Federal Biological Research Centre for Agriculture and Forestry, Biology Division, Braunschweig, Germany. *Parey. Mitt. Biol. Bundesanst. Land- Forstwirtschaft., Berlin.* 27-29 September 1999; 383: 133-141.
- Sinclair CJ, Boxall ABA, Parsons SA, Thomas MR. Prioritization of pesticide environmental transformation products in drinking water supplies. *Environ Sci Technol* 2006; 40: 7283-7289.
- Vischetti C, Cardinali A, Monaci E, Nicelli M, Ferrari F, Trevisan M, et al. Measures to reduce pesticide spray drift in a small aquatic ecosystem in vineyard estate. *Sci Total Environ* 2008; 389: 497-502.
- Xie YF, Chen TB, Lei M, Yang J, Guo QJ, Song B, et al. Spatial distribution of soil heavy metal pollution estimated by different interpolation methods: Accuracy and uncertainty analysis. *Chemosphere* 2011; 82: 468-476.

## Section 2. Fungicides transport in runoff from vineyard plot and catchment: contribution of non-target areas

Marie Lefrancq, Sylvain Payraudeau, Antonio Joaquín García Verdú, Elodie Maillard, Maurice Millet, Gwenaël Imfeld

(Section published in Environmental Science and Pollution Research; Appendices are given in Chapter VII)

### 1. Abstract

Surface runoff and erosion during the course of rainfall events are major processes of pesticide transport from agricultural land to aquatic ecosystem. These processes are generally evaluated either at the plot or the catchment scale. Here, we compared at both scales the transport and partitioning in runoff water of two widely used fungicides, i.e., kresoxim methyl (KM) and cyazofamid (CY). The objective was to evaluate the relationship between fungicide runoff from the plot and from the vineyard catchment. The results show that seasonal export for KM and CY at the catchment were larger than those obtained at the plot. This underlines that non-target areas within the catchment largely contribute to the overall load of runoff-associated fungicides. Estimations show that 85 and 62 % of the loads observed for KM and CY at the catchment outlet cannot be explained by the vineyard plots. However, the partitioning of KM and CY between three fractions, i.e., the suspended solids ( $> 0.7 \mu\text{m}$ ) and two dissolved fractions (i.e., between  $0.22$  and  $0.7 \mu\text{m}$  and  $< 0.22 \mu\text{m}$ ) in runoff water was similar at both scales. KM was predominantly detected below  $0.22 \mu\text{m}$ , whereas CY was mainly detected in the fraction between  $0.22$  and  $0.7 \mu\text{m}$ . Although KM and CY have similar physicochemical properties and are expected to behave similarly, our results show that their partitioning between two fractions of the dissolved phase differs largely. It is concluded that combined observations of pesticide runoff at both the catchment and the plot scales enable to evaluate the sources areas of pesticide off-site transport.

**Keywords:** Pesticide; Scale; Sorption; Partitioning; Deposition

## 2. Introduction

Pesticides are transported in the environment through different pathways, such as surface runoff and/or erosion (Oliver et al. 2012a). Pesticide transport is often evaluated at the plot scale or at the catchment scales (Viglizzo et al. 2011) but more rarely at both scales simultaneously. Combining experimental information obtained at different scales within the same catchment is necessary to identify the areas of off-site pesticide transport and to evaluate how pesticide runoff varies at different scales. At the plot scale, studies are generally conducted to identify the climatic or chemical factors affecting pesticide transport. These factors include the physicochemical properties of pesticides (Dores et al. 2009; Rice et al. 2010), rainfall and irrigation patterns (Candela et al. 2010; Silburn et al. 2013), or agricultural management (Warnemuende et al. 2007). At the catchment scale, studies generally focus on the temporal change of pesticide concentrations in relation to hydrological events (Davis et al. 2012; Oliver et al. 2012b) or on the transport pathways of pesticides based on hydrograph separation (Duffner et al. 2012; Taghavi et al. 2011). Several studies have shown that diffuse herbicide loss to surface waters may originate from a limited part of a catchment (Freitas et al. 2008; Frey et al. 2009). Spatial arrangement of the plots and agricultural practices also influence pesticide loss (Wohlfahrt et al. 2010). Studies including different observation scales have emphasised that pesticide dilution and re-infiltration processes occurred from field edges to the outlet of the catchment (Leu et al. 2004; Louchart et al. 2001). Overall, quantitative knowledge on pesticide transport in runoff combining plot and catchment scales at the same study site remains scarce.

Pesticide transport in runoff occurs either in the dissolved phase or sorbed onto suspended solids, depending mainly on the physico-chemical characteristics of the compound. Most studies to date focus on dissolved pesticide transport. However, more than 50 % of total pesticide loading in runoff can be accounted for by sorption to suspended solids depending on the chemical properties (Dores et al. 2009; Boithias et al. 2011). Hydrophobic pesticides are mainly transported in runoff in association with colloids and dissolved organic carbon (DOC) (Chen et al. 2010; Maillard et al. 2011). Hence, both dissolved and particulate loads should be accounted for when evaluating pesticide transport in agricultural runoff. The presence of pesticides in agricultural runoff due to intensive use in vineyards is a current environmental concern. Fungicides represent 80% of pesticide use in French viticulture (Provost et al. 2007). Kresoxim-methyl (KM) and cyazofamid (CY) are two systemic fungicides which are widely used in foliar spray applications to control grapevine downy mildew (*Plasmopara viticola*) for arable crops, fruit tree crops, and vine. KM and CY are known to be toxic for aquatic crustaceans and mammals, respectively (Table III-3). KM acid, one of the KM transformation products, is on the

priority list of the UK drinking water source protection (Sinclair et al. 2006). Residues of CY in grapes have been reported to exceed the European Union maximum residue level, which underline possible effects on public health (Gonzalez-Rodriguez et al. 2011). Although KM and CY are widely used in Europe (Eurostat, 2007) and may cause ecotoxicological effects, to the best of our knowledge, the transport in runoff of these fungicides has not been reported yet in vineyards. In this study, transport of KM and CY in runoff from a vineyard catchment of 42.7 ha and a representative plot of 878 m<sup>2</sup> was jointly evaluated and compared with respect to rainfall and hydrochemical patterns. The dissolved and particle-associated loads of KM and CY were quantified during a vine-growing season (i.e., May to August 2011) at the plot and the catchment scales in order to compare fungicide runoff and to evaluate the contribution of non-target areas to total pesticide losses at the catchment scale. In this study, non-target areas are defined as the areas where no pesticide applications are intended, such as forests, orchards, or road networks.

### 3. Material and methods

#### 3.1. Chemicals

Physical and chemical characteristics of KM and CY are provided in Table III-3. KM (methyl (E)-methoxyimino[ $\alpha$ -(otolyloxy)-o-tolyl]acetate) belongs to the strobilurin family and is the active substance of the Stroby DF<sup>®</sup> commercial formulation (BASF). CY, (4-chloro-2-cyano-N,N-dimethyl-5-ptolyimidazole-1-sulfonamide) belongs to the cyanoimidazole family and it is the active substance of the Mildicut<sup>®</sup> commercial formulation (ISK Biosciences Europe S.A.). The detailed composition of commercial preparations is provided in Table VII-5 in the Appendices. KM and CY have low vapor pressure (2.3 and  $13.3 \times 10^{-3}$  mPa, respectively) and a log  $K_{ow}$  in the same order of magnitude (3.4 and 3.2, respectively) (see Table III-3). In soil leaching studies, KM and CY were shown to be moderately mobile (Fenoll et al. 2010; Suciu et al. 2011). However, less is known about the environmental behaviour of KM and CY.

**Table III-3. Physico-chemical properties of kresoxim-methyl and cyazofamid. Data were obtained from PPDB (2011)**

		Kresoxim methyl	Cyazofamid
Chemical structure			
Chemical formula		C <sub>18</sub> H <sub>19</sub> NO <sub>4</sub>	C <sub>13</sub> H <sub>13</sub> ClN <sub>4</sub> O <sub>2</sub> S
Family		Strobilurin	Cyanoimidazole
Molecular mass	[g mol <sup>-1</sup> ]	313.35	324.78
Water solubility	[g L <sup>-1</sup> ]	2	0.1
Vapour pressure at 25°C	[10 <sup>-3</sup> mPa]	2.3	13.3
Henry's law constant at 25°C	[Pa m <sup>3</sup> mol <sup>-1</sup> ]	3.60 10 <sup>-4</sup>	4.03 10 <sup>-2</sup>
Log K <sub>ow</sub>	[-]	3.4	3.2
Log K <sub>oc</sub>	[-]	2.5	2.8
Soil degradation DT50	[d]	16	10
Water-Sediment DT50	[d]	1	14
Aqueous hydrolysis DT50 (20°C, pH 7)	[d]	35	25
Aqueous photolysis DT50 (pH 7)	[d]	18.2	0.1
<i>Daphnia</i> toxicity Acute 48 hour EC50	[mg L <sup>-1</sup> ]	0.2	0.2
<i>Oncorhynchus mykiss</i> toxicity Chronic 21 day NOEC	[mg L <sup>-1</sup> ]	0.013	0.13
<i>Rat</i> toxicity short term dietary NOEL	[mg kg <sup>-1</sup> ]	> 146	29.5

### 3.2. Description of the vineyard catchment

The 42.7 ha vineyard catchment is located in Rouffach, Alsace, France (47°57'9 N, 07°17'3 E) and was described previously (Grégoire et al. 2010). The scheme and detailed characteristics of the catchment are provided in Figure III-5 and Table III-4. The study was carried out between 24 May and 31 August 2011, because KM and CY use mainly proceeds during the mildew outbreak, i.e., between the end of May and middle of July. Briefly, 59% of the catchment is covered by vineyards and the main soil type is a calcareous clay loam with medium infiltration capacity. According to the hydrologic soil groups classification of USDA-SCS (1972), the soil surface distribution per soil type is 30% for B (moderately low runoff potential), 43% for C (moderately high runoff potential), and 27% for D (high runoff potential). The mean slope of the catchment is 15%.

The catchment is equipped with a meteorological station providing rainfall data with a resolution of 6 min. The mean precipitation value from 24 May to 31 August was 216 ± 75 mm

(1998 - 2011). Grass cover of vine plots in every two rows has been favoured since the 1980s as a means to reduce erosion and runoff (Tournebize et al. 2012). Hydrological surface connectivity is very low in the catchment due to the grass cover and concave grass strip. Previous observations showed that only 12 % of the catchment effectively contributes to runoff discharges that reach the outlet of the catchment. Rainfall-runoff events statistically occur every week and do not generate a permanent stream in the catchment. The road network accounts for 5% of the catchment area and represents the principal route of water flow within the catchment. Topography and flow direction have been provided in Figure VII-1 in the Appendices. Runoff coefficients ranged from 0.01 to 2.60% (2009 - 2010). Lower runoff coefficients are characteristic for vineyards with grass cover, such as *Lolium perenne* (L.) in the inter-rows (Novara et al. 2011).

### 3.3. Description of the experimental plot

The 878 m<sup>2</sup> plot (68.6 × 12.8 m) encompassed seven vine rows and was separated from adjacent rows with a 30 cm high border to ensure hydraulic separation from other plots (Figure III-5). This plot was cultivated with a *Vitis vinifera* Cv *Riesling* "Grand crus", and was covered every two rows with interrow grass consisting mainly of *Lolium perenne* (L.) (covering 90%), *Galium mollugo* (L.) (5%), and *Medicago lupulina* (L.) (5%). Inter-rows spacing were 280 cm for grass row and 140 cm for weeded rows. Vine feet were spaced about 140 cm each in a row. The vine training system was called single and/or double "Guyot." Overland flow generated from the plot flowed to a road through a 2 m grass strip, at which point it reached the outlet of the catchment (see Figure III-5).

The representativeness of the selected plot is based on (1) the slope (18%; the mean value for the vineyard plots is  $14.4 \pm 7.6\%$ ), (2) the hydrologic soil group (C; i.e., representing 45% of the vineyard soil of the catchment), (3) the occurrence of grass coverage every two vine plant rows (a crop management technique currently applied in France and applied on 69% of the vineyard catchment surface), and (4) the typical pattern of pesticide use (similar to that of the other plots in terms of chemicals, doses, and frequencies (see Tables VII-6 and VII-7 in the Appendices). This plot was therefore considered representative of the vineyard area for evaluating KM and CY transport.

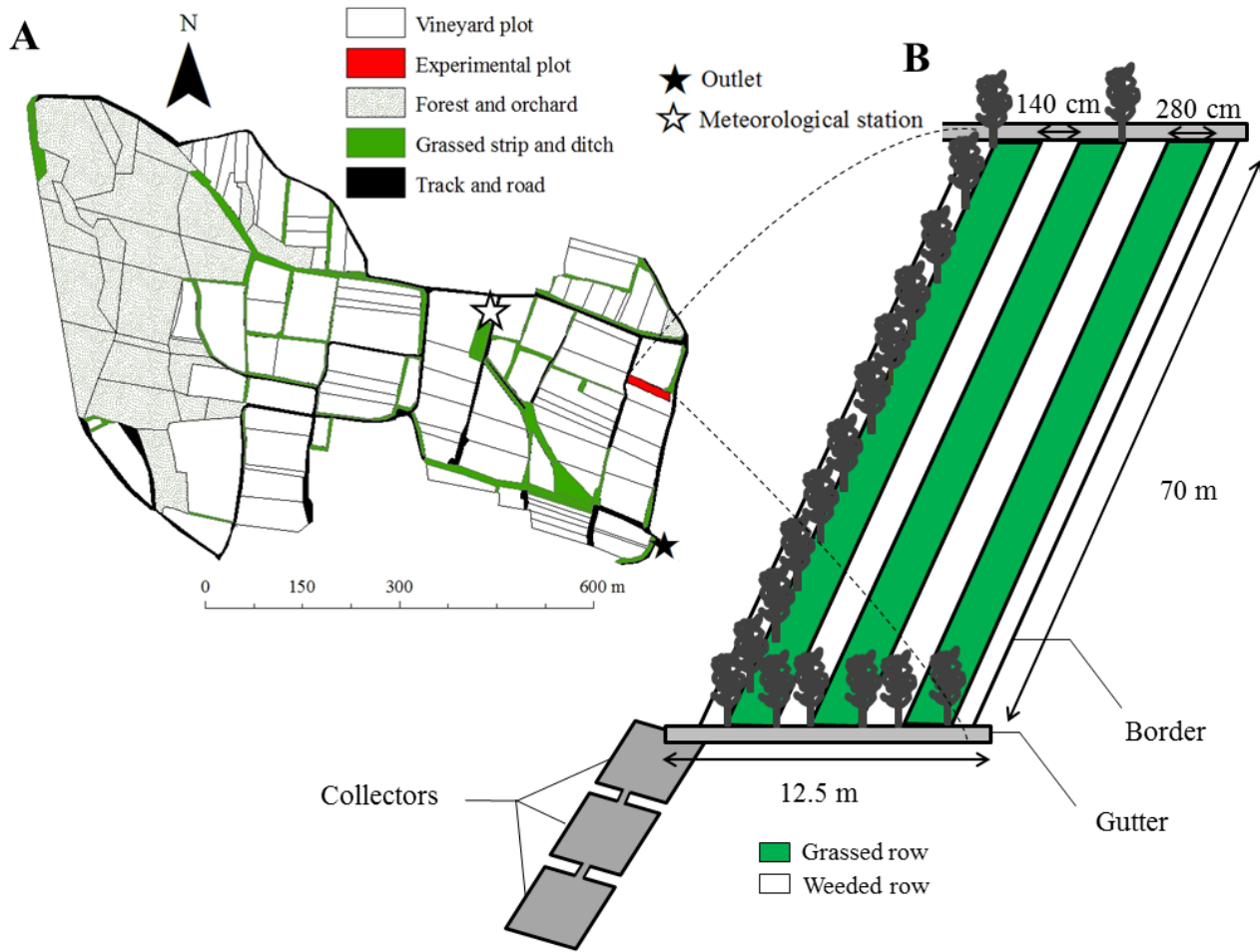


Figure III-5. Scheme of the catchment (A) and the experimental plot (B) (Rouffach, Alsace, France). The geographical coordinates of the meteorological station are 47°57'9N, 07°17'3E.

**Table III-4. Geomorphology and land use, hydrology and hydrochemistry from May 24 to August 31 2011 in the experimental plot and the vineyard catchment (Rouffach, France). Values are provided as the mean and ranges.**

	Parameter	Unit	Catchment	Plot
<b>Geomorphology</b>	Area	[ha]	42.7	0.088
	Elevation	[m]	230 - 379	246 - 252
	Slope	[%]	15	18
<b>Landuse</b>	Vineyard ratio	[%]	59	100
	Road network	[%]	5	0
	Forest/pasture	[%]	29	0
	Others (headland, ...)	[%]	7	0
<b>Hydrology</b>	Number of runoff events	[-]	38	15
	Runoff coefficient	[%]	1.76 (0.32 - 3.97)	0.13 (0.006 - 0.43)
	Normalised runoff volume	[m <sup>3</sup> ha <sup>-1</sup> ]	37.27	4.89
	Quiescent period	[d]	2.13 (0.03 - 7.56)	5.02 (0.16 - 14.96)
<b>Hydrochemistry</b>	pH	[-]	7.22 (6.69 - 7.81)	7.67 (7.10 - 8.35)
	DOC	[mg C L <sup>-1</sup> ]	22.76 (10.15 - 38.77)	23.80 (9.60 - 55.96)
	TOC	[mg C L <sup>-1</sup> ]	24.79 (11.63 - 37.74)	28.31 (9.46 - 57.74)
	NO <sub>3</sub> <sup>-</sup>	[mg L <sup>-1</sup> ]	0.74 (0 - 2.47)	6.40 (0 - 29.90)
	PO <sub>4</sub> <sup>3-</sup>	[mg L <sup>-1</sup> ]	1.96 (1.26 - 2.51)	4.46 (1.56 - 10.17)
	NH <sub>4</sub> <sup>+</sup>	[mg L <sup>-1</sup> ]	0.08 (0 - 0.15)	0.64 (0 - 1.27)
	NO <sub>2</sub> <sup>-</sup>	[mg L <sup>-1</sup> ]	0.07 (0 - 0.19)	0.17 (0 - 0.42)
	SO <sub>4</sub> <sup>2-</sup>	[mg L <sup>-1</sup> ]	7.82 (3.61 - 14.10)	17.81 (0 - 49.48)
	K	[mg L <sup>-1</sup> ]	5.27 (2.03 - 10.96)	16.15 (6.90 - 38.00)
	Fe <sub>t</sub>	[mg L <sup>-1</sup> ]	0.45 (0 - 2.02)	0.94 (0.14 - 2.07)
	Fe II	[mg L <sup>-1</sup> ]	0.27 (0 - 1.80)	0.48 (0.12 - 1.41)
	Mn	[mg L <sup>-1</sup> ]	0.07 (0 - 0.22)	0.10 (0.01 - 0.32)
	Cu	[mg L <sup>-1</sup> ]	0.038 (0.014 - 0.076)	0.135 (0.043 - 0.283)

### 3.4. Pesticide applications and soil deposition

The amount and time of KM and CY use were estimated based on surveys addressed to the vine growers which covered 83% of the total vineyard area in the catchment. Both compounds were applied in the same way and in similar amounts, 1,133 g for KM and 1,387 g for CY in the whole catchment. The soil deposition of fungicides reported in the present study result from the largest application of the vine growing season, and accounted for 97% of the total mass applied for KM on 24 May and 89% for CY on 9 June on 46% of the vineyard area. Additional applications of KM (on 1.2% of the vineyard) and CY (on 4.8% of the vineyard) (Figure III-6C) occurred between 3 June and 4 July. These additional applications (one for KM and two for CY) were carried out at more than 170 m from the experimental plot. Therefore, KM and CY drift on the experimental plot corresponding to these applications was assumed to account for a negligible fraction of the pesticide mass balance. However, these additional applications were taken into account to quantify the total fungicide export at the catchment scale. Fungicide amounts used per vineyard surface were 1.77 and 1.44 times larger at the plot scale than at the catchment scale for KM and CY, respectively (see Table III-5; Figure III-6C, D). Fifty one Petri dishes were used to collect fungicide droplets deposited on the soil surface of vineyard plots and plot margins, such as road networks or grass strips. The sampling procedure for characterising KM deposition on soil has been described previously (Lefrancq et al. 2013) and was identical for CY.

### 3.5. Runoff discharge measurement and water sampling procedure

At the plot outlet, runoff water was collected in a polyethylene gutter that conducted water into three connected stainless steel collectors of 68 L (Figure III-5). The collectors were covered to keep water in the dark. This volumetric measurement was retained instead of dynamic discharge measurement because of a large uncertainty for low outflow. For each runoff event, water height was recorded on a limnometric scale and converted to runoff volume (uncertainty of 0.01 L). Manual samples were taken within an average of 1.9 days after the runoff event. At the catchment outlet (Figure III-5), runoff discharges were continuously monitored from 24 May to 31 August 2011. The water depth was measured using bubbler flow modules with a precision of 1 mm (Hydrologic, Sainte-Foy, Quebec, Canada) combined with a Venturi channel. Three hundred millilitres of water were sampled for every 3 m<sup>3</sup> of discharge using a 4010 Hydrologic automatic sampler (Sainte-Foy, Quebec, Canada). The detailed procedure of sample collection and storage in order to ensure reliable pesticide measurements was tested and described previously (Domange and Grégoire 2006). Briefly, water samples were collected in glass jars, stored in the dark at 4 °C until collection, and placed on ice during transportation to the

laboratory. The series of discrete flow-proportional water samples taken during each week were combined in a single composite sample prior to analysis.

Water samples collected at the plot and the catchment outlet were sequentially filtered maximally within 12 h after collection. Filtrates were obtained following sequential filtration through 0.7 and 0.22  $\mu\text{m}$  filters. Filtrates were stored at  $-20\text{ }^{\circ}\text{C}$  in the dark until analysis. Fungicides in both filtrates were analysed and fungicides transported in the fraction between 0.7 and 0.22  $\mu\text{m}$  were determined by difference. Total suspended solids (TSS) were considered as the fraction larger than 0.7  $\mu\text{m}$ .

### 3.6. Soil sampling and characterization

Dissipation and/or sorption of KM and CY in soil were evaluated in the near-surface layer of soil which is strongly correlated with fungicide mobilisation in runoff (McGrath et al. 2008). Topsoil (0 - 3 cm) samples were collected weekly at the plot scale to measure soil water content and monthly to measure pH and organic matter. Soil samples for fungicide quantification were collected according to a pre-established logarithmic time scale: 0, 1, 3, 8, 14, 21, 34, 50, and 84 days after pesticide application. During each sampling campaign, five soil samples were randomly taken every 10 m from each unweeded vine row to avoid grass removal in the weeded vine row. Soil samples were taken from the weeded row 5 days after application (DAA). Differences on fungicides concentrations between weeded and unweeded rows remained below the analysis uncertainties and were therefore neglected. On the application day, soil samples were additionally analysed every 10 m to evaluate the intra-plot variability of fungicide application. Samples were collected using a stainless steel spoon and were then pooled into a single composite sample. Physicochemical characteristics of the topsoil were (in per cent): organic carbon, 8.2;  $\text{SiO}_2$ , 37.2;  $\text{Al}_2\text{O}_3$ , 6.2;  $\text{MgO}$ , 1.8;  $\text{CaO}$ , 21.8;  $\text{Fe}_2\text{O}_3$ , 3.5;  $\text{MnO}$ , 0.1;  $\text{Na}_2\text{O}$ , 0.4;  $\text{K}_2\text{O}$ , 1.7;  $\text{P}_2\text{O}_5$ , 0.3; and pH 7.1. Detailed norms and methods for pedological measurements are described in Table VII-8 in the Appendices. For fungicides quantification, soil samples were stored in the dark at  $-20\text{ }^{\circ}\text{C}$  until analysis.

### 3.7. Chemical analysis

For the deposition experiment, samples were concentrated using a rotary evaporator and analysed with a GC-MS/MS for KM and reverse phase HPLC at 280 nm for CY. The quantification limit (LOQ) was  $8.10^{-3}\text{ }\mu\text{g m}^{-2}$  for KM and  $2\text{ }\mu\text{g m}^{-2}$  for CY, and analytical uncertainties were 10% for KM and 2% for CY.

Hydrologic processes control the export of organic matter and nutrients from the agricultural land to aquatic ecosystem (Stieglitz et al. 2003; Thompson et al. 2012). The use of nutrients as hydrological tracers could therefore provide information on the hydrological connectivity and the relative contribution of plot margins versus agricultural plots. Concentrations of DOC, dissolved inorganic carbon, total organic carbon, total inorganic carbon,  $\text{NH}_4^+$ ,  $\text{NO}_3^-$ ,  $\text{NO}_2^-$ ,  $\text{PO}_4^{3-}$ ,  $\text{SO}_4^{2-}$ , Na, K, Mg, Ca, Al, Mn, Fe, Cu, Si, and  $\text{Cl}^-$  in water were determined following FR EN ISO standards and laboratory procedures. pH was measured using a WTW multi-350i portable sensors (WTW, Weilheim, Germany).

KM and CY in dissolved water, suspended solids, and soil were analysed according to the NF XPT 90 - 210. Briefly, KM and CY in water were analysed by online SPE LC-MS/MS. Both compounds had a LOQ of  $0.10 \mu\text{g L}^{-1}$  with uncertainties of 23% for KM and 24% for CY and a recovery rate of  $85 \pm 5\%$ . Extraction efficiencies of pesticides were obtained for each water sample set by spiking active substances in runoff water. Further quality control was achieved by using a blank for each set of samples.

KM and CY in soil and TSS were ultrasonically extracted by methanol with a contact time of 30 min, yielding a recovery rate of  $65 \pm 5\%$  and were analysed by LC-MS/MS. LOQ was determined to be  $10 \mu\text{g kg}_{\text{dried}}^{-1}$  with analytical uncertainties of 28% for KM and 33% for CY.

### 3.8. Data analysis and calculation

Hydrological and hydrochemical concentrations at the plot and catchment outlets were compared using the paired nonparametric Wilcoxon signed rank test and the Spearman rank correlation test. Statistical tests were performed using the R software (R development Core Team, 2008; version 2.6.2). When hydrochemical or fungicide concentrations were lower than the LOQ, sample concentration was set to zero for calculating the KM and CY mean concentrations, occurrences, and loadings. To evaluate seasonal load export of KM and CY, a seasonal export coefficient (SEC) was calculated with the quotient of the total load exported over the total mass applied during the season. The runoff coefficients associated with each runoff event were calculated using the entire area of the plot and the catchment. KM and CY applications and loads were normalised by the total vineyard area and expressed in grams per hectare of vineyard to distinguish non-target areas from application areas, such as forests, orchards, and roads, which comprise 41% of the catchment.

## 4. Results

### 4.1. Hydrology

Hydrological characteristics from 24 May through 31 August 2011 are provided in Table III-4 and Figure III-6A, B. Daily mean temperature varied between 10.6 and 27.6 °C and potential daily evapotranspiration ranged from 1.5 to 6.9 mm. Rainfall events were defined by a minimal interruption of 2 h with dry period. Fifty four rainfall events were monitored from 24 May to 31 August 2011, which amounted to 214.9 mm. These events varied in terms of range of total rainfall amounts (0.2 - 23.9 mm), durations (6 - 690 min), and intensities (0.03 - 1.00 mm min<sup>-1</sup>). Among these rainfall events, 38 produced runoff at the catchment scale (95% of the total rainfall during the investigation period) and among them, only 15 at the plot scale (79% of the total rainfall). Runoff events occurred at the plot scale with a minimum rainfall intensity threshold of 0.33 mm min<sup>-1</sup>. At the plot outlet runoff volume varied between 2 and 84 L (mean ± SD, 27 ± 29 L) (Figure III-6b; Table III-4). Runoff coefficients ranged between 0.006 and 0.429 % (mean ± SD, 0.130 ± 0.134). The quiescent period between two runoff events had a range of 0.16 to 14.96 days (mean ± SD, 5.02 ± 4.60 days) during the investigation period. The gravimetric water content in the plot soil samples ranged from 2 to 33% for the study period. A significant negative correlation was observed between water content and number of days without rainfall ( $p < 0.01$ ).

At the catchment outlet, runoff events occurred with a minimum rainfall intensity threshold of 0.10 mm min<sup>-1</sup>. The runoff volume for each event during the investigation period had a range of 1.91 to 195.41 m<sup>3</sup> (mean ± SD, 41.88 ± 50.23 m<sup>3</sup>) (Figure III-6A; Table III-4) generating a total volume of 1591.28 m<sup>3</sup>. Runoff coefficients varied between 0.32 and 3.97% (mean ± SD, 1.76 ± 0.73%). The mean quiescent period between two runoff events ranged from 0.03 to 7.56 days (mean ± SD, 2.13 ± 2.42 days) during the investigation period. Hydrochemical patterns of runoff generated from the plot and the catchment were also compared.

### 4.2. Hydrochemistry

Detailed hydrochemical characteristics are provided in Table III-4. Comparison of hydrochemical conditions between the plot and the catchment revealed no significant changes in either organic carbon, inorganic carbon, nitrites or sulphate concentrations during the investigation period ( $p > 0.05$ ) (see Table VII-9 in the Appendices). The concentration of DOC did not significantly differ between the plot and the catchment ( $p > 0.05$ ). The total DOC mass exported during the investigation period reached 151 g ha<sup>-1</sup> at the plot and 680 g ha<sup>-1</sup> at the

catchment scales. In contrast, nutrients, i.e.,  $\text{NO}_3^-$ ,  $\text{NH}_4^+$ ,  $\text{PO}_4^{3-}$ , and major elements, i.e., Cu, Al, Si, K, Na, Mg, and pH differed significantly between the plot and catchment samples (see Table VII-9 in the Appendices). Concentrations of nutrients and major element were generally higher at the plot scale than at the catchment scale (Table III-4).

#### 4.3. Deposition of KM and CY on soil

KM and CY deposition on the vineyard soil varied widely in space and time. For the study plot, KM concentration reached  $0.12 \text{ mg m}^{-2}$ . Deposition concentrations ranged between  $0.09$  and  $1.20 \text{ mg m}^{-2}$  in the catchment. CY deposition for 9 June resulted in a concentration of  $0.27 \text{ mg m}^{-2}$  at the study plot, and ranged between  $0.02$  and  $0.30 \text{ mg m}^{-2}$  in the catchment. At the catchment scale, the total mass of fungicides deposited on the vineyard plots was estimated to be  $60 \text{ g}$  (7% of the total mass applied) for KM and  $18 \text{ g}$  (2% of the total mass applied) for CY. Fungicide losses on plot margins were estimated by linear interpolation at maximally  $20 \text{ g}$  (2% of the total mass applied) for KM and  $6 \text{ g}$  (1% of the total mass applied) for CY with  $5.2 \text{ g}$  for KM and  $1.4 \text{ g}$  for CY only on roads. Details on KM deposition, estimates, and interpolation calculations have been described previously for KM (Lefrancq et al. 2013). A similar approach has been applied for CY deposition. This deposition resulted in a fungicide pool in the top layer of soil that could be mobilised during runoff.

#### 4.4. KM and CY mobilisation in the runoff dissolved phase ( $< 0.7 \mu\text{m}$ )

At the plot scale, KM and CY were not detected in the soil before applications. Following application, KM and CY concentrations in the soil were detected and gradually decreased down to no detection after 8 days for KM and 11 days for CY (see Table III-5; Figure III-6G). The spatial variability of fungicide concentrations observed directly after application in the plot area remained below analytical uncertainties.

Of the 15 water samples collected at the plot outlet, 28 and 50% had KM and CY concentrations above the LOQ. The first runoff events that occurred 8 and 6 days following application accounted for 3% of the total mass exported for KM and 50% for that of CY. KM and CY concentrations in runoff reached  $1.20$  and  $12.00 \mu\text{g L}^{-1}$ , respectively (Table III-5; Figure III-6D). The maximum pesticide concentration in runoff was observed 30 DAA for KM and 6 DAA for CY. The last runoff event in which KM and CY was quantified occurred 50 DAA for KM and 34 DAA for CY, though at this point KM and CY concentrations in the soil could not be quantified (Figure III-6G). Admittedly, the LOQ for pesticides analysis in water was two orders of

magnitude lower than for soil. Runoff events recorded at the plot scale yielded a total load of 0.06 and 0.17 mg, corresponding to a SEC of 0.01‰ for KM and 0.02‰ for CY (Table III-5; Figure III-6F). When the concentrations below the LOQ were set to the LOQ for water ( $< 0.7 \mu\text{m}$ ), the corresponding SEC estimates were 0.01 for KM and 0.03‰ for CY.

At the catchment outlet, 28 (KM) and 21% (CY) of water samples collected ( $n=16$ ) contained concentrations above the LOQ. KM and CY concentrations in runoff at the catchment scale rapidly decreased in 8 DAA (Figure III-6C); 16% for KM and 54% for CY of the total mass exported in runoff were already exported 8 DAA. Concentrations reached  $0.17 \mu\text{g L}^{-1}$  for KM and  $0.60 \mu\text{g L}^{-1}$  for CY. Maximum concentrations were measured in the first runoff event following the application of both compounds (see Table III-5; Figure III-6C). Runoff events yielded a total load of 72.01 and 57.44 mg corresponding to a SEC of 0.06‰ for KM and 0.04‰ for CY (Figure III-6E). When the concentrations were below the LOQ for water ( $< 0.7 \mu\text{m}$ ) and were set to the LOQ after the application, the corresponding SEC was estimated to 0.14‰ for KM and 0.13‰ for CY. KM and CY concentrations in runoff did not significantly differ between the plot and the catchment ( $p > 0.05$ ). KM loads were  $0.68 \text{ mg ha}_{\text{vineyard}}^{-1}$  at the plot and  $2.86 \text{ mg ha}_{\text{vineyard}}^{-1}$  at the catchment. CY loads were  $1.93 \text{ mg ha}_{\text{vineyard}}^{-1}$  at the plot and  $2.28 \text{ mg ha}_{\text{vineyard}}^{-1}$  at the catchment's outlet. These results underline that larger amounts of KM were exported at the catchment compared with those of CY, whereas at the plot scale the opposite trend was observed (Table III-5). These results underscore the different behaviour in KM and CY export in runoff, which may be reflected in the partitioning of KM and CY between suspended solids and two fractions of the dissolved phase.

**Table III-5. Kresoxim methyl and cyazofamid application and transport from May 24 to August 31 2011 in the experimental plot and the vineyard catchment (Rouffach, France). Values are provided as the mean and ranges.**

Parameter	Unit	Catchment		Plot		
		Kresoxim-methyl	Cyazofamid	Kresoxim-methyl	Cyazofamid	
<b>Application</b>	Amount	[g ha <sub>vineyard</sub> <sup>-1</sup> ]	45.06	55.17	79.55	79.55
	Soil concentration	[mg kg <sup>-1</sup> ]	-	-	(0 - 0.14)	(0 - 0.17)
<b>Soil</b>	Last detection after application	[d]	-	-	4-8	7-11
	Occurrence ( <i>n</i> )	[%]	28 (16)	21 (16)	28 (15)	50 (15)
<b>Water in dissolved phase (&lt; 0.7 µm)</b>	Concentration	[µg L <sup>-1</sup> ]	(0 - 0.17)	(0 - 0.60)	(0 - 1.20)	(0 - 12.00)
	Load	[mg ha <sub>vineyard</sub> <sup>-1</sup> ]	2.86	2.28	0.68	1.93
	Load	[mg ha <sup>-1</sup> ]	1.69	1.35	0.68	1.93
	Seasonal Export Coefficient (SEC)	[‰]	0.06	0.04	0.01	0.02

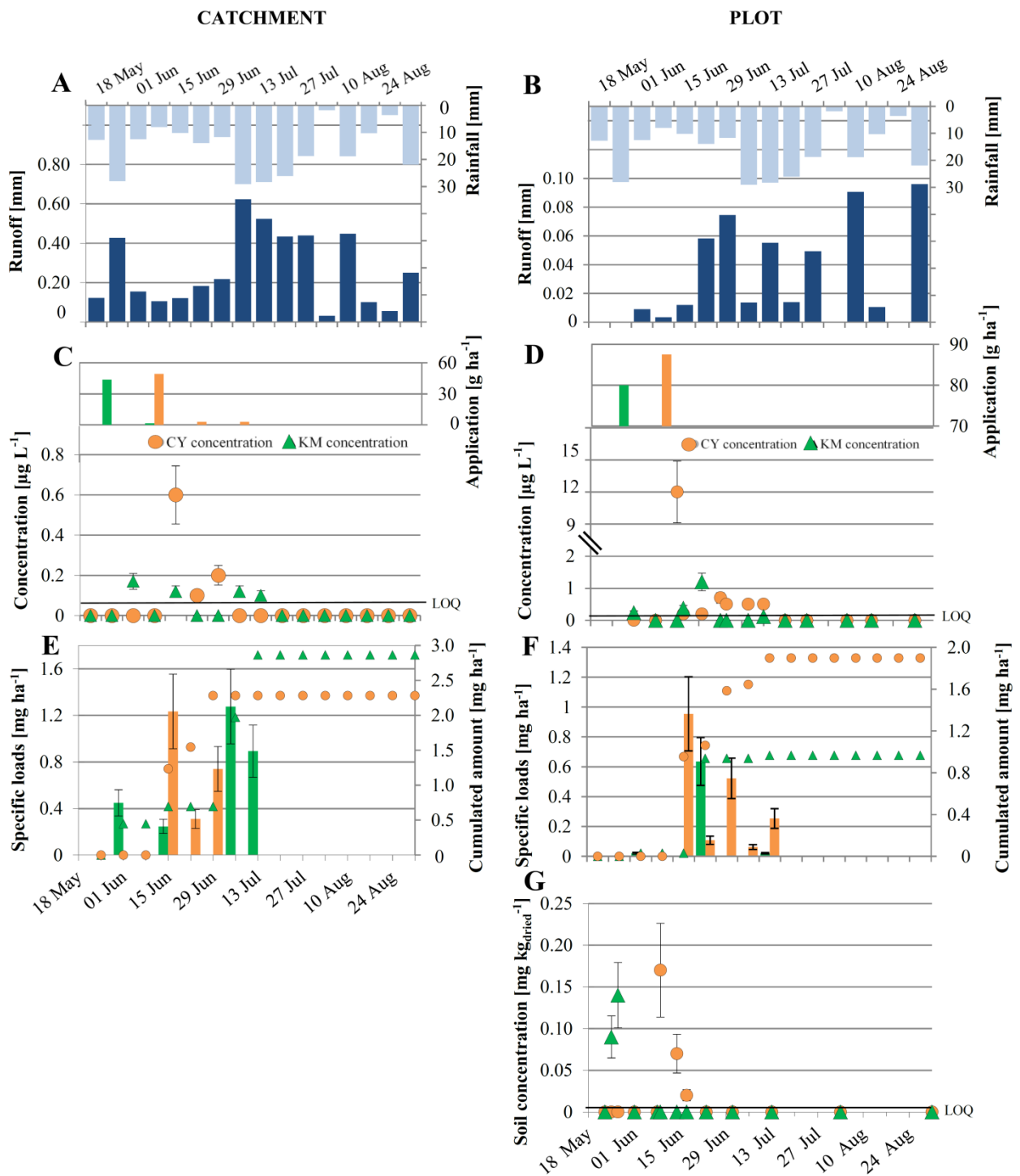


Figure III-6. Temporal changes in the hydrological conditions (A and B), the fungicides application (green bars for KM, orange bars for CY) and the concentrations in runoff water (C and D), the specific loads (green bars for KM, orange bars for CY) in runoff water (E and F), with the cumulated amount (markers) and fungicides concentrations in soil (G) at the catchment scale (left) and at the plot scale (right) from May 24 to August 31 2011. ▲ = KM and ● = CY. Figure III-6C and III-6D: error bars show the analytical uncertainty of pesticides measurements. Figure III-6E and III-6F: error bars show the total uncertainty associated with the pesticides measurement and the discharge measurement.

4.6. Partitioning of KM and CY in runoff

KM and CY were not detected in suspended solids ( $> 0.7 \mu\text{m}$ ) at plot or catchment scales for the duration of the study; 64.1 (0.04 mg) and 91.8% (66.10 mg) of total KM load occurred in the dissolved fraction of runoff below  $0.22 \mu\text{m}$  at both the plot and the catchment scale, respectively (see Figure III-7). KM concentrations below  $0.22 \mu\text{m}$  reached  $0.55 \mu\text{g L}^{-1}$  at the plot scale and  $0.27 \mu\text{g L}^{-1}$  at the catchment scale. Concerning CY, 98.7 (0.17 mg) and 100% (57.44 mg) of the exported load occurred in the dissolved fraction between  $0.22$  and  $0.7 \mu\text{m}$  for the plot and catchment scale, respectively (see Figure III-7). CY concentrations in the dissolved fraction below  $0.22 \mu\text{m}$  reached  $0.3 \mu\text{g L}^{-1}$  at the plot scale, although it was not detected in this fraction at the catchment scale.

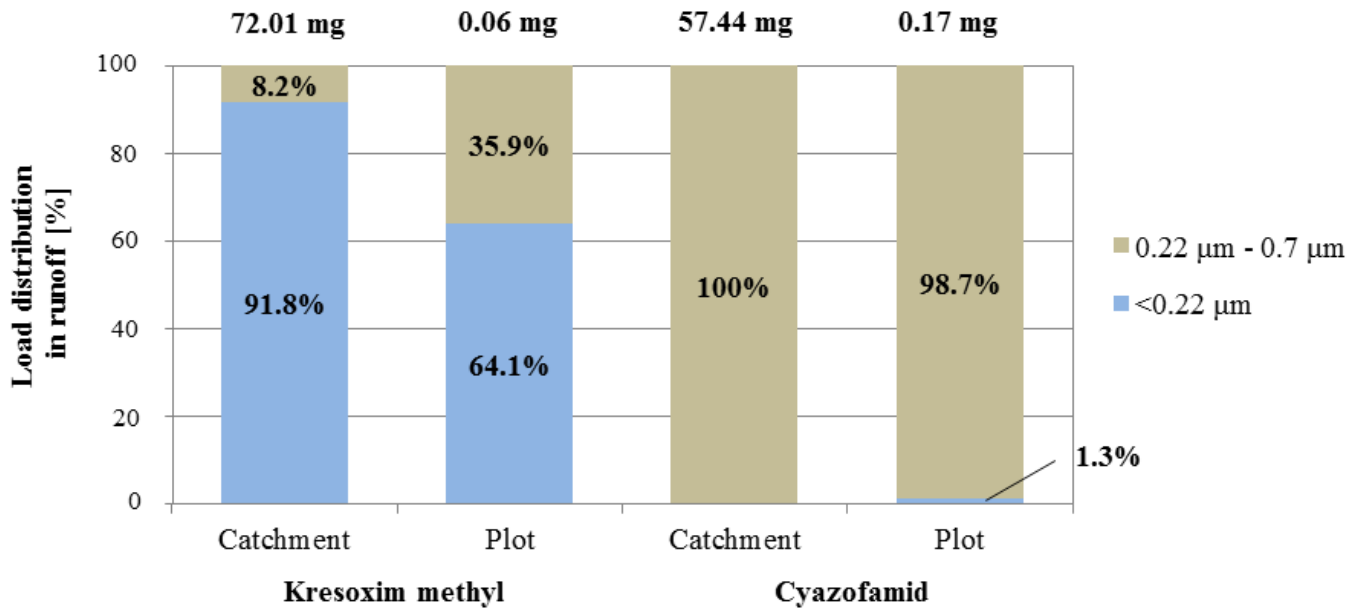


Figure III-7. Load distribution between the dissolved and particulate phases in runoff water at the catchment and plot scales (Rouffach, France). The total loads exported are reported at the top of the barplots.

## 5. Discussion

The off-site transport of fungicides in both dissolved and particulate phases needs to be better understood for an identification of environmental factors controlling fungicide runoff. Therefore, information obtained at both plot and catchment scales can be combined to evaluate the relative contribution of the plots and the plot margins to fungicide runoff.

At both scales, SEC remains very low and was lower than the values obtained in previous studies (Grégoire et al. 2010). However, previous studies showed lower pesticide concentrations at the catchment scale than at the plot scale, which indicates a dilution effect on pesticide concentrations due to non-treated areas, such as plot margins, and infiltration to groundwater (Leu et al. 2004; Louchart et al. 2001). The latter results differ from our observations in so far, as no significant difference could be observed between fungicide concentrations in runoff at the plot and catchment scales. In addition, loads normalised per vineyard area were larger at the catchment scale than at the plot scale. Fungicide loads at the catchment outlet can be estimated by extrapolating pesticide export observed at the experimental plot to the entire pesticide application area of the catchment. This estimation shows that 85 and 62% of the loads observed at the catchment outlet cannot be explained by an export from the vineyard plots. This result underscores that non-target areas within the catchment, such as plot margins, largely contribute to overall fungicide loads in runoff. In this study, only small storm events generating runoff occurred during the period close to the application. If larger storms were to occur shortly after the application of pesticides, the contribution of the plots to the overall pesticide loads at the catchment's outlet is expected to be higher. The different contributions from plots and plot margins to runoff-associated fungicide export at the catchment scale is discussed in the following with respect to hydrological and hydrochemical conditions, as well as fungicide deposition.

Lower occurrence and amount of runoff at the plot compared with the catchment scale can be explained by the grass cover on plots and the dense impermeable road network within the catchment. Consequently, the areas prone to generate runoff, and thus pesticide runoff, encompass the road network directly connected to the catchment outlet and plots when the runoff threshold is exceeded. At the catchment scale, hydrological connectivity between fields and plot margins is a major factor which determines the transport of pesticides from fields to the catchment outlet (Wohlfahrt et al. 2010). The decrease of nutrients and major ion concentrations such as Cu, Na, K, Si, and Al from the plot to the catchment outlet underlines the attenuation and/or dilution effect on hydrochemical concentrations between the scales

(Haygarth et al. 2005). The provision of DOC from the forest, dirt road or from bare soil plots likely led to higher DOC loads observed at the catchment compared with that at the plot. In addition, significant amounts of KM and CY deposited on non-target areas attested that fungicide drift represents a critical source of contamination leading to fungicide runoff. The higher deposited mass of KM on the plot margins (2.2% of the total mass applied) compared with that of CY (0.6% of the total mass applied) resulted in larger KM export at the catchment scale compared with CY, while at the plot scale, the opposite trend was observed. Our results also highlight that a similar partitioning of KM and CY within the dissolved phase of runoff occurred at both scales. KM was mainly found below 0.22  $\mu\text{m}$ , whereas CY was mostly found in the fraction between 0.22 and 0.7  $\mu\text{m}$ . Although KM and CY have similar physico-chemical properties, these results show that their partitioning in the dissolved phase in field samples differs. However, these properties are often specific for the active ingredient and given soil characteristics and may not be appropriate for understanding sorption of commercial products on suspended solids and/or DOC (Pose-Juan et al. 2011; Vryzas et al. 2007). This suggests that the physico-chemical properties are insufficient to quantitatively evaluate and predict the in situ partitioning of KM and CY within the dissolved phase. Besides, theoretical partitioning coefficients are often obtained under equilibrium conditions using static sorption experiments (Wauchope et al. 2002). However, under field conditions, sorption equilibrium is rarely reached because agricultural systems are highly dynamic and hydrological and chemical conditions are likely to vary over time and space (Lafrance and Caron 2012).

In pesticide transport studies, data collection and process knowledge mostly originate from the plot scale (Viglizzo et al. 2011), whereas transport models and management actions for pesticides often operate at the catchment and/or the regional scale (Reichenberger et al. 2007). Down or upscaling of experimental data or physicochemical processes are therefore considered to be critical in hydrology, hydrochemistry, and pesticide transport studies (Capel et al. 2001; Cerdan et al. 2004; Haygarth et al. 2005). Several studies have emphasised that runoff and pesticide losses were statistically similar for different plot size (Mounirou et al. 2012; Wauchope et al. 2004), and the results obtained at the smaller scale may be extrapolated for larger areas. However, these studies do not integrate different landscape elements typically found in agricultural catchments, such as plot margins and roads. A representative surface unit for off-site pesticide transport extrapolation at the catchment scale should include the different agricultural landscape elements, such as roads and plot boundaries. The inter-annual variability of off-site pesticide transport may be reduced with increasing scale size (Capel et al. 2001). This result can be explained by the fact that the catchment integrates pesticide runoff from tens to thousands of agricultural plots and plot margins, which may compensate pesticide loads from

year to year. In contrast, variability in meteorological conditions and application time largely accounts for changes in pesticide losses at the plot scale. The accuracy of an extrapolation of pesticide loads across the scales highly depends on pesticide properties. For pesticides with short half-life in the soil, such as KM and CY, it is difficult to predict across scales a common export pattern, because they are generally less detected in surface water at larger scale due to fast degradation (Capel et al. 2001). Studies at complementary scales multiply the cost, the time, and the measurements and may lead to methodological inconsistencies (Viglizzo et al. 2011). However, combining hydrological and chemical observations at different scales of an agricultural catchment can improve the knowledge on the respective contribution of plots and plot margins in the off-site transport of pesticides. The latter approach may consolidate predictions of pesticide transport at a particular scale.

## 6. Conclusion

Our results provide quantitative field data of transport and partitioning of KM and CY in runoff in both particulate and dissolved phases. Combining observations of pesticide runoff at both the catchment and plot scales enables to evaluate the source areas of off-site transport of agricultural pesticides. Altogether, our results highlight that (1) plots were not the main contributors of KM and CY load exports at the catchment scale during the investigated growing season, (2) fungicide drift on roads is a major transport pathway of KM and CY to the outlet of the catchment, (3) catchment complexity cannot be restricted to a group of individual agricultural plots generating pesticide loads for predicting off-site pesticide transport, and (4) that fungicide partitioning within the dissolved phase may greatly differ according to chemicals. Quantitative estimates of off-site pesticide transport may support the design and adaptation of mitigation strategies, including reducing pesticide drift on boundary areas.

## 7. Acknowledgements

The authors are members of REALISE, the Network of Laboratories in Engineering and Science for the Environment in the Alsace Region (France) (<http://realise.u-strasbg.fr>), from which support is gratefully acknowledged. This research has been funded by the Research Program EC2CO (CNRS-INSU) and the PhytoRET project (C.21) of the European INTERREG IV program Upper Rhine. Marie Lefrancq and Elodie Maillard were supported by a fellowship of the Rhine-Meuse Water Agency and the Alsace Region, respectively. The authors wish to thank the Agricultural and Viticulture College of Rouffach, the City of Rouffach and the farmers of the Hohrain domain, Rouffach, France. Special appreciation goes to the soil laboratory EOST UMS830 CNRS with Martine Trautmann for the soil analysis. We specially acknowledge as well René Boutin, Thomas Dreidemy, Romy Durst, Sophie Gangloff, Agnès Herrmann, Carole Lutz, Marie-Pierre Ottermatte, Eric Pernin, Brian Sweeney and Nicolas Tissot for their support in sampling, analysis or/and writing.

## 8. References

- Boithias L, Sauvage S, Taghavi L, Merlina G, Probst JL, Perez JMS (2011) Occurrence of metolachlor and trifluralin losses in the Save river agricultural catchment during floods. *J Hazard Mater* 196: 210-219
- Candela L, Caballero J, Ronen D (2010) Glyphosate transport through weathered granite soils under irrigated and non-irrigated conditions - Barcelona, Spain. *Sci Total Environ* 408: 2509-2516
- Capel PD, Larson SJ, Winterstein TA (2001) The behaviour of 39 pesticides in surface waters as a function of scale. *Hydrol Process* 15: 1251-1269
- Cerdan O, Le Bissonnais Y, Govers G, Lecomte V, van Oost K, Couturier A, King C, Dubreuil N (2004) Scale effect on runoff from experimental plots to catchments in agricultural areas in Normandy. *J Hydrol* 299: 4-14
- Chen GA, Lin C, Chen LA, Yang H (2010) Effect of size-fractionation dissolved organic matter on the mobility of prometryne in soil. *Chemosphere* 79: 1046-1055
- Davis AM, Lewis SE, Bainbridge ZT, Glendenning L, Turner RDR, Brodie JE (2012) Dynamics of herbicide transport and partitioning under event flow conditions in the lower Burdekin region, Australia. *Mar Pollut Bull* 65: 182-193
- Domange N, Grégoire C (2006) Quality of in situ data about pollutant concentration. *Trac-Trend Anal Chem* 25: 179-189
- Dores EFGC, Spadotto CA, Weber OLS, Carbo L, Vecchiato AB, Pinto AA (2009) Environmental Behaviour of Metolachlor and Diuron in a Tropical Soil in the Central Region of Brazil. *Water Air Soil Poll* 197: 175-183

- Duffner A, Ingwersen J, Hugenschmidt C, Streck T (2012) Pesticide Transport Pathways from a Sloped Litchi Orchard to an Adjacent Tropical Stream as Identified by Hydrograph Separation. *J Environ Qual* 41: 1315-1323
- Eurostat (2007 Edition) The use of plant protection products in the European Union: Data 1992-2003. statistical book.
- Fenoll J, Ruiz E, Flores P, Hellin P, Navarro S (2010) Leaching potential of several insecticides and fungicides through disturbed clay-loam soil columns. *Int J Environ An Ch* 90: 276-285
- Freitas LG, Singer H, Muller SR, Schwarzenbach RP, Stamm C (2008) Source area effects on herbicide losses to surface waters - A case study in the Swiss Plateau. *Agr Ecosyst Environ* 128: 177-184
- Frey MP, Schneider MK, Dietzel A, Reichert P, Stamm C (2009) Predicting critical source areas for diffuse herbicide losses to surface waters: Role of connectivity and boundary conditions. *J Hydrol* 365: 23-36
- Gonzalez-Rodriguez RM, Cancho-Grande B, Simal-Gandara J (2011) Decay of fungicide residues during vinification of white grapes harvested after the application of some new active substances against downy mildew. *Food Chem* 125: 549-560
- Grégoire C, Payraudeau S, Domange N (2010) Use and fate of 17 pesticides applied on a vineyard catchment. *Int J Environ Anal Chem* 90: 406-420
- Haygarth PM, Wood FL, Heathwaite AL, Butler PJ (2005) Phosphorus dynamics observed through increasing scales in a nested headwater-to-river channel study. *Sci Total Environ* 344: 83-106
- Lafrance P, Caron E (2012) Impact of vegetated filter strips on sorbed herbicide concentrations and sorption equilibrium in agricultural plots. *J Environ Sci Health B* 47: 967-974
- Lefrancq M, Imfeld G, Payraudeau S, Millet M (2013) Kresoxim methyl deposition, drift and runoff in a vineyard catchment. *Sci Total Environ* 442: 503-508
- Leu C, Singer H, Stamm C, Muller SR, Schwarzenbach RP (2004) Variability of herbicide losses from 13 fields to surface water within a small catchment after a controlled herbicide application. *Environ Sci Technol* 38: 3835-3841
- Louchart X, Voltz M, Andrieux P, Moussa R (2001) Herbicide Transport to Surface Waters at Field and Watershed Scales in a Mediterranean Vineyard Area. *J Environ Qual* 30: 982-991
- Maillard E, Payraudeau S, Faivre E, Grégoire C, Gangloff S, Imfeld G (2011) Removal of pesticide mixtures in a stormwater wetland collecting runoff from a vineyard catchment. *Sci Total Environ* 409: 2317-2324
- McGrath GS, Hinz C, Sivapalan M (2008) Modeling the effect of rainfall intermittency on the variability of solute persistence at the soil surface. *Water Resour Res* 44: W09432
- Mounirou LA, Yacouba H, Karambiri H, Paturel JE, Mahe G (2012) Measuring runoff by plots at different scales: Understanding and analysing the sources of variation. *Cr Geosci* 344: 441-448
- Novara A, Gristina L, Saladino SS, Santoro A, Cerda A (2011) Soil erosion assessment on tillage and alternative soil managements in a Sicilian vineyard. *Soil Till Res* 117: 140-147
- Oliver DP, Kookana RS, Anderson JS, Cox JW, Waller N, Smith LH (2012a) Off-site transport of pesticides in dissolved and particulate forms from two land uses in the Mt. Lofty Ranges, South Australia. *Agr Water Manage* 106: 78-85

- Oliver DP, Kookana RS, Anderson JS, Cox J, Waller N, Smith L (2012b) The off-site transport of pesticide loads from two land uses in relation to hydrological events in the Mt. Lofty Ranges, South Australia. *Agr Water Manage* 106: 70-77
- Pose-Juan E, Rial-Otero R, Paradelo M, Lopez-Periago JE (2011) Influence of the adjuvants in a commercial formulation of the fungicide "Switch" on the adsorption of their active ingredients: Cyprodinil and fludioxonil, on soils devoted to vineyard. *J Hazard Mater* 193: 288-295
- Provost D, Cantagrel A, Lebailly P, Jaffre A, Loyant V, Loiseau H, et al. (2007) Brain tumours and exposure to pesticides: a case-control study in southwestern France. *Occup Environ Med* 64: 509-14.
- Reichenberger S, Bach M, Skitschak A, Frede HG (2007) Mitigation strategies to reduce pesticide inputs into ground- and surface water and their effectiveness; A review. *Sci Total Environ* 384: 1-35
- Rice PJ, Horgan BP, Rittenhouse JL (2010) Pesticide Transport with Runoff from Creeping Bentgrass Turf: Relationship of Pesticide Properties to Mass Transport. *Environ Toxicol Chem* 29: 1209-1214
- Silburn DM, Foley JL, deVoil RC (2012) Managing runoff of herbicides under rainfall and furrow irrigation with wheel traffic and banded spraying. *Agr Ecosyst Environ* (in press)
- Sinclair CJ, Boxall ABA, Parsons SA, Thomas MR (2006) Prioritization of pesticide environmental transformation products in drinking water supplies. *Environ Sci Technol* 40: 7283-7289
- Stieglitz M, Shaman J, McNamara J, Engel V, Shanley J, Kling GW (2003) An approach to understanding hydrologic connectivity on the hillslope and the implications for nutrient transport. *Global Biogeochem Cy* 17
- Suciu NA, Ferrari T, Ferrari F, Trevisan M, Capri E (2011) Pesticide removal from waste spray-tank water by organoclay adsorption after field application to vineyards. *Environ Sci Pollut R* 18: 1374-1383
- Taghavi L, Merlina G, Probst JL (2011) The role of storm flows in concentration of pesticides associated with particulate and dissolved fractions as a threat to aquatic ecosystems Case study: the agricultural watershed of Save river (Southwest of France). *Knowl Manag Aquat Ec* 400: 06
- Thompson JJD, Doody DG, Flynn R, Watson CJ (2012) Dynamics of critical source areas: Does connectivity explain chemistry? *Sci Total Environ* 435, 499-508
- Tournebize J, Grégoire C, Coupe RH, Ackerer P (2012) Modelling nitrate transport under row intercropping system: Vines and grass cover. *J Hydrol* 440: 14-25
- USDA-SCS (1972) National Engineering Handbook. Part 360. Government Printing Office: Washington, D.C.
- Viglizzo EF, Ricard MF, Jobbagy EG, Frank FC, Carreno LV (2011) Assessing the cross-scale impact of 50 years of agricultural transformation in Argentina. *Field Crop Res* 124: 186-194
- Vryzas Z, Papadopoulou-Mourkidou E, Soulios G, Prodromou K (2007) Kinetics and adsorption of metolachlor and atrazine and the conversion products (deethylatrazine, deisopropylatrazine, hydroxyatrazine) in the soil profile of a river basin. *Eur J Soil Sci* 58: 1186-1199
- Wauchope RD, Yeh S, Linders JBHJ, Kloskowski R, Tanaka K, Rubin B, Katayama A, Kordel W, Gerstl Z, Lane M, Unsworth JB (2002) Pesticide soil sorption parameters: theory, measurement, uses, limitations and reliability. *Pest Manag Sci* 58: 419-445
- Wauchope RD, Truman CC, Johnson AW, Sumner HR, Hook JE, Dowler CC, Chandler LD, Gascho GJ, Davis JG (2004) Fenamiphos losses under simulated rainfall: Plot size effects. *T Asae* 47: 669-676

Warnemuende EA, Patterson JP, Smith DR, Huang CH (2007) Effects of tilling no-till soil on losses of atrazine and glyphosate to runoff water under variable intensity simulated rainfall. *Soil Till Res* 95: 19-26

Wohlfahrt J, Colin F, Assaghir Z, Bockstaller C (2010) Assessing the impact of the spatial arrangement of agricultural practices on pesticide runoff in small catchments: Combining hydrological modeling and supervised learning. *Ecol Indic* 10: 826-839

Overall, the investigation of drift and transport of fungicides in vineyard catchment demonstrated that (i) pesticide drift onto roads is not negligible and represents a major transport pathway to surface water in such vineyard catchments strongly impacted by anthropogenic forcing, (ii) erosion was negligible in such a catchment where grass cover of vine plots in every two rows has been favoured since the 1980s, (iii) fungicide partitioning within the dissolved phase may greatly differ according to chemical properties and (iv) combined observations of pesticide runoff at both the catchment and the plot scales enable to evaluate the sources areas of pesticide off-site transport.

# Chapter IV. Herbicide transport and attenuation via runoff and erosion in arable crop catchment

---

For better understanding of pesticide transport via erosion, we studied pesticide transport in a corn catchment where erosion may occur significantly compared to the vineyard catchment. The two scales approach was therefore likewise applied in an arable crop catchment in Alsace (Alteckendorf, Alsace, France), prone to frequent mudflows.

Chloroacetanilide herbicides are used to control annual grasses and broad-leaved weeds on a variety of crops including corn, sugar beet and sunflower. They are applied pre-emergence to row crops which are therefore easily prone to runoff and erosion. *S*-metolachlor and acetochlor are among the ten most commonly used herbicides in the European Union and the United States. The transport and partitioning of *S*-metolachlor and acetochlor were evaluated. *S*-metolachlor comprises of four stable stereoisomers with an asymmetric carbon atom and an axial chirality. Its degradation in agricultural soil may lead to an enrichment of the heavier isotope and/or one specific enantiomer, which might be reflected during pesticide transport.

The transport by runoff and erosion of these two herbicides was evaluated in a headwater agricultural catchment and a combination of three methods was tested to assess the in situ degradation of *S*-metolachlor in runoff water at catchment scale: analysis of (i) parent and (ii) daughter compound concentrations, (iii) enantiomer ratios.

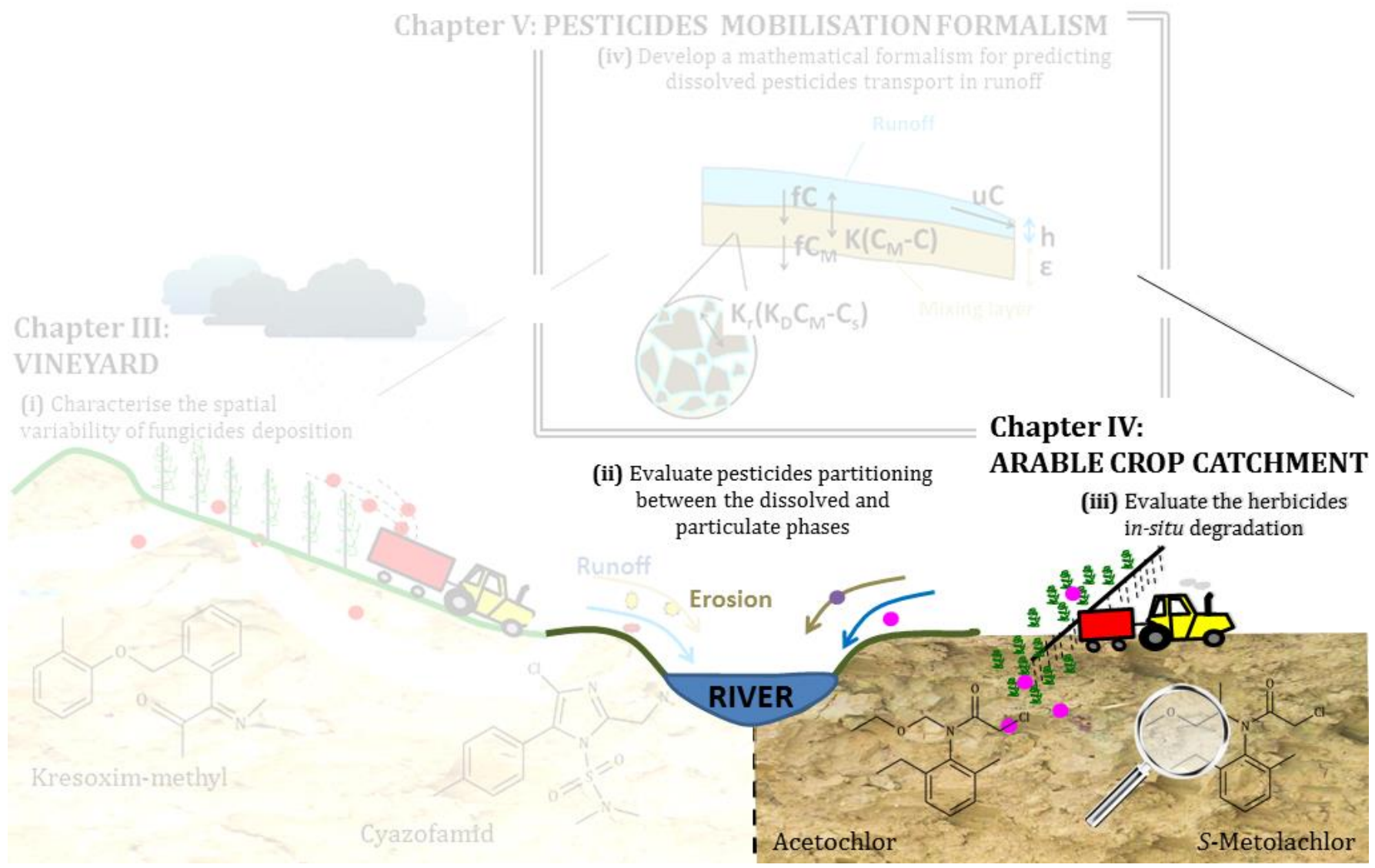


Figure IV-1. Graphical outline of the PhD thesis (Chapter IV)

## Section 1. Transport and attenuation of chloroacetanilides in an agricultural headwater catchment

Marie Lefrancq, Gwenaël Imfeld, Benoit Guyot, Maurice Millet, Sylvain Payraudeau

(This part is in preparation for publication, Appendices are given in Chapter VII)

### 1. Abstract

Chloroacetanilides are pre-emergent herbicides used on corn and sugar beet and are applied to bare soil, which is prone to runoff and erosion. Determination of their transport in the dissolved and particulate phases of runoff water and degradation in agricultural catchments is currently lacking. The objectives of this study were i) to assess the export of two chloroacetanilides (*S*-metolachlor and acetochlor) and four degradation products (ethane sulfonic (ESA) and oxanilic acid (OXA) degradates of metolachlor (MESA and MOXA) and acetochlor (AcESA and AcOXA)) in an agricultural catchment to account for both the dissolved and particulate phases over an agriculture season, and ii) to apply enantiomer analyses to evaluate *S*-metolachlor biodegradation. Runoff, erosion, hydrochemistry and chloroacetanilide transport were evaluated at both the plot and catchment scales. Partitioning between the dissolved and particulate chloroacetanilide phases largely varied over time and was dependent on the suspended solid concentrations and rainfall-runoff event characteristics. *S*-metolachlor degradation products strongly persisted in the runoff water compared to the acetochlor degradation products. Enantiomeric fractionation was observed at the catchment outlet with low concentrations of *S*-metolachlor, suggesting that *S*-enantioselective degradation occurred. Thus far, this is the first investigation that has combined the degradation products and enantiomer analyses of *S*-metolachlor in different environmental matrices (soil, suspended solids and water) within an agricultural catchment. We anticipate that our results will be a starting point for the improved understanding and prediction of the transport and degradation of chloroacetanilides at the agricultural catchment scale.

#### Keywords:

Runoff; Sorption; Herbicides; Enantiomeric fractionation; Biodegradation; Partitioning

## 2. Introduction

Pre-emergent herbicides are applied to bare soil, which is prone to runoff and erosion. Chloroacetanilides are primary pre-emergent herbicides used on corn and sugar beet (Eurostat, 2007) and have a moderate to high chronic toxicity for aquatic vertebrates, invertebrates, and aquatic plants (Cai et al., 2007; He et al., 2013; Liu and Xiong, 2009; Zhang et al., 2013). The acetochlor and metolachlor chemical structures differ only in their alkoxyalkyl moiety attached to the N-atom in the acetanilide group, resulting in differences in terms of toxicity, transport and degradation (Figure IV-3) (Barbash, 2014; Elsayed et al., 2014; Saha et al., 2012). *S*-metolachlor is a chiral molecule and presents four stable stereoisomers (two pairs of enantiomers and two pairs of diastereomers) resulting from two chiral elements: one from an asymmetrically substituted carbon and the other from a hindered rotation around the C-N axis (Figure VII-2) (Buser et al., 2000). Among chloroacetanilides, metolachlor and acetochlor have been observed as being more highly sorbed in soil (Liu et al., 2000). Chloroacetanilides exported in both the dissolved and particulate phases should be accounted for in catchments prone to hard runoff and erosion (Oliver et al., 2012). *S*-metolachlor and acetochlor are frequently detected along side their degradation products in global surface waters (Freitas et al., 2008; Steele et al., 2008; Ye, 2003). Chloroacetanilides undergo degradation that results in the production of more than 30 and 25 different degradation products for *S*-metolachlor and acetochlor, respectively (Hladik et al., 2008b; Roberts et al., 1999; Steele et al., 2008). The ethane sulfonic (ESA) and oxanilic acid (OXA) degradates of metolachlor (MESA and MOXA) and acetochlor (AcESA and AcOXA) are the most prevalent *S*-metolachlor and acetochlor degradation products and were frequently detected in laboratory studies, groundwater systems and surface water bodies (Baran and Gourcy, 2013; Dictor et al., 2008; Steele et al., 2008). However, the analysis of the degradation products may have limitations when used to quantify the degradation processes. In particular, the degradation of the commercial formulation results in the formation of degradation products that are mostly unknown and for which few analytical standards are currently available, limiting their identification (Boxall et al., 2004; Hladik et al., 2008a). Therefore, alternative approaches are required to evaluate the relative contribution of different attenuation processes, such as sorption, dilution or degradation in the environment (Turner et al., 2006).

Although the enantiomer ratios are not affected by abiotic attenuation processes for chiral compounds, biological processes, such as microbial degradation, may be enantioselective. Thus, enantiomer analyses may indicate the occurrence of biodegradation and have already been successfully applied to assess the biodegradation of various pesticides, such as metalaxyl in batch experiments (Celis et al., 2013) or phenoxyacid herbicides in groundwater systems

(Milosevic et al., 2013). However, little is known of the fate of metolachlor stereoisomers in the environment, and the enantioselective biodegradation of metolachlor in various environmental compartments remains controversial (Buser et al., 2000; Klein et al., 2006; Kurt-Karakus et al., 2010). The objectives of this study were i) to assess the export of two chloroacetanilides, i.e., *S*-metolachlor and acetochlor, and four degradation products (ethane sulfonic (ESA) and oxanilic acid (OXA) degradates of metolachlor (MESA and MOXA) in an agricultural catchment to account for both the dissolved and particulate phases over an agriculture season, and ii) to apply enantiomer analyses to evaluate *S*-metolachlor biodegradation. The transport of chloroacetanilide in the surface water at the outlet of a drain, plot and catchment was jointly evaluated and compared to the rainfall and hydrochemical patterns. The study was carried out between March 12 and August 14, 2012 because the use of *S*-metolachlor and acetochlor proceeds in March-April for the pre-emergence control of weeds and because springtime is a mudslide risk period resulting from extensive bare soil.

### **3. Material and methods**

#### **3.1. Description of the study site**

The 47-ha catchment is located 30 km north of Strasbourg (Alteckendorf, Alsace, France) (Figure IV-2). The mean slope is 6.7% ( $\pm$  4.8%), and the altitude ranges between 190 and 230 m. Geological features of the lower hills of the Vosges include Mesozoic marls and limestone that are overlain by silty material assumed to have originated from loess alteration.

The spatial variability of the soil was characterised by 48 soil surface samples (0 - 20 cm) in April 2011 and six 2-m soil profiles in November 2012. The main soil type is calcareous brown earth, and there are calcic soils on hillsides and calcic colluvial soils in the central thalweg. The grain size distributions of 6 soil profiles presented low variation ( $n = 30$ ) (mean  $\pm$  SD in percent): clay  $29.5 \pm 5.8$ , silt  $64.2 \pm 6.5$  and sand  $6.4 \pm 2.9$ . The soil characteristics (mean  $\pm$  SD) were  $\text{CaCO}_3$   $10.7 \pm 8.1\%$ , organic matter  $1.1 \pm 0.8\%$ , pH  $7.2 \pm 0.6$ , phosphorus  $0.04 \pm 0.04 \text{ g kg}^{-1}$  and CEC  $12.7 \pm 2.8 \text{ cmol}^+ \text{ kg}^{-1}$ . The detailed norms and methods of the soil measurements are described in Table VII-10 in the Appendices.

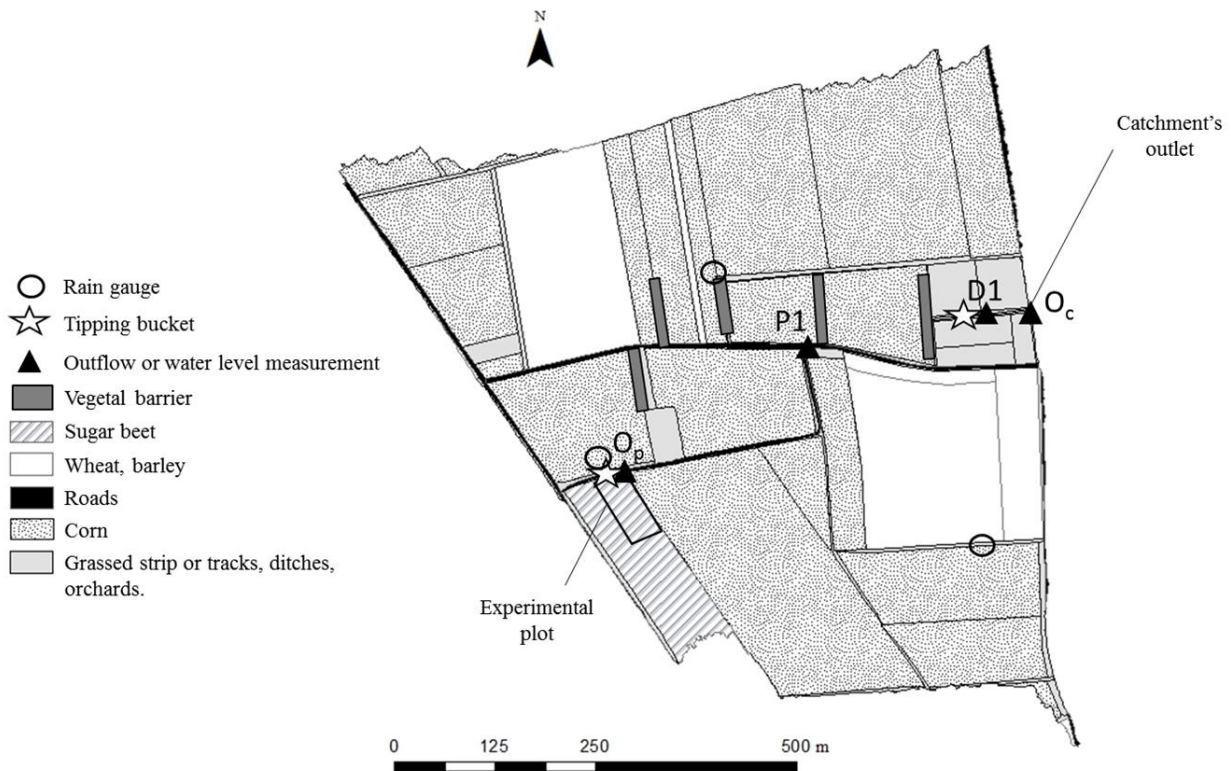
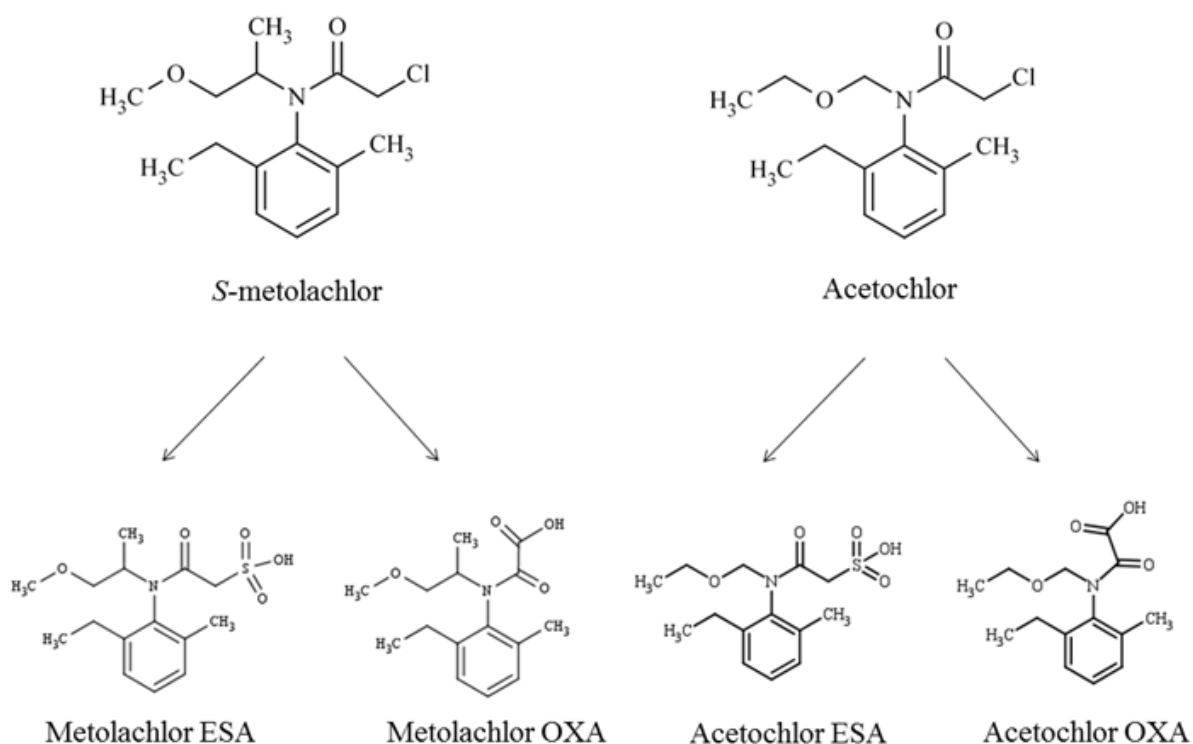


Figure IV-2. Scheme of the catchment (Alteckendorf, Alsace, France).

Water was conducted to the outlet of the catchment via ditches to a 50 cm diameter pipe under the road (Figure IV-2). A drainage system has existed since 1950; one drain (D1, see Figure IV-2) was detected as active during the campaign and flowed to a ditch 102 m from the outlet. No flow was observed for the other drains during the study period. The mean precipitation from March 12 to August 14 was  $295 \pm 69$  mm (2005 - 2011). The catchment was intensively cultivated; 88% was arable land, and corn (68%), winter wheat (16%) and sugar beet (4%) were the principal crops in 27 farming plots. Corn and sugar beet are usually sown between mid-March and the end of May, leading to the prevalence of bare soil during this period. The catchment study area is prone to significant mudslides every two years (Heitz et al., 2012). In 2009, five vegetative barriers were installed on the water pathways to decrease the water velocity and to retain sediments during large rainfall-runoff events (Figure IV-2). Within the catchment, a 77.2- $m^2$  sugar beet plot was located in the uphill region and hydrologically isolated from the adjacent plots by a 60-cm high HDPE border at 30-cm soil depth (Figure IV-2). The plot slope was 4.7%, and the plot instrumentation was removed on July 10, 2012 as a result of agricultural operations.

### 3.2. Herbicides characteristics and applications

*S*-metolachlor (2-chloro-N-(2-ethyl-6-methylphenyl)-N-[(1*S*)-2-methoxy-1-methylethyl]acetamide) is the active compound of the commercial formulations Mercantor Gold, Dual Gold and Camix (Syngenta) (Figure IV-3). Acetochlor (2-chloro-N-(ethoxymethyl)-N-(2-ethyl-6-methylphenyl)acetamide) is the active compound of the commercial formulation Harness (Dow Agrosciences) (Figure IV-3). *S*-metolachlor and acetochlor are nonionic (Bedmar et al., 2011) and moderately soluble in water (solubility of 480 and 282 mg L<sup>-1</sup> and Log *K*<sub>ow</sub> of 3.05 and 4.14, respectively). The reported organic carbon normalised soil water partition coefficient (*K*<sub>oc</sub>) values in soil batch studies ranged from 62 to 372 L kg<sup>-1</sup> for *S*-metolachlor and 86 to 328 L kg<sup>-1</sup> for acetochlor depending on the soil characteristics (Alletto et al., 2013; Hiller et al., 2008). Less is known of the environmental fate of *S*-metolachlor and the acetochlor degradates ESA and OXA (Figure IV-3) (Baran and Gourcy, 2013; Dictor et al., 2008). ESA and OXA have a higher polarity and solubility and lower *K*<sub>d</sub> values than their respective parent compounds (Krutz et al., 2004; McCarty et al., 2014). Because of their large solubility (in the order of 10<sup>5</sup> mg L<sup>-1</sup>), only dissolved concentrations of ESA and OXA were measured in this study.



**Figure IV-3. Chemical structure of *S*-metolachlor, acetochlor and their degradation products: ethane sulfonic (ESA) and oxanilic acids (OXA) metabolites of metolachlor (MESA and MOXA) and acetochlor (AcESA and AcOXA)**

Racemic metolachlor and acetochlor were applied in the study site from the early and late 1990s, respectively. Since 1998-2000, metolachlor has been replaced by *S*-metolachlor (the herbicidally active enantiomer), which is isomerically enriched in the enantiomer-*S* (80/20%) (Blaser, 2002). The amounts, timing and location of the acetochlor and *S*-metolachlor applications were estimated based on surveys addressed to the farmers who covered 88% of the catchment crop area, and identical application practices were assumed for the remaining area. A total of 10.44 and 10.95 kg of acetochlor and *S*-metolachlor, respectively, were applied for the 10 days following corn and sugar beet sowing in the catchment during the study period (Figure IV-4). The Mercantor Gold commercial formulation (Syngenta) was applied twice (April 12 and May 1) on the plot, and no acetochlor was applied.

### 3.3. Hydrological measurements and sampling procedure

Two tipping buckets and 3 cumulative rain gauges were installed within the study catchment (Figure IV-2) and read every week to evaluate spatial variation in rainfall. At the catchment outlet (Figure IV-2), water discharge was measured using a Doppler flowmeter (2150 Isco, Lincoln, Nebraska, USA). Flow proportional water samples were systematically collected every 20 m<sup>3</sup> using a cooled automatic sampler (Isco Avalanche, Lincoln, Nebraska, USA). A punctual water sample at the catchment outlet was collected in November 2012.

At the plot scale, runoff water was collected by a polyethylene gutter. Water level measurements ( $O_p$  in Figure IV-2) were conducted using a Venturi channel combined with a surface water level sensor (ISMA, Forbach, France). Because of plot border overflowing, the water mass balance could not be precisely estimated at the plot scale. Flow proportional water samples were collected every 7 L by a cooled automatic sampler (Isco Avalanche, Lincoln, Nebraska, USA). Point water sampling was collected weekly at the drain (D1, Figure IV-2) until July 10. The water samples were collected in glass flasks, stored in the dark at 4 °C after each runoff event and placed on ice during transportation to the laboratory for chemical analysis.

Sediments were collected monthly at the outlet of the catchment for chemical and granulometric analyses. At the plot scale, the topsoil (0 - 3 cm) samples were collected before the application and 5, 12, 20, 27, 33, 40, 47, 60, 75 and 89 days following the application. On July 10, one 1-m depth core were extracted at the plot scale to estimate the vertical herbicide transport. The soil samples were kept frozen at -20 °C until pesticide analysis.

### 3.4. Hydrochemical and soil analysis

The conductivity, pH, dissolved oxygen and redox potential were continuously measured at the catchment outlet using Acteon 3000 sensors (Ponsel, Caudan, France). Nine hydrochemical parameters (TIC, DIC, TOC, DOC,  $\text{PO}_4^{3-}$ ,  $\text{P}_{\text{tot}}$ ,  $\text{NO}_3^-$ ,  $\text{NO}_2^-$  and  $\text{NH}_4^+$ ) were determined by FR EN ISO standards and laboratory procedures. The water samples were filtered through 0.7- $\mu\text{m}$  glass fibre filters to separate the dissolved and particulate phases. Organic matter, pH and water content of the soil samples were determined over time according to FR EN ISO standards and internal procedures (Table VII-10).

### 3.5. Chloroacetanilide analysis

#### 3.5.1 Chemicals

Chromasolv Plus methylene chloride, methanol and ethyl acetate at analytical grade purity ( $\geq 99.9\%$ ) (Sigma Aldrich, St Quentin Fallavier, France) were used for the chloroacetanilide analyses. Metolachlor- $\text{d}_6$  and alachlor- $\text{d}_{13}$  were obtained from Dr. Ehrenstorfer GmbH (Augsburg, Germany) and used as internal standards for the chloroacetanilide quantification. The analytical standards of metolachlor, acetochlor and the ethane sulfonic (ESA) and oxanilic acids (OXA) degradates of metolachlor (MESA and MOXA) and acetochlor (AcESA and AcOXA) (Pestanal, analytical grade purity  $>95\%$ ; Sigma Aldrich, St Quentin Fallavier, France) were used to develop the analytical method.

#### 3.5.2 Extraction

The chloroacetanilide quantification was conducted on the suspended solid ( $4 \pm 9$  g), sediment (5 g) and soil (5 g) samples with 4 mL of ACN/pure water (v:v 60/40) by shaking for 1 min (Vortex), incubating for 30 min at  $115^\circ\text{C}$ , shaking for an additional 1 min and centrifuging for 10 min at 3500 rpm. The supernatant was then collected, and a second extraction was carried out using the same protocol with the addition of 0.1%  $\text{H}_3\text{PO}_4$ . The supernatant was then filtered using a 0.2- $\mu\text{m}$  PTFE filter, concentrated with rotary evaporation to one droplet, resuspended in 50 mL of pure water and extracted by solid-phase extraction (SPE).

The SPE of the water, suspended solids, sediments and soil samples were performed using SolEx  $\text{C}_{18}$  cartridges and an AutoTrace 280 SPE system (Dionex, CA, USA). The extraction cartridges were washed with 5 mL of ethyl acetate, followed by 5 mL of methylene chloride and

sequentially conditioned by 10 mL of methanol and 10 mL of deionised water. The conditioned cartridges were then loaded with the samples and dried with nitrogen for 10 min. The elution of the chloroacetanilide herbicides and their degradation products was performed successively with 3 mL of ethyl acetate and 2 mL of methylene chloride. Samples were concentrated under nitrogen flux to 1 droplet, and 2 mL of methylene chloride were added.

### **3.5.3 Quantification of the chloroacetanilides and their degradation products**

The chloroacetanilides were quantified by a GC-MS/MS (ITQ 700 model, Thermo Fisher Scientific, Les Ulis, France) using metolachlor-*d*<sub>6</sub> and alachlor-*d*<sub>13</sub> as internal standards (100 µg L<sup>-1</sup>) for *S*-metolachlor and acetochlor, respectively. The chloroacetanilide separation was conducted on a 5% phenyl - 95% dimethylpolysiloxane fused-silica capillary column using a 30 m x 0.25 mm ID, and 0.25-µm film thickness OPTIMA 5MS (Macherey Nagel GmbH, Düren, Germany) with helium as a carrier gas at a flow rate of 1 mL min<sup>-1</sup>. The quantification limits for the water samples were 0.02 and 0.05 µg L<sup>-1</sup> with a recovery efficiency of 96% and 43% for metolachlor and acetochlor, respectively, with a mean analytical uncertainty of 8%. The detection limits, retention times and selected ions used for identification are detailed in Table VII-11. The quantification limits of the solid samples were 0.01 and 0.05 mg kg<sup>-1</sup> with a recovery efficiency of 74% and 63% and analysis uncertainty of 16% and 22% for metolachlor and acetochlor, respectively.

MESA, MOXA, AcESA and AcOXA were analysed using a TSQ Quantum ACCESS LC-MS/MS equipped with a Thermo Scientific Accela autosampler with a temperature-controlled sample tray (15 °C) (Thermo Fisher, Les Ulis, France). The analytical column was an EC 150/3 Nucleodur Polar Tec (particle size 3 µm, length 150 mm and internal diameter 3 mm) and a precolumn EC 4/3 Polar Tec 30 mm (Macherey Nagel, France). The mass spectrometer (MS) was a Thermo TSQ Quantum triple quadrupole mass spectrometer (Thermo Fisher, Les Ulis, France) operated using a heated electrospray ionisation (HESI) source. The best sensitivity in the multiple reaction monitoring operation was achieved through the acquisition of selected reaction monitoring (SRM) transitions with the MRM mode. For the identification of the studied compounds, two SRM transitions and the correct ratio between the abundances of the two optimised SRM transitions (SRM1/SRM2) were used along with retention time matching. The quantification limits were 0.10 and 0.06 µg L<sup>-1</sup> for MOXA and MESA, respectively, and 0.10 and 0.02 µg L<sup>-1</sup> for AcOXA and AcESA, respectively. Information on the SRM transitions, detection limits and analytical uncertainties are provided in Table VII-11.

### 3.5.4 Enantiomer analysis of *S*-metolachlor

Chiral analyses were performed with a GC-MS (Trace GC 2000 series, Thermo Scientific, Les Ulis, France) using a 30 m x 0.25 mm ID, 0.25- $\mu$ m film with 20% tert-butyldimethylsilyl-beta-cyclodextrin dissolved in a 15% phenyl - 85% methylpolysiloxane column (BGB Analytik, Boeckten, Switzerland) with helium as a carrier gas at a flow rate of 1.0 mL min<sup>-1</sup>. The stereoisomer elution was *aS1'S*; *aS1'R*; *aR1'S*; and *aR1'R* (Figure VII-3). The four isomers can be grouped into two pairs of enantiomers whereby the *aS1'S*- and *aR1'S*-isomers constitute one pair of enantiomers, and the *aS1'R*- and *aR1'R*-isomers constitute the other pair. The enantiomeric excess (EE) was defined as the excess of the *1'S*-isomers over the *1'R*-isomers (Buser et al., 2000) as follows:

$$EE = \frac{(aS1'S + aR1'S) - (aS1'R + aR1'R)}{(aS1'R + aR1'S + aS1'R + aR1'R)} \quad (4)$$

The diastereoisomer excess (DE) was similarly defined as the excess of one pair of diastereomers (*aS1'S* and *aR1'R*) over the other pair (*aR1'S* and *aS1'R*) as follows:

$$DE = \frac{(aS1'S + aR1'R) - (aR1'S + aS1'R)}{(aS1'S + aR1'R + aR1'S + aS1'R)} \quad (5)$$

The EE and DE from the commercial product Mercantor Gold were  $0.73 \pm 0.01$  and  $0.07 \pm 0.02$ , respectively ( $n = 8$ ). The racemic metolachlor spiked at 9 different concentrations (25 – 2500  $\mu$ g L<sup>-1</sup>) was injected 3 times each to determine the precision in EE measurements. The mean and standard deviations were  $0.01 \pm 0.03$  ( $n = 27$ ), indicating that there were no concentration effects on the EE values. In addition, no enantiomeric fractionation occurred during the extraction and dilution procedures (data not shown).

### 3.5.5 Data analysis

Herbicide concentrations below the quantification limit were set to zero. The runoff coefficients, herbicide exported loads and export coefficient were calculated as previously explained (Grégoire et al., 2010). Data were compared using the paired non-parametric Wilcoxon signed rank test and Spearman rank correlation test. Statistical tests were performed using the R software (R development Core Team, 2008; version 2.6.2). The partition coefficient of the chloroacetanilides between the dissolved and particulate phases ( $K_d$ ) were calculated as the ratio of the particulate concentration against the dissolved concentration when both concentrations exceeded the quantification limits. The soil organic carbon water partitioning coefficient ( $K_{oc}$ ) was calculated based on the ratio of  $K_d$  against the particulate organic carbon

(POC). The field half-life in the soil was estimated assuming an exponential decrease of the soil concentration over time. To quantify the transport of the total chloroacetanilide loading within the agricultural catchment, ESA and OXA, as chloroacetanilide-derived compounds, were expressed as a parent compound mass equivalence. The mass equivalent load of the parent compound (P) ( $MEL_P$ ) was calculated according to the following equation:

$$MEL_P = Load_P + \left\{ Load_{OXA} \left[ \frac{MW_P}{MW_{OXA}} \right] \right\} + \left\{ Load_{ESA} \left[ \frac{MW_P}{MW_{ESA}} \right] \right\} \quad (1)$$

where  $MW_P$  is the molecular weight of S-metolachlor ( $283.8 \text{ g mol}^{-1}$ ) or acetochlor ( $269.8 \text{ g mol}^{-1}$ ),  $MW_{OXA}$  is the molecular weight of MOXA ( $279.3 \text{ g mol}^{-1}$ ) or AcOXA ( $265.30 \text{ g mol}^{-1}$ ), and  $MW_{ESA}$  is the molecular weight of MESA ( $329.1 \text{ g mol}^{-1}$ ) or AcESA ( $314.37 \text{ g mol}^{-1}$ ). The relationship between the chloroacetanilides and degradation products were evaluated by calculating the %OXA (ESA) as a percentage of the total loads of the chloroacetanilides, ESA and OXA according to the following equations:

$$\%OXA = \frac{[OXA]}{[P] + [ESA] + [OXA]} \quad (2)$$

$$\%ESA = \frac{[ESA]}{[P] + [ESA] + [OXA]} \quad (3)$$

where [ESA], [OXA] and [P] are the respective molar loadings of ESA, OXA and the parent compounds in water. A %OXA (ESA) equal to zero indicates that either ESA, OXA and the parent compound were below the quantification limit or that only OXA (resp. ESA) was below the limit.

## **4. Results and discussion**

### **4.1. Chloroacetanilide attenuation in the plot soil**

The concentration of S-metolachlor in the topsoil from the experimental plot was  $6.0 \mu\text{g kg}_{\text{dry}}^{-1}$  (Figure IV-4), and no acetochlor was detected before the applications because an acetochlor application had not occurred in the previous 5 years at the plot scale. The soil concentrations of S-metolachlor after Mercantor Gold application gradually decreased from  $2.1 \text{ mg kg}_{\text{dry}}^{-1}$  to  $0.5 \text{ mg kg}_{\text{dry}}^{-1}$  at 89 days after application (Figure IV-4). The field half-life in the soil was estimated at 54 days following an exponential decrease ( $R^2 = 0.75$ ,  $p < 0.001$ ) (Figure IV-4), which was consistent with the values of previous field and modelling studies (half-lives from 13 to  $> 90$  days) (Boithias et al., 2011; Cabrera et al., 2012; Leu et al., 2010; Shaner et al., 2006). S-metolachlor leached up to a 1 m depth on July 10 with concentrations of  $4 \times 10^{-3} \text{ mg kg}_{\text{dry}}^{-1}$ . The dissolved S-metolachlor concentrations in the runoff water at the plot scale decreased over time and were correlated with concentrations of the soil surface samples ( $\rho=0.93$ ,  $p < 0.001$ )

(Figure IV-4), emphasising that the lower *S*-metolachlor amount could be mobilised over time for surface transport.

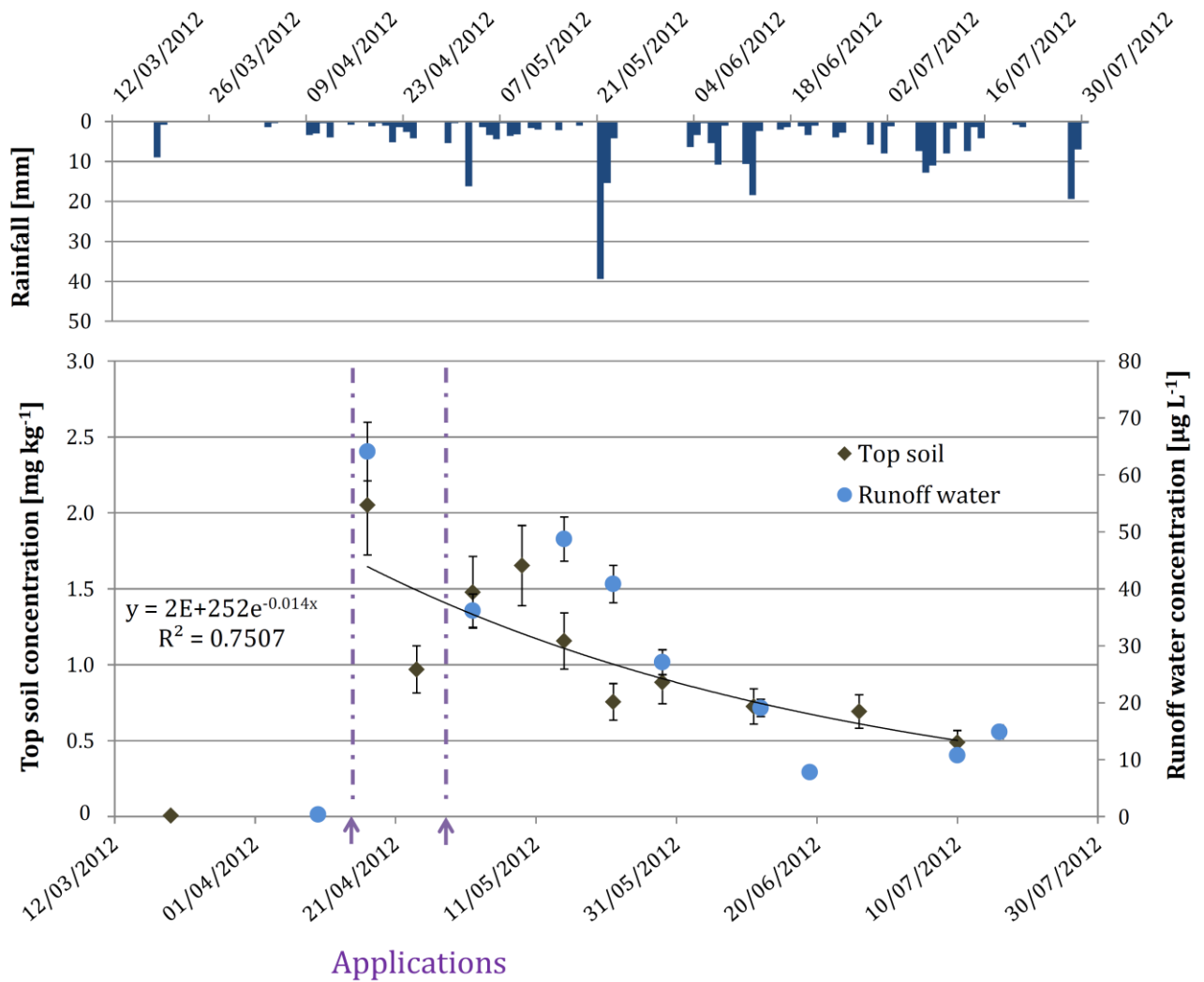


Figure IV- 4. Temporal changes of *S*-metolachlor concentration in soil and dissolved runoff water samples at the plot scale

## 4.2. Influence of hydrology and hydrochemistry on chloroacetanilide export and partitioning

### 4.2.1 Hydrochemical and chloroacetanilide load variations

Based on the five rain gauges, rainfall showed a low spatial variation ( $\pm 3.5$  mm on a weekly basis) and was considered homogeneous at the catchment scale. Eighty-eight rainfall events were monitored from March 12 to August 14 and amounted to 316 mm. A total outflow water volume of 17,419 m<sup>3</sup> was measured at the catchment outlet (Figure IV-5). The meteorological, hydrological, and hydrochemical characteristics during the study period are provided in Tables IV-1 and IV-2 and Figure IV-5 A and C.

**Table IV-1. Hydrological characteristics from March 12 to August 14 2012 in the catchment (Alsace, France). Values are provided as the mean and ranges. Bold number corresponds to May 21.**

	<b>Parameter</b>	<b>Unit</b>	
<b>Meteorology</b>	Daily mean temperature	[°C]	15.8 ± 4.8 (4.9 – 26.0)
	Daily mean humidity	[%]	68.2 ± 10.9 (37.8 - 89.4)
	Daily potential evapotranspiration	[mm]	3.8 ± 1.2 (1.3 - 7.4)
	Rainfall events amounts	[mm]	3.6 ± 6.4 (0.4 - <b>54.4</b> )
	Maximal rainfall events intensities	[mm h <sup>-1</sup> ]	4 ± 4 (2 - <b>18</b> )
	Rainfall events duration	[mn]	114 ± 114 (8 - 462)
<b>Hydrology (events &gt; 10 m<sup>3</sup>)</b>	Outflow volume	[m <sup>3</sup> ]	1314 ± 3472 (22 - <b>10568</b> )
	Event duration	[mn]	136 ± 116 (38 - <b>413</b> )
	Runoff coefficient	[%]	7.8 ± 12.6 (0.2 - <b>40.8</b> )
	Maximum outflow	[mm h <sup>-1</sup> ]	1.17 ± 1.72 (0 – <b>5.56</b> )
	Estimation of the drainage contribution to the runoff volume	[%]	8.6 ± 6.7 ( <b>1.5</b> - 22.5)

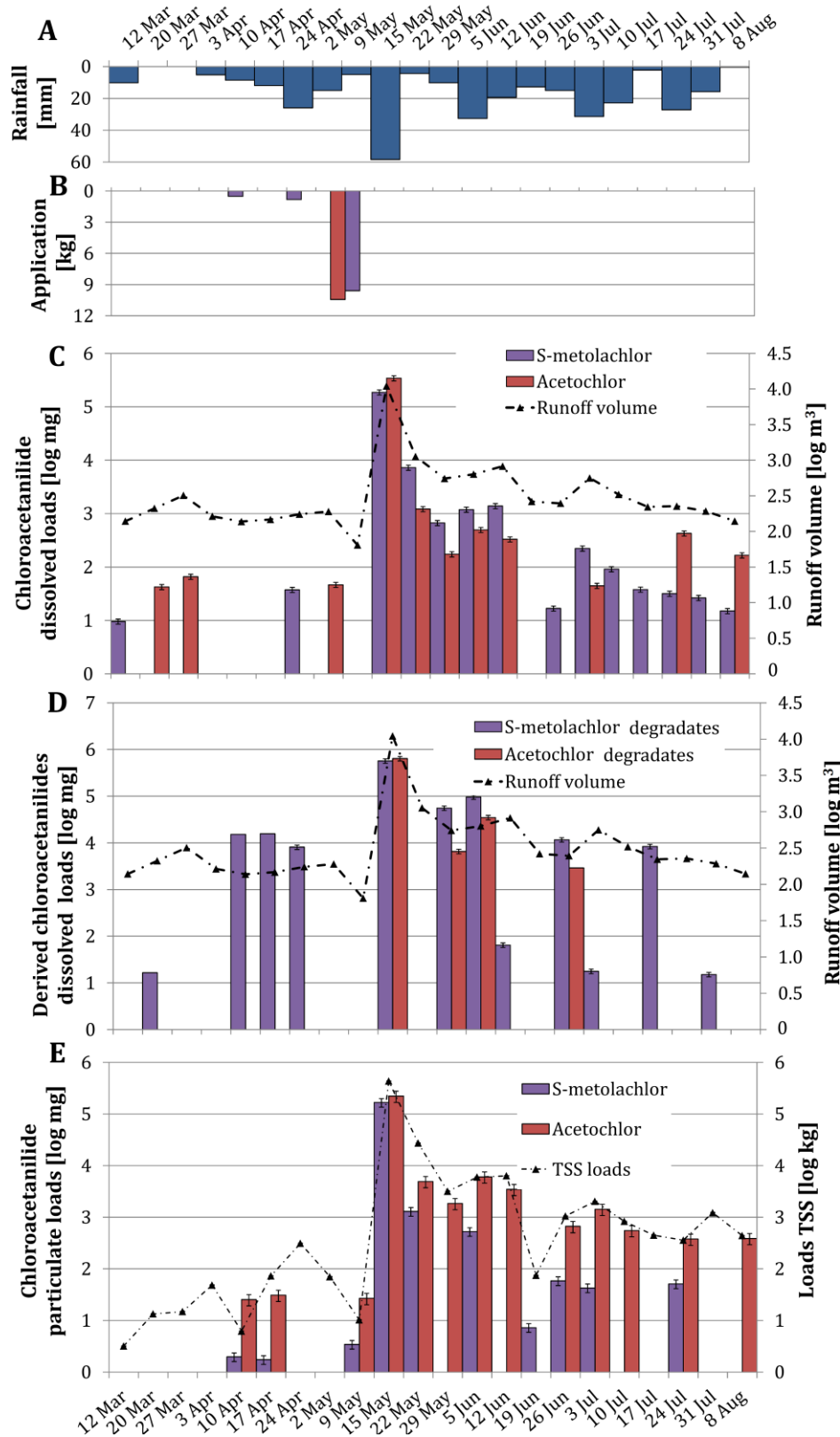


Figure IV-5. Temporal changes of rainfall (A), the chloroacetanilide application (B), the dissolved exported loads (< 0.7  $\mu\text{m}$ ) of the parent compound (C), those of the degradation products (D) and the particulate loads (> 0.7  $\mu\text{m}$ ) of the parent compounds (E) at the catchment outlet (Alteckendorf, Alsace, France) with red bars for acetochlor and purple bars for S-metolachlor. For chloroacetanilide and metabolite loads, error bars were calculated via error propagation, incorporating analytical uncertainties as well as the uncertainty of suspended solids and water volume measurements.

During the growing season, a total of 581 tons of TSS, 0.33 tons of dissolved organic carbon (DOC) and 44 tons of POC were exported at the outlet of the catchment (Figure IV-5). The TSS export represented 1006 t km<sup>-2</sup> and corresponded to a soil loss of 0.4 mm over the catchment. This severe soil loss was in the range of the regional annual erosion (Neboit, 1991). Based on linear hydrograph separation, the drainage contribution from drain D1 (Figure IV-2) was estimated at 33% of the total outflowing water during the growing season. Compared to the hydrochemical conditions of the drain, plot and catchment water during the investigation period, the drain had significantly different concentrations of TIC, DIC, TOC, DOC, PO<sub>4</sub><sup>3-</sup>, P<sub>tot</sub>, NO<sub>2</sub><sup>-</sup> and NH<sub>4</sub><sup>+</sup> ( $p < 0.05$ ) (see Table IV-2 and Table VII-12 in Appendices). Drainage water typically has lower concentrations of pesticides (14 to 96 times) than surface runoff from a catchment or plot (Table IV-3), which was previously shown (Brown and van Beinum, 2009). At the catchment scale, the total chloroacetanilide concentrations differed between high and low flow periods ( $p < 0.01$ ). This suggests a higher contribution of surface runoff during the high flow conditions to discharge and to chloroacetanilide export at the catchment scale.

A total export coefficient of 3.4% and 5.8% for *S*-metolachlor and acetochlor were estimated for both the particulate and dissolved phases at the catchment outlet. A 40-year return period rainfall event on May 21 corresponded to 20% of the total rainfall and 53% of the total outflow volume. This major event accounted for 92% of the TSS, 42% of the DOC, 87% of the POC and 96% of the chloroacetanilides exported during the study period (Figure IV-5). The May 21 event occurred 7 days after and 16 days after the final applications of *S*-metolachlor and acetochlor, respectively. Therefore, the period that included the days following the chloroacetanilide application when bare soil was prevalent appeared to be risky for chloroacetanilide export. More than 40% of the total chloroacetanilide export occurred in the particulate phase for both *S*-metolachlor and acetochlor (Figure VII-4), ranging according to error propagation between 38 and 53%, emphasising that a large portion of exported chloroacetanilides occurred in association with particles. Not counting this extreme event, the total exported load in the dissolved phase was 85 and 13% of the total loads exported for *S*-metolachlor and acetochlor respectively, emphasising the large temporal variability of the chloroacetanilide partitioning between the dissolved and particulate phase.

**Table IV-2. Hydrochemistry characteristics from March 12 to August 14 2012 in the plot, drain and catchment's outlet (Alsace, France). Values are provided as the mean and ranges. Bold number corresponds to May 21.**

	Parameter	Unit	Plot	Drain	Catchment
	Samples number	[ - ]	10	16	33
<b>Erosion</b>	Total suspended solids (> 0.7µm)	[mg L <sup>-1</sup> ]	1.70 ± 2.57 (0.05 - 7.66)	0.16 ± 0.29 (0 - 1.00)	5.85 ± 11.27 (0.02 - <b>59.70</b> )
	Volatile organic carbon (> 0.7µm)	[%]	18.73 ± 12.9 (11.04 - 46.32)	24.27 ± 22.62 (3.03 - 75.76)	11.1 ± 5.16 (4.76 - 30.16)
<b>Hydrochemistry</b>	Nitrite (NO <sub>2</sub> <sup>-</sup> )	[mg L <sup>-1</sup> ]	0.50 ± 0.36 (0.11 - 1.22)	0.13 ± 0.03 (0.11 - 0.19)	0.83 ± 1.31 (0.11 - 5.60)
	Nitrate (NO <sub>3</sub> <sup>-</sup> )	[mg L <sup>-1</sup> ]	114.05 ± 157.02 (10.17 - 425.15)	31.52 ± 12.87 (18.75 - 62.66)	27.16 ± 20.71 (2.32 - <b>92.18</b> )
	Ammonium (NH <sub>4</sub> <sup>+</sup> )	[mg L <sup>-1</sup> ]	12.11 ± 23.95 (0.42 - 69.45)	1.16 ± 1.63 (0.12 - 3.04)	4.14 ± 7.39 (0.12 - 29.59)
	Ion phosphate (PO <sub>4</sub> <sup>3-</sup> )	[mg P L <sup>-1</sup> ]	1.85 ± 2.32 (0.13 - 6.38)	0.36 ± 0.39 (0.01 - 1.05)	0.44 ± 0.37 (0.01 - 1.61)
	Total inorganic carbon (TIC)	[mg C L <sup>-1</sup> ]	22.51 ± 35.43 (1.46 - 93.4)	87.37 ± 2.79 (82.32 - 91.42)	74.9 ± 18.47 (18.71 - 107.77)
	Total organic carbon (TOC)	[mg C L <sup>-1</sup> ]	64.86 ± 78.55 (10.43 - 221.51)	2.87 ± 1.08 (1.72 - 5.23)	20.44 ± 28.10 (1.20 - 120.42)
	Dissolved inorganic carbon (DIC)	[mg C L <sup>-1</sup> ]	23.97 ± 38.55 (0.09 - 87.44)	80.07 ± 22.76 (3.74 - 92.31)	58.42 ± 27.26 (0.12 - 93.17)
	Dissolved organic carbon (DOC)	[mg C L <sup>-1</sup> ]	50.11 ± 75.65 (3.16 - 228.90)	4.12 ± 3.85 (1.84 - 14.46)	21.6 ± 26.45 (1.30 - 111.80)
Total phosphorus (P)	[mg L <sup>-1</sup> ]	2.87 ± 1.90 (1.44 - 6.20)	0.64 ± 0.38 (0.35 - 1.26)	7.43 ± 7.20 (0.84 - <b>29.00</b> )	

Table IV-3. Chloroacetanilides concentrations and occurrences from March 12 to August 14 2012 in the plot, drain and catchment's outlet (Alsace, France). Values are provided as the mean and ranges. Bold number corresponds to May 21.

	Parameter	Unit	Plot	Drain	Catchment	
Runoff Water	Samples number	[-]	10	16	33	
	Occurrence	[%]	100	63	64	
	<i>S</i> -metolachlor (< 0.7 µm)	Dissolved concentration	[µg L <sup>-1</sup> ]	26.98 ± 20.21 (0.36 - 64.10)	0.28 ± 0.53 (0 - <b>2.21</b> )	4.14 ± 12.79 (0 - <b>62.09</b> )
		Enantiomeric excess (EE)	[-]	0.72 ± 0.05 (0.6 - 0.75)	0.68 ± 0.12 (0.34 - 0.74)	0.71 ± 0.15 (-0.02 - <b>0.77</b> )
		Diastereoisomer excess (DE)	[-]	0.09 ± 0.03 (0.04 - <b>0.14</b> )	0.11 ± 0.02 (0.07 - 0.16)	0.10 ± 0.02 (0.07 - 0.13)
	<i>S</i> -metolachlor (> 0.7 µm)	Occurrence	[%]	70	54	44
		Particulate concentration	[mg kg <sup>-1</sup> ]	0.77 ± 1.50 (0 - 4.83)	0.62 ± 1.65 (0 - 6.35)	1.14 ± 6.05 (0 - <b>34.29</b> )
		Enantiomeric excess (EE)	[-]	0.74 ± 0.04 (0.67 - <b>0.77</b> )	0.74 ± 0.04 (0.64 - <b>0.77</b> )	0.70 ± 0.13 (0.28 - <b>0.75</b> )
	Metolachlor (< 0.7 µm) ESA -OXA	Diastereoisomer ratio (DR)	[-]	0.11 ± 0.02 (0.07 - 0.14)	0.19 ± 0.05 ( <b>0.10</b> - 0.25)	0.11 ± 0.04 (0.00 - 0.16)
		Occurrence (MESA)	[%]	56	n.a	29
		Occurrence (MOXA)	[%]	89	n.a	53
		<i>S</i> -metolachlor ESA	[µg L <sup>-1</sup> ]	28.66 ± 67.03 (0 - 199.94)	n.a	41.64 ± 82.30 (0 - 316.17)
	Acetochlor (< 0.7 µm)	<i>S</i> -metolachlor OXA	[µg L <sup>-1</sup> ]	122.33 ± 208.46 (0 - 659.32)	n.a	6.52 ± 18.84 (0 - 91.84)
		Occurrence	[%]	40	38	45
	Acetochlor (> 0.7 µm)	Dissolved concentration	[µg L <sup>-1</sup> ]	0.28 ± 0.55 (0 - 1.75)	0.15 ± 0.24 (0 - <b>0.85</b> )	3.86 ± 12.32 (0 - <b>59.33</b> )
		Occurrence	[%]	25	38	22
	Acetochlor (< 0.7 µm) ESA-OXA	Particulate concentration	[mg kg <sup>-1</sup> ]	3.69 ± 11.78 (0 - 41.03)	1.70 ± 5.47 (0 - 21.94)	3.28 ± 14.57 (0 - <b>82.95</b> )
		Occurrence (AcESA)	[%]	0	n.a	12
		Occurrence (AcOXA)	[%]	0	n.a	21
Acetochlor ESA		[µg L <sup>-1</sup> ]	0 ± 0 (0 - 0)	n.a	1.35 ± 4.17 (0 - 17.51)	
Acetochlor OXA		[µg L <sup>-1</sup> ]	0 ± 0 (0 - 0)	n.a	10.01 ± 23.55 (0 - 96.25)	
Soil	Metolachlor					
	Samples number	[-]	11	n.a	n.a	
	Concentration	[mg kg <sup>-1</sup> ]	0.86 ± 0.52 (0.00 - 1.36)	n.a	n.a	
	Enantiomeric excess (EE)	[-]	0.73 ± 0.04 (0.62 - 0.78)	n.a	n.a	
	Diastereoisomer ratio (DR)	[-]	0.09 ± 0.01 (0.07 - 0.11)	n.a	n.a	

n.a. not analysed

### 4.2.2 Chloroacetanilide partitioning

Rainfall intensities were correlated with the total suspended solid (TSS) concentrations ( $\rho=0.6$ ;  $p < 0.001$ ) as well as the *S*-metolachlor and acetochlor concentrations in both the dissolved and particulate phases ( $\rho=0.39$ ,  $p < 0.001$ ). This underscores the impact of intensive events on TSS and chloroacetanilide export. The herbicide concentrations and loads during the study period are provided in Figure IV-5 and Table IV-3. Drastic changes in *S*-metolachlor and acetochlor partitioning between the dissolved and particulate phases were observed over time (Figure VII-4). The  $K_d$  values of *S*-metolachlor and acetochlor were significantly correlated together ( $\rho=0.85$ ,  $p < 0.05$ ), suggesting that these two herbicides were similarly mobilised over time. The  $K_{oc}$  values ranged between 71 and 9395 L kg<sup>-1</sup> for *S*-metolachlor and between 97 and 137,818 L kg<sup>-1</sup> for acetochlor. Higher  $K_{oc}$  values for acetochlor compared to *S*-metolachlor were consistent with its higher hydrophobicity and lower solubility. The  $K_d$  values of both chloroacetanilides presented significant negative correlations with the suspended solid flux ( $\rho=-0.92$  and  $\rho=-0.54$ ,  $p < 0.001$  and  $p < 0.05$  for *S*-metolachlor and acetochlor, respectively), indicating that chloroacetanilide adsorption onto particles decreased with increasing TSS concentrations. It is further supported by the decrease of POC together with the increase of TSS ( $\rho=-0.55$ ,  $p < 0.001$ ). These observations are consistent with other studies and highlight the impoverishment in organic carbon of eroded materials (Boithias et al., 2014; Cerro et al., 2014). The TSS concentrations may also impact the required level of Gibbs free energy during partitioning, which may largely affect the partitioning coefficient over time (Goss and Schwarzenbach, 2003). Large variations of *S*-metolachlor and acetochlor partitioning over time may be related to their large solubility relative to their log  $K_{ow}$  (Boithias et al., 2014) and the nature of the sorbents (size of the particles, aromaticity and polarity), which may change over time and under different erosive events (Boithias et al., 2014; Si et al., 2009). The conductivity and pH appear to have no influence on the  $K_d$  values, most likely because the pH ( $7.9 \pm 0.2$ ) and conductivity ( $633 \pm 239 \mu\text{S cm}^{-1}$ ) were relatively constant during the study period.

Few studies have focused on partitioning coefficients, such as  $K_d$  or  $K_{oc}$ , stemming from runoff pesticide concentration measurements (Boithias et al., 2014; Taghavi et al., 2011). The calculated  $K_{oc}$  values were five orders of magnitude lower than the chloroacetanilide  $K_{oc}$  values estimated in the Save River in the western France (Boithias et al., 2014) and one to two orders of magnitude larger than those in soil-water batch studies at equilibrium (Alletto et al., 2013; Hiller et al., 2008). The diversity of the experimental approaches, equilibrium sorption time and sorbent characteristics make it difficult to compare the partitioning coefficients.

### **4.3. Dynamics of ESA and OXA degradation products**

Although ESA and OXA were less frequently detected than their parent compounds (Table IV-3), they often presented larger molar concentrations than their parent compounds (70% and 47% of the samples at the plot and catchment scales, respectively), indicating that the degradation process occurred during the study period. At the plot scale, dissolved AcESA and AcOXA could not be detected in the water because acetochlor had not been applied in the previous 5 years. Eighty-six percent of the plot water samples presented higher molar concentrations of MOXA than MESA (Figure VII-5). At the catchment scale, MESA, MOXA, AcESA and AcOXA correlated over time ( $\rho=0.68$ ,  $p < 0.001$ ), suggesting that they had similar transformation and transportation pathways, as previously shown in batch studies (Graham et al., 1999). On a weekly basis, 41% and 100% of the catchment samples presented greater OXA concentrations than ESA concentrations for *S*-metolachlor and acetochlor, respectively (Figure VII-5). Based on the MELp calculation (Eq.1), an export coefficient of ESA and OXA parent compound mass equivalent loads of 7.3% and 6.7% of the total mass applied for *S*-metolachlor and acetochlor, respectively, were estimated, indicating the large relative contributions of the ESA and OXA loads.

Only the *S*-metolachlor degradation products could be detected at the catchment scale from March 12 to March 15, although both *S*-metolachlor and acetochlor were used during this period (Figure IV-5). The occurrence of metolachlor degradation products can be explained by the rapid degradation from earlier and smaller applications of *S*-metolachlor (April 12 and May 1) or by the large quantities of *S*-metolachlor that had accumulated in soils because of the 10 additional years of metolachlor use within the study site. From May 15 to July 3, 5 runoff events larger than 10 m<sup>3</sup> occurred and led to a high detection frequency and larger exported loads of the chloroacetanilides ESA and OXA. Among the runoff events, the event of May 21 explained 9% and 94% of the total exported loads for ESA and OXA of *S*-metolachlor and acetochlor, respectively, suggesting that a smaller amount of ESA was available in the soil surface or that MOXA was more mobile than ESA, which is still controversial (Baran and Gourcy, 2013; Bayless et al., 2008; Krutz et al., 2004). The persistence of *S*-metolachlor degradation products compared to those of acetochlor were observed at the catchment outlet at the end of the study period (from July 3 to August 14), whereas the acetochlor degradation products were not detected (Figure IV-5), which is consistent with other studies (Steele et al., 2008).

Chloroacetanilide degradation may occur both biotically (Field and Thurman, 1996; McCarty et al., 2014) and abiotically (Bian et al., 2009; Zeng et al., 2012). It is commonly supposed that ESA

and OXA chloroacetanilides are produced by the oxidation of glutathione-metolachlor conjugates during biotic processes (Field and Thurman, 1996) that result in the removal of a chlorine atom and addition of a sulfonic acid functional group (ESA) or carboxyl group (OXA) (Figure IV-3). During abiotic processes in the presence of sulphate-reducing conditions, sulphides can react through a nucleophilic attack (Stamper and Tuovinen, 1998) and replace the chlorine with the reactive sulphite species. Although this reaction may occur in agricultural soil, it is unlikely that it prevails under mostly aerobic conditions and when biotic processes are mostly expected to occur. The temporal variability in the formation and transport of degradation products is also reflected in the enantiomer analysis of *S*-metolachlor.

#### **4.4. *S*-metolachlor enantiomeric signatures as indicator of in-situ degradation**

The EE values were in the range of those of the commercial products (0.72 - 0.74) for most of the samples during the study period (Figure IV-6), suggesting that *S*-enantioselective degradation was not significant during the observed timespan (4 months following application). The low EE value (0.6) in a point water sample in November at the catchment outlet 6 months after the metolachlor application confirmed that significant *S*-enantioselective degradation may occur over the course of several months (Figure IV-7). The enantiomeric fractionation of metolachlor was previously observed in a Swiss lake between years but not within the same year (Poiger *et al.*, 2002; Buser *et al.*, 2000).

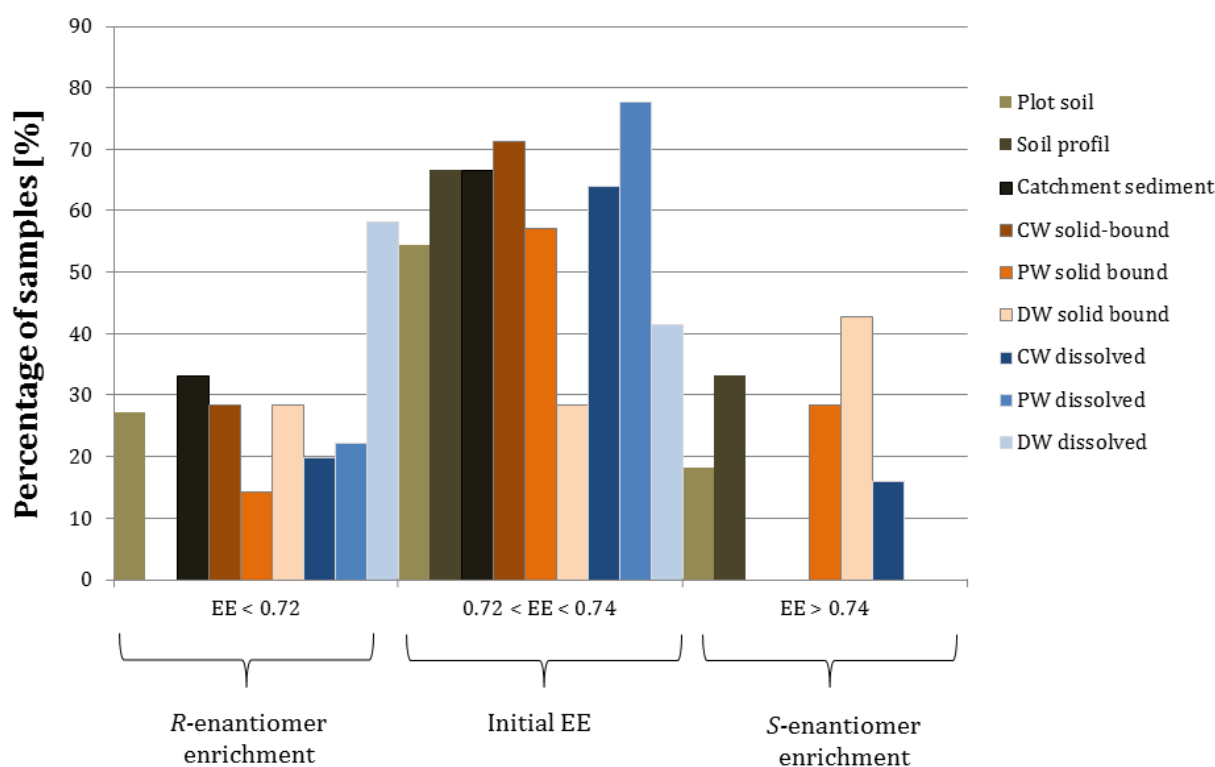


**Figure IV-6. Distribution of enantiomeric excess of *S*-metolachlor in dissolved and solid bound surface water samples from the drain (DW), plot (PW) and catchment (CW) outlets and in soil (plot) and sediment (catchment) samples.**

The EE ranged between -0.02 and 0.77 in the dissolved phase of runoff and 0.28 and 0.77 in the particulate phase (Figure IV-7 and Table IV-3). The EE increased from 0.6 to 0.75 and from -0.02 to 0.75 in the runoff water at the plot and catchment scales just after application (Figure IV-7). *S*-metolachlor could not be quantified on suspended solids before the application, which prevented an enantiomeric analysis. At the catchment scale, the EE in the dissolved and particulate phases revealed a significant correlation with the *S*-metolachlor concentration in those phases ( $\rho=0.64$  and  $0.87$ ,  $p < 0.001$ ). The EE values increased from 0.62 to 0.74 in the plot soil samples just after the first application (Figure IV-7). Afterwards, the EE average was  $0.74 \pm 0.02$ , which suggested that *S*-metolachlor was not degraded enantioselectively within the observed time span (71 days after last application) (Figure IV-7). The EE decreased from 0.80 to 0.64 over the soil depth and was correlated with the *S*-metolachlor concentration ( $\rho=0.88$ ,  $p < 0.05$ ). The EE decreased from 0.75 to 0.66 ( $n = 3$ ) over time in the sediments in front of the dike at the catchment outlet (Figure IV-7). Overall, a slight correlation existed between the EE values in the different environmental samples and *S*-metolachlor concentrations [ppm] ( $\rho=0.22$ ,  $p < 0.05$ ,  $n=94$ ). There was no significant difference between the EE values among the environmental compartments ( $p > 0.1$ ), suggesting that the environmental compartments could

not be distinguished based on their enantiomers signatures. The DE in nearly all of the samples (water, suspended solids and soils) did not show significant shifts, suggesting that metolachlor biodegradation was not diastereoisomer-selective under the environmental conditions described in this study (Table IV-3).

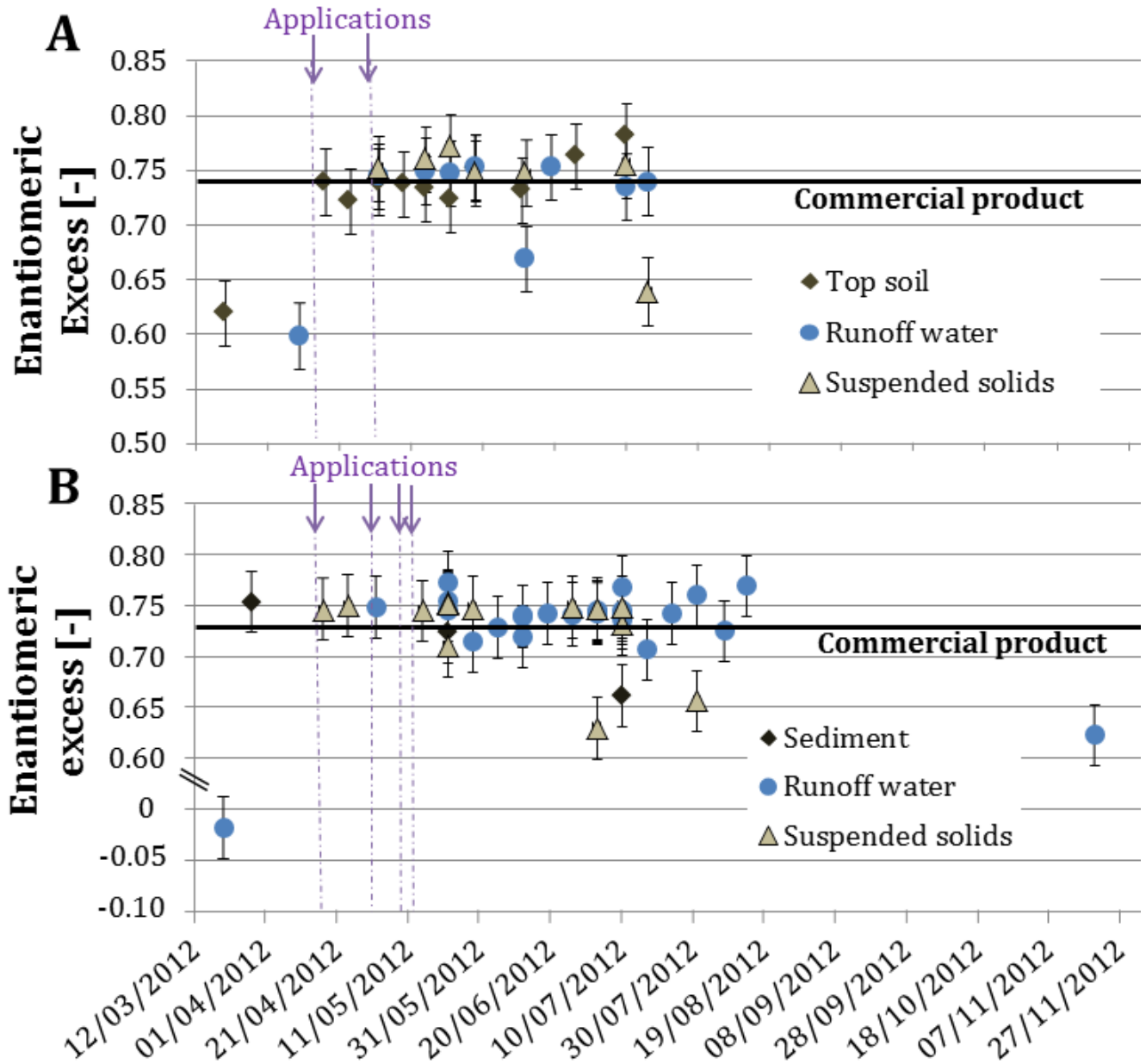


Figure IV- 7. Temporal changes of the enantiomeric excess of metolachlor at the plot outlet (A) and at the catchment outlet (B) in different environmental compartments.

Although few studies of the stereoselectivity of metolachlor have been conducted, the stereoselective degradation of *S*-metolachlor is still a controversial topic (Buser et al., 2000; Klein et al., 2006; Kurt-Karakus et al., 2010). In a laboratory study, spiked soil samples presented stereoselective degradation of racemic metolachlor with a decrease in the *aR1'S* isomer (Polcaro et al., 2004). In this study, the ratio  $(aSS-aRS)/(aSS+aRS)$  did not significantly change and was not significantly correlated with the *S*-metolachlor concentration, suggesting that only enantiomers were subject to isomer-selective degradation. Samples with lower concentrations of *S*-metolachlor were associated with an enrichment in the *R*-enantiomer, indicating *S*-enantioselective degradation. No correlation was observed between the EE and MOXA or MESA concentrations, which might partially be a result of the different contributions of other commercial formulations (Dual Gold and Camix) that have different isomeric signatures. Contrary to the EE, the DE of a chiral compound can vary largely depending on the batch and conditions during synthesis (Buser et al., 2000). Variations of the EE according to the different commercial products are unlikely to occur (Kurt-Karakus et al., 2010). In addition, *S*-enantioselective degradation may not involve the formation of such degradation products, and the presence of enzymes capable of degrading the enantiomers or/and interconversion reaction cannot be excluded (Milosevic et al., 2013; Polcaro et al., 2004), interfering with the enantiomeric signatures of the bulk sample.

## 5. Conclusion

The transport and degradation of the widely used chloroacetanilides *S*-metolachlor and acetochlor were evaluated at both the plot and catchment scales using different analytical approaches, which included the quantification of the chloroacetanilides and four of their degradation products and enantiomer analyses. Our results showed that an important amount of the pesticide load is missed when only the dissolved concentration of the parent compound is analysed. The total export coefficients for *S*-metolachlor and acetochlor and their degradation products were 11.4 and 11.8%, respectively, which includes both the dissolved and particulate loads. The partitioning of *S*-metolachlor and acetochlor between the dissolved and particulate phases varied widely over time and was linked to the suspended solid concentrations. The concentration dynamics of acetochlor, *S*-metolachlor and their metabolites (ESA and OXA) in runoff were similar within the agricultural catchment. MESA and MOXA were found to be more persistent than AcESA and AcOXA. However, an evaluation of the amount of degradation products in the soil is lacking within the catchment, and such an evaluation would help determine the formation mechanisms of the degradation products in the field prior to their export in runoff. These measurements will be the topic of future investigations. Our results show

that *S*-enantioselective biodegradation occurs and is negatively correlated with *S*-metolachlor concentrations. However, no relationship could be found between the EE values and MESA and MOXA concentrations. The present field study indicates the potential of enantiomer analyses for assessing chloroacetanilide biodegradation and could be efficiently complemented with future laboratory benchmark studies on enantiomeric fractionation during chloroacetanilide degradation combined with an analysis of the degradation products to determine the extent of biodegradation in agro-ecosystems.

## **6. Acknowledgements**

The authors are members of REALISE, the Network of Laboratories in Engineering and Science for the Environment in the Alsace Region (France; <http://realise.unistra.fr>), and the support of REALISE is gratefully acknowledged. This research was funded by the research program EC2CO (CNRS-INSU) and the PhytoRET project (C.21) of the European INTERREG IV program in the Upper Rhine. Marie Lefrancq was supported by a fellowship of the Rhine-Meuse Water Agency and Alsace Region. The authors wish to thank the farmers for their support. We acknowledge the soil laboratory EOST UMS830 CNRS and Martine Trautmann, Anne Véronique Auzet, Tristan Meyer, Diogo Reis, Jeanne Dollinger, Thomas Dreidemy, Célia Kennel, René Boutin, Sophie Gangloff, Marie-Pierre Ottermatte, Eric Pernin and Brian Sweeney for their support in sampling, analysis and/or writing.

## 7. References

- Alletto, L., Benoit, P., Bolognesi, B., Couffignal, M., Bergheaud, V., Dumeny, V., Longueval, C., Barriuso, E., 2013. Sorption and mineralisation of S-metolachlor in soils from fields cultivated with different conservation tillage systems. *Soil & Tillage Research*. 128, 97-103.
- Baran, N., Gourcy, L., 2013. Sorption and mineralization of S-metolachlor and its ionic metabolites in soils and vadose zone solids: Consequences on groundwater quality in an alluvial aquifer (Ain Plain, France). *Journal of Contaminant Hydrology*. 154, 20-28.
- Barbash, J.E., 2014. The Geochemistry of Pesticides. In: *Treatise on Geochemistry (Second Edition)*. Vol., H.D. Holland, K.K. Turekian, eds. Elsevier, Oxford, pp. 535-572.
- Bayless, E.R., Capel, P.D., Barbash, J.E., Webb, R.M.T., Hancock, T.L.C., Lampe, D.C., 2008. Simulated fate and transport of metolachlor in the unsaturated zone, Maryland, USA. *Journal of Environmental Quality*. 37, 1064-1072.
- Bedmar, F., Daniel, P.E., Costa, J.L., Gimenez, D., 2011. Sorption of Acetochlor, S-Metolachlor, and Atrazine in Surface and Subsurface Soil Horizons of Argentina. *Environmental Toxicology and Chemistry*. 30, 1990-1996.
- Bian, H.T., Chen, J.W., Cai, X.Y., Liu, P., Wang, Y., Huang, L.P., Qiao, X.L., Hao, C., 2009. Dechlorination of chloroacetanilide herbicides by plant growth regulator sodium bisulfite. *Water Research*. 43, 3566-3574.
- Blaser, H.U., 2002. The chiral switch of (S)-metolachlor: A personal account of an industrial odyssey in asymmetric catalysis. *Advanced Synthesis & Catalysis*. 344, 17-31.
- Boithias, L., Sauvage, S., Taghavi, L., Merlina, G., Probst, J.L., Perez, J.M.S., 2011. Occurrence of metolachlor and trifluralin losses in the Save river agricultural catchment during floods. *Journal of Hazardous Materials*. 196, 210-219.
- Boithias, L., Sauvage, S., Merlina, G., Jean, S., Probst, J.-L., Sánchez Pérez, J.M., 2014. New insight into pesticide partition coefficient  $K_d$  for modelling pesticide fluvial transport: Application to an agricultural catchment in south-western France. *Chemosphere*. 99, 134-142.
- Boxall, A.B.A., Sinclair, C.J., Fenner, K., Kolpin, D., Maud, S.J., 2004. When synthetic chemicals degrade in the environment. *Environmental Science & Technology*. 38, 368a-375a.
- Brown, C.D., van Beinum, W., 2009. Pesticide transport via sub-surface drains in Europe. *Environmental Pollution*. 157, 3314-3324.
- Buser, H.R., Poiger, T., Muller, M.D., 2000. Changed enantiomer composition of metolachlor in surface water following the introduction of the enantiomerically enriched product to the market. *Environmental Science & Technology*. 34, 2690-2696.
- Cabrera, A., Papiernik, S.K., Koskinen, W.C., Rice, P.J., 2012. Sorption and dissipation of aged metolachlor residues in eroded and rehabilitated soils. *Pest Management Science*. 68, 1272-1277.
- Cai, X.Y., Sheng, G.Y., Liu, W.P., 2007. Degradation and detoxification of acetochlor in soils treated by organic and thiosulfate amendments. *Chemosphere*. 66, 286-292.

- Celis, R., Gamiz, B., Adelino, M.A., Hermosin, M.C., Cornejo, J., 2013. Environmental behavior of the enantiomers of the chiral fungicide metalaxyl in Mediterranean agricultural soils. *Science of The Total Environment*. 444, 288-297.
- Cerro, I., Sanchez-Perez, J.M., Ruiz-Romera, E., Antigüedad, I., 2014. Variability of particulate (SS, POC) and dissolved (DOC, NO<sub>3</sub>) matter during storm events in the Alegria agricultural watershed. *Hydrological Processes*. 28, 2855-2867.
- Dictor, M.C., Baran, N., Gautier, A., Mouvet, C., 2008. Acetochlor mineralization and fate of its two major metabolites in two soils under laboratory conditions. *Chemosphere*. 71, 663-670.
- Elsayed, O.F., Maillard, E., Vuilleumier, S., Nijenhuis, I., Richnow, H.H., Imfeld, G., 2014. Using compound-specific isotope analysis to assess the degradation of chloroacetanilide herbicides in lab-scale wetlands. *Chemosphere*. 99, 89-95.
- Eurostat, 2007. The use of plant protection products in the European Union: data 1992–2003. Statistical book. European Communities, Luxembourg.
- Field, J.A., Thurman, E.M., 1996. Glutathione conjugation and contaminant transformation. *Environmental Science & Technology*. 30, 1413-1418.
- Freitas, L.G., Singer, H., Muller, S.R., Schwarzenbach, R.P., Stamm, C., 2008. Source area effects on herbicide losses to surface waters - A case study in the Swiss Plateau. *Agriculture Ecosystems & Environment*. 128, 177-184.
- Goss, K.U., Schwarzenbach, R.P., 2003. Rules of thumb for assessing equilibrium partitioning of organic compounds: Successes and pitfalls. *Journal of Chemical Education*. 80, 450-455.
- Graham, W.H., Graham, D.W., Denoyelles, F., Smith, V.H., Larive, C.K., Thurman, E.M., 1999. Metolachlor and alachlor breakdown product formation patterns in aquatic field mesocosms. *Environmental Science & Technology*. 33, 4471-4476.
- Grégoire, C., Payraudeau, S., Domange, N., 2010. Use and fate of 17 pesticides applied on a vineyard catchment. *International Journal of Environmental Analytical Chemistry*. 90, 406-420.
- He, H.Z., Chen, G.K., Yu, J., He, J.B., Huang, X.L., Li, S.F., Guo, Q., Yu, T.H., Li, H.S., 2013. Individual and Joint Toxicity of Three Chloroacetanilide Herbicides to Freshwater Cladoceran *Daphnia carinata*. *Bulletin of Environmental Contamination and Toxicology*. 90, 344-350.
- Heitz, C., Flinois, G., Glatron, S., 2012. Protection against muddy floods: perception for local actors in Alsace (France) of a protection measure (fascines). *International Disaster Risk Conference, Davos, Suisse, 26-30 Août 2012*.
- Hiller, E., Krascenits, Z., Cernansky, S., 2008. Sorption of acetochlor, atrazine, 2,4-D, chlorotoluron, MCPA, and trifluralin in six soils from Slovakia. *Bulletin of Environmental Contamination and Toxicology*. 80, 412-416.
- Hladik, M.L., Bouwer, E.J., Roberts, A.L., 2008a. Neutral degradates of chloroacetamide herbicides: Occurrence in drinking water and removal during conventional water treatment. *Water Research*. 42, 4905-4914.
- Hladik, M.L., Bouwer, E.J., Roberts, A.L., 2008b. Neutral chloroacetamide herbicide degradates and related compounds in Midwestern United States drinking water sources. *Science of The Total Environment*. 390, 155-165.

- Klein, C., Schneider, R.J., Meyer, M.T., Aga, D.S., 2006. Enantiomeric separation of metolachlor and its metabolites using LC-MS and CZE. *Chemosphere*. 62, 1591-9.
- Krutz, L.J., Senseman, S.A., Dozier, M.C., Hoffman, D.W., Tierney, D.P., 2004. Infiltration and adsorption of dissolved metolachlor, metolachlor oxanilic acid, and metolachlor ethanesulfonic acid by buffalograss (*Buchloe dactyloides*) filter strips. *Weed Science*. 52, 166-171.
- Kurt-Karakus, P.B., Bidleman, T.F., Muir, D.C.G., Struger, J., Sverko, E., Cagampan, S.J., Small, J.M., Jantunen, L.M., 2010. Comparison of concentrations and stereoisomer ratios of mecoprop, dichlorprop and metolachlor in Ontario streams, 2006-2007 vs. 2003-2004. *Environmental Pollution*. 158, 1842-1849.
- Leu, C., Schneider, M.K., Stamm, C., 2010. Estimating Catchment Vulnerability to Diffuse Herbicide Losses from Hydrograph Statistics. *Journal of Environmental Quality*. 39, 1441-1450.
- Liu, H.J., Xiong, M.Y., 2009. Comparative toxicity of racemic metolachlor and S-metolachlor to *Chlorella pyrenoidosa*. *Aquatic Toxicology*. 93, 100-106.
- Liu, W.P., Gan, J.Y., Papiernik, S.K., Yates, S.R., 2000. Structural influences in relative sorptivity of chloroacetanilide herbicides on soil. *Journal of Agricultural and Food Chemistry*. 48, 4320-4325.
- McCarty, G.W., Hapeman, C.J., Rice, C.P., Hively, W.D., McConnell, L.L., Sadeghi, A.M., Lang, M.W., Whitall, D.R., Bialek, K., Downey, P., 2014. Metolachlor metabolite (MESA) reveals agricultural nitrate-N fate and transport in Choptank River watershed. *Science of The Total Environment*. 473-474, 473-482.
- Milosevic, N., Qiu, S., Elsner, M., Einsiedl, F., Maier, M.P., Bensch, H.K.V., Albrechtsen, H.J., Bjerg, P.L., 2013. Combined isotope and enantiomer analysis to assess the fate of phenoxy acids in a heterogeneous geologic setting at an old landfill. *Water Research*. 47, 637-649.
- Neboit, R., 1991. L'homme et l'érosion: l'érosion des sols dans le monde, Vol., Association des Publications de la Faculté des Lettres et Sciences Humaines de Clermont-Ferrand.
- Oliver, D.P., Kookana, R.S., Anderson, J.S., Cox, J.W., Waller, N., Smith, L.H., 2012. Off-site transport of pesticides in dissolved and particulate forms from two land uses in the Mt. Lofty Ranges, South Australia. *Agricultural Water Management*. 106, 78-85.
- Poiger, T., Muller, M.D., Buser, H.R., 2002. Verifying the chiral switch of the pesticide metolachlor on the basis of the enantiomer composition of environmental residues. *Chimia*. 56, 300-303.
- Polcaro, C.M., Berti, A., Mannina, L., Marra, C., Sinibaldi, M., Viel, S., 2004. Chiral HPLC resolution of neutral pesticides. *Journal of Liquid Chromatography & Related Technologies*. 27, 49-61.
- Roberts, T.R., Hutson, D.H., Services, R.S.o.C.I., 1999. *Metabolic Pathways of Agrochemicals: Insecticides and fungicides*, Vol., Royal Society of Chemistry.
- Saha, S., Dutta, D., Karmakar, R., Ray, D.P., 2012. Structure-toxicity relationship of chloroacetanilide herbicides: Relative impact on soil microorganisms. *Environmental Toxicology and Pharmacology*. 34, 307-314.
- Shaner, D.L., Brunk, G., Belles, D., Westra, P., Nissen, S., 2006. Soil dissipation and biological activity of metolachlor and S-metolachlor in five soils. *Pest Management Science*. 62, 617-623.
- Si, Y.B., Takagi, K., Iwasaki, A., Zhou, D.M., 2009. Adsorption, desorption and dissipation of metolachlor in surface and subsurface soils. *Pest Management Science*. 65, 956-962.

- Stamper, D.M., Tuovinen, O.H., 1998. Biodegradation of the acetanilide herbicides alachlor, metolachlor, and propachlor. *Critical Reviews in Microbiology*. 24, 1-22.
- Steele, G.V., Johnson, H.M., Sandstrom, M.W., Capel, P.D., Barbash, J.E., 2008. Occurrence and fate of pesticides in four contrasting agricultural settings in the United States. *Journal of Environmental Quality*. 37, 1116-32.
- Taghavi, L., Merlina, G., Probst, J.L., 2011. The role of storm flows in concentration of pesticides associated with particulate and dissolved fractions as a threat to aquatic ecosystems Case study: the agricultural watershed of Save river (Southwest of France). *Knowledge and Management of Aquatic Ecosystems* 400-06.
- Turner, J., Albrechtsen, H.J., Bonell, M., Duguet, J.P., Harris, B., Meckenstock, R., McGuire, K., Moussa, R., Peters, N., Richnow, H.H., Sherwood-Lollar, B., Uhlenbrook, S., van Lanen, H., 2006. Future trends in transport and fate of diffuse contaminants in catchments, with special emphasis on stable isotope applications. *Hydrological Processes*. 20, 205-213.
- Ye, C., 2003. Environmental behavior of the herbicide acetochlor in soil. *Bulletin of Environmental Contamination and Toxicology*. 71, 919-923.
- Zeng, T., Chin, Y.P., Arnold, W.A., 2012. Potential for Abiotic Reduction of Pesticides in Prairie Pothole Porewaters. *Environmental Science & Technology*. 46, 3177-3187.
- Zhang, J.N., Liang, W.J., Wu, X., Jiang, S.W., Li, Q., 2013. Toxic Effects of Acetochlor on Mortality, Reproduction and Growth of *Caenorhabditis elegans* and *Pristionchus pacificus*. *Bulletin of Environmental Contamination and Toxicology*. 90, 364-368.

# Chapter V. Modelling pesticide runoff at the headwater catchment scale

---

## Overview

Pesticide runoff in two different agricultural contexts representative of headwater catchments of the Rhineland area were investigated in this thesis. However, physico-chemical processes observed from one agricultural context during one season could only be confirmed and further extended with the help of modelling.

Runoff and erosion in agro-ecosystems are largely influenced by drastic changes of the dynamics of soil surface state and hydrodynamic parameters during the growing season (Alaoui et al., 2011). Knowledge of soil surface state and hydrodynamic parameters is crucial for understanding and predicting pesticide transport processes in agro-ecosystems. Currently, few pesticide transport models account for the effects of agricultural practices on hydrodynamic parameters and soil surface characteristics and most of them are deemed inappropriate for investigating headwater catchments with a very fine temporal resolution ( $\leq 1$  min, see Chapter 1, §2.2.4). Furthermore, pesticide-runoff models rarely integrate erosion processes, and thus neglect pesticide transport in the particulate phase. This underscores that an event based, spatially distributed pesticide-fate model at the headwater catchment scale is needed to address pesticide mobilisation and transport in agricultural headwater catchments.

A new calibration approach was developed for predicting runoff and erosion processes with meaningful input parameters based on an hydrological and erosion model LISEM (Limbourg Soil Erosion Model) (DeRoo et al., 1996) in order to account for the temporal variability of the soil surface and hydrodynamic parameters along the growing season (Section 1, *in prep*). A mathematical formalism was developed to predict pesticide mobilisation and transport via runoff in the dissolved phase based on the distributed mixing layer theory (Wallender et al., 2008) (Section 2). This formalism was integrated in LISEM.

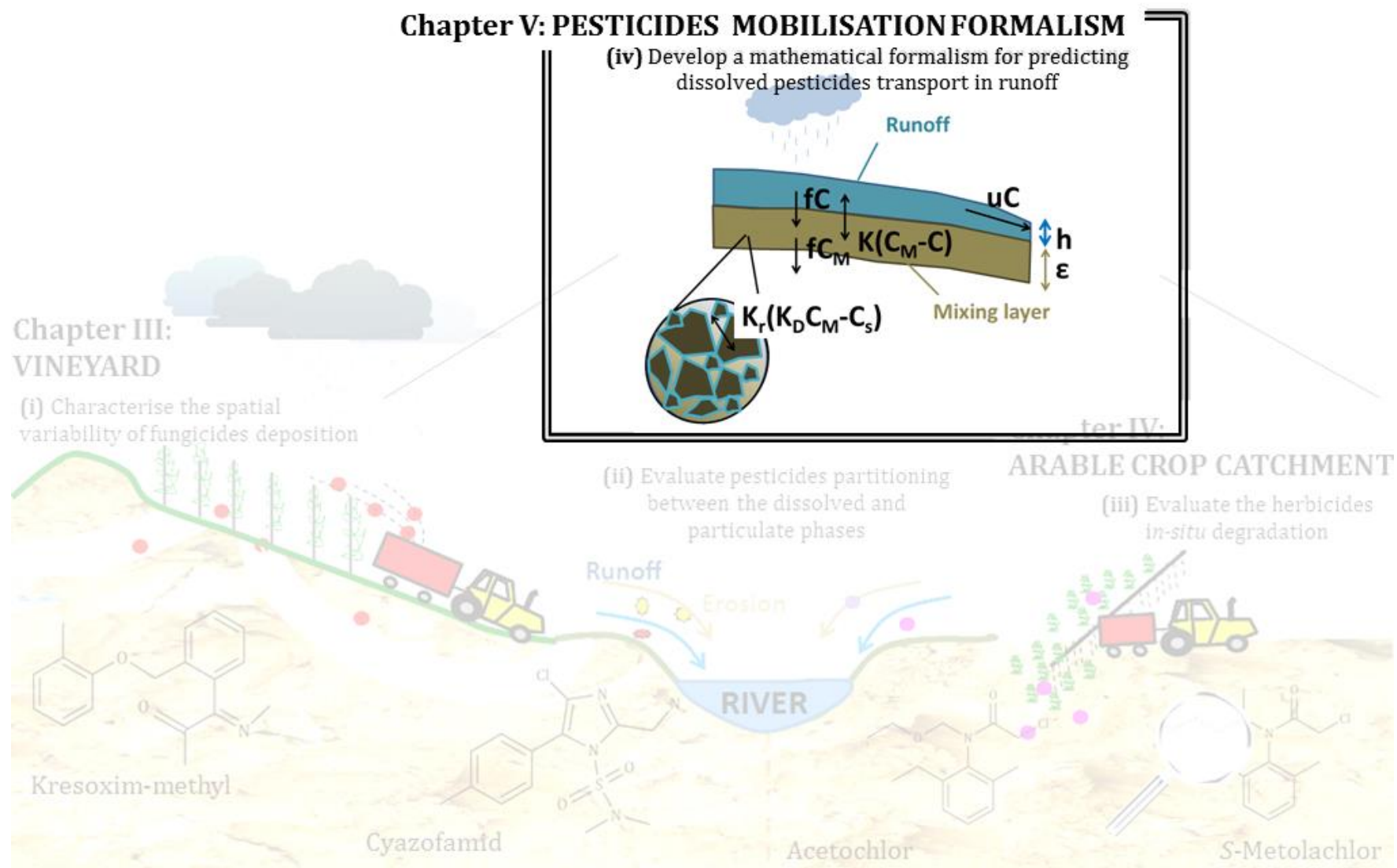


Figure V-1. Graphical outline of the PhD thesis (Chapter V)

## Section 1. Agronomical insights for improving runoff prediction in headwater agricultural catchments

Marie Lefrancq, Paul Van Dijk, Matthieu Schwob, Sylvain Payraudeau

(This part is in preparation for publication, Appendices are given in Chapter VII)

### 1. Abstract

Predicting runoff and erosion in agricultural areas is inherently difficult because of rapid changes in soil surface characteristics, hydrodynamic parameters and vegetation. Obtaining distributed input parameters for mechanistic approaches remains difficult, and model calibration often leads to “equifinality” as a result of over-parameterisation. In this study, a novel approach was developed for reducing the dimensionality of calibration issues to improve runoff prediction at the event scale within headwater agricultural catchments. The originality of this approach is the combination of the event-based hydrological model LISEM (Limbourg Soil Erosion Model) and agronomic continuous model  $I_{DR}$  to provide the temporal variability of soil surface characteristics, soil hydrodynamic parameters and vegetation changes during a growing season. Applied at a study site located in eastern France, the approach developed in this work showed that runoff prediction at the outlet and within the catchment was enhanced during a growing season based on limited supplementary knowledge of the input parameters. Combining a hydrological event-based model and agronomic continuous model provided an accurate spatial prediction of erosion for the largest observed erosive event. The sensitivity of 21 input parameters of LISEM was assessed and differed according to the intensity and volume of the 9 significant runoff events observed during the growing season. Simulated runoff volume was less sensitive to the initial water content and saturated hydraulic conductivity during intensive runoff events. The sensitivity analysis showed that the Green and Ampt infiltration parameters, i.e., saturated and initial water content, suction at the wetting front and saturated hydraulic conductivity, were major factors influencing the total runoff volume for the 9 runoff events. The full coupling of a distributed hydrological event-based model with an agronomic model should be further developed to account for spatial and temporal variation of the initial soil surface characteristics and hydrodynamic parameters.

**Key words:** Erosion; Soil hydraulic properties; Equifinality; Temporal variability; Soil surface characteristics; Tillage

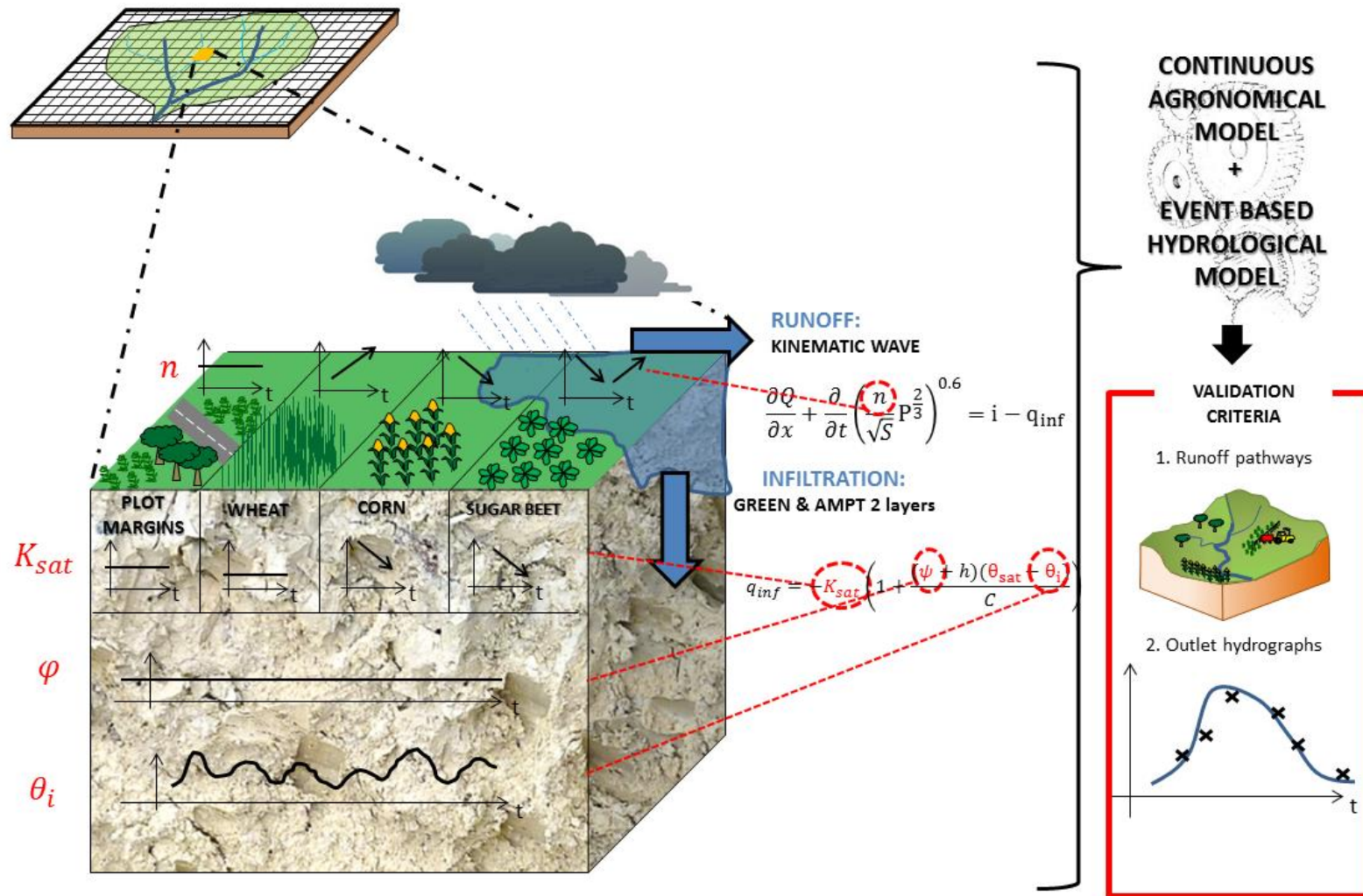


Figure V-2. Graphical abstract.

## 2. Introduction

Agricultural practices strongly impact the generation, dynamics and pathways of both runoff and erosion worldwide (Dotterweich, 2013). Common agricultural practices of removing perennial vegetation (Xu et al., 2013), maintaining areas of bare soil (Durán-Zuazo et al., 2013), and tilling (Meijer et al., 2013) promote soil erosion and runoff and the subsequent transport of pesticides.

Cultivated soils have specific soil surface characteristics such as soil cover, topsoil structure and soil crusting that are known to largely influence the partitioning of rainfall between infiltration and runoff (Pare et al., 2011). Hortonian runoff prevails in agricultural areas in the early growth stages (spring and early summer) (Armand et al., 2009; Van den Putte et al., 2013), and soil hydrodynamics significantly change over time during a growing season (Alaoui et al., 2011; Ali, 2008; O'Hare et al., 2010). For example, surface soil hydraulic conductivity ( $K_{sat}$ ) may exhibit higher values immediately after tillage (e.g., 30-35 mm h<sup>-1</sup>) and gradually decrease from April to September (e.g., 5-10 mm h<sup>-1</sup>) for loess soils (Ali, 2008) as a result of the breakdown of aggregates caused by rainfall and the clogging of larger pores (Zeng et al., 2013). Manning's coefficient ( $n$ ) is influenced by soil surface characteristics, which are rendered smoother by the rainfall events, and the friction dissipation from crop growth that maintains resistance for the water flow (Augustin et al., 2009; Li and Zhang, 2001). Determining the soil surface characteristics and hydrodynamics is crucial for predicting hydrological processes in agricultural catchments. However, few studies have attempted to develop predictive models that emphasise the impact of agricultural practices on hydrodynamic parameters and soil surface characteristics (Green et al., 2003; Pare et al., 2011).

Erosion and hydrological models have been steadily improving throughout recent decades (Aksoy and Kavvas, 2005; Mitsova et al., 2013). A single rainfall event can cause more than half of the annual measured erosion within a catchment (Edwards and Owens, 1991), and only parts of a catchment might contribute to runoff (Dunne and Black, 1970). Determining the generation, dynamics and pathways of both surface runoff and sediment transport at an event scale is therefore essential (Evrard et al., 2009; Fiener et al., 2011). Continuous models are not usually designed to detail the runoff from single events and generally lack sufficient spatial and temporal details (Merritt et al., 2003). Event-based models are often simpler because they do not account for all of the processes required in a continuous model, such as evapotranspiration, water redistribution and plant growth (Berthet et al., 2009), and enable finer temporal and spatial discretisation. However, reducing the gap between measurement availability and parameter estimation for physically based models still remains a challenge.

The initial conditions in event-based models are set from additional external information (Tramblay et al., 2010) and often require calibration for each rainfall-runoff event (Baartman et al., 2012). Calibration steps may hamper the selection of unique spatial parameter sets that best describe catchment dynamics and may lead to “equifinality” as a result of over-parameterisation (Beven, 2006; Kirchner, 2006). Several approaches have been developed to tackle the issue of non-unique parameter sets (Efstratiadis and Koutsoyiannis, 2010; Gupta et al., 2009; Wallner et al., 2013). These approaches include multi-objective calibrations with different types and/or locations of observations. Considering the complexity of interactions between physical processes, several observation locations within the catchment can significantly improve the calibration and validation of a distributed model (Lee et al., 2012). Because sediment transport is conditioned by runoff dynamics (Aksoy and Kavvas, 2005), additional erosion characterisation within the catchment may assist in the spatial validation of predicted runoff velocities and flow depths.

The objective of this study was to develop a novel approach to improve runoff prediction at the event scale during a growing season within headwater agricultural catchments. The novelty of the approach was in the combination of the event-based hydrological model LISEM (DeRoo et al., 1996) and the continuous agronomic model  $I_{DR}$  (Van Dijk et al., in prep.) to provide the temporal variability of soil surface characteristics, soil hydrodynamic parameters and vegetation changes during a growing season. A constraint calibration method (CCM) was developed and tested using the  $I_{DR}$  model outputs to improve the consistency and to reduce the equifinality of the LISEM parameters calibrated for an event based on a growing season. To quantify the benefit in terms of the consistency and equifinality of the CCM approach, a basic calibration method (BCM) of the LISEM parameters was applied for each event without considering the evolution of the agronomical properties along the growing season. The consistency of the model prediction was evaluated by the ability of LISEM to i) simulate the runoff dynamics at the outlet and runoff patterns within the catchment and ii) predict the amount of eroded soil at the outlet and erosion patterns within the catchment for intensive event. The CCM approach was tested for a case study located 30 km northeast of Strasbourg (Alsace, France).

### 3. Material and methods

#### 3.1. Model description

The hydrological model used for the calibration testing was LISEM (Limbourg Soil Erosion Model) (DeRoo et al., 1996), which is a physically based runoff and soil erosion model for event-based predictions in small agricultural catchments (<10,000 ha).

The selection of LISEM was motivated by 3 main reasons. The first reason was to select an event-based model that was fully distributed for headwater catchments and that considered erosion processes. The second reason was that LISEM was designed to describe agricultural landscape components with crusted and compacted zones and soil surface structure (Liu et al., 2003). The third reason was that this model was validated in various agricultural contexts and hydrological conditions (Baartman et al., 2012; Hessel et al., 2006; Hessel and Jetten, 2007; Sheikh et al., 2010). The theory and structures of LISEM were previously described (Baartman et al., 2012). Briefly, rainfall interception by vegetation is first calculated based on a canopy storage function (de Jong and Jetten, 2007). Then, the water partitioning between infiltration and the surface is calculated by the Green and Ampt equations for one or two soil layers (Kutilek and Nielsen, 1994) (Eq. 1):

$$q_{inf} = -K_{sat} \left( 1 + \frac{(\psi + h)(\theta_{sat} - \theta_i)}{F} \right) \quad (\text{Eq. 1})$$

where  $q_{inf}$  is the infiltration rate [ $\text{m s}^{-1}$ ],  $K_{sat}$  is the saturated hydraulic conductivity [ $\text{m s}^{-1}$ ],  $F$  is the cumulative infiltration from the beginning of the event [ $\text{m}$ ],  $\psi$  is the average matrix suction at the wetting front [ $\text{m}$ ],  $h$  is the overpressure depth of the water layer at the soil surface [ $\text{m}$ ],  $\theta_{sat}$  is the saturated water content [-], and  $\theta_i$  is the initial water content of the layer [-]. The maximum depression storage in the micro-relief was estimated based on an empirical equation from Kamphorst et al. (2000). Once the maximum depression storage was exceeded, runoff was generated. Erosion detachment was generated by rainfall splash based on rainfall kinetic energy (Sanchez-Moreno et al., 2012) and/or overland flow. Flow detachment was calculated with a stream-power based transport capacity based on the EUROSEM formalism (Morgan et al., 1998). Sediment traps can be used to represent the vegetal barriers as observed within the catchment. The flow velocity was calculated with the Manning equation, and surface runoff was routed over the landscape with the 1D kinetic wave equation (Eq. 2) (Chow et al., 2013).

$$\frac{\partial Q}{\partial x} + \frac{\partial}{\partial t} \left[ \frac{n}{\sqrt{S}} P^{\frac{2}{3}} \right]^{0.6} = q_{sur} \quad (\text{Eq. 2})$$

where  $Q$  is the discharge [ $\text{m}^3 \text{s}^{-1}$ ],  $n$  is the Manning coefficient [-],  $S$  is the sine of the slope gradient [-],  $P$  is the wet perimeter [m], and  $q_{\text{sur}}$  is the infiltration surplus [ $\text{m}^2 \text{s}^{-1}$ ]. Equations 1 and 2 indicate that the compensation in rainfall-runoff model parameters may occur in one cell during the water partitioning between runoff and infiltration (Eq. 1) or spatially between the cells during the transport step (Eq. 2). Transport equations (water and sediment) are solved in one spatial dimension and routed from upstream to downstream over a predefined flow network that connects cells in 8 directions (quasi 2D). In this study, LISEM refers to version 1.79 of OpenLISEM (<http://blogs.itc.nl/lisem/>). For each predicted runoff event, the initial surface soil characteristics, hydrodynamic parameters and initial water content were required for the hydrological predictions with LISEM and were provided by the continuous agronomic model  $I_{\text{DR}}$ .

### **3.2. Continuous agronomic model: $I_{\text{DR}}$**

Soil surface and vegetation characteristics, including vegetation and crop residue cover, random roughness and saturated hydraulic conductivity, vary in space during the crop growing season.  $I_{\text{DR}}$ , or indicator of runoff dynamics, is a continuous field scale model.  $I_{\text{DR}}$  predicts the soil surface state and hydrodynamic parameters as a function of the cropping system, e.g., crop, tillage, climate and soil type (Van Dijk et al., in prep.). Physical processes and equations included in  $I_{\text{DR}}$  are detailed in the Appendices. Briefly,  $K_{\text{sat}}$  is determined in two steps: the saturated hydraulic conductivity of the soil matrix is estimated based on the pedotransfer function (Cosby et al., 1984), which only depends on the soil texture, and then the soil tillage and progressive soil clogging under the influence of rainfall are considered. The approach for estimating soil moisture in the topsoil layer is based on the soil moisture depletion model from Kohler and Linsley (1951). Vegetation cover is calculated according to a sigmoidal curve based on the growth equation of Hunt (1982). Random roughness (RR) is calculated based on the equations of Potter (1990).

### 3.3. Case study

#### 3.3.1 Description of the study site

The 47-ha catchment is located 30 km northeast of Strasbourg (Alsace, France) and has a mean annual temperature of 11.7 °C, mean annual rainfall of 605 mm ( $\pm 141$  mm) and evapotranspiration of 820 mm ( $\pm 28$  mm) (2005-2011, Meteo France station in Waltenheim sur Zorn, which is located 7 km from the study site).

The mean slope is 6.7% ( $\pm 4.8\%$ ), and the altitude ranges between 190 and 230 m. The catchment outlet forms a retention basin (maximum capacity of 6700 m<sup>3</sup>) during large runoff events, and water is conducted to the catchment outlet (P0 in Figure V-3) via ditches into a 50-cm diameter pipe under the road, which yields a maximum outflow of 550 L s<sup>-1</sup>. A pipe (P1 in Figure V-3) was constructed to conduct the runoff under a track. The catchment is intensively cultivated, and 88% is arable land with corn (68%), winter wheat (16%) and sugar beet (4%) as principal crops. A drainage system has existed since 1950, and one drain (Figure V-3) was active during the study period and flowing in a ditch. No flow was observed in the other drains during the study period.

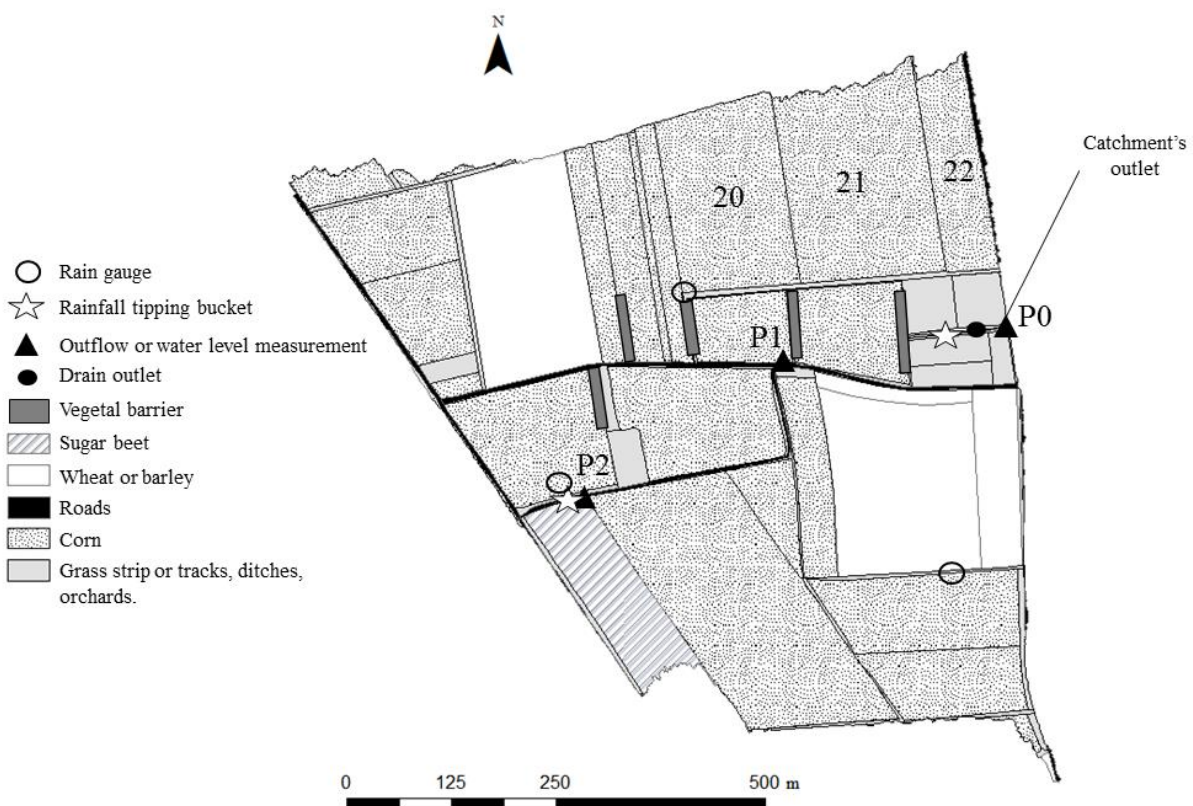


Figure V-3. Scheme of the study catchment (Alteckendorf, Alsace, France).

The spatial variability of the soil was characterised by 48 soil surface samples (0 - 20 cm) in April 2011 and six 2-m soil profiles in November 2012. The main soil type is calcareous brown earths and calcic soils on hillsides and colluvial calcic soils in the central thalweg (Figure VII-6 in the Appendices). The grain size distributions of the soil profiles presented low variations ( $n = 30$ ) (mean  $\pm$  SD in percent): clay  $29.5 \pm 5.8$ , silt  $64.2 \pm 6.5$  and sand  $6.4 \pm 2.9$ . The soil characteristics (mean  $\pm$  SD) were  $\text{CaCO}_3$   $10.7 \pm 8.1\%$ , organic matter  $1.1 \pm 0.8\%$ , pH  $7.2 \pm 0.6$ , phosphorus  $0.04 \pm 0.04 \text{ g kg}^{-1}$  and CEC  $12.7 \pm 2.8 \text{ cmol}^+ \text{ kg}^{-1}$ . The detailed norms and methods for the soil measurements are described in Table VII-10. The soil characteristics showed little variability within the studied catchment (Figure VII-6) and were considered homogeneous in this study. A compacted layer was observed at a depth between 20 and 30 cm along the soil profiles corresponding to the plough base. Undisturbed soil samples of  $100 \text{ cm}^3$  were taken at 6 depths along the 2 m depth profile to characterise the hydrodynamic properties.

The saturated hydraulic conductivity of the soil matrix was determined under steady conditions (Table VII-10), and it was measured at  $6.3 \pm 8.8 \text{ mm h}^{-1}$  in the soil samples from the first depth (0 - 10 cm) ( $n = 6$ ). The study catchment was prone to significant muddy flows nearly every year (Heitz et al., 2012), and the soil was sensitive to soil crusting and compaction. In 2009, five vegetal barriers were installed in the flow path to decrease the water velocity and to retain the soil particles during large events (Figure V-3). Springtime is a muddy flow risk period because of the extensive bare soil. Runoff discharges were continuously monitored between March 12 and August 14, 2012 and corresponded to the crop-growing season.

### 3.3.2 Hydrological procedure and experimental results

The catchment area was equipped with two tipping bucket rain gauges and 3 cumulative rain gauges to measure the weekly rainfall spatial variability (Figure V-3). Based on the five rain gauges, a low spatial variation of the rainfall was observed within the catchment ( $\pm 3.5 \text{ mm}$  on a weekly basis). Therefore, the rainfall was considered to be homogeneous for the simulation.

Water discharge was measured at the catchment outlet (P0 in Figure V-3) using a Doppler flowmeter (2150 Isco, Lincoln, Nebraska, USA) with a volume precision of 3%. Within the catchment, 2 runoff detectors were installed at P1 and P2 to indicate the runoff pathways within the catchment (see Figure V-3). The water level was measured using a pressure-sensor datalogger (Orpheus mini, OTT, Kempten, Germany) in a pipe (P1) in which the water was conducted from a ditch. P2 was located at the outlet of a sugar beet plot upstream in the catchment; it was left as a bare area from March to May like 72% of the crop area. The runoff

water was collected by a polyethylene gutter, and the water level was measured with a Venturi channel combined with a surface water level sensor (ENDRESS and HAUSER, Huningue, France) (P2 in Figure V-3).

Each week, topsoil samples (0 - 3 cm) were collected in the sugar beet plot (P2), and water content, organic carbon and pH of the samples were measured. To allow for the spatial validation of the simulated patterns, field observations were performed on runoff pathways and erosion and deposition patterns after the most intense events on May 2 and May 21 because the traces of surface runoff and erosion were visible.

Nine rainfall events that each yielded more than 10 m<sup>3</sup> of runoff at the outlet of the catchment were observed during the study period (Table V-1). The largest event was on May 21 and corresponded to 20% of the total rainfall and 53% of the total discharge during the study period. For this event, the water retention in front of the dike began 130 min after the beginning of the rainfall and reached 1.8 m, which modified the water velocities and peak outflow. After this event, the soil surface of the arable land was completely crusted, facilitating the production of runoff during subsequent rainfall events (Table V-1).

**Table V-1. Meteorological and hydrological characteristics of the 9 runoff events yielding at least 10 m<sup>3</sup> at the outlet of the catchment and occurring from May 2 to August 15 2012.**

	Unit	May 2	May 21	May 23	June 7	June 11	June 12	July 10	July 08	July10
<b>Rainfall amount</b>	[mm]	16.2	54.4	3.8	10.8	5.8	10.8	12.8	11.0	6.2
<b>Rainfall duration</b>	[min]	179	204	29	106	20	180	30	164	41
<b>Rainfall effective duration</b>	[min]	45	106	12	24	10	53	27	49	11
<b>6 min-peak rainfall intensity</b>	[mm h <sup>-1</sup> ]	38	72	26	56	50	20	40	16	46
<b>Total discharge</b>	[m <sup>3</sup> ]	22.2	10567.9	143.6	208.0	147.6	408.3	227.4	79.0	23.2
<b>Drainage contribution</b>	[%]	22.5	1.5	13.7	3.5	5.3	6.2	4.8	13.3	6.5
<b>Runoff event duration</b>	[min]	75	413	55	98	84	193	91	179	38
<b>Runoff coefficient</b>	[%]	0.2	40.8	7.0	4.0	6.5	5.8	3.6	1.3	0.7
<b>Maximum outflow</b>	[L s <sup>-1</sup> ]	11.2	*	105.0	131.0	0.7	125.0	229.0	30.5	20.2
<b>Peak time discharge**</b>	[min]	184	*	27	84	19	53	34	90	10

\* Flood retention

\*\* Time after beginning of rainfall event

### 3.3.3 Erosion characterisation

Because sediment transport is sensitive to flow hydraulics, erosion characterisation could help to validate runoff predictions. At the outlet of the plot and catchment (P2 and P0, respectively, in Figure V-3), flow-proportional water samples were systematically collected every 7 L and 20 m<sup>3</sup>, respectively, using an automatic sampler (Isco Avalanche, Lincoln, Nebraska, USA). The water samples were filtered through 0.7- $\mu$ m glass fibre filters for the quantification of total suspended solids (TSS). On average during the study period, 90% of the water was sampled each week, excluding the week of May 21, in which only 4% of the water discharge volume was sampled because of the automatic sampling strategy and large amount of discharge.

Erosion characteristics were mapped on May 21 because the rill patterns and deposition enabled the measurement and quantification of erosion. Along a representative length profile of the plots, the width and depth measurements of the rills were performed for each plot and extrapolated to the whole plots as proposed by Takken et al. (1999). The deposited soil volume was measured below each vegetal barrier; the sediment amount stored in numerous small deposition areas was much harder to measure in the field and may have been proportionally important, which rendered the quantification uncertain. The erosion and deposition mass budget was quantified assuming a homogeneous bulk density of the sediment. The bulk density of the deposited material was measured below each vegetal barrier within the catchment in triplicate, and on average it was  $2200 \pm 77 \text{ kg m}^{-3}$ .

At the outlet of the catchment, a total amount of TSS of 433 t was exported during the May 21 event. Assuming the homogeneity of the erosion and bulk density in the catchment, the total amount of exported TSS corresponded to an erosion rate of  $9 \text{ t ha}^{-1}$  and represented a soil loss depth of 0.4 mm over the catchment. The sediment deposition occurred in the (i) main flow path in front of the vegetal barriers, (ii) plots, as a result of slope changes, and (iii) downslope areas where the flow direction suddenly changed, as a result of tillage perpendicular to the flow direction (headlands) or at the interface between corn and grass strips. No sign of erosion could be observed for the wheat and barley fields characterised by dense vegetation cover. The main erosion and deposition processes are illustrated in Figure VII-7. The rill erosion rates were estimated for each plot and ranged between 0 and  $382 \text{ t ha}^{-1}$ . The erosion and deposition budget estimates are detailed in Table V-5.

### 3.5. Input parameters

The input parameters for the hydrological modelling are detailed in Table V-2. The catchment boundary was determined with ArcGIS 10.1 (ESRI, Redlands, United States) based on airborne lidar measurements (8 points per m<sup>2</sup> with a vertical accuracy of 15 cm). The catchment was discretised over 4-m<sup>2</sup> cells to describe the smallest agricultural element, i.e., a grass strip. The soil profile was discretised in two layers at 0-25 and 25-175 cm to represent the observed compacted layers corresponding to the plough base. The input parameters for each layer are noted with subscripts 1 (0-25 cm) or 2 (25-175 cm).

Eleven different land uses were determined: corn crop, cereal crop (wheat, alfalfa and oat), sugar beet crop, dirt road, asphalt road, grass road, grass strip, ditch, fallow land, orchard and hedge. The initial and saturated water content ( $\theta_{i,1,2}$  and  $\theta_{sat,1,2}$ ), average suction at the wetting front ( $\Psi_{1,2}$ ), soil depth for both layers ( $soildep_{1,2}$ ) and saturated hydraulic conductivity for the second layer ( $K_{sat2}$ ) were assumed to be homogeneous within the catchment. Parameter values and estimation methods are detailed in Table V-2. The measured topsoil water content (0 - 3 cm) could not be used directly in the model because it represents the water content of a very thin soil surface layer compared to the topsoil layer (0 - 25 cm) represented in LISEM; however, temporal variations in measured topsoil water content were compared with the calibrated initial water content. The surface parameters, i.e., random roughness ( $RR$ ),  $n$ ,  $K_{sat}$  and vegetation parameters, were assumed to only vary according to the crops because the spatial variations of the soil types and the slope were limited within the catchment. The vegetation parameters and  $RR$  were determined using  $I_{DR}$  for each crop (Table V-2). The erosion input parameters for May 21 are detailed for each crop in Table V-3.

**Table V-2. Description of the LISEM input parameters and their spatial and temporal discretisation for the both calibration methods: BCM and CCM. “Spatialised” indicates that input parameters are discretised for each cell, “crop” that input parameters are homogeneous according to each 11 landuses and “homogeneous” that the input parameters were lumped for the catchment. “Fixed” indicates that input parameters are fixed over time, “temporally” that input parameters were fixed but may vary over time and “calibrated” indicates that the input parameters were calibrated.**

Calibration methods		Spatial variation		Temporal variation		Method-source	
		Basic and constraint		Basic	Constraint	Basic	Constraint
<b>Catchment morphology</b>		<b>Units</b>					
	Digital elevation model		Spatialised		Fixed		Measurement (Lidar)
	Slope		Spatialised		Fixed		Calculated based on DEM
	Local drainage direction		Spatialised		Fixed		Calculated based on DEM
<b>Soil surface</b>							
	RR	[cm]	Crop		Temporally		Field measurement and I <sub>DR</sub>
	Manning		Crop				
	<i>for plot margins</i>	[-]		Calibrated	Fixed	Expert advice ± 20%	Constraint n°=2
	<i>for corn/sugarbeet</i>	[-]		Calibrated	Calibrated	0.07 - 0.13	Constraint n°=5
	<i>for wheat</i>	[-]		Calibrated	Calibrated	0.12 - 0.21	Constraint n°=5
<b>Vegetation</b>							
	Landuse		Crop		Fixed		Orthophoto and field observation
	Surface Cover	[-]	Crop		Temporally		Field observations and I <sub>DR</sub>
	Crop height	[m]	Crop		Temporally		Field observations
	Leaf area Index	[-]	Crop		Temporally		Lisem user guide
<b>Infiltration</b>							
	Saturated hydraulic conductivity		Crop				
	<i>for plot margins</i>	[mm h <sup>-1</sup> ]		Calibrated	Fixed	Expert advice ± 20%	Constraint n°=2
	<i>for corn/sugarbeet</i>	[mm h <sup>-1</sup> ]		Calibrated	Calibrated	0.5 - 60	Constraint n°=4
	<i>for wheat</i>	[mm h <sup>-1</sup> ]		Calibrated	Fixed	0.5 - 60	Constraint n°=3
Layer 1	Initial water content	[-]	Homogeneous		Calibrated		I <sub>DR</sub> value ± 20%
	Saturated water content	[-]	Homogeneous		Fixed: 0.42		Field measurement
	Suction at the wetting front	[cm]	Homogeneous	Calibrated	Fixed: 61.7	6.1 - 139.4	Constraint n°=1 (Saxton and Rawls, 2006)
	Soil depth	[m]	Homogeneous		Fixed: 0.25		Field observations
Layer 2	Saturated hydraulic conductivity	[mm h <sup>-1</sup> ]	Homogeneous		Fixed: 15.1		Measurement
	Initial water content	[-]	Homogeneous		Fixed: 0.3		pF curve
	Saturated water content	[-]	Homogeneous		Fixed: 0.36		Field measurement
	Suction at the wetting front	[cm]	Homogeneous		Fixed: 80.26		(Saxton and Rawls, 2006)
	Soil depth	[m]	Homogeneous		Fixed: 1.75		Field observations

Table V-3. LISEM erosion parameters related to each crop for May 21.

Landuse	Aggregate stability [-]	Cohesion [kPa]	Additive root cohesion [kPa]
Pasture	*	3	2
Impermeable surfaces	*	50	0
Dirt road	*	10	0
Corn (tilled)	10	0.88	0
winter cereals (tilled)	7	1	1
Sugar beet (tilled)	8	0.59	0.2

\* indicates that aggregate stability estimation is based only on cohesion

### 3.6. Calibration strategy

The basic calibration (BCM) was evaluated by calibrating each runoff event individually to illustrate how classical calibration fails to predict runoff pathways within a catchment. To reduce the dimensionality of the parameter calibration problem, a constraint calibration method (CCM) was developed with five supplementary constraints (Table V-2):

- (1)  $\Psi$  was considered constant following the conclusion of previous studies that indicated that the Green and Ampt model could not be improved by calibrating  $\Psi$  in addition to  $K_{sat}$  (Risse et al., 1994; Van den Putte et al., 2013);
- (2)  $K_{sat}$  and  $n$  for the plot margins, such as the road, buffer strip and ditch, were fixed over time according to expert rules and were not calibrated because their soil surface presented less temporal variability than agricultural plots;
- (3)  $K_{sat}$  for winter wheat was considered constant during the investigated period because wheat was already well implanted in March and was not harvested in July. Its value was based on the  $I_{DR}$  prediction;
- (4)  $K_{sat}$  for corn and sugar beet were predicted to decrease during the growing season, as previously observed (Van den Putte et al., 2013; Zeng et al., 2013) and validated by the  $I_{DR}$  prediction.
- (5)  $n$  increased for wheat and decreased for corn and sugar beet until mid-June and then increased as the vegetation tended to dominate other resistance processes (O'Hare et al., 2010; Van den Putte et al., 2013).

### 3.7. Model calibration and sensitivity analysis

Except for the May 21 event, the calibration was based on the outflow dynamics at the outlet of the catchment for both calibration methods. Because ponding occurred in the retention basin and modified the peak flow, the calibration for the May 21 event was based on the first 150 min of the hydrograph and total exported discharge volume. The calibration and sensitivity analyses were conducted using the PEST algorithm (Doherty, 2002). PEST uses a classical optimisation approach based on the minima in error surfaces and incorporates the Gauss-Marquardt-Levenberg (GML) algorithm. PEST minimises an objective function that is the sum of the weighted square deviation between the measured and predicted outflow (Doherty, 2002). The drawback of this method is that the algorithm might converge to a local minima depending on the error surface and start values for the optimisation run (Cullmann et al., 2011). The initial value for calibration is therefore crucial and must be accurately estimated before calibration.

To assess the input parameters that most significantly influenced the model results, a sensitivity analysis that varied one factor at a time was performed using the SENSAN component of PEST (Doherty, 2002). It was performed by increasing and decreasing each individual input variable and parameter by 20% and examining the model output in terms of total discharge. Although the one factor-at-a-time method overlooks the interactions and non-linear effects of the input parameters (Saltelli et al., 2004), it provides a preliminary appreciation of the primary influence of the input parameters on the total discharge predictions and emphasises the input parameters for which measurement and calibration efforts are most required.

### 3.8. Evaluation criteria and data analysis

The predicted and observed total discharge, peak discharge and peak time discharge were first compared at the outlet of the catchment. Comparisons of the predicted and observed hydrographs were assessed qualitatively (visual comparison) and quantitatively based on a multi-criteria analysis. Three criteria were calculated: (i) the Nash Suttcliff coefficient (NSE), (ii) Kling-Gupta efficiency (KGE), and (iii) bias indicator (BIAS) (Milella et al, 2012). The NSE and KGE assess the consistency of the peak flow with respect to the timing and discharge peaks (Eq. 3):

$$NSE = 1 - \frac{\sum_{i=1}^n (Q_{i_{obs}} - Q_{i_{sim}})^2}{\sum_{i=1}^n (Q_{i_{obs}} - \bar{Q}_{obs})^2} \quad (\text{Eq. 3})$$

where  $i$  is the time step,  $Q_{i_{obs}}$  is the observed outflow at  $i$ ,  $Q_{i_{sim}}$  is the predicted outflow at  $i$ , and  $\overline{Q_{obs}}$  is the average observed outflow during the event. KGE (Gupta et al., 2009) is estimated as follows (Eq. 4):

$$KGE = 1 - \sqrt{(r - 1)^2 + (\alpha - 1)^2 + (\beta - 1)^2} \quad (\text{Eq. 4})$$

where  $r$  is the linear correlation coefficient between the simulated and observed discharge.  $\alpha$  and  $\beta$  are determined as follows:  $\alpha = \frac{\sigma_s}{\sigma_o}$ ;  $\beta = \frac{\mu_s}{\mu_o}$ ; where  $\sigma$  is the standard deviation,  $\mu$  is the mean value, subscript 's' represents simulations, and 'o' represents observations. BIAS produces a global concept of the overestimation or underestimation (Eq. 5):

$$BIAS = 100 \times \frac{\sum_{i=1}^n (Q_{i_{obs}} - Q_{i_{sim}})}{\sum_{i=1}^n Q_{i_{obs}}} \quad (\text{Eq. 5})$$

Considering the complexity of the interactions among physical processes, performing the validation at the outlet can mask important spatial variation in the catchment (Lee et al., 2012). Therefore, for each runoff event, the predicted runoff pathways were compared to the runoff detectors within the catchments (P1 and P2, Figure V-3) and the spatial observations after the 2 largest events on May 2 and May 21. The percentage of the catchment area where runoff occurred and the percentage of such area hydrologically connected to the outlet *via* surface runoff were calculated based on LISEM output maps with ArcGIS 10.1.

The calibrated parameters and their sensitivity were compared to the measured system properties using the paired nonparametric Wilcoxon signed rank test and the Spearman rank correlation test. Statistical tests were performed using the R software (R development Core Team, 2008; version 2.6.2).

## 4. Results

### 4.1. Basic calibration method (BCM)

The basic calibration method (BCM) was first assessed by calibrating the LISEM parameters independently for each runoff event. For the 9 runoff events, measured hydrographs were systematically under-predicted by the BCM, as shown by the negative BIAS values (Table V-4). The observed hydrographs were fitted by LISEM with the BCM approach (Figure VII-10), resulting in NSE and KGE values ranging from 0.4 to 0.97 (Table V-4). On the contrary, runoff pathways were not adequately simulated, particularly for May 2 and May 21. Although observed runoff occurred at the two internal control points (P1 and P2) for these 2 events, only the runoff at internal control point P1 was predicted by the BCM. According to the LISEM predictions for

the 9 runoff events, an average of 63% of the cereal surfaces triggered runoff and were hydrologically connected *via* surface runoff to the outlet of the catchment, whereas the field observations revealed that runoff mostly occurred on the bare soil.

As expected for the event-based calibrations (Van den Putte et al., 2013), equifinality occurred. A clear compensation between the  $K_{sat}$  and  $\Psi$  parameters was observed during the partitioning between the runoff and infiltration (Figure VII-8), and there was also a compensation between the  $K_{sat}$  parameters for the different land uses. For example, the calibrated  $K_{sat \text{ wheat}}$  increased from 4 to 60 mm h<sup>-1</sup> between June 11 and June 12, whereas in the same time period,  $K_{sat \text{ corn}}$  decreased from 60 to 6 mm h<sup>-1</sup>; This is clearly unrealistic in only one day. Contrasting runoff pathways were predicted for a similarly predicted hydrograph at the outlet with different  $K_{sat}$  for wheat and corn (Figure VII-9). The parameters obtained with BCM are therefore poorly constrained, highly interdependent and not consistent with agronomical knowledge. These results highlighted the weakness of calibrations performed independently for each event.

**Table V-4. Comparisons of measured and predicted runoff events in terms of total discharge [m<sup>3</sup>], peak time discharge [min], peak discharge [L s<sup>-1</sup>] and performance criteria for each runoff events.**

	Total discharge [m <sup>3</sup> ]			Peak discharge [L s <sup>-1</sup> ]			Peak time discharge [min]		
	Obs	CCM	% Diff	Obs	CCM	% Diff	Obs	CCM	% Diff
May 2	17	26.2	54.1	16	16.6	3.6	184	188.6	2.5
May 21	10411	5800.4	-44.3	*	1929.0	*	*	235.3	*
May 23	124	165.2	33.3	105	96.6	-8.7	27	26.5	-1.9
June 7	201	179.8	-10.5	131	156.0	16.0	84	82.3	-2.0
June 11	140	137.1	-2.1	129	127.8	-0.9	19	20.5	7.9
June 12	383	177.4	-53.7	125	125.1	0.1	53	57.2	7.9
July 7	217	232.6	7.2	229	228.1	-0.4	34	33.8	-0.6
July 8	69	40.0	-42.0	30	30.0	0.0	90	111.6	24.0
July 10	22	8.1	-63.2	37	7.6	-79.5	10	13.2	32.0

	BIAS		KGE		Nash coefficient	
	BCM	CCM	BCM	CCM	BCM	CCM
May 2	-38.87	11.30	0.45	0.55	0.57	0.02
May 21	-0.97**	4.49**	0.69**	0.44**	0.94**	0.10**
May 23	-2.12	-0.62	0.85	0.84	0.78	0.68
June 7	-3.31	-14.70	0.96	0.82	0.97	0.82
June 11	8.88	-7.80	0.75	0.82	0.76	0.68
June 12	-28.60	-56.45	0.70	0.35	0.73	0.21
July 7	-15.17	1.81	0.52	0.76	0.53	0.52
July 8	-19.56	-48.04	0.75	0.40	0.82	-0.01
July 10	-10.85	-75.36	0.45	-0.28	0.40	-0.17

\*flood retention

\*\*between the beginning of the rainfall event and the flooding of the pipe

#### **4.2. Constraint calibration method (CCM)**

To overcome the limitation of the BCM strategy, the more constrained CCM approach was developed and tested on the study site. In general, the BIAS criteria indicated that the predictions underestimated the runoff water volume. The adequacies for the total discharge, peak discharge, and peak time discharge between predicted and measured runoff and the NSE are presented for the 9 runoff events (Figure VII-10). The KGE ranged between -0.28 and 0.84, and the NSE obtained with the CCM were always lower than those obtained by the BCM; however, certain events presented a better KGE for the CCM than the BCM (Table V-4). For May 2 and July 10, the LISEM could reproduce two peaks with the CCM compared to the BCM method (Figure VII-10), indicating that the hydrological processes and their spatial amplitudes were better represented. This improvement could only be confirmed with KGE for May 2 (Table V-4). The runoff pathways were significantly improved because the runoff was observed for the 9 events at the 2 internal control points P1 and P2, which were simulated by LISEM. Moreover, for the largest event (May 21), the predicted runoff pathways corresponded to the observations (Figure VII-11). Fifty-four percent of the catchment surface was hydrologically connected to the outlet *via* surface runoff according to the LISEM runoff mapping during the crop growing season. As observed in the field, wheat, alfalfa and oat plots were not primary contributors to the predicted runoff, and only 2% of the cereal areas were hydrologically connected. The slight decrease of the criteria based on the discharge fitting was counterbalanced by a clear improvement of the runoff pathways within the catchment.

The temporal variation of the calibrated value of  $\theta_{il}$  (0 - 25 cm) follows the same tendency as the measured topsoil water content (0 - 3 cm) (Figure V-4). The calibrated  $K_{sat}$  values varied between 0.7 and 1.5 mm h<sup>-1</sup> and were in the range of values obtained in previous studies for similar agricultural catchments in temperate areas (Risse et al., 1995). Despite the constraint rules, a small increase of  $K_{sat}$  for corn and sugar beet values was necessary for June 7 to improve the predictions of runoff at P0 (Figure V-4). An increase of  $K_{sat}$  was previously observed during the cropping seasons (Mubarak et al., 2009) and could partly be a result of the restructuring of the soil 17 days after the intensive rainfall event of May 21 and the soil drying cycle (Mubarak et al., 2009) because no rainfall occurred between May 23 and June 2.

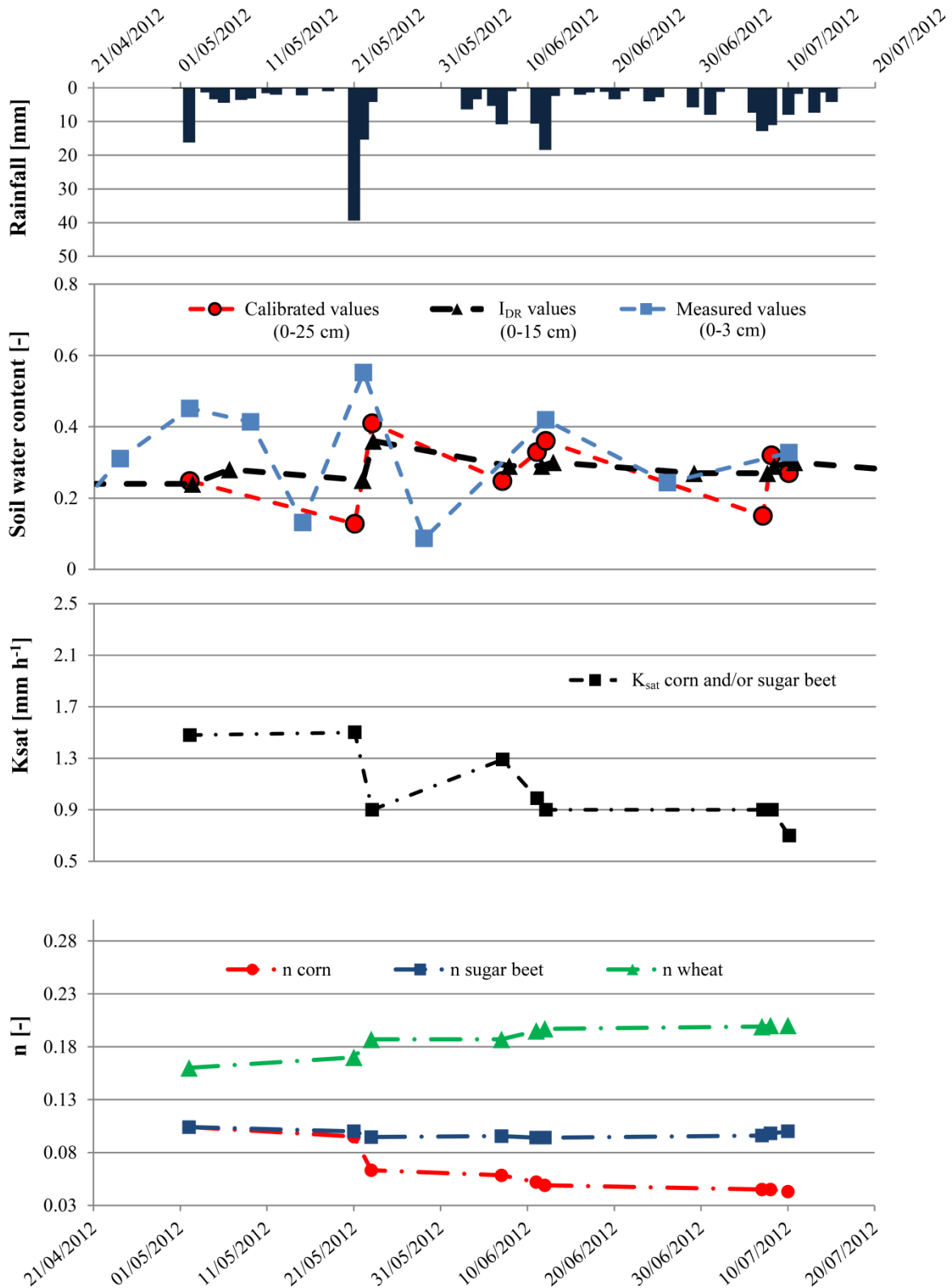


Figure V-4. Temporal changes of calibrated initial water content, saturated hydraulic conductivity and Manning coefficient related to the daily rainfall from May 2 to July 10 2012.

### 4.3. Sensitivity analysis of input parameters

A sensitivity analysis was conducted for each event to observe the influence of input parameters over time on the model results and to allocate efforts in the calibration method focused on the most influential input parameter. A sensitivity analysis of the 21 parameters of LISEM was assessed for the CCM calibrated input parameters. The results showed that the Green and Ampt parameters, i.e.,  $\theta_{sat1}$ ,  $\theta_{i1}$ ,  $K_{sat1}$ , and  $\Psi_1$ , were the major factors that influenced the total discharge for the 9 runoff events (Figure V-5), which was previously shown (Sheikh et al., 2010; Zeng et al., 2013).

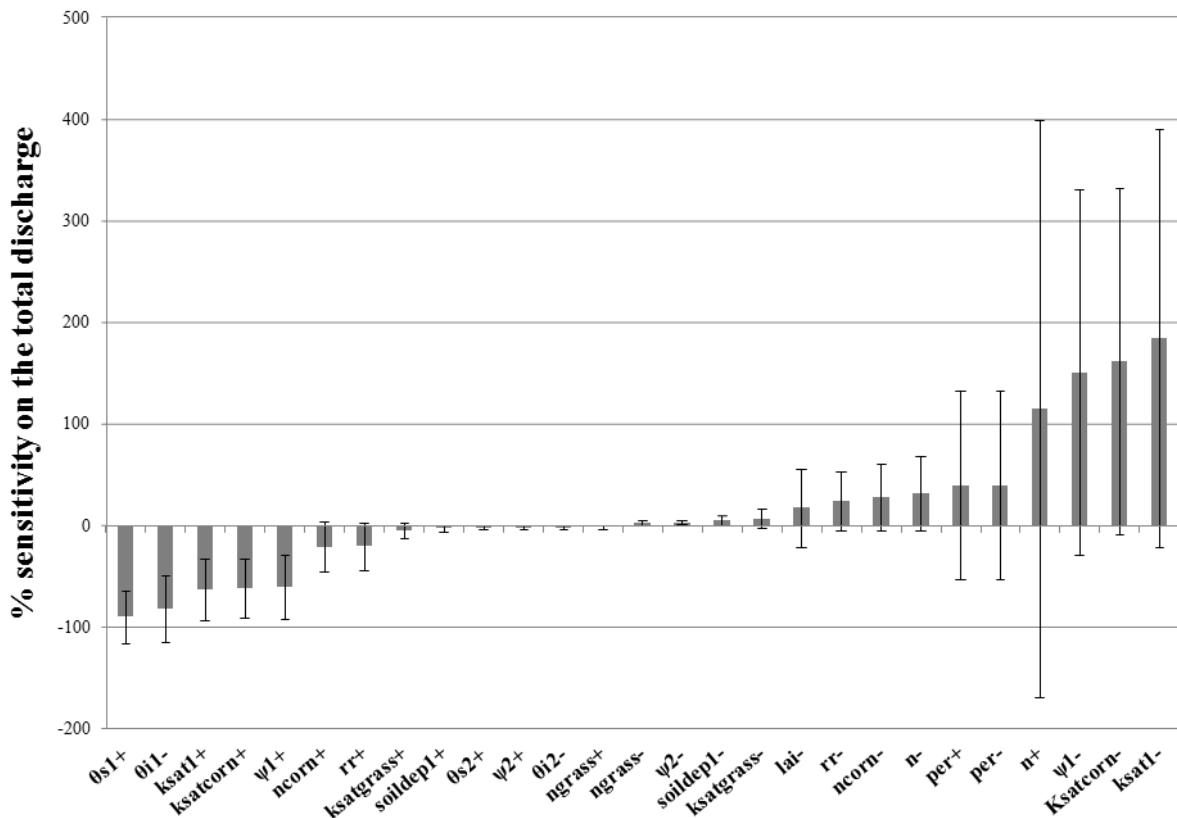


Figure V-5. Relative sensitivity of total discharge [%] for 20% variation of each input parameter separately. Only parameters for which total discharge sensitivity exceeded 1% were represented. Abbreviations for the input parameters are explained in the nomenclature. Plus or minus symbol indicates 20% increase or decrease respectively. Errors bars represent the temporal variability of the sensitivity within the 9 runoff events.

$K_{sat2}$ ,  $\Psi_2$ , and  $soildep_2$  were relatively insensitive to the total discharge (from -2 to 2% of the total discharge for 20% of the change) (Figure V-5), suggesting the importance of the topsoil layers for Hortonian runoff generation. The impact of vegetation interception ranged from 0.8% of the total rainfall for the May 21 event to 19.8% for the July 10 event. The sensitivity of the leaf area index of corn was significantly correlated with the corn coverage fractions ( $\rho = 0.9$ ,  $p < 0.001$ ) and indicated that the sensitivity of the vegetation increased with the vegetation growth at the end of the season. The sensitivity analysis of the 21 parameters did not significantly differ

between the 9 runoff events ( $p > 0.5$ ). The sensitivity of the initial moisture on the total discharge was lower (between 10 to 300 times less important) for intensive events, such as on May 21, compared to other events, which was previously shown by Sheikh (Sheikh et al., 2010). The observed runoff coefficient presented a significant negative correlation with the sensitivity of  $K_{sat1}$  to the total discharge ( $\rho = -0.98$ ,  $p < 0.001$ ), suggesting that  $K_{sat1}$  was also less sensitive during intensive runoff events. These results showed that conducting a sensitivity analysis on a single event was definitely not representative of the sensitivity over a crop-growing season.

#### **4.4. Erosion characterisation and prediction: focus on May 21**

The event on May 21 was the largest event of the study period, and calibration was only possible at the beginning of its hydrograph because discharge was not limited by the discharge capacity of the outlet pipe. The erosion observations may help to validate the predicted runoff pathways. The predicted deposits and eroded masses were clearly underestimated, which was expected because of the underestimation of the total discharge (Table V-4 and V-5). However, the simulated deposition in the vegetal barrier compared to the simulated total deposition was in the same range as the field measurements following the event. Similarly, an identical proportion of the flow detachment erosion compared to the total erosion was found between the field measurements and simulations. The predicted erosion rates ranged between 6 and 82 ton ha<sup>-1</sup> according to each plot and were represented against the observations (Figure VII-12). LISEM strongly over-predicted the erosion rates in cereal fields and under-predicted the erosion rates in plots 20, 21 and 22 (Figure V-3 and Figure VII-12). This result was confirmed by Takken (1999), who observed that the spatial variation in erosion rates for different crop types was not well-predicted. The poor spatial agreement of the spatial erosion prediction with the observations may be partly due to the fact that the effect of tillage on the runoff pattern was not taken into account, which may have had an important effect on the predicted local erosion rates (Takken et al., 1996) or by an incomplete or incorrect predictive impact of vegetation on the erosion processes. The predicted suspended solid concentrations obtained by LISEM were in the same order of magnitude as the measured results (Table V-5).

Measured			Predicted		
<i>Mass budget</i>	[ton]	[%]		[ton]	[%]
<i>Erosion</i>					
Rill/interrill	2414	91	Flow detachment	1445	95
Diffusive	No quantified : $\approx 250$	9	Splash detachment	78	5
<i>Deposition</i>					
Vegetal barrier	1482	67	Sediment traps	795	63
Topography**	666	30	Other type of deposition	458	37
Headlands	63	3			
<i>Soil loss at the outlet</i>					
	433			246	
<i>Mean TSS concentrations</i>					
	[g L <sup>-1</sup> ]			[g L <sup>-1</sup> ]	
Plot (P2)	2.9			7	
Catchment (P0)	59.7			46	

**Table V-5. Measured and predicted total erosion and deposition [ton] within the catchment and the total soil loss at the outlet of the catchment.**

\*\* Deposition in the plot in front of the dike was included in topographical deposition

## 5. Discussion and conclusion

Predicting runoff in agricultural areas is inherently difficult because of rapid changes in the surface characteristics, hydrodynamic parameters and vegetation. Advances in model accuracy can be achieved by investing more effort in calibration methods based on agronomical information, spatial validation and erosion prediction.

The LISEM parameters were calibrated independently for each event (BCM approach); however, predictions did not correctly represent the runoff pathways within the catchment despite constraining the input parameters within their physical extent. Furthermore, the temporal variations of the input parameters were unlikely to occur. The developed constraint calibration approach (CCM) clearly showed that considering the temporal variability of hydrodynamic parameters along the growing season helped to enhance the model prediction from a limited amount of supplementary information despite a slight degradation of evaluation criteria of the prediction at the catchment outlet. Therefore, our results confirm the observations of Risse et al.

(1994) and Van den Putte et al. (2013), who stated that the performance of the Green and Ampt model could not be improved by calibrating  $\Psi$  in addition to  $K_{sat}$ .

We anticipate that the CCM method is readily transposable for agricultural areas where a similar soil surface evolution is observed. Because the main factors influencing the runoff were the Green and Ampt parameters, the main initial assumptions regarding the homogeneity of the initial and saturated water content ( $\theta_{i1}$  and  $\theta_{sat1}$ ) within the catchment and the homogeneity of the permeability for each crop may be relaxed in future studies. The spatial variability of the soil moisture content could have a major impact on the predictions (Craig et al., 2010; Kale and Sahoo, 2011). Spatial variations of  $\theta_{i1}$  can be estimated with a simple soil water balance model that can be used in continuous time periods to predict each pre-event  $\theta_i$  (Sheikh et al., 2009). The constant under-estimation of the total discharge, shown by the BIAS parameters for both the BCM and CCM, could be partly explained by the drainage contribution. Drainage could also explain the wider shape of the observed hydrographs compared to the predicted hydrographs. The peak rainfall intensity presented a significant negative correlation with the drainage contribution ( $\rho = -0.73$ ;  $p < 0.05$ ), which suggested that the drainage contribution was important for smaller events. The observed drainage contribution showed a significant correlation with the sensitivity of  $\theta_{i2}$  ( $\rho = 0.81$ ,  $p < 0.05$ ), suggesting that the humidity of the deeper layers and the low flow component prevailed when the drainage was dominant compared to the runoff. The frequency of significant muddy flows observed in the catchment, which were prone to soil crusting and compaction, confirmed the major role of surface runoff.

Erosion predictions may help to validate runoff predictions. Runoff velocity reduction and sediment deposition in headlands, when the tillage orientation changed, was not predicted by LISEM. The impact of tillage direction on runoff and erosion pathways may be improved by the Tillage-Controlled Runoff Pattern model (TCRP) because it can change the local flow direction according to the tillage practices (Takken et al., 2001; van Dijk et al., 2005).

The full coupling of a distributed hydrological event-based model with an agronomical model should be further investigated when considering the dynamics of the initial soil surface characteristics and hydrodynamic parameters. This coupling should enhance the model accuracy and reduce the equifinality. This future approach may help to bridge the gap between events and continuous-based modelling.

## 6. Acknowledgements

The authors are members of REALISE, the Network of Laboratories in Engineering and Science for the Environment in the Alsace Region (France; <http://realise.unistra.fr>), and the support from REALISE is gratefully acknowledged. This research was funded by the PhytoRET project (C.21) of the European INTERREG IV program in the Upper Rhine. Marie Lefrancq was supported by the European INTERREG IV program in the Upper Rhine and Water Agency of Rhine Meuse. We acknowledge, in particular, Anne-Véronique Auzet for her considerable knowledge of erosion and soil surface states, the soil laboratory UMS830 EOST/CNRS, Martine Trautmann for the soil analysis and Jean-Bernard Bardiaux for his hydraulic expertise. We would like to thank Gwenaël Imfeld for helpful comments.

## 7. References

- Aksoy, H., Kavvas, M.L., 2005. A review of hillslope and watershed scale erosion and sediment transport models. *Catena*. 64, 247-271.
- Alaoui, A., Lipiec, J., Gerke, H.H., 2011. A review of the changes in the soil pore system due to soil deformation: A hydrodynamic perspective. *Soil & Tillage Research*. 115, 1-15.
- Ali, B., 2008. Typologie fonctionnelle des états de surface du sol [EDS] pour l'extrapolation des propriétés hydro-érosives. . Thèse, Université Louis Pasteur de Strasbourg – CNRS. Institut de Mécanique des Fluides et des Solides. 206 pp.
- Armand, R., Bockstaller, C., Auzet, A.V., Van Dijk, P., 2009. Runoff generation related to intra-field soil surface characteristics variability Application to conservation tillage context. *Soil & Tillage Research*. 102, 27-37.
- Augustin, L.N., Irish, J.L., Lynett, P., 2009. Laboratory and numerical studies of wave damping by emergent and near-emergent wetland vegetation. *Coastal Engineering*. 56, 332-340.
- Baartman, J.E.M., Jetten, V.G., Ritsema, C.J., de Vente, J., 2012. Exploring effects of rainfall intensity and duration on soil erosion at the catchment scale using openLISEM: Prado catchment, SE Spain. *Hydrological Processes*. 26, 1034-1049.
- Berthet, L., Andreassian, V., Perrin, C., Javelle, P., 2009. How crucial is it to account for the antecedent moisture conditions in flood forecasting? Comparison of event-based and continuous approaches on 178 catchments. *Hydrology and Earth System Sciences*. 13, 819-831.
- Beven, K., 2006. A manifesto for the equifinality thesis. *Journal of Hydrology*. 320, 18-36.
- Chow, V., Maidment, D., Mays, L., 2013. *Applied Hydrology*, 2nd Edition, Vol., McGraw-Hill Companies, Incorporated.
- Cosby, B.J., Hornberger, G.M., Clapp, R.B., Ginn, T.R., 1984. A Statistical Exploration of the Relationships of Soil-Moisture Characteristics to the Physical-Properties of Soils. *Water Resources Research*. 20, 682-690.

- Craig, J.R., Liu, G., Soulis, E.D., 2010. Runoff-infiltration partitioning using an upscaled Green-Ampt solution. *Hydrological Processes*. 24, 2328-2334.
- Cullmann, J., Krausse, T., Saile, P., 2011. Parameterising hydrological models - Comparing optimisation and robust parameter estimation. *Journal of Hydrology*. 404, 323-331.
- de Jong, S.M., Jetten, V.G., 2007. Estimating spatial patterns of rainfall interception from remotely sensed vegetation indices and spectral mixture analysis. *International Journal of Geographical Information Science*. 21, 529-545.
- DeRoo, A.P.J., Wesseling, C.G., Ritsema, C.J., 1996. LISEM: A single-event physically based hydrological and soil erosion model for drainage basins .1. Theory, input and output. *Hydrological Processes*. 10, 1107-1117.
- Doherty, J., 2002. PEST Model-Independent Parameter Estimation. *Watermark Numerical Computing*.
- Dotterweich, M., 2013. The history of human-induced soil erosion: Geomorphic legacies, early descriptions and research, and the development of soil conservation-A global synopsis. *Geomorphology*. 201, 1-34.
- Dunne, T., Black, R.D., 1970. Partial Area Contributions to Storm Runoff in a Small New England Watershed. *Water Resources Research*. 6, 1296-1311.
- Durán-Zuazo, V.H., Francia-Martínez, J.R., García-Tejero, I., Tavira, S.C., 2013. Implications of land-cover types for soil erosion on semiarid mountain slopes: Towards sustainable land use in problematic landscapes. *Acta Ecologica Sinica*. 33, 272-281.
- Edwards, W.M., Owens, L.B., 1991. Large Storm Effects on Total Soil-Erosion. *Journal of Soil and Water Conservation*. 46, 75-78.
- Efstratiadis, A., Koutsoyiannis, D., 2010. One decade of multi-objective calibration approaches in hydrological modelling: a review. *Hydrological Sciences Journal-Journal Des Sciences Hydrologiques*. 55, 58-78.
- Evrard, O., Cerdan, O., van Wesemael, B., Chauvet, M., Le Bissonnais, Y., Raclot, D., Vandaele, K., Andrieux, P., Bielders, C., 2009. Reliability of an expert-based runoff and erosion model: Application of STREAM to different environments. *Catena*. 78, 129-141.
- Fiener, P., Auerswald, K., Van Oost, K., 2011. Spatio-temporal patterns in land use and management affecting surface runoff response of agricultural catchments-A review. *Earth-Science Reviews*. 106, 92-104.
- Green, T.R., Ahuja, L.R., Benjamin, J.G., 2003. Advances and challenges in predicting agricultural management effects on soil hydraulic properties. *Geoderma*. 116, 3-27.
- Gupta, H.V., Kling, H., Yilmaz, K.K., Martinez, G.F., 2009. Decomposition of the mean squared error and NSE performance criteria: Implications for improving hydrological modelling. *Journal of Hydrology*. 377, 80-91.
- Heitz, C., Flinois, G., Glatron, S., 2012. Protection against muddy floods: perception for local actors in Alsace (France) of a protection measure (fascines). *International Disaster Risk Conference, Davos, Suisse, 26-30 Août 2012*.

- Hessel, R., van den Bosch, R., Vigiak, O., 2006. Evaluation of the LISEM soil erosion model in two catchments in the East African Highlands. *Earth Surface Processes and Landforms*. 31, 469-486.
- Hessel, R., Jetten, V., 2007. Suitability of transport equations in modelling soil erosion for a small Loess Plateau catchment. *Engineering Geology*. 91, 56-71.
- Hunt, R., 1982. *Plant growth curves*. Edward Arnold, London, 248.
- Kale, R.V., Sahoo, B., 2011. Green-Ampt Infiltration Models for Varied Field Conditions: A Revisit. *Water Resources Management*. 25, 3505-3536.
- Kamphorst, E.C., Jetten, V., Guerif, J., Pitkanen, J., Iversen, B.V., Douglas, J.T., Paz, A., 2000. Predicting depression storage from soil surface roughness. *Soil Science Society of America Journal*. 64, 1749-1758.
- Kirchner, J.W., 2006. Getting the right answers for the right reasons: Linking measurements, analyses, and models to advance the science of hydrology. *Water Resources Research*. 42.
- Kohler, M.A., Linsley, R.K., 1951. Predicting the runoff from storm rainfall. *US weather Bureau Res.*
- Kutilek, M., Nielsen, D.R., 1994. *Soil hydrology*, Vol., Catena Verlag.
- Lee, G., Tachikawa, Y., Sayama, T., Takara, K., 2012. Catchment responses to plausible parameters and input data under equifinality in distributed rainfall-runoff modeling. *Hydrological Processes*. 26, 893-906.
- Li, Z., Zhang, J.T., 2001. Calculation of field Manning's roughness coefficient. *Agricultural Water Management*. 49, 153-161.
- Liu, G.B., Xu, M.X., Ritsema, C., 2003. A study of soil surface characteristics in a small watershed in the hilly, gullied area on the Chinese Loess Plateau. *Catena*. 54, 31-44.
- Meijer, A.D., Heitman, J.L., White, J.G., Austin, R.E., 2013. Measuring erosion in long-term tillage plots using ground-based lidar. *Soil & Tillage Research*. 126, 1-10.
- Merritt, W.S., Letcher, R.A., Jakeman, A.J., 2003. A review of erosion and sediment transport models. *Environmental Modelling & Software*. 18, 761-799.
- Milella, P., Bisantino, T., Gentile, F., Iacobellis, V., Liuzzi, G.T., 2012. Diagnostic analysis of distributed input and parameter datasets in Mediterranean basin streamflow modeling. *Journal of Hydrology*. 472, 262-276.
- Mitasova, H., Barton, M., Ullah, I., Hofierka, J., Harmon, R.S., 2013. 3.9 GIS-Based Soil Erosion Modeling. In: *Treatise on Geomorphology*. Vol., J.F. Shroder, ed. eds. Academic Press, San Diego, pp. 228-258.
- Morgan, R.P.C., Quinton, J.N., Smith, R.E., Govers, G., Poesen, J.W.A., Chisci, G., Torri, D., 1998. The EUROSEM model. *Modelling Soil Erosion by Water*. 55, 389-398.
- Mubarak, I., Mailhol, J.C., Angulo-Jaramillo, R., Ruelle, P., Boivin, P., Khaledian, M., 2009. Temporal variability in soil hydraulic properties under drip irrigation. *Geoderma*. 150, 158-165.
- O'Hare, M.T., McGahey, C., Bissett, N., Cailes, C., Henville, P., Scarlett, P., 2010. Variability in roughness measurements for vegetated rivers near base flow, in England and Scotland. *Journal of Hydrology*. 385, 361-370.
- Pare, N., Andrieux, P., Louchart, X., Biarnes, A., Voltz, M., 2011. Predicting the spatio-temporal dynamic of soil surface characteristics after tillage. *Soil & Tillage Research*. 114, 135-145.

- Potter, K.N., 1990. Soil Properties Effect on Random Roughness Decay by Rainfall. *Transactions of the Asae*. 33, 1889-1892.
- Risse, L.M., Nearing, M.A., Savabi, M.R., 1994. Determining the Green-Ampt Effective Hydraulic Conductivity from Rainfall-Runoff Data for the Wepp Model. *Transactions of the Asae*. 37, 411-418.
- Risse, L.M., Nearing, M.A., Zhang, X.C., 1995. Variability in Green-Ampt Effective Hydraulic Conductivity under Fallow Conditions. *Journal of Hydrology*. 169, 1-24.
- Saltelli, A., Tarantola, S., Campolongo, F., Ratto, M., 2004. *Sensitivity Analysis in Practice: A Guide to Assessing Scientific Models*, Vol., Wiley.
- Sanchez-Moreno, J.F., Mannaerts, C.M., Jetten, V., Loffler-Mang, M., 2012. Rainfall kinetic energy-intensity and rainfall momentum-intensity relationships for Cape Verde. *Journal of Hydrology*. 454, 131-140.
- Sheikh, V., Visser, S., Stroosnijder, L., 2009. A simple model to predict soil moisture: Bridging Event and Continuous Hydrological (BEACH) modelling. *Environmental Modelling & Software*. 24, 542-556.
- Sheikh, V., van Loon, E., Hessel, R., Jetten, V., 2010. Sensitivity of LISEM predicted catchment discharge to initial soil moisture content of soil profile. *Journal of Hydrology*. 393, 174-185.
- Takken, I., Beuselinck, L., Nachtergaele, J., Govers, G., Poesen, J., Degraer, G., 1999. Spatial evaluation of a physically-based distributed erosion model (LISEM). *Catena*. 37, 431-447.
- Takken, I., Govers, G., Jetten, V., Nachtergaele, L., Steegen, A., Poesen, J., 2001. Effects of tillage on runoff and erosion patterns. *Soil & Tillage Research*. 61, 55-60.
- Tramblay, Y., Bouvier, C., Martin, C., Didon-Lescot, J.F., Todorovik, D., Domergue, J.M., 2010. Assessment of initial soil moisture conditions for event-based rainfall-runoff modelling. *Journal of Hydrology*. 387, 176-187.
- Van den Putte, A., Govers, G., Leys, A., Langhans, C., Clymans, W., Diels, J., 2013. Estimating the parameters of the Green-Ampt infiltration equation from rainfall simulation data: Why simpler is better. *Journal of Hydrology*. 476, 332-344.
- Van Dijk, P., Villerd, J., Koller, R., Bockstaller, C., in prep. A predictive indicator for overland flow potential of cropping systems: accounting for farmers' control on key variables.
- Van Dijk, P.M., Auzet, A.V., Lemmel, M., 2005. Rapid assessment of field erosion and sediment transport pathways in cultivated catchments after heavy rainfall events. *Earth Surface Processes and Landforms*. 30, 169-182.
- Wallner, M., Haberlandt, U., Dietrich, J., 2013. A one-step similarity approach for the regionalization of hydrological model parameters based on Self-Organizing Maps. *Journal of Hydrology*. 494, 59-71.
- Xu, Q.X., Wang, T.W., Cai, C.F., Li, Z.X., Shi, Z.H., Fang, R.J., 2013. Responses of Runoff and Soil Erosion to Vegetation Removal and Tillage on Steep Lands. *Pedosphere*. 23, 532-541.
- Zeng, C., Wang, Q.J., Zhang, F., Zhang, J., 2013. Temporal changes in soil hydraulic conductivity with different soil types and irrigation methods. *Geoderma*. 193, 290-299.

LISEM provided consistent prediction i) of discharge, volume at the outlet of the studied crop catchment and ii) of the runoff pathways within the catchment associated to runoff events along a crop growing season. A mathematical formalism for assessing dissolved pesticide runoff transport was therefore developed and integrated in LISEM to evaluate different study case scenarios. The mathematical formalism is introduced in the following section.

## **Section 2. A comprehensive mathematical model for mobilisation and transport of dissolved pesticide from the soil surface to runoff: the mixing layer approach.**

### **1. Introduction**

On soil surfaces, runoff and associated erosion represent a primary mode of mobilisation and transfer of pesticides from agricultural land to surface water (Oliver et al., 2012). Pesticide mobilisation from soil into runoff involves complex combination of various transport mechanisms including raindrop-driven processes, diffusion induced by the pesticide concentration gradient, erosion of sediment with adsorbed pesticide and adsorption/desorption of pesticides in soil-water systems (Gao et al., 2005; Shi et al., 2011; Wallach et al., 2001). Many models have been developed for predicting pesticide transfer between soil-water and runoff (Borah and Bera, 2003; Holvoet et al., 2007; Kohne et al., 2009; Payraudeau and Grégoire, 2012; Quilbe et al., 2006).

Predicting runoff, erosion and the subsequent transport of pesticides in agricultural areas is inherently difficult because of rapid changes in soil surface characteristics and hydrodynamic parameters. Currently, few pesticide runoff models account for the effects of agricultural practices on hydrodynamic parameters and soil surface characteristics and most of them are deemed inappropriate for investigating headwater catchment scale with a very fine temporal resolution ( $\leq 1$  min) (Chap. I. §2.2.4). This emphasises the need for an event based, spatially distributed pesticide transport model at the catchment scale integrating changes in soil surface characteristics and soil hydrodynamic parameters (Payraudeau and Grégoire, 2012). LISEM (Limbourg Soil Erosion Model), an event based model, that is fully distributed, was designed to explicitly describe the soil surface structures including crusted and compacted zones, and the diversity of agricultural landscape components, i.e. plots and plots margins in headwater catchments (Liu et al., 2003). An additional reason, which has motivated the selection of LISEM, lies in its consideration for erosion processes which opens doors for further investigation on solid-bound pesticide prediction. The objective of this study was therefore to predict the mobilisation and the transport of dissolved pesticide in runoff.

Pesticide mobilisation between soil, soil water and runoff is usually modelled as either a diffusion-like process or a mixing model (Gao et al., 2005; Shi et al., 2011). In the diffusion

models, a boundary layer is described as an interfacial diffusion-controlled process driven by the concentration gradient. The mixing layer concept is probably the most commonly used in pesticide fate models due to its numerical simplicity and its realistic representation, as Hortonian runoff processes have repeatedly been shown to be initiated as a near-surface process (Gao et al., 2004; McGrath et al., 2008; Wallender et al., 2008). This concept assumes that the transport is controlled by a mixing layer below the soil surface, in which rainwater, soil solution and runoff water completely and instantaneously mix (Havis et al., 1992). The soil depth interacting with runoff water is variable ranging from 0.25 to 2 cm according to various experimental and modelling studies (Ahuja et al., 1981; Havis et al., 1992; Wallender et al., 2008). Previous studies have shown that the effective depth of interaction is related to the degree of soil aggregation and increases with soil slope, kinetic energy of raindrops and rainfall intensity (Havis et al., 1992). In fact, the observed mixing-layer depth is often much shallower than the depth required for fitting models to field data (Gao et al., 2004). In reality, rainfall water and soil water are incompletely mixed because soil water inside soil aggregates is partly inaccessible and the hydraulic turbulences produced by rainfall impact decrease with depth (Shi et al., 2011). The concept of a 'film transport coefficient' was therefore introduced to describe the transfer rate between soil water and runoff water (Havis et al., 1992; Shi et al., 2011). In dynamic conditions existing in the field, pesticide sorption equilibrium could take several hours (Lafrance and Caron, 2012). Given the short time steps used in the model ( $\leq 1$  min), a first-order kinetic reaction was used to describe pesticide sorption/desorption in the mixing zone (Wallender et al., 2008).

Combining chemical processes, i.e. sorption and diffusion, and transport processes requires significant computational effort due to the non-linearity of the equations (Wallach et al., 2001). Two main approaches exist to solve the coupled equations for transient flow and solute transport: (i) the operator splitting approach, in which the transport via runoff and the chemistry are solved sequentially, and (ii) the one-step global implicit approach in which the transport and the chemistry equations are solved simultaneously (Jacques et al., 2006). Operator splitting techniques are often used to solve complex equation systems by splitting the governing equations into sub-equations, wherein each subset of equations capture a portion of the physics present in the system (Ren et al., 2014). Among the operator splitting techniques, the sequential non-iterative approach (SNIA) consists in solving sequentially the transport then the chemistry part of the problem without iteration (Carrayrou et al., 2004). Operator splitting techniques provide efficient numerical approaches for developing resolution modules separately and including them in an existing physically based-model (Lagneau and van der Lee, 2010). However, the operator splitting techniques often lead to mass balance errors and impose small

time steps during fast chemical kinetics (Carrayrou et al., 2004). In contrast, the main advantages of the global implicit method are that all processes are solved simultaneously, the method is mass-conservative and the approach is less sensitive to the large time step (Jacques et al., 2006), which may be an important consideration to address pesticide mobilisation and transport at catchment scale. However, this method is generally more complex mathematically and may require large computing memory (Jacques et al., 2006). To the best of our knowledge, very few studies used (pseudo-)analytical resolution, i.e. an analytical solution after spatial differentiation, to solve the implicit numerical schemes. This type of resolution may reduce the computing errors due to discretisation errors associated with the operator approximations (Carrayrou et al., 2004).

Two different numerical approaches were therefore tested and compared in order to (i) evaluate the influence of the solution procedure, (ii) retain the best approach for evaluating pesticides mobilisation and transport in runoff at catchment scale, and (iii) ensure an acceptable mass balance both for water and pesticide. First, an operator splitting approach (SNIA) was used to solve the pesticide mobilisation and transport equations (LISEM-psni model). The second approach considered a pseudo-analytical solution of the global implicit method (LISEM-pa model). Accuracy and robustness of LISEM-psni and LISEM-pa models were estimated by comparing results against the theoretical tests and the experimental data. By using a mass balance formulation and testing their stability over different time steps, both schemes were compared on three test cases: (i) steady state flow on one cell ( $1\text{m}^2$ ), (ii) an experimental case under constant rainfall at plot scale ( $4.5\text{ m}^2$ ) (Joyce, 2008) and (iii) a rainfall-runoff event in the Alteckendorf study catchment ( $470,000\text{ m}^2$ ) (previously presented in Chapter IV).

## 2. Mathematical theory and approach

### 2.1. Openlsem

Openlsem is an accessible and easy-to-use version of the soil erosion model LISEM (DeRoo et al., 1996). Openlsem is implemented in C++. Version 1.79 was used and modified under the cross-platform Qt version 4.8.3 (<http://qt-project.org/>) and the Visual Studio debugging tool 2010 (<http://msdn.microsoft.com>). The theory and structures of LISEM were described previously (Chap.V - Section 1-§2.4 and Annex 1). Only hydrological equations and numerical schemes, which are needed for the pesticide-water coupling are detailed here. Briefly, the water partitioning between infiltration and surface runoff was calculated with the Green and Ampt equations solved explicitly (Eq. 1) (Kutílek and Nielsen, 1994).

$$q_{inf} = -K_{sat} \left( 1 + \frac{(\psi + h)(\theta_{sat} - \theta_i)}{F} \right) \quad (\text{Eq. 1})$$

where  $q_{inf}$  is the infiltration rate [ $\text{m s}^{-1}$ ],  $K_{sat}$  the saturated hydraulic conductivity [ $\text{m s}^{-1}$ ],  $F$  the cumulative infiltration from the beginning of the event [ $\text{m}$ ],  $\psi$  the average matrix suction at the wetting front [ $\text{m}$ ],  $h$  the overpressure depth of the water layer at the soil surface [ $\text{m}$ ],  $\theta_{sat}$  the saturated water content [-] and  $\theta_i$  the initial water content of the soil layer [-]. Flow velocity was calculated for the infiltration surplus, i.e. surface runoff, with the Manning equation and surface runoff was routed over the landscape with the 1D kinetic wave equation (quasi 2D) (Eq. 2). The kinematic wave method is based on Chow et al. (2013) which combines the momentum and mass conservation equations in a classic way:

$$\frac{\partial A}{\partial t} + \frac{\partial Q}{\partial x} = q \quad (\text{Eq. 2})$$

where  $A$  is the wet cross section [ $\text{m}^2$ ],  $Q$  the discharge [ $\text{m}^3 \text{s}^{-1}$ ],  $q$  the infiltration surplus [ $\text{m}^2 \text{s}^{-1}$ ] and  $x$  and  $t$  the localisation [ $\text{m}$ ] and time [ $\text{s}$ ]. When surface runoff was routed over a grid cell that still had the capacity to infiltrate inside the kinematic wave routine, infiltration took place. The relation between  $A$  and  $Q$  is given by:

$$\begin{cases} A = \alpha Q^\beta \\ \alpha = \left[ \frac{n}{\sqrt{S}} P^{2/3} \right]^\beta \end{cases} \quad (\text{Eq. 3})$$

where  $P$  is the wet perimeter [ $\text{m}$ ],  $n$  the Manning's coefficient [-],  $S$  the sine of the slope gradient and  $\beta$  is a constant (0.6). Differentiation and combination of equations 2 and 3 gave the implicit

numerical scheme (Eq. 4) which was solved using a Newton backward-difference method (Chow et al., 2013).

$$\begin{cases} \alpha\beta Q^{\beta-1} \frac{\partial Q}{\partial t} + \frac{\partial Q}{\partial x} = q \\ \alpha\beta \bar{Q}^{\beta-1} \frac{Q_{i+1}^{n+1} - Q_{i+1}^n}{\Delta t} + \frac{Q_{i+1}^{n+1} - Q_i^{n+1}}{\Delta x} = q \text{ with } \bar{Q} = \frac{1}{2}(Q_i^{n+1} + Q_{i+1}^n) \end{cases} \quad (\text{Eq. 4})$$

where n is the current time step, n+1 the end of the time step, i the upstream side of a grid cell, i+1 the downstream side of grid cell,  $Q_{i+1}^{n+1}$  the new discharge [ $\text{m}^3 \text{s}^{-1}$ ],  $Q_i^{n+1}$  the new discharge at the “upstream end” of the grid cell which is the sum of all incoming water generated by the kinematic wave [ $\text{m}^3 \text{s}^{-1}$ ],  $Q_{i+1}^n$  the discharge of the previous time step which is outflowing the grid cell [ $\text{m}^3 \text{s}^{-1}$ ],  $\bar{Q}$  the diagonal average discharge in a space time diagram [ $\text{m}^3 \text{s}^{-1}$ ], q the average infiltration surplus over the length of the grid cell [ $\text{m}^2 \text{s}^{-1}$ ]. At each time step, the grid cells were re-arranged in order to start the flow calculation at the top of the branches of the drainage network and progress towards the outlet, using as input for the downstream grid cell the sum of the discharges of the upstream grid cells at the end of the time step.

As a future objective is to predict solid-bound pesticide transport, consistency with the numerical scheme used to solve the sediment and pesticide transport equations was targeted. Before computing the kinematic wave, splash, flow detachment and sediment deposition were solved separately based on rainfall intensity and updated velocity calculated with effective rainfall depth. Erosion procedures give an intermediate sediment concentration noted  $C^*$  (calculations are not detailed here). Suspended sediment in runoff is then routed using a similar equation as equation 2:

$$\frac{\partial Q_s}{\partial x} + \frac{\partial CA}{\partial t} = 0 \quad (\text{Eq. 5})$$

where  $Q_s$  is the sediment flux [ $\text{kg s}^{-1}$ ] and C the sediment concentration [ $\text{kg m}^{-3}$ ]. After differentiation and discretisation, we have:

$$\left\{ \begin{array}{l} \frac{\partial Q_s}{\partial x} + A \frac{\partial C}{\partial t} + C \frac{\partial A}{\partial t} = e - d \\ \frac{Q_{s,i+1}^{n+1} - Q_{s,i}^{n+1}}{\Delta x} + \bar{A} \frac{C_{i+1}^{n+1} - C_{i+1}^*}{\Delta t} + \bar{C} \alpha \beta \bar{Q}^{\beta-1} \frac{Q_{i+1}^{n+1} - Q_{i+1}^n}{\Delta t} = e - d \\ \frac{Q_{s,i+1}^{n+1} - Q_{s,i}^{n+1}}{\Delta x} + \alpha \bar{Q}^{\beta} \frac{C_{i+1}^{n+1} - C_{i+1}^*}{\Delta t} + \bar{C} \alpha \beta \bar{Q}^{\beta-1} \frac{Q_{i+1}^{n+1} - Q_{i+1}^n}{\Delta t} = e - d \end{array} \right. \quad (\text{Eq. 6})$$

where  $\bar{A} = \alpha \bar{Q}^{\beta}$  and  $\bar{C} = \frac{Q_{s,i}^{n+1} + Q_{s,i+1}^*}{Q_{i+1}^{n+1} + Q_{i+1}^n}$

Where \* indicates that concentration and flux are intermediary and yet considering the erosion or deposition processes of the new time step. Therefore, equation 6 was rewritten to calculate the new sediment flux (Eq. 7).

$$Q_{s,i+1}^{n+1} = \frac{\alpha \bar{Q}^{\beta} \Delta x \frac{Q_{s,i+1}^*}{Q_{i+1}^n} + \Delta t Q_{s,i}^{n+1} - \bar{C} \alpha \beta \bar{Q}^{\beta-1} \Delta x (Q_{i+1}^{n+1} - Q_{i+1}^n)}{\Delta t + \alpha \bar{Q}^{\beta} \frac{\Delta x}{Q_{i+1}^{n+1}}} \quad (\text{Eq. 7})$$

## 2.2. Mixing model

Pesticide mobilisation at the soil/surface runoff interface was predicted by assuming that a very thin layer at the soil surface exists where water from infiltration, runoff and soil pore mix instantaneously (Wallender et al., 2008). The developed conceptual model is shown in Figure V-6.

Pesticide loss below the mixing zone was considered as a sink term as the modelling focused on pesticide transport in runoff. The governing equations describing pesticide transport in runoff water were as follows:

$$\left\{ \begin{array}{l} \frac{1}{\Delta x} \left( \frac{\partial A C}{\partial t} + \frac{\partial Q_p}{\partial x} \right) = K_{film} (C_M - C) - q_{inf} C \\ \theta_s \varepsilon \frac{\partial C_M}{\partial t} = K_{film} (C - C_M) + q_{inf} (C - C_M) - \varepsilon \rho_b k_r (K_D C_M - C_s) \\ \frac{\partial C_s}{\partial t} = k_r (K_D C_M - C_s) \end{array} \right. \quad (\text{Eq. 8})$$

Where  $Q_p$  is pesticide flux [ $\text{kg s}^{-1}$ ],  $A$  the wet cross section [ $\text{m}^2$ ],  $q_{inf}$  the infiltration rate [ $\text{m s}^{-1}$ ],  $K_{film}$  the film transport coefficient [ $\text{m s}^{-1}$ ],  $k_r$  the rate of desorption [ $\text{s}^{-1}$ ],  $K_D$  soil water partition coefficient [ $\text{m}^3 \text{kg}^{-1}$ ],  $C$  the pesticide concentration in runoff [ $\text{kg m}^3$ ],  $C_M$  the pesticide

concentration in the soil water in the mixing zone [ $\text{kg m}^{-3}$ ],  $C_s$  the mass of pesticides adsorbed per dry unit weight of soil in the mixing zone [ $\text{kg kg}^{-1}$ ],  $\theta_s$  the soil porosity [ $\text{m}^3 \text{m}^{-3}$ ],  $\varepsilon$  the mixing layer depth [m] and  $\rho_b$  the soil bulk density [ $\text{kg m}^{-3}$ ]. This three equations' system is valid only if runoff occurs. Two hydrological cases were therefore considered: (1) runoff and (2) no runoff. The numerical limit ( $Q_{\text{lim}}$ ) for considering runoff has been defined as a minimum condition on the discharge outflowing the grid cell ( $Q$ ) and its value is discussed further. The case without runoff was treated similarly in both resolution approaches. When  $Q < Q_{\text{lim}}$  during runoff recession, exchanges via the  $K_{\text{film}}$  coefficient between runoff and mixing layer were interrupted and pesticide mass currently in runoff was infiltrated and transported over the system until pesticide runs out.

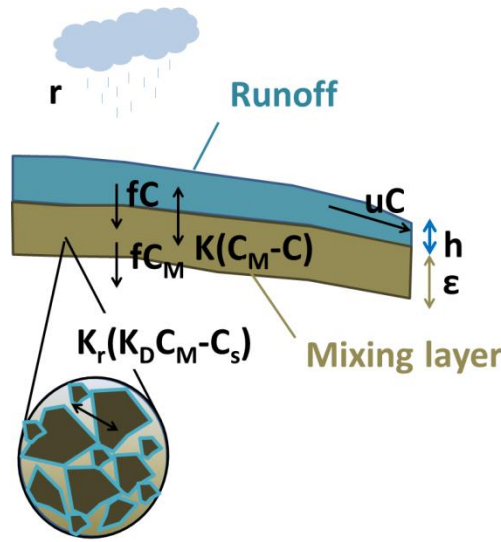


Figure V- 6. Conceptual mixing layer model for pesticide mobilisation (Adapted from Wallender (2008))

### 2.3. Numerical resolution with operator splitting (LISEM-psni)

The transport and chemical set of equations were first solved similarly to the sediment transport resolution in LISEM leading to the development of LISEM-psni. The resolution consisted in the sequential resolution of the chemical set of equations, noted with  $\chi$ -subscript (Eq. 9) and transport equations, noted with T-subscript (Eq. 10).

$$\begin{cases} \left( \frac{\partial C}{\partial t} \right)_{\chi} = K_{\text{film}} (C_M - C) - q_{\text{inf}} C \\ \left( \frac{\partial C_M}{\partial t} \right)_{\chi} = \frac{1}{\theta_s \varepsilon} (K_{\text{film}} (C - C_M) + q_{\text{inf}} (C - C_M) - \varepsilon \rho_b k_r (K_D C_M - C_s)) \\ \left( \frac{\partial C_s}{\partial t} \right)_{\chi} = k_r (K_D C_M - C_s) \end{cases} \quad (\text{Eq. 9})$$

$$\left. \frac{\partial CA}{\partial t} \right)_T = -\frac{\partial Q_p}{\partial x} \quad (\text{Eq. 10})$$

For the case of runoff, equations concerning pesticides in the soil water and the solid-phase of soil were equivalent to the differential equations system in matrix form (Eq. 11):

$$\begin{pmatrix} \frac{\partial C_M}{\partial t} \\ \frac{\partial C_s}{\partial t} \end{pmatrix} = \underbrace{\begin{pmatrix} -K_{film} - q_{inf} - \varepsilon \rho_b k_r K_D & \rho_b k_r \\ \theta_s \varepsilon & \theta_s \\ k_r K_D & -k_r \end{pmatrix}}_A \begin{pmatrix} C_M \\ C_s \end{pmatrix} + \underbrace{\begin{pmatrix} (K_{film} + q_{inf}).C \\ \theta_s \varepsilon \\ 0 \end{pmatrix}}_b \quad (\text{Eq. 11})$$

If pesticide concentration in runoff water (C) was supposedly constant over a time step and known from the previous time step ( $C^n$ ), the system (11) is a system of first-order linear differential equations and has therefore an unique vector-values solution ( $C, C_M, C_s$ ) for any given initial vector-values ( $C_0, C_{M0}, C_{S0}$ ). Analytical expressions for  $C_s$  and  $C_M$  were therefore computed with Maple 17©. A potential mass of pesticide in runoff ( $M_{runoff}$ ) was then calculated as follows:

$$M_{runoff}^{n+1} = M_{runoff}^n - (K_{film} + q_{inf}) \Delta x^2 \Delta t C^n + K_{film} \Delta x^2 \int_{n\Delta t}^{(n+1)\Delta t} C_M dt \quad (\text{Eq. 12})$$

Where  $\Delta t$  is the time step,  $\Delta x$  the spatial resolution,  $(n+1)\Delta t$  the new time of the calculation and  $n\Delta t$  the precedent time of calculation. Large time steps may lead to the calculation of negative pesticide masses in runoff. To avoid numerical problems during simulations, negative  $M_{runoff}^{n+1}$  values were artificially set to zero which may lead to inaccuracy in predicted pesticide concentrations. The obtained mass of pesticide leads to the calculation of an intermediate pesticide concentration in runoff  $C^*$  by considering the water volume in the cell at time  $n+1$ . This calculation is performed for all cells before moving to the next time step. Since the resolution was done from upstream to downstream, the transport equation (Eq. 10) was developed using the approach used for sediment transport resolution. Therefore,  $Q_p$  is the pesticide flux [ $\text{kg s}^{-1}$ ] defined by (Eq. 14).

$$\frac{\partial AC}{\partial t} + \frac{\partial Q_p}{\partial x} = 0 \quad (\text{Eq. 13})$$

$$Q_{p,i+1}^{n+1} = \frac{\Delta t Q_{p,i}^{n+1} + \alpha \bar{Q}^\beta \Delta x \frac{Q_{p,i+1}^*}{Q_{i+1}^n} - \bar{C} \alpha \beta \bar{Q}^{\beta-1} \Delta x (Q_{i+1}^{n+1} - Q_{i+1}^n)}{\Delta t + \alpha \bar{Q}^\beta \frac{\Delta x}{Q_{i+1}^{n+1}}} \quad (\text{Eq. 14})$$

## 2.4. Pseudo-analytical resolution (LISEM-pa)

The transport and chemical set of equations were solved analytically after spatial discretisation leading to the development of LISEM-pa. The first equation of the system (10) was transformed by differentiating the temporal derivation and by assuming that the wetted section, A, was constant over a time step (Eq. 15).

$$\begin{cases} \frac{\partial AC}{\partial t} + \frac{\partial Q_p}{\partial x} = \Delta x (K(C_M - C) - q_{inf} C) \\ \frac{\partial C}{\partial t} + \frac{\partial Q_p}{\partial x} = \Delta x (K(C_M - C) - q_{inf} C) \end{cases} \quad (\text{Eq. 15})$$

The system of ordinary differential equations is then:

$$\begin{cases} \frac{\partial C}{\partial t} + \frac{(Q^{n+1}C - Q_{upstream}^{n+1}C_{upstream}^{n+1})}{\Delta x} = \Delta x (K_{film}C_M - C(K_{film} + q_{inf})) \\ \alpha \bar{Q}^\beta \frac{\partial C}{\partial t} + \frac{(Q^{n+1}C - Q_{upstream}^{n+1}C_{upstream}^{n+1})}{\Delta x} = \Delta x (K_{film}C_M - C(K_{film} + q_{inf})) \\ \frac{\partial C}{\partial t} = \frac{1}{\alpha \bar{Q}^\beta} \left( -\frac{Q^{n+1}}{\Delta x} - K_{film}\Delta x - q_{inf}\Delta x \right) C + \frac{K_{film}\Delta x}{\alpha \bar{Q}^\beta} C_M + \frac{Q_{upstream}^{n+1}}{\alpha \bar{Q}^\beta \Delta x} C_{upstream}^{n+1} \end{cases} \quad (\text{Eq. 16})$$

Therefore, the system (1) and the development (16) can be converted in the following matrix form:

$$\begin{pmatrix} \frac{\partial C}{\partial t} \\ \frac{\partial C_M}{\partial t} \\ \frac{\partial C_s}{\partial t} \end{pmatrix} = \underbrace{\begin{pmatrix} a & b & 0 \\ d & e & f \\ 0 & h & i \end{pmatrix}}_A \underbrace{\begin{pmatrix} C \\ C_M \\ C_s \end{pmatrix}}_b + \begin{pmatrix} k \\ 0 \\ 0 \end{pmatrix} \quad (\text{Eq. 17})$$

where  $a = \frac{1}{\alpha \bar{Q}^\beta} \left( -\frac{\bar{Q}}{\Delta x} - K_{film}\Delta x - q_{inf}\Delta x \right)$ ;  $b = \frac{K_{film}\Delta x}{\alpha \bar{Q}^\beta}$

$$d = \frac{K_{film} + q_{inf}}{\theta_s \varepsilon}; e = \frac{-K_{film} - q_{inf} - \varepsilon \rho_b k_r K_D}{\theta_s \varepsilon}$$

$$f = \frac{\rho_b k_r}{\theta_s}; h = k_r K_D; i = -k_r; k = \frac{Q_{upstream}^{n+1}}{\alpha \bar{Q}^\beta \Delta x} C_{upstream}^{n+1}$$

The entries of the matrix A are constant over each time step. The system (17) has an unique vector-values solution  $(C, C_M, C_S)$  for any given initial vector-values  $(C_0, C_{M0}, C_{S0})$ . In order to compute the vector-values solution, eigenvalues and eigenvectors of the matrix A were calculated. The eigenvalues of the matrix A are the roots of the characteristic polynomial which is a cubic real polynomial. These eigenvalues are the solutions of equation 18:

$$\begin{aligned} P(x) &= x^3 - (i+e+a)x^2 - (hf - ie - ia + db - ea)x + hfa + idb - iea = 0 \\ &= x^3 + \alpha x^2 + \beta x + \gamma \end{aligned} \quad (\text{Eq. 18})$$

The nature of the roots of P depends on the sign of its discriminant defined by:

$$\Delta = 18\alpha\beta\gamma + \alpha^2\beta^2 - 4\alpha^3\gamma - 4\beta^3 - 27\gamma^2 \quad (\text{Eq. 19})$$

According to the sign of  $\Delta$ , it leads to three cases:

**Case 1:** If  $\Delta = 0$ , the polynomial P has a multiple root and all roots are real  $(\lambda_0, \lambda_0, \lambda_0)$  or  $(\lambda_0, \lambda_0, \lambda_1)$

**Case 2:** If  $\Delta > 0$ , the polynomial P has three real roots in the form  $(\lambda_1, \lambda_2, \lambda_3)$

**Case 3:** If  $\Delta < 0$ , the polynomial P has one real root and two non-real conjugate roots  $(\lambda_1, \lambda_2, \overline{\lambda_2})$ .

A particular solution of the equation system is noted  $x_p$ . For the case 1, general solutions are detailed in Annex 1. For case 2, the general solution is:

$$x(t) = C_1 \overline{v_{p_1}} e^{\lambda_1 t} + C_2 \overline{v_{p_2}} e^{\lambda_2 t} + C_3 \overline{v_{p_3}} e^{\lambda_3 t} + x_p(t) \quad (\text{Eq. 20})$$

And for case 3, the general solution is:

$$\begin{aligned} x(t) &= C_1 \overline{v_{p_1}} e^{\lambda_1 t} + C_2 e^{\lambda_2 t} (\overline{v_{r_{p_2}}} \cos(bt) - \overline{v_{i_{p_2}}} \sin(bt)) \\ &+ C_3 e^{\lambda_2 t} (\overline{v_{r_{p_2}}} \sin(bt) + \overline{v_{i_{p_2}}} \cos(bt)) + x_p(t) \end{aligned} \quad (\text{Eq. 21})$$

where  $\overline{v_{r_{p_j}}}$  denotes the real part of the eigenvector related to  $\lambda_j$  and  $\overline{v_{i_{p_j}}}$  denotes the complex part. As the sign of  $\Delta$  was not known, the three cases were implemented in the model. The sign of  $\Delta$  was tested using 100,000 Monte Carlo simulations within the physical extent of each parameter involved in the matrix A entries. These parameters and their physical extent are detailed in Table V-6. The results showed that the sign of  $\Delta$  remains positive for all the Monte Carlo simulations, which indicates that the general solution (20) is mostly to occur.

Table V-6. Parameters involved in the pesticides mobilisation and transport resolution and their physical range.

	Parameters	units	range
	Spatial discretisation ( $\Delta x$ )	[m]	1 - 10
Pesticides	Film transport coefficient ( $K_{film}$ )	[m s <sup>-1</sup> ]	0 - 10 <sup>-3</sup>
	Desorption rate ( $k_r$ )	[s <sup>-1</sup> ]	0 - 1
	Porosity	[-]	0.2 - 0.6
	Depth of the mixing layer ( $\epsilon$ )	[m]	10 <sup>-3</sup> - 10 <sup>-1</sup>
	Soil water partition coefficient ( $K_D$ )	[m <sup>3</sup> kg <sup>-1</sup> ]	0 - 10 <sup>-1</sup>
	Soil bulk density ( $\rho$ )	[kg m <sup>-3</sup> ]	1200 - 1800
Hydrology	Manning coefficient	[-]	0.01 - 0.5
	Water height (h)	[m]	10 <sup>-10</sup> - 10 <sup>-1</sup>
	Slope	[m m <sup>-1</sup> ]	0.001 - 0.8
	infiltration rate ( $q_{inf}$ )	[m s <sup>-1</sup> ]	0 - 10 <sup>-4</sup>

## 2.5. Mass balance errors calculations

Mass balance errors were calculated at every time step. For both numerical approaches, LISEM-psi and LISEM-pa, a cumulative mass balance error ( $M_{err}$ ) was calculated within the same approach (Eq 22):

$$\begin{aligned}
 M_{err}^{n+1} = & \left( M_{applied} - \underbrace{\sum_{i,j} C_M^{n+1} \epsilon \theta_s \Delta x^2}_{\text{Pesticides in soil water}} - \underbrace{\sum_{i,j} C_s^{n+1} \epsilon \rho_b \Delta x^2}_{\text{Pesticides sorbed on the soil}} - \underbrace{M_{runoff}^{n+1}}_{\text{Pesticides in runoff water}} \right. \\
 & \left. - \underbrace{\sum_n \sum_{i,j} q_{inf} \Delta x^2 \int_{n\Delta t}^{(n+1)\Delta t} C_M dt}_{\text{Pesticides leaving the system by infiltration}} - \underbrace{\sum_n Q_{outlet}^{n+1} \Delta x^2 \int_{n\Delta t}^{(n+1)\Delta t} C dt}_{\text{Pesticides leaving the system by surface runoff}} \right) \times 100 / M_{applied} \quad (\text{Eq. 22})
 \end{aligned}$$

Where  $M_{applied}$  is the pesticide mass initially present in the system [kg], i and j refer to the space coordinated, n refers to the time step.

## 2.6. Case study scenarios

Three test cases were analysed for evaluating both numerical schemes, i.e. LISEM-psni and LISEM-pa (Figure V-7).

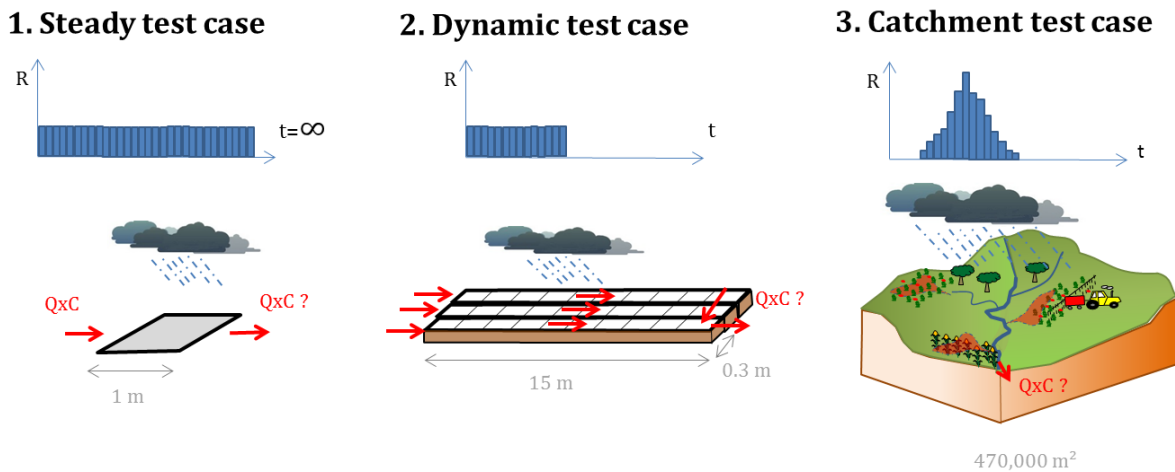


Figure V- 7. Schemes of the three case study scenarios

Specific input parameters for each test case were detailed in Table V-7.

- The first test considered the transport and the mobilization of one hypothetical pesticide through one cell ( $1 \text{ m}^2$ ) in steady state flow and upstream runoff conditions. The cell was subjected to constant rainfall and constant flux of pesticides [ $\text{kg s}^{-1}$ ] ( $50 \times 10^{-6} [\text{kg m}^{-3}] \times 9 \times 10^{-6} [\text{m}^3 \text{s}^{-1}]$ ) until reaching the steady state of pesticide concentrations in the three compartments (runoff, soil and soil water). This test case was used to evaluate the influence of time step and of the  $Q_{\text{lim}}$  value on the predicted concentrations and to verify the accuracy of the algorithms, as the exact steady state solution is known.
- The second test consisted in predicting pesticide mobilisation and transport from the soil surface under experimental conditions in a plot of  $4.5 \text{ m}^2$  under artificial rainfall published by Wallender et al., (2008). The accuracy of the model was evaluated against experimental data.
- The last test consisted in predicting pesticide mobilisation and transport from a contaminated soil surface based on non-homogeneous pesticide application (*S*-metolachlor was applied on 29.8% of the catchment area) on the study catchment of Alteckendorf ( $470,000 \text{ m}^2$ ). Predictions were grounded on the hydrological modelling previously explained (Chap V -Section 1) and compared with the experimental data

previously presented (Chap IV). Two runoff events, May 21 and June 7, were selected for two reasons: (i) the selected runoff events were well predicted by LISEM in terms of runoff pathways and discharge rate at the catchment outlet. (ii) they were associated with contrasting runoff hydrological forcing with 41 and 4% runoff coefficients (yielding to 10,568 and 208 m<sup>3</sup>), respectively and they occurred on average 15 days and 32 days after *S*-metolachlor applications.

**Table V-7. Description of the input parameters of LISEM-psni and LISEM-pa in the three different study scenarios**

		Steady test case	Dynamic test case	Catchment test case
Parameters	units			
Applied rate	[kg m <sup>-2</sup> ]	1.74 10 <sup>-5</sup>	1.74 10 <sup>-5</sup>	Spatially variable based on the farmers survey
Depth of the mixing layer ( $\epsilon$ )	[mm]	1	1	30
Film transport coefficient ( $K_{film}$ )	[mm h <sup>-1</sup> ]	59.8	12.6	2.3 10 <sup>-4</sup>
Desorption rate ( $k_r$ )	[h <sup>-1</sup> ]	4.32	4.32	4.32
Soil water partition coefficient ( $K_D$ )	[L kg <sup>-1</sup> ]	6.17	6.17	2900
Porosity	[-]	0.25	0.37	0.42
Manning coefficient	[-]	0.1	0.1	Chapter V - Section 1
Rainfall intensity	[mm h <sup>-1</sup> ]	150	37.9	Measurements
Rainfall duration	[h]	$\infty$	1	Measurements
Saturated hydraulic conductivity	[mm h <sup>-1</sup> ]	2.3	1.2	Chapter V - Section 1
Initial water content	[-]	0.25	0.3	Chapter V - Section 1
Saturated water content	[-]	0.37	0.37	Chapter V - Section 1
Average suction at the wetting front	[mm]	1100	1100	Chapter V - Section 1

### 3. Results and discussion

#### 3.1. Steady test case

A simple case at steady state was used to evaluate the stability and the accuracy of both numerical schemes, i.e. LISEM-psni and LISEM-pa. Once steady state is reached for transport, LISEM-psni and LISEM-pa solutions were almost the same (48.39  $\mu\text{g L}^{-1}$  in runoff) and reached the theoretical solution with the same error of 0.54% according to different time steps (ranging from 0.1 to 80 s) and  $Q_{lim}$  value ( $10^{-3}$  and  $10^{-6}$  L s<sup>-1</sup>).

Cumulative mass balance errors were in the order of  $10^{-13}\%$  of the total pesticide mass initially present in the system for both solutions, which are in the order of round-off errors. A standard sequential non-iterative scheme generally induces a global error of order  $\Delta t$  (Carrayrou et al., 2004). An increase of the time step should therefore lead to greater mass balance errors. Surprisingly, the mass balance errors due to operator splitting from LISEM-pnsi were comparable to those of LISEM-pa and did not significantly change according to the different time steps. When using large time steps, pesticides loads and fluxes calculated by equations (12) and (14) may indeed lead to negative values. However, to avoid numerical problems during simulations, negative values were artificially set to zero. Pesticides fluxes were also constrained maximally to the pesticide amount in the cell. These constraints may limit the mass balance errors. Without those constraints, mass balance errors degraded along with an increase of the time step (in the order of 2% for this test case) and calculations lead to negative values.

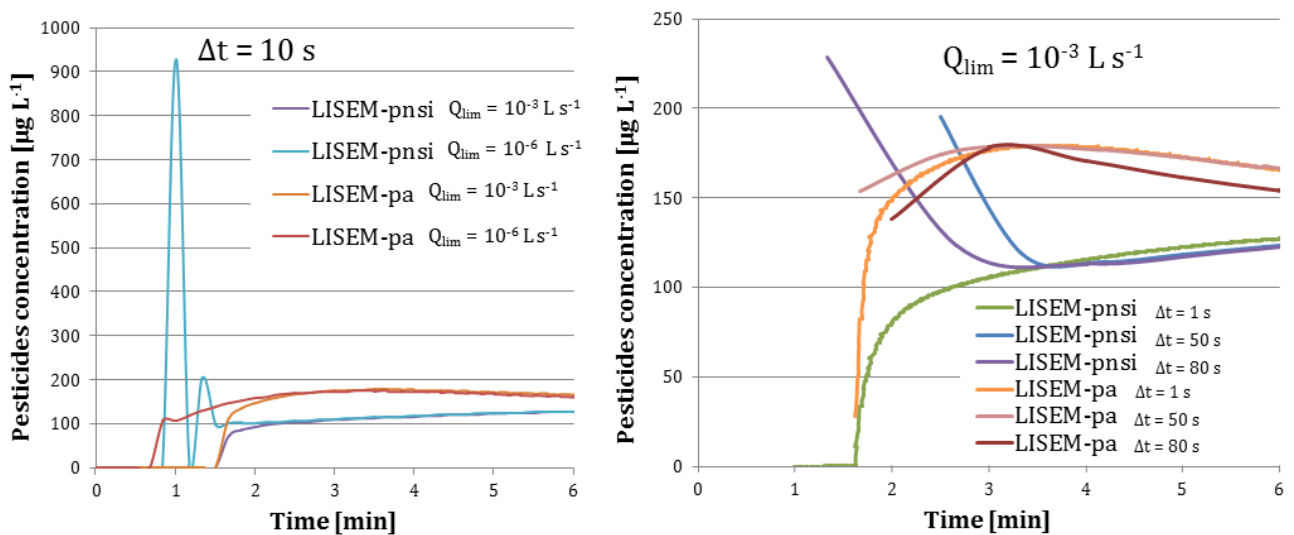


Figure V- 8 . Influence of  $Q_{\text{lim}}$  value (left) and time step (right) on the pesticide concentration in runoff water during the transient period

Figure V-8 shows the pesticide concentration in runoff water during the transient period. The first five minutes of the simulation exhibited drastic changes of the pesticide concentration according to the time step and  $Q_{\text{lim}}$  value for LISEM-pnsi compared to LISEM-pa.  $Q_{\text{lim}}$  value impacted the beginning of pesticide mobilisation in runoff. Concentration peaks that occurred during the transient period for LISEM-pnsi when  $Q_{\text{lim}}=10^{-6} \text{ L s}^{-1}$  or when  $\Delta t > 40 \text{ s}$ , highlighted the non-stability of the operator splitting method resolution for extreme conditions. Predicted concentration of pesticide in runoff via LISEM-pa appeared more stable as no fluctuations or severe spikes occurred during the transient period. According to different  $Q_{\text{lim}}$  values,

predictions via LISEM-pa appeared only delayed in time. LISEM-pnsi seemed therefore not appropriate and was therefore not used for further test cases.

### 3.2. Dynamic test case: an experimental plot

The previous section demonstrated that LISEM-pa was robust and accurate at the pixel scale for steady state hydrological forcing. In the second test, the LISEM-pa predictions were compared against experimental data at a plot scale obtained under unsteady state forcing.

A spatial discretisation of 0.1 m was used to represent the plot experiment. Influence of the time step was tested on the predicted discharge and pesticide concentration dynamic with  $\Delta t = 10, 5$  and 1 s. The predicted maximal runoff velocity was on average  $0.018 \text{ m s}^{-1}$  for the three time step conditions in the domain indicating that a time step of 5 seconds was sufficient for model accuracy according to the Courant condition (CFL condition) (Rai et al., 2010). Predicted outflow rate and pesticide concentrations presented very small variation according to the three different time steps for this test case. A time step of 5 s was therefore used to simulate the pesticide concentration dynamic in the Figure V-9. Measured and simulated runoff are presented in Figure V-9A. LISEM predicted acceptably both cumulative runoff (97.3 compared to 84.7 L observed) and runoff rates with a Nash coefficient of 0.9 (Wallender et al., 2010). Pesticides concentrations in runoff water predicted by LISEM-pa were similar to field observations, and showed large sensitivity to  $Q_{lim}$  (Figure V-9B). A  $Q_{lim}$  value of  $3 \cdot 10^{-3} \text{ L s}^{-1}$  has been shown to be the most appropriate value for fitting the experimental values.

The observed and predicted pesticide concentration peaks were  $177$  and  $162 \mu\text{g L}^{-1}$ , yielding 8.8 and 10.6 mg, respectively. Further investigations are needed to evaluate the influence and the physical meaning of the  $Q_{lim}$  value. At the beginning and at the end of the predicted pesticide concentration dynamic of LISEM-pa, small fluctuations occurred as a result of the sequential arrival of each horizontal profile of the domain at the outlet, located in the bottom right-hand corner as shown in Figure V-7. Discrepancies between observed and predicted runoff by LISEM-pa may partly explain differences between pesticide concentration predictions. The runoff water samples were collected in stainless retention-tanks and the experimental study did not mention the duration of the integrative samplings which renders comparison with the experimental data difficult (Wallender et al., 2010).

Pesticide concentration in runoff increased during runoff recession. This can be explained by less dilution due to lower water height or by the fact that the release of pesticide from soil solids, governed by  $k_r$ , is the limiting factor in determining runoff concentrations. When  $K_{film}$  is large with respect to  $k_r$ , desorption is the limiting process. This effect has already been observed under field conditions (Wallender et al., 2010). The concentration dynamics in the soil water ( $C_M$ ) is illustrated in Figure V-10 and was similar for the three  $Q_{lim}$  values cases; it may be divided into four phases: (1) a sharp decrease of  $C_M$  during high infiltration period, (2) a rebalance of soil and water compartments when soil is saturated, (3) a decrease of  $C_M$  when soil is saturated and runoff occurred, mobilising pesticides in runoff water and (4) a rebalance of soil and water compartments due to runoff recession.

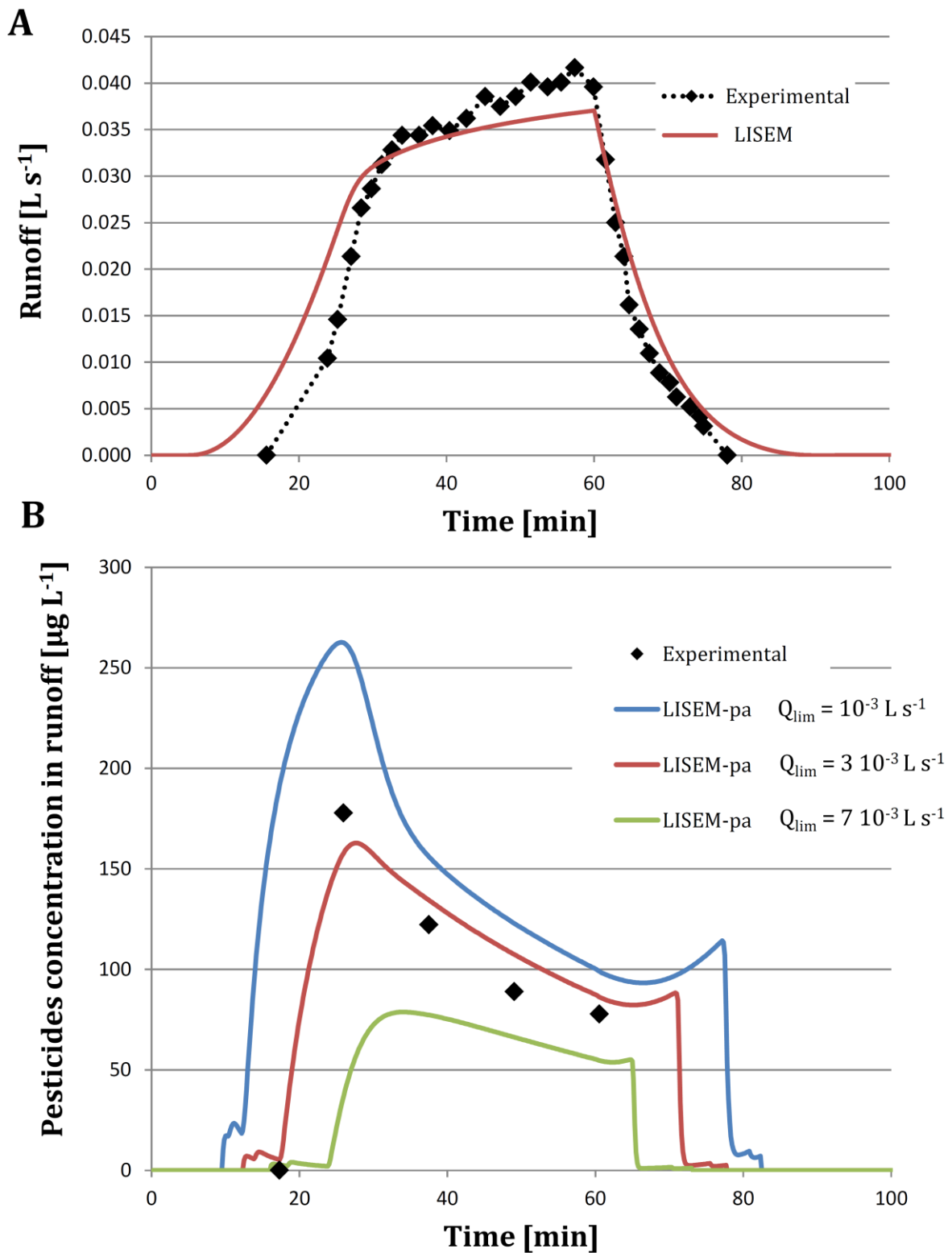


Figure V-9. Observed and simulated runoff on the experimental plot (A) and associated pesticides concentration in runoff water (B)

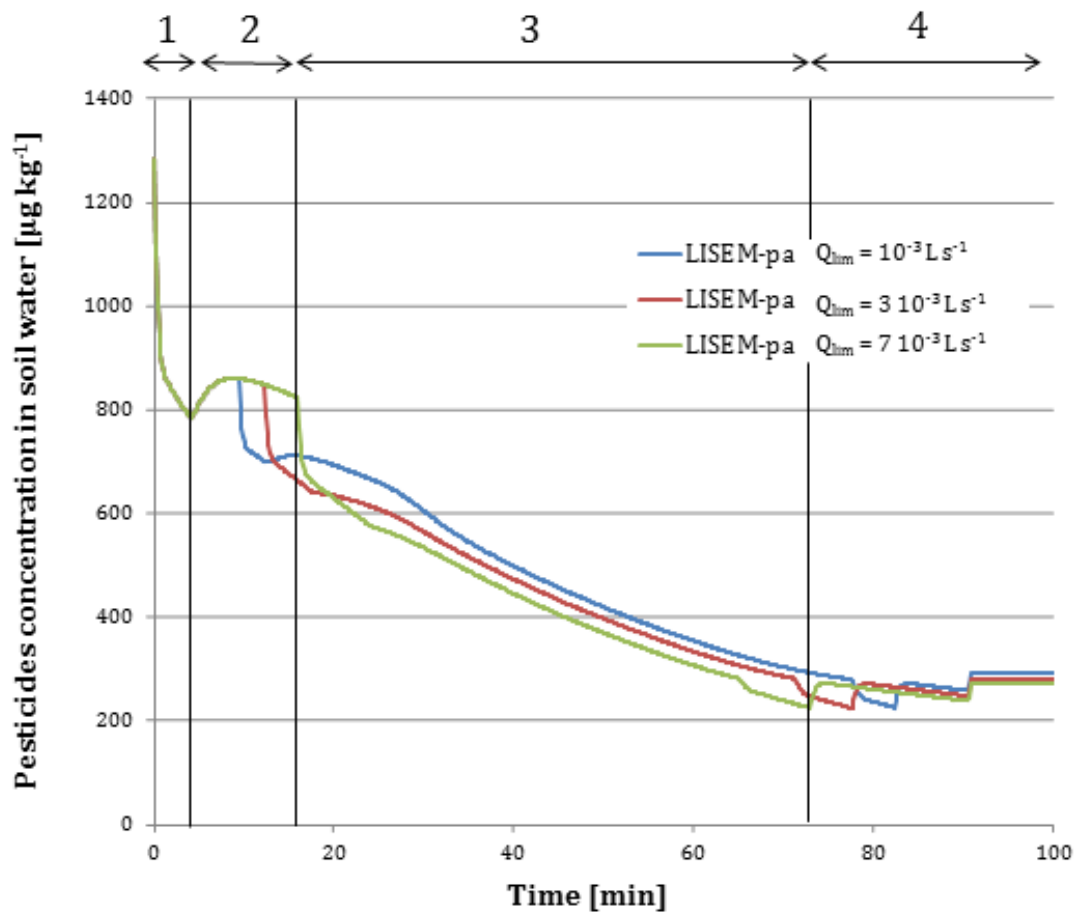


Figure V- 10. Simulated pesticide concentration in soil water ( $C_M$ ). Numbers indicate the 4 phases of  $C_M$  dynamics

The results of the first two case scenarios underlined the stability and accuracy of LISEM-pa which does not require any time step limitation, in contrast to LISEM-psi. The third test was specifically designed to apply LISEM-pa at larger scale to the arable crop catchment presented in Chapter IV.

### 3.3. A case study in an agricultural headwater catchment: Alteckendorf

LISEM-pa predictions were compared against experimental data at headwater catchment scale under a dynamic rainfall runoff event and with a non-homogeneous application, i.e. variability of pesticide application within the catchment. According to the application rate for each plot, initial concentrations of pesticides in soil and soil water were calculated as follows:

$$C_M = \frac{PCA}{\varepsilon\theta_s + \rho\varepsilon K_D}; C_S = C_M K_D \text{ and } C = 0 \quad (23)$$

Where PCA, the mass of pesticide applied per unit surface area, was provided by the farmers [ $\text{kg ha}^{-1}$ ]. The attenuation of the initial pool of available pesticide in the near surface soil layer on

May 21 and June 7 was estimated using a first-order exponential decay law with a half-life of 54 days (see Chap IV - §4.1 for detailed estimation of the half-life value). The mixing layer depth ( $\epsilon$ ) was estimated at 3 cm to be consistent with the field soil sampling (Chap IV - §3.3).  $K_d$  and  $K_r$  values of *S*-metolachlor were not supposedly known in this study site during the crop growing season. Measured  $K_d$  values for *S*-metolachlor, determined in 24 h batch conditions, was 2.9 L kg<sup>-1</sup> for the agricultural calcisol undergoing deep tillage (Alletto et al., 2013).

$K_d$  has been observed to increase with aging time since application (Louchart and Voltz, 2007). Field  $K_d$  have been shown to be up to 164 times higher than their laboratory estimated  $K_d$  value for diuron, having a similar log  $K_{ow}$  to metolachlor, i.e., 2.87 and 3.05 for diuron and *S*-metolachlor respectively (Louchart and Voltz, 2007). A field  $K_d$  value for *S*-metolachlor of 2900 L kg<sup>-1</sup> was therefore used for the test at the catchment scale. The calibrated  $k_r$  value for diazinon, having a similar log  $K_{ow}$  (3.69) to metolachlor, ranged between 1.69 and 5.76 h<sup>-1</sup> with a mean value of 4.32 h<sup>-1</sup> (Wallender et al., 2010). A  $k_r$  value of 4.32 h<sup>-1</sup> was therefore tested for the catchment case. The conceptual parameter,  $K_{film}$  was calibrated on the event of June 7 and used for the event of May 21. This test required the estimation of  $K_{film}$  (8). This parameter cannot be extracted from soil data due to its conceptual nature. Few studies addressed the range of  $K_{film}$  in the context of pesticide mobilisation and transport from plot or catchment. Calibrated  $K_{film}$  values ranged between 5.0 and 42.1 mm h<sup>-1</sup> for diazinon (Wallender et al., 2010) and between 102.6 and 356.0 mm h<sup>-1</sup> for bromide (Havis et al., 1992). The  $K_{film}$  value was manually calibrated to 2.3.10<sup>-4</sup> mm h<sup>-1</sup> on the event of June 7 for the catchment study, which is 5 order of magnitude lower than those of Havis et al. (1992) or Wallender et al. (2010). A lower  $K_{film}$  value within the arable crop catchment may be partly explained by the presence of a soil crust which may reduce the exchange between runoff and mixing layer or by the ageing of pesticides in soil (Louchart and Voltz, 2007), 32 days after application. This may increase the partitioning  $K_d$  coefficient and decrease the mobility of pesticides. As only  $K_{film}$  was calibrated, a change of  $K_d$  may be counterbalanced by a change of  $K_{film}$ .

Twenty-one minutes after the beginning of the runoff event, pesticides reached the catchment's outlet. This time lapse can be related to the distribution of applications occurring only on upstream plots within the agricultural catchment (Figure V-11). At the catchment outlet, flow-proportional water samples were systematically collected every 20 m<sup>3</sup>, however, only one combined sample was analysed for the event of June 7 and 3 for the event of May 21. Observed and predicted values were 2.79 and 0.3 µg L<sup>-1</sup> respectively at the catchment outlet (Figure V-11). The simulated pesticide concentration peak was predicted to 24.5 µg L<sup>-1</sup>. The total observed and predicted exported loads were 580 and 290 mg, respectively. To validate the calibrated value of

$K_{film}$ , LISEM-pa was applied on the largest runoff event observed on May 21 associated with 96% of *S*-metolachlor load observed over the crop growing season. Three mixing samples were collected during this event corresponding to 62, 40 and 16  $\mu\text{g L}^{-1}$ , however, 4% of water was sampled preventing a comparison of the exported loads. The 3 simulated values for the same sampling period were 0, 0.5 and 55  $\mu\text{g L}^{-1}$  at the catchment outlet. Predictive pesticide concentration reached 42  $\text{mg L}^{-1}$ . The sampling strategy did not allow to characterise the peak of pesticide concentration. The predicted pesticide peak concentration occurred at the end of the hydrogram (Fig. V-11). This could be partly due to the fact that pesticide application occurred in upstream catchment areas or by less dilution effect at the end of the runoff event.

Further evaluation and validation of LISEM-pa is required against measurements at finer temporal resolution. LISEM-pa provided a map of cumulative pesticide mass in runoff at the event scale as illustrated in Figure V-12 for the event of May 21. Spatial patterns of pesticide loads in runoff clearly showed that it represents the intersection of the application zone area and the connected hydrologically active area. This spatial pattern allowed identification of the critical sources areas (CSA).

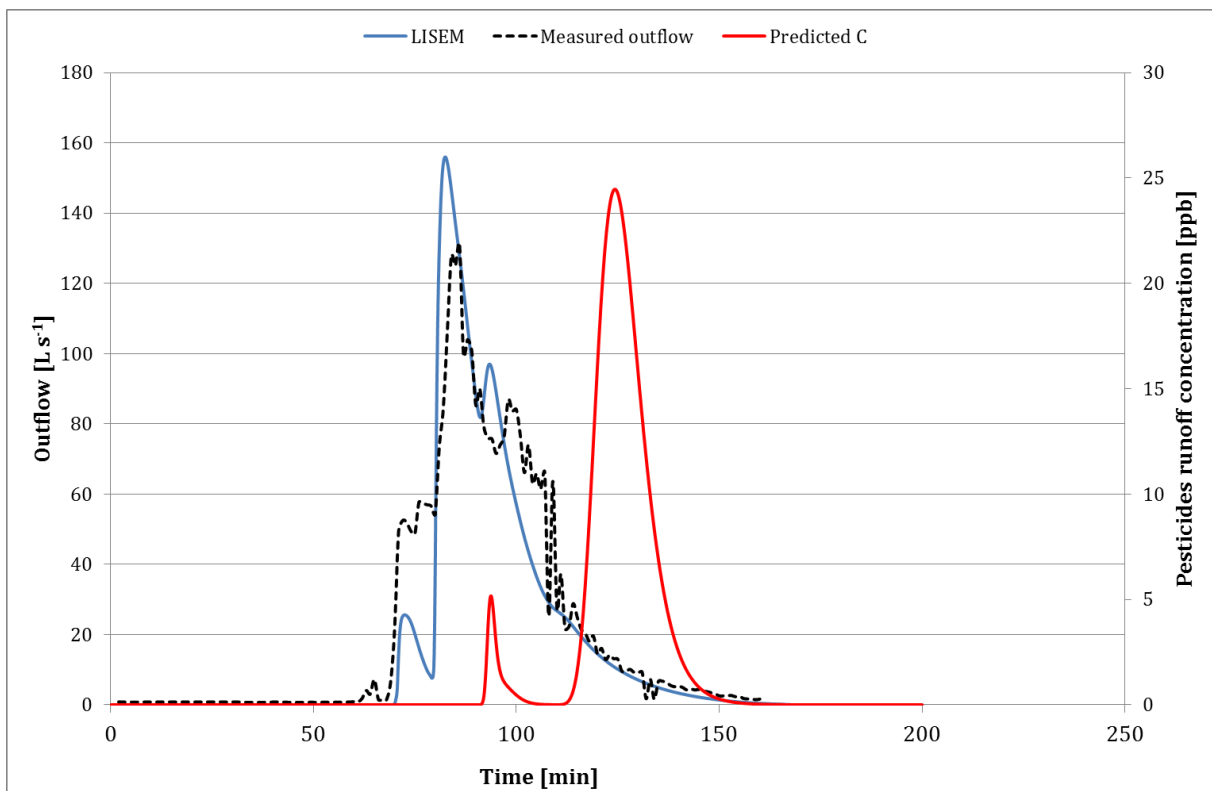


Figure V-11. Measured and simulated runoff and associated pesticides concentration in runoff water at the catchment outlet

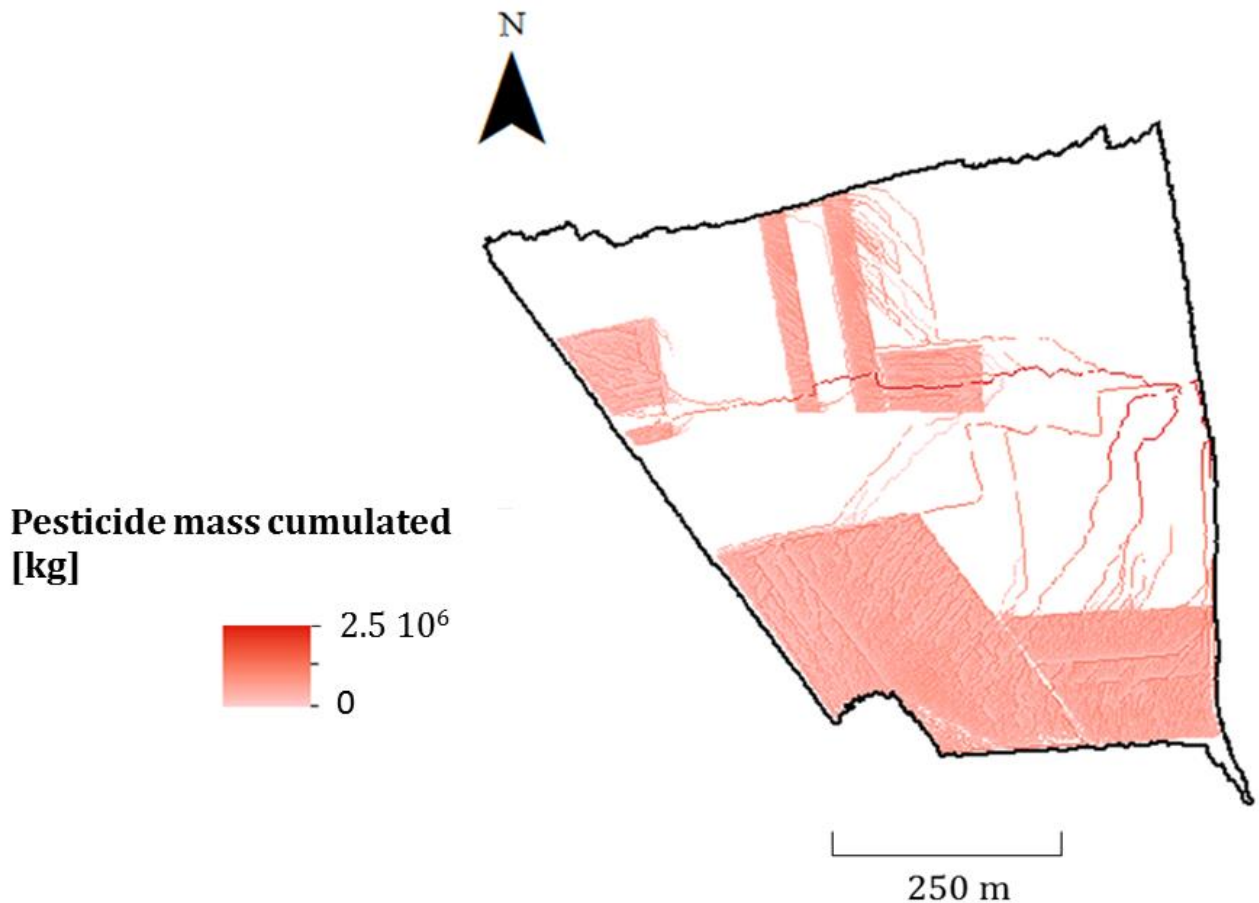


Figure V- 12. Spatial pattern of pesticides runoff in the study catchment on May 21

## 4. Conclusion

Few pesticide runoff models account for the effects of agricultural practices on hydrodynamic parameters and soil surface characteristics and most of them are deemed inappropriate for investigating headwater catchments at a very fine temporal resolution ( $\leq 1$  min). An event based, spatially distributed model is therefore required for predicting the mobilisation and transport of pesticides at the catchment scale.

In this study, we developed and tested two numerical approaches, i.e. one operator splitting approach and a pseudo-analytical approach, for the prediction of pesticide mobilisation and transport in runoff water. The adopted formalism enabled to take into account the sorption-desorption process during rainfall-runoff events. Both formalisms were integrated in LISEM, an event based, hydrological and erosion model. The sequential non-iterative approach, LISEM-psni, was tested due to its simplicity and its similarity with the existing sediment transport resolution in LISEM. However, its numerical instability, due to split operator and time integration scheme, was demonstrated by the first study case scenario. LISEM-pnsi seemed

therefore not appropriate for predicting pesticide transport within an agricultural catchment. An original pseudo-analytical approach, LISEM-pa was jointly evaluated and was validated on simple test cases and was able to simulate the dynamics of discharge and pesticide export from an experimental plot. The formalism showed consistency and robustness both for runoff and pesticide concentration dynamics. The preliminary results of LISEM-pa at the catchment scale presented reasonable order-of-magnitude predictions but clearly need additional exploration.

Further investigations are required, and include (i) the validation of the predicted pesticide concentrations on different rainfall-runoff events where the dynamics of pesticide concentration were precisely characterised using fine temporal discretisation, (ii) the spatial validation of pesticide concentrations using internal control points of measurements, (iii) the evaluation of the spatial pattern of initial concentrations of pesticides in soil and soil water, and (iv) the evaluation of the influence of  $Q_{lim}$  and individual model input parameters such as  $K_{film}$ ,  $kr$  and  $\epsilon$  in order to estimate parameter sensitivity for measurement and calibration guidelines.

These preliminary results can be anticipated as a starting point for better predicting pesticide export in runoff during rainfall-runoff events in agricultural catchments. Solid-bound pesticide prediction will be the focus of further investigation.

## 5. Acknowledgements

The authors are members of REALISE, the Network of Laboratories in Engineering and Science for the Environment in the Alsace Region (France; <http://realise.unistra.fr>), from which support is gratefully acknowledged. This research has been funded by the PhytoRET project (C.21) of the European INTERREG IV program Upper Rhine. Marie Lefrancq was supported by a fellowship of the Rhine-Meuse Water Agency and the Alsace Region. We acknowledge Jérôme Carrayrou, Sylvain Weill, Alain Clement and Raphaël Di Chiara and especially Philippe Ackerer for their help in the numerical development. We acknowledge Victor Jetten for his support on OpenLisem and Qt creator.

## 6. References

- Ahuja, L.R., Sharpley, A.N., Yamamoto, M., Menzel, R.G., 1981. The Depth of Rainfall-Runoff-Soil Interaction as Determined by P-32. *Water Resources Research*. 17, 969-974.
- Alletto, L., Benoit, P., Bolognesi, B., Couffignal, M., Bergheaud, V., Dumeny, V., Longueval, C., Barriuso, E., 2013. Sorption and mineralisation of S-metolachlor in soils from fields cultivated with different conservation tillage systems. *Soil & Tillage Research*. 128, 97-103.
- Borah, D.K., Bera, M., 2003. Watershed-scale hydrologic and nonpoint-source pollution models: Review of mathematical bases. *Transactions of the Asae*. 46, 1553-1566.
- Carrayrou, J., Mose, R., Behra, P., 2004. Operator-splitting procedures for reactive transport and comparison of mass balance errors. *Journal of Contaminant Hydrology*. 68, 239-268.
- Chow, V., Maidment, D., Mays, L., 2013. *Applied Hydrology*, 2nd Edition, Vol., McGraw-Hill Companies, Incorporated.
- DeRoo, A.P.J., Wesseling, C.G., Ritsema, C.J., 1996. LISEM: A single-event physically based hydrological and soil erosion model for drainage basins .1. Theory, input and output. *Hydrological Processes*. 10, 1107-1117.
- Gao, B., Walter, M.T., Steenhuis, T.S., Hogarth, W.L., Parlange, J.Y., 2004. Rainfall induced chemical transport from soil to runoff: theory and experiments. *Journal of Hydrology*. 295, 291-304.
- Gao, B., Walter, M.T., Steenhuis, T.S., Parlange, J.Y., Richards, B.K., Hogarth, W.L., Rose, C.W., 2005. Investigating raindrop effects on transport of sediment and non-sorbed chemicals from soil to surface runoff. *Journal of Hydrology*. 308, 313-320.
- Havis, R.N., Smith, R.E., Adrian, D.D., 1992. Partitioning Solute Transport between Infiltration and Overland-Flow under Rainfall. *Water Resources Research*. 28, 2569-2580.
- Holvoet, K.M.A., Seuntjens, P., Vanrolleghem, P.A., 2007. Monitoring and modeling pesticide fate in surface waters at the catchment scale. *Ecological Modelling*. 209, 53-64.
- Jacques, D., Simunek, J., Mallants, D., van Genuchten, M.T., 2006. Operator-splitting errors in coupled reactive transport codes for transient variably saturated flow and contaminant transport in layered soil profiles. *Journal of Contaminant Hydrology*. 88, 197-218.
- Kohne, J.M., Kohne, S., Simunek, J., 2009. A review of model applications for structured soils: b) Pesticide transport. *Journal of Contaminant Hydrology*. 104, 36-60.
- Kutilek, M., Nielsen, D.R., 1994. *Soil hydrology*, Vol., Catena Verlag.
- Lafrance, P., Caron, E., 2012. Impact of vegetated filter strips on sorbed herbicide concentrations and sorption equilibrium in agricultural plots. *Journal of Environmental Science and Health Part B- Pesticides Food Contaminants and Agricultural Wastes*. 47, 967-974.
- Lagneau, V., van der Lee, J., 2010. Operator-splitting-based reactive transport models in strong feedback of porosity change: The contribution of analytical solutions for accuracy validation and estimator improvement. *Journal of Contaminant Hydrology*. 112, 118-129.
- Liu, G.B., Xu, M.X., Ritsema, C., 2003. A study of soil surface characteristics in a small watershed in the hilly, gullied area on the Chinese Loess Plateau. *Catena*. 54, 31-44.

- Louchart, X., Voltz, M., 2007. Aging effects on the availability of herbicides to runoff transfer. *Environmental Science & Technology*. 41, 1137-1144.
- McGrath, G.S., Hinz, C., Sivapalan, M., 2008. Modeling the effect of rainfall intermittency on the variability of solute persistence at the soil surface. *Water Resources Research*. 44.
- Oliver, D.P., Kookana, R.S., Anderson, J.S., Cox, J.W., Waller, N., Smith, L.H., 2012. Off-site transport of pesticides in dissolved and particulate forms from two land uses in the Mt. Lofty Ranges, South Australia. *Agricultural Water Management*. 106, 78-85.
- Payraudeau, S., Grégoire, C., 2012. Modelling pesticides transfer to surface water at the catchment scale: a multi-criteria analysis. *Agronomy for Sustainable Development*. 32, 479-500.
- Quilbe, R., Rousseau, A.N., Lafrance, P., Leclerc, J., Amrani, M., 2006. Selecting a pesticide fate model at the watershed scale using a multi-criteria analysis. *Water Quality Research Journal of Canada*. 41, 283-295.
- Rai, R.K., Upadhyay, A., Singh, V.P., 2010. Effect of variable roughness on runoff. *Journal of Hydrology*. 382, 115-127.
- Ren, Z., Xu, C., Lu, T., Singer, M.A., 2014. Dynamic adaptive chemistry with operator splitting schemes for reactive flow simulations. *Journal of Computational Physics*. 263, 19-36.
- Shi, X.N., Wu, L.S., Chen, W.P., Wang, Q.J., 2011. Solute Transfer from the Soil Surface to Overland Flow: A Review. *Soil Science Society of America Journal*. 75, 1214-1225.
- Wallach, R., Grigorin, G., Rivlin, J., 2001. A comprehensive mathematical model for transport of soil-dissolved chemicals by overland flow. *Journal of Hydrology*. 247, 85-99.
- Wallender, W.W., Joyce, B.A., Ginn, T.R., 2008. Modeling the Transport of Spray-Applied Pesticides from Fields with Vegetative Cover. *Transactions of the Asabe*. 51, 1963-1976.
- Wallender, W.W., Joyce, B.A., Mailapalli, D.R., 2010. Application of pesticide transport model for simulating diazinon runoff in California's central valley. *Journal of Hydrology*. 395, 79-90.

# Chapter VI. General conclusions and perspectives

## 1. Summary and conclusion

The contamination of surface water bodies by pesticides and their degradation products poses a serious threat to aquatic ecosystems (Vorosmarty et al., 2010). Understanding the transport and the transformation of pesticides has become of utmost importance for the preservation of soils and water resources. Among water bodies, headwater catchments (0 – 1 km<sup>2</sup>) may have a major impact on downstream water quality due to their major contribution to the downstream water volume and the solute fluxes (Dodds and Oakes, 2008; Freeman et al., 2007; Salmon-Monviola et al., 2013). However, headwater catchments are generally disregarded and poorly investigated (Rasmussen et al., 2013). Agricultural headwater streams are particularly vulnerable to contamination due to their close connections with treated areas and the rapid mobilisation of pesticides during rainfall-runoff events (Botta et al., 2012; Tang et al., 2012). Pesticide fate in agricultural headwater catchments remains poorly understood.

Even though significant research effort has been dedicated to characterise the transport and degradation of pesticides in agricultural catchments throughout recent decades, it still remains difficult to understand pesticide mobility, transport and transformation under specific field conditions, from sources to sinks within agro-ecosystems (Fenner et al., 2013). Pesticide adsorption onto soil particles is known to influence their transport in runoff and erosion and decrease pesticide bioavailability and toxicity (Barbash, 2014). However, information on partitioning of pesticides between the dissolved and particulate phases is currently scarce under field conditions whereas it is crucial for better understanding pesticide transport and attenuation in agro-ecosystems.

In this context, this thesis aimed at gaining knowledge about pesticide transport and attenuation in agricultural headwater catchments, with a particular emphasis on pesticide partitioning between the dissolved and particulate phases in runoff. The following scientific questions have arisen, for which this PhD thesis attempted to provide evidence:

- What are the spatial patterns of fungicide deposition following a vineyard application, and how does the spatial variability of fungicide deposition influence off-site movement in runoff?
- How are pesticides distributed between the dissolved and particulate phases in runoff water in relation to each compound's characteristics and the hydrological and hydrochemical conditions?
- What is the potential contribution of analytical approaches, such as enantiomer analysis of chiral pesticides, to identifying, characterising and quantifying the *in situ* degradation of pesticides at the headwater-catchment scale?
- Finally, how is it possible to predict the impact of erosion processes and pesticide partitioning between the dissolved and particulate phases on pesticide transport into surface water?

Interlocked scales and analytical approaches were combined in this PhD thesis to evaluate pesticide transport and degradation from the plot application area (source) to the catchment's outlet in contrasting agricultural catchments, i.e. vineyard versus arable crops, representative of temperate agro-ecosystems. Several transport and attenuation processes may simultaneously and synergistically control pesticide fate and their degradation products in agricultural catchments. Therefore, field characterisation and modelling were combined to investigate pesticide runoff and degradation processes based on complementary analytical techniques.

The drift of two fungicides and the spatial variability of the depositions were first investigated under foliar application conditions in a vineyard catchment (Chapter III - Section 1). The impact of hydrological and hydrochemical characteristics on pesticide export and partitioning were then evaluated in a vineyard catchment (Chapter III - Section 2) and an arable crop catchment (Chapter IV). An integrative approach that combines the analyses of the parent pesticides (e.g., *S*-metolachlor and acetochlor here), the degradation products (ethane sulfonic (ESA) and oxanilic acid (OXA)) and the enantiomers of metolachlor was then applied to elucidate processes involved in pesticide attenuation during their transport from the plot to the catchment scales (Chapter IV). In order to better understand pesticide transport within agricultural catchments, 'Critical source areas' (CSA) regarding runoff and erosion, i.e., areas that contribute the major fraction of exported pesticides in runoff and erosion, were evaluated based on a distributed modelling approach at runoff event scale (Chapter V – Section 1). Finally, a mathematical model

was developed to predict the dissolved pesticide mobilisation and runoff transport (Chapter V - Section 2). The developed model can be applied in various agricultural catchments.

The following discussion is structured in five points that answer the research questions of this thesis and correspond to the main messages of the thesis.

We first discuss the spatial variability of pesticide deposition following an application (§1.1). The relevance of combination of plot and catchment scales observations is discussed in order to characterise and predict pesticide transport and attenuation (§1.2) in which the importance of combining modelling following a characterisation phase is examined (§1.3). These two combinations emphasise that runoff and associated erosion represent a primary mode of mobilisation and transfer of pesticides from agricultural land to surface water. The issue of pesticide partitioning in runoff is therefore addressed (§1.4). Finally, the evaluation of pesticide degradation at the catchment scale based on different analytical approaches is discussed (§1.5). Longer-term research perspectives are then presented.

### **1.1. The spatial variability of pesticides deposition during application impacts pesticide runoff**

The spatial variability of pesticide deposition during their application on crops is expected to greatly influence their transport during runoff events (Gascuel-Oudoux et al., 2009). Pesticide drift and deposition largely depend on the equipment, farming practices, the vegetation growth and the topography (Gil and Sinfort, 2005; Nuyttens et al., 2009). The spatial variability of deposition and its impact on pesticide runoff largely differ in the two contrasting study catchments and are therefore discussed in the following with respect to (i) the factors influencing pesticide drift and (ii) the hydrological forcing in the two study catchments.

Results obtained in the present thesis showed that the spatial variability of kresoxim-methyl and cyazofamid deposition in the vineyard greatly varied in space and time and occurred at a distance of more than 40 m (Chapter III – Section 1). Fungicides are preventatively applied on vine leaves, and deposition on the vineyard soil is therefore considered as a loss. The total estimated amount of fungicides deposited onto soil in the vineyard catchment represented 7% and 2% of the total mass applied for kresoxim-methyl and cyazofamid, respectively. Similar results are expected for other pesticides that are foliar applied in vineyards, such as fungicides used to control grapevine mildews, like cymoxanil, dithiocarbamate and metalaxyl (Vischetti et al., 2008), whereas for

example glyphosate application is often carried out directly at the foot of the vine (Chung et al., 2013) which may reduce pesticide drift.

In the studied arable crop catchment (Chapter IV), pre-emergent herbicides were applied to bare soil. Chloroacetanilides deposition was evaluated on the experimental plot (data not shown) and  $84 \pm 15\%$  of the applied dose was detected on the soil surface. This highlights a lower spatial variability of pesticide deposition compared to that observed in the vineyard catchment because pesticide application was carried out directly on soil.

The pesticide deposition patterns are directly influenced by the pesticide spraying equipment, which largely differ between vine and arable crops. Foliar application in vineyards is carried out at 2 m height in every vine row, which results in significant pesticide drift. Six-meter boom length sprayers, i.e., 12 m length in total, are often used to limit passings on the agricultural plots in arable crop catchment (Chung et al., 2013). Application duration is therefore often shorter in arable crop catchments compared to that in the vineyard. Climatic conditions, such as wind speed, temperature or atmospheric humidity, also play a major role in the spatial variability of pesticide deposition. For example, lower atmospheric humidity results in greater pesticide drift (Nuyttens et al., 2007). An entire day of application in the vineyard catchment inevitably involves a low humidity period.

In addition, vineyards often present impermeable surfaces, which are easily prone to pesticide runoff (Salifu et al., 2013). Kresoxim-methyl and cyazofamid loads on roads represented 0.57% and 0.16% of the total mass applied. Although it represents a small fraction of the total mass applied, estimates showed that 85 and 62% of the exported loads in runoff for kresoxim-methyl and cyazofamid at the catchment outlet cannot be explained by the vineyard plots (Chapter III - Section 2). During the experimental study, May to August 2011, only small storm events generating runoff occurred during the period following application. If larger storms occur shortly after the application of pesticides, the contribution of the plots to the overall pesticide loads at the catchment outlet is expected to be higher. It is suggested that hydrological conditions trigger the CSA patterns, as highlighted by Thompson et al. (2012) who showed that CSA patterns for nutrient runoff on drained grassland varied depending of rainfall intensity. Event-based runoff coefficients for water largely differed in both types of catchment, and ranged between 0.3 and 4.0% in the vineyard and between 0.2 and 40.8% in the arable crop catchment (Chapter III - Section 2; Chapter IV). The export rates of both fungicides in the vineyard catchment along the growing season in 2011 were in the order of 0.01‰ (Chapter III - Section 2), whereas those of both herbicides in the arable crop catchment along the growing

season in 2012 were in the order of 5% in the dissolved and the particulate phases (Chapter IV). This emphasised that pesticide dynamics and mobilisation largely differed in the two types of agricultural catchments depending on the climatic and hydrological forcing.

We conclude that non-target areas within catchment may largely contribute to the overall load of runoff-associated fungicides depending on the hydrological forcing. From a management perspective, the reduction of pesticide drift on boundary areas or the limitation of impermeable surfaces within the agricultural catchment may decrease the contribution of plot margins to the total exported loads of pesticides within a catchment. From a modelling viewpoint, pesticide runoff predictions are often based on input contamination maps which include generally only agricultural plots, therefore neglecting the impact of pesticide drift on non-target areas. Pesticide runoff predictions may therefore misrepresent the reality. From a risk assessment point of view, pesticide drift is highly dependent on the commercial formulations (Hilz and Vermeer, 2013) and meteorological conditions (Nuyttens et al., 2007) which render any extrapolation of our results to other agricultural contexts and substances difficult. This study is the first to quantitatively evaluate pesticide losses via drift at the catchment scale. Such quantitative evaluation is required for the creation of a comprehensive database of available estimates of spray drift for gaining overall trends on pesticide drift at global scale via meta-analyses and defining optimal and worst pesticide drift scenarios (Donkersley and Nuyttens, 2011).

Overall, the present work enabled to characterise the variability of pesticide deposition for better understanding their mobilisation during rainfall-runoff events within both agricultural catchments.

### **1.2. Combining plot and catchment scales observations is critical for assessing off-site exports of pesticides**

Many studies have demonstrated the successful application of combining characterisation at the catchment scale and simulation models for understanding and predicting pesticide fate in environment (Bertuzzo et al., 2013; Borah and Bera, 2003; Holvoet et al., 2007; Zanardo et al., 2012). Catchment scale studies are widely recognised for delineating CSA within the catchment (Fan et al., 2013; Frey et al., 2009). However, agricultural headwater catchments integrate numerous agricultural plots, which renders a comprehensive understanding of the source and sink areas for pesticide transport difficult. In addition, such integrated information gathered

from catchment studies is hardly transferable at the farm or plot scale where the best management practices (BMPs) are implemented (Ghebremichael et al., 2013; Macary et al., 2014; Thompson et al., 2012). In addition, most models employed at the catchment scale lack a detailed representation of agricultural landscape components and soil surface conditions related to agricultural practices (Pare et al., 2011; Wohlfahrt et al., 2010).

In this thesis, interlocked investigation scales were used to characterise pesticide transport and degradation processes at the catchment scale, based on the hypothesis that field-process understanding of pesticide transport is a prerequisite to a larger scale view. From a methodological perspective, combining observations of pesticide runoff at both the plot and the catchment scales enabled the delineation of CSA (Chapter III – Section 2). Observations at agricultural plot scale provide information about runoff activation in relation to hydrological conditions (Jencso et al., 2009) and agricultural soil surface characteristics, such as crusted and compacted zones as a first-order control on runoff source area (Chapter III – Section 2 and Chapter IV). Catchment models are typically developed from a sparse number of observations at a few points (Jencso et al., 2009). Several hydrological measurement points within a studied area are necessary for reducing the equifinality issue and validating a fully distributed model considering the interaction complexity of the hydrological processes (Chapter V – Section 1). Many studies focused on pesticide export via surface runoff at the catchment scale (Boithias et al., 2011; De Gerónimo et al.). Evaluation of the available pesticide pool in agricultural plots prior to their export in runoff facilitates the evaluation of their mobilisation at a larger observation scale (Chapter III – Section 2 and Chapter IV).

This embedded characterisation approach enables estimating the respective contribution of plots and plot margins in the off-site transport of pesticides in order to delineate CSA that mainly contribute to pesticide mobilisation and transport. For bridging the gap between investigation scales, physically based modelling may also help in assessing pesticide export according to the spatio-temporal variability of the patterns of CSA (Zanardo et al., 2012).

### 1.3. Predicting pesticide transport processes in the agricultural catchments

Current pesticide runoff models rarely account for the effects of agricultural practices on hydrodynamic parameters such as the saturated hydraulic conductivity or the Manning's coefficient and soil surface characteristics (Pare et al., 2011). Most models are deemed inappropriate for investigating the headwater catchment scale at discrete temporal resolution ( $\leq 1$  min). Pesticide transport in runoff occurs either in the dissolved phase or sorbed on suspended solids, and models rarely integrate processes related to the particulate pesticide fraction in runoff water, which may account for more than 50% of the total load depending on pesticide properties (Boithias et al., 2011).

The runoff and associated erosion mobilise pesticides mainly from a thin near-surface soil layer (McGrath et al., 2010). In this thesis, the concept of mixing layer was therefore implemented in LISEM to improve the description of dissolved pesticide export at catchment scales grounded on a physically-based model (Chapter V – Section 2). A pseudo-analytical resolution was developed and integrated in an erosion model LISEM (Limbourg Soil Erosion Model) (DeRoo et al., 1996). The model was validated on simple test cases and was able to simulate the dynamics of discharge and pesticide export from an experimental plot. The preliminary results of the mathematical formalism at the catchment scale presented reasonable order of magnitude of pesticides concentrations, i.e., a few  $\mu\text{g L}^{-1}$ , and exported loads, i.e., hundreds of mg, compared to the observations at the arable crop catchment outlet but clearly need additional exploration and validation (Chapter V – Section 2). This model represents a valuable tool to dynamically assess CSA patterns within agricultural catchments.

Runoff and erosion prediction, grounded on fully distributed models, may help to delineate CSA for pesticide export and identify zones where runoff and erosion occurred and contributed to runoff at the catchment's outlet (Fan et al., 2013; Frey et al., 2009). The hydrological predictions with LISEM showed that impermeable surfaces in the vineyard catchment explained on average 90% of the total outflowing water occurring at the outlet of the catchment during the growing season (Payraudeau et al., 2010). Pesticide deposition on roads in the vineyard catchment may therefore result in rapid pesticide export in runoff. In the arable crop catchment, runoff and erosion are largely influenced by drastic changes in the soil surface states and the hydrodynamic parameters during the growing season in agro-ecosystems (Alaoui et al., 2011). A novel calibration approach was therefore developed for improving predictions of runoff and erosion processes such as flow and splash detachment, with meaningful input parameters based on the temporal variability of the soil surface and the hydrodynamic parameters during the growing

season (Chapter V – Section 1). Bare soil prevails from beginning of March to mid-May in corn and sugar beet cultivated areas and these were shown to more frequently cause runoff and erosion compared to wheat areas. Coupling the agronomical observations with the event-based hydrological modelling helped to describe with additional precision the dynamics of the initial soil surface.

The further validation of the new formalism against fine dynamics of dissolved pesticide concentrations measurements in the runoff, in the soil and the soil water during rainfall-runoff events, may also enhance the prediction of solid-bound pesticide transport in agro-ecosystems.

### **1.4. Pesticides partitioning is crucial for pesticide export under field condition**

Pesticide adsorption onto soil particles is known to decrease pesticide bioavailability and thus their toxicity. The “bioavailability” of a compound is the extent to which it is accessible for uptake by living organisms (Gevao et al., 2000). Thus, the decrease of pesticide bioavailability due to adsorption processes is expected to limit their biodegradation, affecting the available pesticide amount at the soil surface before the occurrence of a rainfall-runoff event (Barbash, 2014). Significant erosion occurred in the arable crop catchment compared to the vineyard catchment. A total soil loss rate of 1006 t km<sup>-2</sup> was measured from March 12 to August 14 2012 in the arable crop catchment, which was in the range of regional annual erosion (Neboit, 1991) (Chapter IV). Reduction of erosion was promoted in the Alsatian vineyard since the 1980s with the use of grass cover in every two-vine row. A total soil loss rate of 5.3 t km<sup>-2</sup> was measured from March to August 2011 in the vineyard catchment (Chapter III - Section 2). This observation suggested that pesticide transport on suspended solids may account for a large fraction of exported pesticides in agricultural catchments vulnerable for erosion, as previously shown with long-term sediment associated with copper-based-fungicides from agricultural fields (van der Perk and Jetten, 2006).

Specific management practices may therefore focus on solid pesticide export in limiting the erosion processes by establishing vegetated barriers on runoff pathways, in encouraging low tillage or in limiting corn and sugar beet farming in vulnerable catchments. More than 40% of the total export in runoff water occurred in the particulate phase (> 0.7 µm) for both chloroacetanilides (Chapter IV). Partitioning of pesticides between the dissolved and particulate phases is therefore crucial for better evaluating pesticides export in runoff (Boithias et al., 2014).

This issue can be addressed by evaluating the different fractions of the total pesticide loads using, for example, a sequential filtration approach (Goody et al., 2007).

The nature of the sorbents may change over time and under different erosive events and may influence pesticide sorption (Boithias et al., 2014). Pesticide sorption can typically occur on mineral surfaces, but to a larger extent on the organic fraction of soil (Taghavi et al., 2011) or to finer particles such as dissolved organic carbon (Rodriguez-Liebana et al., 2011). In order to decipher the contribution of three different classes of particles for pesticides export, sequential filtration was attempted on the runoff water in this PhD thesis. In the vineyard catchment, three different classes of particles, 0 - 0.22  $\mu\text{m}$ , 0.22 - 0.7  $\mu\text{m}$  and > 0.7  $\mu\text{m}$  were investigated (Chapter III – Section 2). Although kresoxim-methyl and cyazofamid have similar laboratory-physicochemical properties, these results showed that their partitioning in the dissolved phase in field samples differs. In the arable crop catchment, the soil-water partitioning of *S*-metolachlor and acetochlor between the dissolved (< 0.7  $\mu\text{m}$ ) and the particulate (> 0.7  $\mu\text{m}$ ) phases largely varied over time and was shown to be linked to suspended solid concentrations (Chapter IV).

The limited validity of laboratory-derived  $K_d$  values in order to describe the transport of dissolved pesticides has frequently been reported (Vereecken et al., 2011). Theoretical partitioning is indeed often specific to the combination “active ingredient and soil characteristics” and may not be appropriate for understanding sorption of commercial products on suspended solids and/or dissolved organic carbon. Besides, theoretical partition coefficients are often obtained under equilibrium conditions using static sorption experiments (Papiernik et al., 2009). Under field conditions, sorption equilibrium is rarely reached because agricultural systems are highly dynamic in which hydrological and chemical conditions are likely to vary over time and space. A better characterisation of interaction between pesticides and mineral and/or organic matter under dynamic conditions existing in the field would help to model and predict their accumulation, biodegradation, mobility and toxicity in agro-ecosystems.

From a modelling point of view, empirical approaches to evaluate pesticide partitioning appears more suitable, e.g., for fluvial transport (Boithias et al., 2014). However, few studies attempted to establish a relationship between environmental factors and the pesticide field partition coefficient  $K_d$  in runoff water. As reported by many researchers from the early 1980s, enrichment of sorbed pesticides was observed in eroded sediments compared to that in the soil (Ghadiri and Rose, 1993). Fine sediments are more readily eroded than coarse sediments due to their larger specific surface area. Although multiclass erosive models exist and have been

evaluated (Van Oost et al., 2004), no models have been conceived to predict pesticide transport among the different grain size particles. This may partly reflect the lack of experimental data on pesticides among the different grain fractions.

In-depth knowledge about the impact of particle size and the nature of the sorbents on pesticide sorption is definitely required to understand the large temporal variability of field soil-water distribution coefficients, as well as the discrepancies between field and laboratory soil-water distribution coefficient values.

### **1.5. Combining analytical approaches enhances the evaluation of pesticide degradation within agricultural headwater catchment**

Degradation is the only process that actually results in a mass-depletion of pesticides in the environment (Fenner et al., 2013), and leads simultaneously to the formation of degradation products. Improving the evaluation of the degradation processes in agricultural catchments is therefore crucial. It is often impossible to distinguish between biotic and abiotic degradation processes because all of these processes may occur simultaneously or sequentially, making a mechanistic understanding difficult, especially under field conditions (Barbash, 2014). Current approaches to directly identify pesticide degradation processes in the environment rely on the detection of parent compound disappearance (Fenner et al., 2013), detection of degradation products (Steele et al., 2008a) or molecular evidence of an intrinsic transformation potential (Milosevic et al., 2013).

Mass depletion of the four model compounds were investigated in the soil samples at the plot scale in both study catchments. Kresoxim-methyl and cyazofamid concentrations in the vineyard soil rapidly decreased after the application with an estimated half-life of 2 and 5 days respectively (Chapter III – Section 2), whereas the field half-life in soil of *S*-metolachlor in the arable crop catchment was estimated at 54 days (Chapter IV). However, the measurement of parent pesticide concentrations in the field alone does not allow to distinguish transformation from other processes such as dilution, leaching or sorption.

In order to evaluate the relative contribution of the different attenuation processes in the environment, including degradation, the use of complementary analytical techniques is therefore required (Turner et al., 2006). Transformation pathways are often poorly understood (Fenner et al., 2013) and analytical standards for degradation products are currently not commercially available, limiting their identification (Boxall et al., 2004; Hladik et al., 2008).

Chiral pesticide biodegradation may lead to the enrichment of the remaining fraction of non-degraded pesticides in one or another enantiomer. Enantiomeric analyses of chiral pesticides have therefore been successfully used to assess pesticide degradation (Celis et al., 2013; Milosevic et al., 2013).

In this PhD thesis, enantiomer and degradation product analyses were used to provide some qualitative evidence of chloroacetanilide degradation in the arable crop catchment (Chapter IV). ESA and OXA degradates of chloroacetanilides are reported as the most prevalent *S*-metolachlor and acetochlor degradation products (Baran and Gourcy, 2013) and their transport was therefore investigated at the catchment scale (Chapter IV). Biodegradation was expected to be the largest contributor to chloroacetanilide degradation within the arable agricultural catchment. ESA and OXA often presented larger molar concentrations than those of their parent compounds (Chapter IV), in agreement with previous field studies (Steele et al., 2008a). Based on the molar equivalent loads calculation, an export coefficient of ESA and OXA parent compound mass equivalent loads of 7.3% and 6.7% of the total mass applied of *S*-metolachlor and acetochlor respectively was estimated underscoring the large relative contribution of ESA and OXA loads. Furthermore, ESA and OXA have been shown to persist in agricultural soils for more than 4 years after application (Phillips et al., 1999). Such an evaluation would help to determine the production rates of the degradation products in the field with respect to soil characteristics, prior to their export in runoff. The evaluation of the ESA and OXA pools in weekly plot soils samples and in a core soil sample in the arable crop catchment will therefore be the topic of further investigation.

The potential of enantiomer analysis to assess the degradation of *S*-metolachlor in soil, suspended solids and runoff water samples at the catchment scale was evaluated in this PhD thesis (Chapter IV). Enantiomer analyses may serve as integrating indicators of degradation processes across a range of scales, occurring at molecular scale and enabling its evaluation at catchment scale. Although few studies of the stereoselectivity of metolachlor have been conducted, stereoselective degradation of *S*-metolachlor is still a controversial topic (Kurt-Karakus et al., 2010). Our results showed that the enantiomeric excess of the *S*-enantiomer negatively correlated with *S*-metolachlor concentrations suggesting enantioselective biodegradation in the different environmental compartments. From a scientific view point, pronounced enantiomer fractionation in the field was observed indicating the occurrence of pesticides degradation in soil and runoff water which demonstrates that enantiomer analyses may be a useful approach for the assessment of biodegradation of chiral pesticides at catchment scale.

No relationship could be found between enantiomeric excess values of *S*-metolachlor and MESA and MOXA concentrations. Preferential degradation of the *S*-enantiomer may not involve the formation of such degradation products or interconversion reaction may interfere with the enantiomer signature (Milosevic et al., 2013; Polcaro et al., 2004) and render the field data interpretation complicated. Little is known on the environmental fate of stereoisomers and enantiomer fractionation shift references are currently missing for evaluating the extent of degradation at catchment scale, and additional, benchmark-laboratory experiments to quantify enantioselective degradation are necessary to interpret the enantiomer signatures retrieved from the field experiments. From a regulatory point of view, there is a growing need to consider pesticide active ingredients manufactured as isomeric mixtures as individual pesticide stereoisomers, for which individual information on the efficacy, toxicity and environmental fate should be required (Kurt-Karakus et al., 2010).

The combination of different approaches in this PhD thesis enabled to assess, model and predict pesticide transport and degradation in the dynamic conditions existing in the field, which opens doors for novel research perspectives.

## 2. Implications and perspectives

This thesis demonstrated the relevance of combining observations from interlocked scales and analytical approaches to evaluate pesticide transport and attenuation from the plot application area (sources) to the catchment outlet in contrasting agricultural catchments (vineyard versus arable crops). This PhD thesis attempted to respond to the need for an event based, spatially distributed pesticide transport model at the catchment scale designed to describe agricultural landscape components with crusted and compacted zones and soil surface structure. Furthermore, this study constitutes a starting point to combine the quantification of the parent pesticides and their degradation products with enantiomer analyses to evaluate and predict the degradation of chiral pesticides in agro-ecosystems.

The complexity of pesticide fate and the prediction of their transport in agro-ecosystems involve the dynamic interplay of microbial, hydrological and hydrochemical processes which make this a rich topic, with many short- and longer-term research perspectives. These are detailed in the following perspectives and formulated as open research questions.

## **2.1. How to address the variability of pesticide deposition during application in pesticides runoff studies?**

Pesticide drift in agricultural systems remains poorly investigated at the catchment scale and its thorough evaluation appears crucial for delineating CSA for pesticide export. Pesticide runoff predictions are often based on the input contamination map, which includes only the agricultural plots, therefore neglecting the impact of pesticide drift on non-target areas. Drift field characterisation is costly, time consuming and challenging at the catchment scale due to the variability of the meteorological conditions (Gregorio et al., 2014), commercial formulations (Hilz and Vermeer, 2013) and the application modes (Nuyttens et al., 2007), rendering an extrapolation difficult to other contexts, if not impossible (Donkersley and Nuyttens, 2011).

Therefore, a physically-based model predicting the drift processes may help in evaluating the spatial extent of pesticide deposition and its variability at the catchment scale. Most common pesticide drift models are limited to pesticide transport and the deposition into areas directly surrounding the application plots, and generally require local meteorological data and specific details on operation modes and droplet size (Ellis and Miller, 2010; Lebeau et al., 2011). As micro-meteorological conditions may play a crucial role in pesticide drift, pesticide drift evaluation may be assessed towards a new generation of high-resolution meteorological input data (Leimer et al., 2011) combined with an atmospheric pesticide transport model. Pesticide transport models include plume dispersion models based on a Gaussian distribution of the concentrations when long drift distances need to be predicted such as ADMS, (Baetens et al., 2009) or droplet tracking models based on a random walk such as IDEFICS (Holterman et al., 1997) or AgDrift (Teske et al., 2009). Such a new combined model, i.e. meteorological and atmospheric pesticide transport modelling, could be applied in both study catchments, and particularly in the vineyard catchment to precisely estimate the contribution of pesticide deposition on the total export of pesticides in runoff at the catchment outlet. Bridging the gap between plot and catchment scales for drift prediction is complex and appears crucial for better evaluating CSA in different agricultural contexts and under different meteorological conditions.

## **2.2. How to improve the evaluation the pesticides partitioning in runoff water?**

There is a need to better understand sorption processes under dynamic climatic, hydrological and chemical condition existing in the field. In-depth knowledge about the influence of the nature of soil particles requires further investigation. Laboratory experiments with selected sorbents varying in their nature and quantity, similar to those for studying erosion processes (Balacco, 2013) but with the aim of examining the mobilisation of pesticides in runoff and

erosion under different erosive condition (Ulrich et al., 2013), may help in the characterisation of pesticide partitioning in runoff water.

The influence of particle size on pesticide export may be evaluated in analysing pesticides in different particle fractions using for example sequential ultrafiltration. Measurements of aromaticity (measured by UV-Vis spectrophotometer) and electrical conductivity have been shown to be valuable tools in assessing pesticide sorption (Rodríguez-Liébaña, 2013). Clay mineral determination may also help in the characterisation of pesticide sorption (Spark, 2002). These methods may be combined under controlled conditions in laboratory studies. To bridge the gap between laboratory and field studies, such laboratory experiments needs to be based on more realistic conditions, including the use of commercial formulations (with surfactants) instead of active ingredients, or complex water and soil matrices in order to disentangle the underlying drivers of pesticide and sorbent characteristics on pesticide sorption.

### **2.3. How to evaluate the degradation of chiral pesticides under field conditions?**

The environmental fate of the individual stereoisomers of chiral pesticides remains poorly understood (Celis et al., 2013). Several studies attempted to evaluate enantioselective degradation of chiral compounds to gain mechanistic insights on pesticide degradation under complex field dynamic conditions (Buser et al., 2000; Kurt-Karakus et al., 2010; Milosevic et al., 2013). However, such field studies are difficult to interpret in quantitative terms when laboratory reference studies on enantiomer fractionation for degradation of such compounds are missing. Laboratory references aim at investigating the degradation of such pesticides under controlled conditions such as aerobic and anaerobic condition or presence of selected microorganisms. These references may allow the systematic assessment of the enantiomer fractionation of chiral compounds and the formation of degradation products in a comprehensive survey. The use of emerging analytical techniques such as Orbitrap-Based Mass Spectrometry or Time-of-Flight Mass Spectrometry measurements can constitute a valuable method to identify degradation products that remain unknown and quantify the degradation extent (Eichhorn et al., 2012). Supplementary complementary approaches, such as CSIA and enantiomer-specific isotope analyses for chiral compounds, may be combined to better understand pesticide transformation processes (Milosevic et al., 2013). Hence, both enantiomer and isotope enrichment factors could be retrieved in benchmark experiment studies related to a stringent mass balance between the mass depletion of the parent compound and the mass increase of the degradation products. These enrichment factors may be used to evaluate, and possibly quantify the *in situ* biodegradation under more complex field conditions.

From a modelling point of view, degradation processes amplify uncertainty associated with predictions of pesticide and degradation product transport and attenuation (Gassmann et al., 2014). Pesticide half lives and sorption parameters were correlated to each other suggesting that sorption and degradation processes may counterbalance each other in the prediction of pesticide transport. Few quantitative published data are available with regard to the partitioning properties or persistence of the degradation products (Steele et al., 2008b) which introduces additional uncertainty in predictions. Reactive transport models that incorporate isotope fractionation are becoming a popular method for predicting pesticide degradation in groundwater systems (D'Affonseca et al., 2011) and in surface water (Lutz et al., 2013). Based on enrichment factors retrieved from laboratory reference studies, models may predict enantiomer fractionation under field conditions and thus assist complex data interpretation from field-relevant situations.

Each pesticide is expected to behave uniquely with respect to its environmental transport and degradation. This PhD thesis attempted to address novel aspects of pesticide reactive transport in complex environments, such as agro-ecosystems. Overall, gaining knowledge on the fate of ancient and emerging pollutants is crucial for the preservation of soils and water resources.

### 3. References

- Alaoui, A., Lipiec, J., Gerke, H.H., 2011. A review of the changes in the soil pore system due to soil deformation: A hydrodynamic perspective. *Soil & Tillage Research*. 115, 1-15.
- Baetens, K., Ho, Q.T., Nuyttens, D., De Schampheleire, M., Endalew, A.M., Hertog, M.L.A.T.M., Nicolai, B., Ramon, H., Verboven, P., 2009. A validated 2-D diffusion-advection model for prediction of drift from ground boom sprayers. *Atmospheric Environment*. 43, 1674-1682.
- Balacco, G., 2013. The interrill erosion for a sandy loam soil. *International Journal of Sediment Research*. 28, 329-337.
- Baran, N., Gourcy, L., 2013. Sorption and mineralization of S-metolachlor and its ionic metabolites in soils and vadose zone solids: Consequences on groundwater quality in an alluvial aquifer (Ain Plain, France). *Journal of Contaminant Hydrology*. 154, 20-28.
- Barbash, J.E., 2014. The Geochemistry of Pesticides. In: *Treatise on Geochemistry (Second Edition)*. Vol., H.D. Holland, K.K. Turekian, ed. Elsevier, Oxford, pp. 535-572.
- Bertuzzo, E., Thomet, M., Botter, G., Rinaldo, A., 2013. Catchment-scale herbicides transport: Theory and application. *Advances in Water Resources*. 52, 232-242.
- Boithias, L., Sauvage, S., Taghavi, L., Merlina, G., Probst, J.L., Perez, J.M.S., 2011. Occurrence of metolachlor and trifluralin losses in the Save river agricultural catchment during floods. *Journal of Hazardous Materials*. 196, 210-219.
- Boithias, L., Sauvage, S., Merlina, G., Jean, S., Probst, J.-L., Sánchez Pérez, J.M., 2014. New insight into pesticide partition coefficient  $K_d$  for modelling pesticide fluvial transport: Application to an agricultural catchment in south-western France. *Chemosphere*. 99, 134-142.
- Borah, D.K., Bera, M., 2003. Watershed-scale hydrologic and nonpoint-source pollution models: Review of mathematical bases. *Transactions of the Asae*. 46, 1553-1566.
- Botta, F., Fauchon, N., Blanchoud, H., Chevreuil, M., Guery, B., 2012. Phyt'Eaux Cites: Application and validation of a programme to reduce surface water contamination with urban pesticides. *Chemosphere*. 86, 166-176.
- Boxall, A.B.A., Sinclair, C.J., Fenner, K., Kolpin, D., Maud, S.J., 2004. When synthetic chemicals degrade in the environment. *Environmental Science & Technology*. 38, 368a-375a.
- Buser, H.R., Poiger, T., Muller, M.D., 2000. Changed enantiomer composition of metolachlor in surface water following the introduction of the enantiomerically enriched product to the market. *Environmental Science & Technology*. 34, 2690-2696.
- Celis, R., Gamiz, B., Adelino, M.A., Hermosin, M.C., Cornejo, J., 2013. Environmental behavior of the enantiomers of the chiral fungicide metalaxyl in Mediterranean agricultural soils. *Science of The Total Environment*. 444, 288-297.
- Chung, A.W., Ghebremichael, M., Robinson, H., Brown, E., Choi, I., Rolland, M., Dugast, A., Suscovich, T.J., Liao, L., Mahan, A.E., Streeck, H., Rerks-Ngarm, S., Nitayaphan, S., de Souza, M.S., Pitisuttithum, P., Francis, D., Michael, N.L., Kim, J.H., Bailey-Kellog, C., Ackerman, M.E., Alter, G., 2013. Distinct HIV-

- Specific Antibody Fc-Profiles in RV144 and VAX003 Vaccinees. *Aids Research and Human Retroviruses*. 29, A63-A64.
- D'Affonseca, F.M., Prommer, H., Finkel, M., Blum, P., Grathwohl, P., 2011. Modeling the long-term and transient evolution of biogeochemical and isotopic signatures in coal tar-contaminated aquifers. *Water Resources Research*. 47.
- De Gerónimo, E., Aparicio, V.C., Bárbaro, S., Portocarrero, R., Jaime, S., Costa, J.L., 2014. Presence of pesticides in surface water from four sub-basins in Argentina. *Chemosphere*, in press.
- DeRoo, A.P.J., Wesseling, C.G., Ritsema, C.J., 1996. LISEM: A single-event physically based hydrological and soil erosion model for drainage basins .1. Theory, input and output. *Hydrological Processes*. 10, 1107-1117.
- Dodds, W.K., Oakes, R.M., 2008. Headwater influences on downstream water quality. *Environmental Management*. 41, 367-377.
- Donkersley, P., Nuyttens, D., 2011. A meta analysis of spray drift sampling. *Crop Protection*. 30, 931-936.
- Eichhorn, P., Pérez, S., Barceló, D., 2012. Chapter 5 - Time-of-Flight Mass Spectrometry Versus Orbitrap-Based Mass Spectrometry for the Screening and Identification of Drugs and Metabolites: Is There a Winner? In: *Comprehensive Analytical Chemistry*. Vol. Volume 58, R.F.-A. Amadeo, ed.^eds. Elsevier, pp. 217-272.
- Ellis, M.C.B., Miller, P.C.H., 2010. The Silsoe Spray Drift Model: A model of spray drift for the assessment of non-target exposures to pesticides. *Biosystems Engineering*. 107, 169-177.
- Fan, X.D., Liu, E., Freudenreich, O., Copeland, P., Hayden, D., Ghebremichael, M., Cohen, B., Ongur, D., Goff, D.C., Henderson, D.C., 2013. No Effect of Adjunctive, Repeated-Dose Intranasal Insulin Treatment on Psychopathology and Cognition in Patients With Schizophrenia. *Journal of Clinical Psychopharmacology*. 33, 226-230.
- Fenner, K., Canonica, S., Wackett, L.P., Elsner, M., 2013. Evaluating Pesticide Degradation in the Environment: Blind Spots and Emerging Opportunities. *Science*. 341, 752-758.
- Freeman, M.C., Pringle, C.M., Jackson, C.R., 2007. Hydrologic connectivity and the contribution of stream headwaters to ecological integrity at regional scales. *Journal of the American Water Resources Association*. 43, 5-14.
- Frey, M.P., Schneider, M.K., Dietzel, A., Reichert, P., Stamm, C., 2009. Predicting critical source areas for diffuse herbicide losses to surface waters: Role of connectivity and boundary conditions. *Journal of Hydrology*. 365, 23-36.
- Gascuel-Oudou, C., Arousseau, P., Cordier, M.O., Durand, P., Garcia, F., Masson, V., Salmon-Monviola, J., Tortrat, F., Trepos, R., 2009. A decision-oriented model to evaluate the effect of land use and agricultural management on herbicide contamination in stream water. *Environmental Modelling & Software*. 24, 1433-1446.
- Gassmann, M., Khodorkovsky, M., Friedler, E., Dubowski, Y., Olsson, O., 2014. Uncertainty in the river export modelling of pesticides and transformation products. *Environmental Modelling & Software*. 51, 35-44.
- Gevao, B., Semple, K.T., Jones, K.C., 2000. Bound pesticide residues in soils: a review. *Environmental Pollution*. 108, 3-14.

- Ghadiri, H., Rose, C.W., 1993. Water Erosion Processes and the Enrichment of Sorbed Pesticides .1. Enrichment Mechanisms and the Degradation of Applied Pesticides. *Journal of Environmental Management*. 37, 23-35.
- Ghebremichael, L.T., Veith, T.L., Hamlett, J.M., 2013. Integrated watershed- and farm-scale modeling framework for targeting critical source areas while maintaining farm economic viability. *Journal of Environmental Management*. 114, 381-394.
- Gil, Y., Sinfort, C., 2005. Emission of pesticides to the air during sprayer application: A bibliographic review. *Atmospheric Environment*. 39, 5183-5193.
- Goody, D.C., Mathias, S.A., Harrison, I., Lapworth, D.J., Kim, A.W., 2007. The significance of colloids in the transport of pesticides through Chalk. *Science of the Total Environment*. 385, 262-271.
- Gregorio, E., Rosell-Polo, J.R., Sanz, R., Rocadenbosch, F., Solanelles, F., Garcerá, C., Chueca, P., Arnó, J., del Moral, I., Masip, J., Camp, F., Viana, R., Escolà, A., Gràcia, F., Planas, S., Moltó, E., 2014. LIDAR as an alternative to passive collectors to measure pesticide spray drift. *Atmospheric Environment*. 82, 83-93.
- Hilz, E., Vermeer, A.W.P., 2013. Spray drift review: The extent to which a formulation can contribute to spray drift reduction. *Crop Protection*. 44, 75-83.
- Hladik, M.L., Bouwer, E.J., Roberts, A.L., 2008. Neutral degradates of chloroacetamide herbicides: Occurrence in drinking water and removal during conventional water treatment. *Water Research*. 42, 4905-4914.
- Holterman, H.J., van de Zande, J.C., Porskamp, H.A.J., Huijsmans, J.F.M., 1997. Modelling spray drift from boom sprayers. *Computers and Electronics in Agriculture*. 19, 1-22.
- Holvoet, K.M.A., Seuntjens, P., Vanrolleghem, P.A., 2007. Monitoring and modeling pesticide fate in surface waters at the catchment scale. *Ecological Modelling*. 209, 53-64.
- Jencso, K.G., McGlynn, B.L., Gooseff, M.N., Wondzell, S.M., Bencala, K.E., Marshall, L.A., 2009. Hydrologic connectivity between landscapes and streams: Transferring reach-and plot-scale understanding to the catchment scale. *Water Resources Research*. 45.
- Kurt-Karakus, P.B., Bidleman, T.F., Muir, D.C.G., Struger, J., Sverko, E., Cagampan, S.J., Small, J.M., Jantunen, L.M., 2010. Comparison of concentrations and stereoisomer ratios of mecoprop, dichlorprop and metolachlor in Ontario streams, 2006-2007 vs. 2003-2004. *Environmental Pollution*. 158, 1842-1849.
- Lebeau, F., Verstraete, A., Stainier, C., Destain, M.F., 2011. RTDrift: A real time model for estimating spray drift from ground applications. *Computers and Electronics in Agriculture*. 77, 161-174.
- Leimer, S., Pohlert, T., Pfahl, S., Wilcke, W., 2011. Towards a new generation of high-resolution meteorological input data for small-scale hydrologic modeling. *Journal of Hydrology*. 402, 317-332.
- Lutz, S.R., van Meerveld, H.J., Waterloo, M.J., Broers, H.P., van Breukelen, B.M., 2013. A model-based assessment of the potential use of compound-specific stable isotope analysis in river monitoring of diffuse pesticide pollution. *Hydrol. Earth Syst. Sci.* 17, 4505-4524.
- Macary, F., Morin, S., Probst, J.L., Saudubray, F., 2014. A multi-scale method to assess pesticide contamination risks in agricultural watersheds. *Ecological Indicators*. 36, 624-639.

- McGrath, G.S., Hinz, C., Sivapalan, M., Dressel, J., Putz, T., Vereecken, H., 2010. Identifying a rainfall event threshold triggering herbicide leaching by preferential flow. *Water Resources Research*. 46.
- Milosevic, N., Qiu, S., Elsner, M., Einsiedl, F., Maier, M.P., Bensch, H.K.V., Albrechtsen, H.J., Bjerg, P.L., 2013. Combined isotope and enantiomer analysis to assess the fate of phenoxy acids in a heterogeneous geologic setting at an old landfill. *Water Research*. 47, 637-649.
- Neboit, R., 1991. L'homme et l'érosion: l'érosion des sols dans le monde, Vol., Association des Publications de la Faculté des Lettres et Sciences Humaines de Clermont-Ferrand.
- Nuyttens, D., De Schampheleire, M., Baetens, K., Sonck, B., 2007. The influence of operator-controlled variables on spray drift from field crop sprayers. *Transactions of the Asabe*. 50, 1129-1140.
- Nuyttens, D., De Schampheleire, M., Verboven, P., Brusselman, E., Dekeyser, D., 2009. Droplet Size and Velocity Characteristics of Agricultural Sprays. *Transactions of the Asabe*. 52, 1471-1480.
- Papiernik, S.K., Koskinen, W.C., Yates, S.R., 2009. Solute Transport in Eroded and Rehabilitated Prairie Landforms. 2. Reactive Solute. *Journal of Agricultural and Food Chemistry*. 57, 7434-7439.
- Pare, N., Andrieux, P., Louchart, X., Biarnes, A., Voltz, M., 2011. Predicting the spatio-temporal dynamic of soil surface characteristics after tillage. *Soil & Tillage Research*. 114, 135-145.
- Payraudeau, S., Mauree, D., Van Dijk, P., Imfeld, G., Regazzoni, C., Grégoire, C., 2010. Analyzing the temporal variability of the hydrological connectivity to assess the critical source areas for pesticides losses. EGU General Assembly 2010, held 2-7 May, 2010 in Vienna, Austria, p.5130.
- Phillips, P.J., Wall, G.R., Thurman, E.M., Eckhardt, D.A., Vanhoesen, J., 1999. Metolachlor and its metabolites in tile drain and stream runoff in the canajoharie Greek watershed. *Environmental Science & Technology*. 33, 3531-3537.
- Polcaro, C.M., Berti, A., Mannina, L., Marra, C., Sinibaldi, M., Viel, S., 2004. Chiral HPLC resolution of neutral pesticides. *Journal of Liquid Chromatography & Related Technologies*. 27, 49-61.
- Rasmussen, J.J., McKnight, U.S., Loinaz, M.C., Thomsen, N.I., Olsson, M.E., Bjerg, P.L., Binning, P.J., Kronvang, B., 2013. A catchment scale evaluation of multiple stressor effects in headwater streams. *Science of The Total Environment*. 442, 420-431.
- Rodriguez-Liebana, J.A., Mingorance, M.D., Pena, A., 2011. Sorption of hydrophobic pesticides on a Mediterranean soil affected by wastewater, dissolved organic matter and salts. *Journal of Environmental Management*. 92, 650-654.
- Salifu, A., Petrushevski, B., Ghebremichael, K., Modestus, L., Buamah, R., Aubry, C., Amy, G.L., 2013. Aluminum (hydr)oxide coated pumice for fluoride removal from drinking water: Synthesis, equilibrium, kinetics and mechanism. *Chemical Engineering Journal*. 228, 63-74.
- Salmon-Monviola, J., Moreau, P., Benhamou, C., Durand, P., Merot, P., Oehler, F., Gascuel-Oudou, C., 2013. Effect of climate change and increased atmospheric CO<sub>2</sub> on hydrological and nitrogen cycling in an intensive agricultural headwater catchment in western France. *Climatic Change*. 120, 433-447.
- Spark, K. M., Swift, R. S., Effect of soil composition and dissolved organic matter on pesticide sorption. *Science of The Total Environment*. 298, 147-161

- Steele, G.V., Johnson, H.M., Sandstrom, M.W., Capel, P.D., Barbash, J.E., 2008a. Occurrence and fate of pesticides in four contrasting agricultural settings in the United States. *Journal of Environmental Quality*. 37, 1116-1132.
- Steele, G.V., Johnson, H.M., Sandstrom, M.W., Capel, P.D., Barbash, J.E., 2008b. Occurrence and fate of pesticides in four contrasting agricultural settings in the United States. *Journal of Environmental Quality*. 37, 1116-32.
- Taghavi, L., Merlina, G., Probst, J.L., 2011. The role of storm flows in concentration of pesticides associated with particulate and dissolved fractions as a threat to aquatic ecosystems Case study: the agricultural watershed of Save river (Southwest of France). *Knowledge and Management of Aquatic Ecosystems* 400-06.
- Tang, X.Y., Zhu, B., Katou, H., 2012. A review of rapid transport of pesticides from sloping farmland to surface waters: Processes and mitigation strategies. *Journal of Environmental Sciences-China*. 24, 351-361.
- Teske, M.E., Miller, P.C.H., Thistle, H.W., Birchfield, N.B., 2009. Initial Development and Validation of a Mechanistic Spray Drift Model for Ground Boom Sprayers. *Transactions of the Asabe*. 52, 1089-1097.
- Thompson, J.J.D., Doody, D.G., Flynn, R., Watson, C.J., 2012. Dynamics of critical source areas: Does connectivity explain chemistry? *Science of The Total Environment*. 435, 499-508.
- Turner, J., Albrechtsen, H.J., Bonell, M., Duguet, J.P., Harris, B., Meckenstock, R., McGuire, K., Moussa, R., Peters, N., Richnow, H.H., Sherwood-Lollar, B., Uhlenbrook, S., van Lanen, H., 2006. Future trends in transport and fate of diffuse contaminants in catchments, with special emphasis on stable isotope applications. *Hydrological Processes*. 20, 205-213.
- Ulrich, U., Zeiger, M., Fohrer, N., 2013. Soil structure and herbicide transport on soil surfaces during intermittent artificial rainfall. *Zeitschrift Fur Geomorphologie*. 57, 135-155.
- van der Perk, M., Jetten, V.G., 2006. The use of a simple sediment budget model to estimate long-term contaminant export from small catchments. *Geomorphology*. 79, 3-12.
- Van Oost, K., Beuselinck, L., Hairsine, P.B., Govers, G., 2004. Spatial evaluation of a multi-class sediment transport and deposition model. *Earth Surface Processes and Landforms*. 29, 1027-1044.
- Vereecken, H., Vanderborght, J., Kasteel, R., Spiteller, M., Schaffer, A., Close, M., 2011. Do Lab-Derived Distribution Coefficient Values of Pesticides Match Distribution Coefficient Values Determined from Column and Field-Scale Experiments? A Critical Analysis of Relevant Literature. *Journal of Environmental Quality*. 40, 879-898.
- Vischetti, C., Cardinali, A., Monaci, E., Nicelli, M., Ferrari, F., Trevisan, M., Capri, E., 2008. Measures to reduce pesticide spray drift in a small aquatic ecosystem in vineyard estate. *Science of The Total Environment*. 389, 497-502.
- Vorosmarty, C.J., McIntyre, P.B., Gessner, M.O., Dudgeon, D., Prusevich, A., Green, P., Glidden, S., Bunn, S.E., Sullivan, C.A., Liermann, C.R., Davies, P.M., 2010. Global threats to human water security and river biodiversity (vol 467, pg 555, 2010). *Nature*. 468, 334-334.

- Wohlfahrt, J., Colin, F., Assaghir, Z., Bockstaller, C., 2010. Assessing the impact of the spatial arrangement of agricultural practices on pesticide runoff in small catchments: Combining hydrological modeling and supervised learning. *Ecological Indicators*. 10, 826-839.
- Zanardo, S., Basu, N.B., Botter, G., Rinaldo, A., Rao, P.S.C., 2012. Dominant controls on pesticide transport from tile to catchment scale: Lessons from a minimalist model. *Water Resources Research*. 48.

## Chapter VII. Appendices

---

## Appendices for Chapter III:

Table VII-1. Interpolation methods for estimating the total KM deposition at the catchment scale.

	Thiessen Methodology	Inverse Weighting Distance	Ordinary Kriging	Arithmetic mean
<b>Hypothesis</b>	Values of unsampled locations are equal to the value of the nearest sampled point.	Predictions are a linear combination of available data. Greater weighting values are assigned to values closer to the interpolated points.	The parameter being interpolated can be treated as a regionalized variable. The kriging estimator is given by a linear combination of the observed values.	Each petri dish has the same weight
<b>References<sup>1</sup></b>	-	(Ke et al., 2011; Kravchenko, 2003; Sun et al., 2010; Xie et al., 2011)	(Kravchenko, 2003; Leterme et al., 2007; Li et al., 2007; Lindahl et al., 2008; Xie et al., 2011)	-
<b>RMSE [ ]<sup>2</sup></b>	8.5	6.4	7.8	5.3
<b>KMT [g]<sup>3</sup></b>	61	59	58	53

<sup>1</sup> References between the interpolation methods and contaminants spatialisation. <sup>2</sup> Root Mean Square Error (Xie et al., 2011). <sup>3</sup>Total deposition of kresoxim methyl on vineyard plots.

### References

- Ke W, Cheng HP, Yan D, Lin C. The Application of Cluster Analysis and Inverse Distance-Weighted Interpolation to Appraising the Water Quality of Three Forks Lake. *Procedia Environ Sci* 2011; 10, Part C: 2511-2517.
- Kravchenko AN. Influence of spatial structure on accuracy of interpolation methods. *Soil Sci Soc Am J* 2003; 67: 1564-1571.
- Leterme B, Vanclooster M, van der Linden AMA, Tiktak A, Rounsevell MDA. The consequences of interpolating or calculating first on the simulation of pesticide leaching at the regional scale. *Geoderma* 2007; 137: 414-425.
- Li BG, Ran Y, Cao J, Liu WX, Shen WR, Wang J, et al. Spatial structure analysis and kriging of dichlorodiphenyltrichloroethane residues in topsoil from Tianjin, China. *Geoderma* 2007; 141: 71-77.
- Lindahl AML, Soderstrom M, Jarvis N. Influence of input uncertainty on prediction of within-field pesticide leaching risks. *J Contam Hydrol* 2008; 98: 106-114.
- Sun C, Bi CJ, Chen ZL, Wang DQ, Zhang C, Sun YD, et al. Assessment on environmental quality of heavy metals in agricultural soils of Chongming Island, Shanghai City. *J Geogr Sci* 2010; 20: 135-147.
- Xie YF, Chen TB, Lei M, Yang J, Guo QJ, Song B, et al. Spatial distribution of soil heavy metal pollution estimated by different interpolation methods: Accuracy and uncertainty analysis. *Chemosphere* 2011; 82: 468-476.

Table VII-2. Kresoxim methyl soil deposition as a percentage of the applied dose for each integrative petri dish.

Samples name	I1	I2	I3	I4	I5	I6	I7	I8	I9
<b>Period 1</b>									
<b>Opening time</b>	6:10 am	6:10 am	6:10 am	6:10 am	6:30 am	6:24 am	6:41 am	6:38 am	6:46 am
	10:32 am	10:07 am	10:29 am	10:14 am	10:23 am	10:18 am	10:50 am	10:32 am	10:41 am
<b>Mean of the triplicate [%]</b>	1.095	1.353	1.891	0.308	14.447	4.022	1.046	0	0
<b>(±SD)</b>	(±0.035)	(±0.041)	(±0.076)	(±0.046)	(±0.761)	(±0.077)	(±0.068)		
<b>Period 2</b>									
<b>Opening time</b>	10:32 am	10:07 am	10:29 am	10:14 am	10:23 am	10:18 am	10:50 am	10:32 am	10:41 am
	2:37 pm	2:07 pm	2:35 pm	2:18 pm	2:48 pm	2:22 pm	2:45 pm	2:17 pm	2:39 pm
<b>Mean of the triplicate [%]</b>	0.019	0.083	0	1.902	0	2.714	0.081	0	7.690
<b>(±SD)</b>	(±0.003)	(±0.018)		(±0.121)		(±0.187)	(±0.012)		(±0.606)
<b>Period 3</b>									
<b>Opening time</b>	2:37 pm	2:07 pm	2:35 pm	2:18 pm	2:48 pm	2:22 pm	2:45 pm	2:17 pm	2:39 pm
	4:38 pm	4:21 pm	4:36 pm	4:25 pm	4:32 pm	4:28 pm	4:38 pm	4:25 pm	4:33 pm
<b>Mean of the triplicate [%]</b>	0	0.014	0	0	0	0	0.183	15.042	0
<b>(±SD)</b>		(±0.002)					(±0.024)	(±1.069)	
<b>Entire day</b>									
<b>Mean of the triplicate [%]</b>	1.114	1.451	1.891	2.210	14.447	6.737	1.310	15.042	7.690
<b>(±SD)</b>	(±0.038)	(±0.061)	(±0.076)	(±0.167)	(±0.761)	(±0.264)	(±0.104)	(±1.069)	(±0.606)

Table VII-3. Meteorological data for each transect and kresoxim methyl soil deposition as a percentage of the applied dose.

	<b>T1</b>	<b>T2</b>	<b>T3</b>	<b>T4</b>	<b>T5</b>	<b>T6</b>	<b>T7</b>	<b>Rautmann (early)</b>	<b>Rautmann (late)</b>
<b>Opening time</b>	11:54 - 12:26	6:33 - 9:10	9:05 - 10:24	8:41 - 10:05	9:10 - 10:05	14:22 - 15:51	13:43 - 14:50	-	-
<b>Temperature [°C]</b>	26.65	20.69	25.68	25.19	24.50	24.80	25.43	-	-
<b>Wind speed [m s<sup>-1</sup>]</b>	1.85	1.66	1.34	1.32	1.32	2.57	2.81	-	-
<b>Air humidity [%]</b>	29.33	58.43	35.64	39.13	42.8	28.94	29.54	-	-
								-	-
<b>Distance [m]</b>	<b>Mean of the triplicate [%] (±SD)</b>								
<b>0</b>	2.251 (±0.433)	18.240 (±0.953)	3.666 (±0.105)	10.051 (±0.741)	8.113 (±0.449)	1.920 (±0.242)	9.294 (±0.147)	650	1613
<b>1</b>	-	7.827 (±0.531)	3.510 (±0.147)	5.156 (±0.333)	3.354 (±0.733)	2.798 (±0.267)	17.977 (±0.796)	16	45
<b>5</b>	0.082 (±0.019)	1.189 (±0.061)	0.209 (±0.030)	0	0	2.244 (±0.488)	3.400 (±0.119)	1.182	3.618
<b>10</b>	0.055 (±0.012)	0.225 (±0.038)	0	0	0	0.393 (±0.036)	0.689 (±0.091)	0.386	1.228
<b>25</b>	0	0.114 (±0.008)	0	0	0	0.396 (±0.021)	0.150 (±0.014)	0.088	0.294
<b>40</b>	0	0.113 (±0.014)	0	0	0	-	-	0.041	0.141

Table VII-4. Deposition loads on plot margins in the catchment according to the distances. Values are provided as a range.

<b>Buffer from the application area [m]</b>	<b>Surface of plot margins [ha]</b>	<b>Deposition loads on plot margins [g]</b>	<b>Surface of roads [ha]</b>	<b>Deposition loads on roads [g]</b>	<b>Surface of connected roads [ha]</b>	<b>Deposition loads on connected roads [g]</b>
0 - 1 m	0.21	0.41 - 3.16	0.11	0.2 - 1.57	0.09	0.16 - 1.23
1 - 5 m	1.82	2.04 - 15.59	0.39	0.44 - 3.33	0.33	0.37 - 2.83
5 - 10 m	0.68	0 - 1.11	0.15	0 - 0.25	0.14	0 - 0.22
10 - 25 m	0.38	0 - 0.16	0.06	0 - 0.025	0.03	0 - 0.013
25 - 40 m	$6.2 \cdot 10^{-5}$	$0 - 1.26 \cdot 10^{-5}$	$1 \cdot 10^{-6}$	$0 - 2.03 \cdot 10^{-7}$	0	0 - 0
Total	3.09	2.45 - 20.02	0.71	0.64 - 5.18	0.58	0.53 - 4.30

Table VII-5. Commercial products composition (Stroby DF © and Mildicut ©).

<b>Mildicut</b>		<b>Stroby DF</b>	
Cyazofamid	2.03%	Kresoxim methyl	50%
Disodium-phosphonate	< 25%	Lignosulfonic acid, Sodium salt	< 40%
Naphthalenesulfonic acid, methyl-, polymer with formaldehyde, sodium salt	< 5%	Ammonium sulfate	< 20%
Unknown other components	Not provided	Sodium sulfate	< 10%

**Table VII-6. Application dose and frequency of all the synthetic active substances applied in the catchment during the wine growing season of 2011 (substances representing > 2% of the total pesticide mass applied). Values for the catchment are provided as mean of plots values  $\pm$  standard deviation according to the plots. The substances marked in grey were used on the study plot.**

Substances	Plot number <sup>a</sup>	Catchment surface [%] <sup>b</sup>	AD <sup>c</sup> [g ha <sup>-1</sup> ]	AD <sub>study</sub> plot <sup>d</sup> [g ha <sup>-1</sup> ]	AN <sup>e</sup> [-]	AN <sub>study</sub> plot <sup>f</sup> [-]	Mass [%] <sup>g</sup>
Boscalid	1	2.2	625 $\pm$ 0	-	1	-	0.30
Cyazofamid	33	48.8	90.4 $\pm$ 8.2	87.5	1	1	1.03
Cymoxanil	50	73.8	109.3 $\pm$ 13.6	110.4	2.2	2	3.86
Cyprodinil	4	4.3	375 $\pm$ 0	375	1	1	0.36
Difenoconazole	41	59.5	26.4 $\pm$ 2.3	25	1	1	0.36
Dimethomorph	8	14.4	225.8 $\pm$ 0.5	-	1	-	0.73
Disodium phosphonate	33	48.8	904.4 $\pm$ 81.8	875	1	1	10.30
Fenoxycarb	13	21.4	75 $\pm$ 0	-	1	-	0.36
Fludioxonil	4	4.3	250 $\pm$ 0	250	1	1	0.24
Folpel	48	69.2	524.5 $\pm$ 336.9	296.4	2	2	14.27
Fosetyl-aluminium	34	48.6	1462.2 $\pm$ 281.4	1318.8	1.1	1	16.31
Glufosinate-ammonium	2	6.2	525 $\pm$ 0	-	1	-	0.24
Glyphosate	49	67.9	673.7 $\pm$ 238.5	540	1.9	2	6.21
Kresoxim-methyl	32	46.6	81.3 $\pm$ 4.9	80	1	1	0.84
Synthetic latex	30	45.4	72 $\pm$ 0	72	1	1	0.73
Mancozeb	45	65.7	602.1 $\pm$ 407.7	378	1.1	1	8.20
Mefenoxam	30	45.4	45.1 $\pm$ 0	45	1	1	0.46
Metirame-zinc	40	60.8	1171.9 $\pm$ 317	1198	1.9	2	29.86
Metrafenone	34	48.6	91.2 $\pm$ 3.3	90	1	1	0.99
Oryzalin	6	5.3	2240 $\pm$ 655.8	-	1	-	0.87
Oxyfluorfen	6	7.3	593.7 $\pm$ 283	-	1	-	0.28
Propyzamide	6	7.3	463.7 $\pm$ 221	-	1	-	0.22
Pyraclostrobin	13	23	93.8 $\pm$ 15	-	1	-	0.50
Pyrimethanil	5	3.2	1000 $\pm$ 0	-	1	-	0.72
Spiroxamine	8	10.6	300 $\pm$ 0	-	1	-	0.71

<sup>a</sup> Number of plots where the substances is applied at least one time.

<sup>b</sup> Percentage of the catchment surface where the substance is applied at least one time.

<sup>c</sup> Application dose for the applied plots.

<sup>d</sup> Application dose for the study plot.

<sup>e</sup> Application number for the applied plots.

<sup>f</sup> Application number for the study plot.

<sup>g</sup> Percentage of total synthetic pesticide mass applied in the catchment.

**Table VII-7. Number of applications and pesticides use in the catchment during the 2011 wine growing season. Values for the catchment are provided as mean of plots values  $\pm$  standard deviation.**

	<b>Number of applications per plot</b>	<b>Number of active substances used per plot</b>
Catchment plots	21 $\pm$ 5	14 $\pm$ 4
Study plot	24	19

**Table VII-8. Methods and standards for pedological analysis.**

<b>Variables</b>	<b>Methods in brief</b>	<b>Norms and/or procedure</b>
Soil water content	Drying sample in an oven set at 110°C	NF ISO 11465
pH	With KCl at 0.1 mol L <sup>-1</sup>	NF ISO 10390
Organic matter	Loss by ignition at 375°C during 16 h	See Ertlen <i>et al.</i> (2010)
Granulometry	Laser	See Ertlen <i>et al.</i> (2010)
Elementary composition	ICP-AES after lithium metaborate fusion	see Chabaux <i>et al.</i> (2013)

### References

- Chabaux F, Blaes E, Stille P, Roupert RD, Pelt E, Dosseto A, Ma L, Buss HL, Brantley SL (2013) Regolith formation rate from U-series nuclides: Implications from the study of a spheroidal weathering profile in the Rio Icacos watershed (Puerto Rico). *Geochim Cosmochim Acta* 100: 73-95
- Ertlen D, Schwartz D, Trautmann M, Webster R, Brunet D (2010) Discriminating between organic matter in soil from grass and forest by near-infrared spectroscopy. *Eur J Soil Sci* 61: 207-216

**Table VII-9. Hydrochemical comparison of runoff water outflowing from the plot and the catchment using the Wilcoxon Signed Rank test.**

<b>Parameters</b>	<b>p-value<sup>1</sup></b>
Total Organic Carbon	n.s
Dissolved Organic Carbon	n.s
Total Inorganic Carbon	n.s
Dissolved Inorganic Carbon	n.s
pH	**
Na	***
K	***
Mg	**
Ca	n.s
Al	***
Mn	n.s
Fe (II)	*
Fe (Total)	*
Cu	***
Cl <sup>-</sup>	*
SO <sub>4</sub> <sup>2-</sup>	n.s
Si	***
NO <sub>2</sub> <sup>-</sup>	n.s
NO <sub>3</sub> <sup>-</sup>	**
NH <sub>4</sub> <sup>+</sup>	***
PO <sub>4</sub> <sup>3-</sup>	**

<sup>1</sup> n.s. = not significant ( $p \geq 0.05$ ); \*  $p \leq 0.05$ ; \*\*  $p \leq 0.01$ ; \*\*\*  $p \leq 0.001$

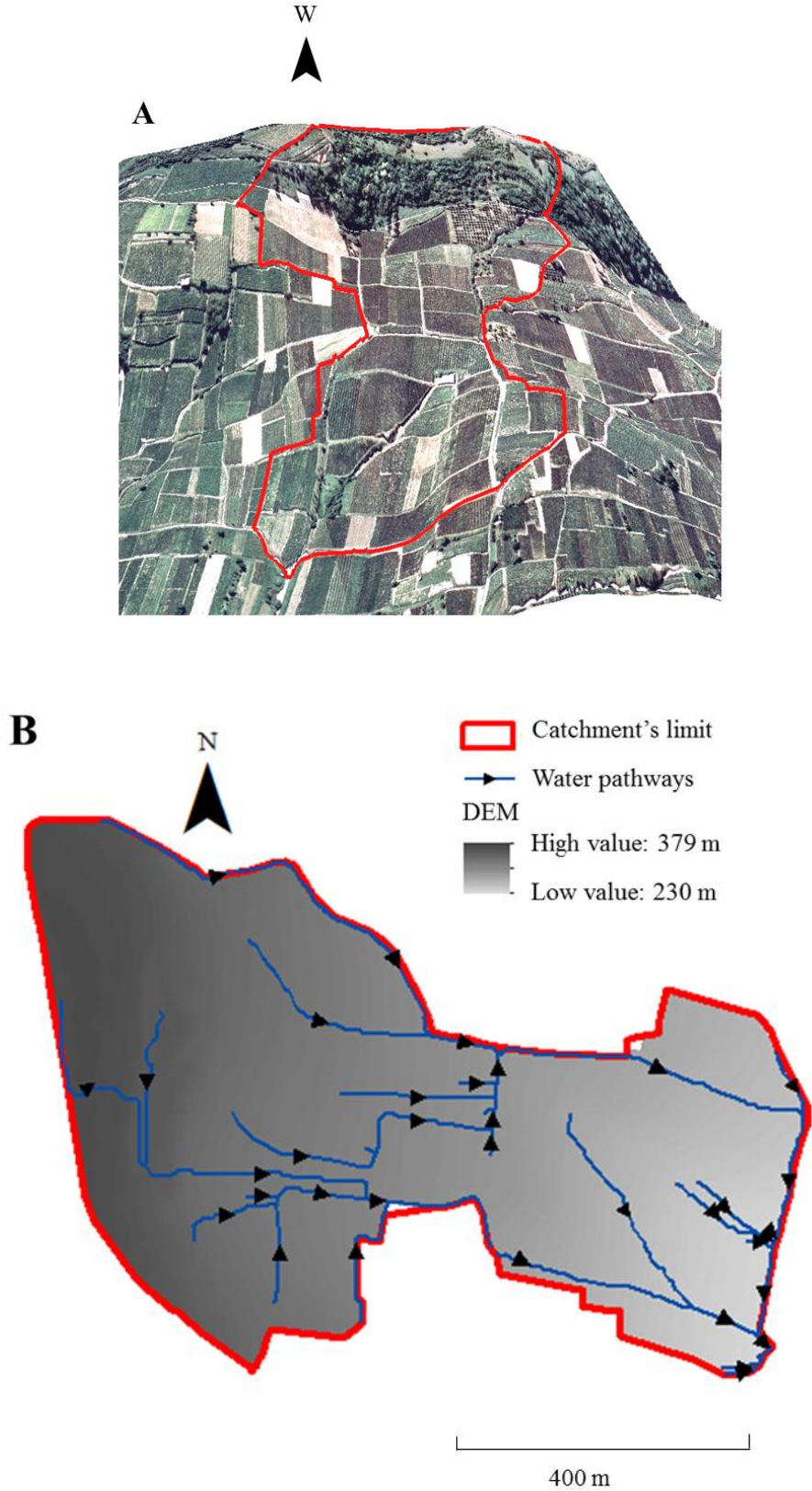


Figure VII-1. 3D orthophotography (A) and topography and water pathways (B) which drained at least 0.5 ha of the vineyard catchment.

## Appendices for Chapter IV

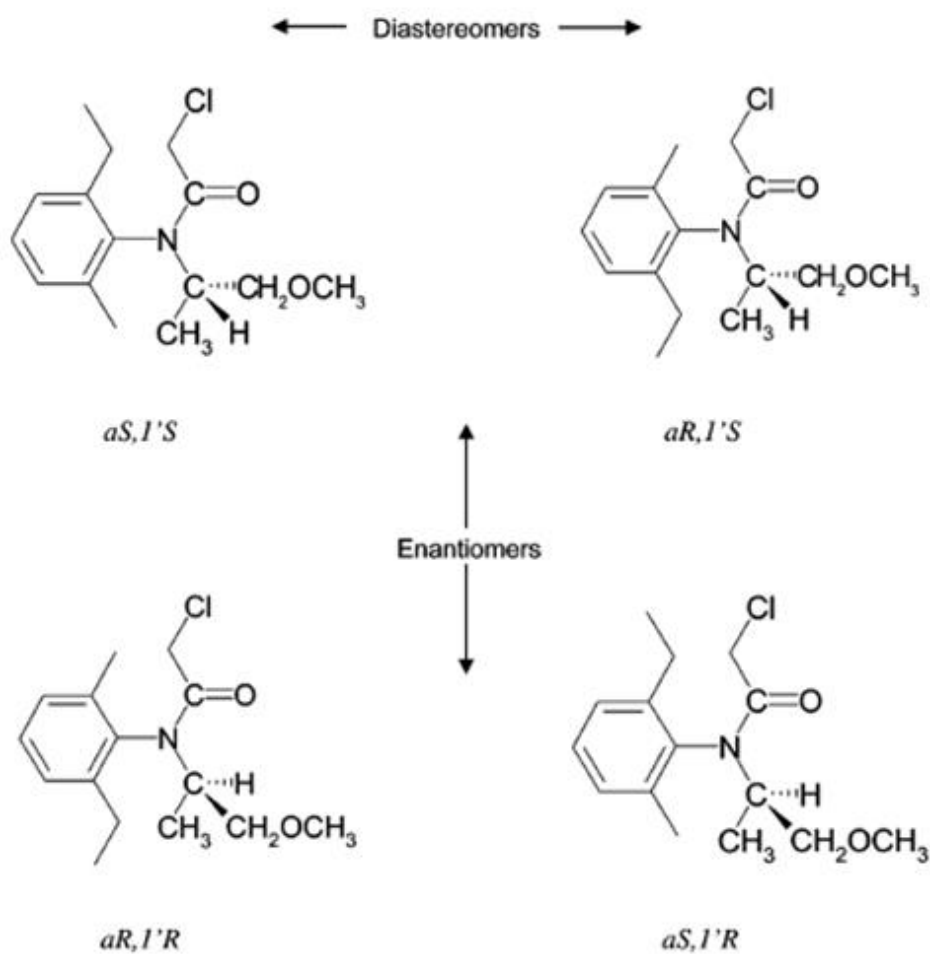


Figure VII-2. Four Metolachlor stereoisomers (2 diastereomers and 2 enantiomers) (Kabler and Chen, 2006)

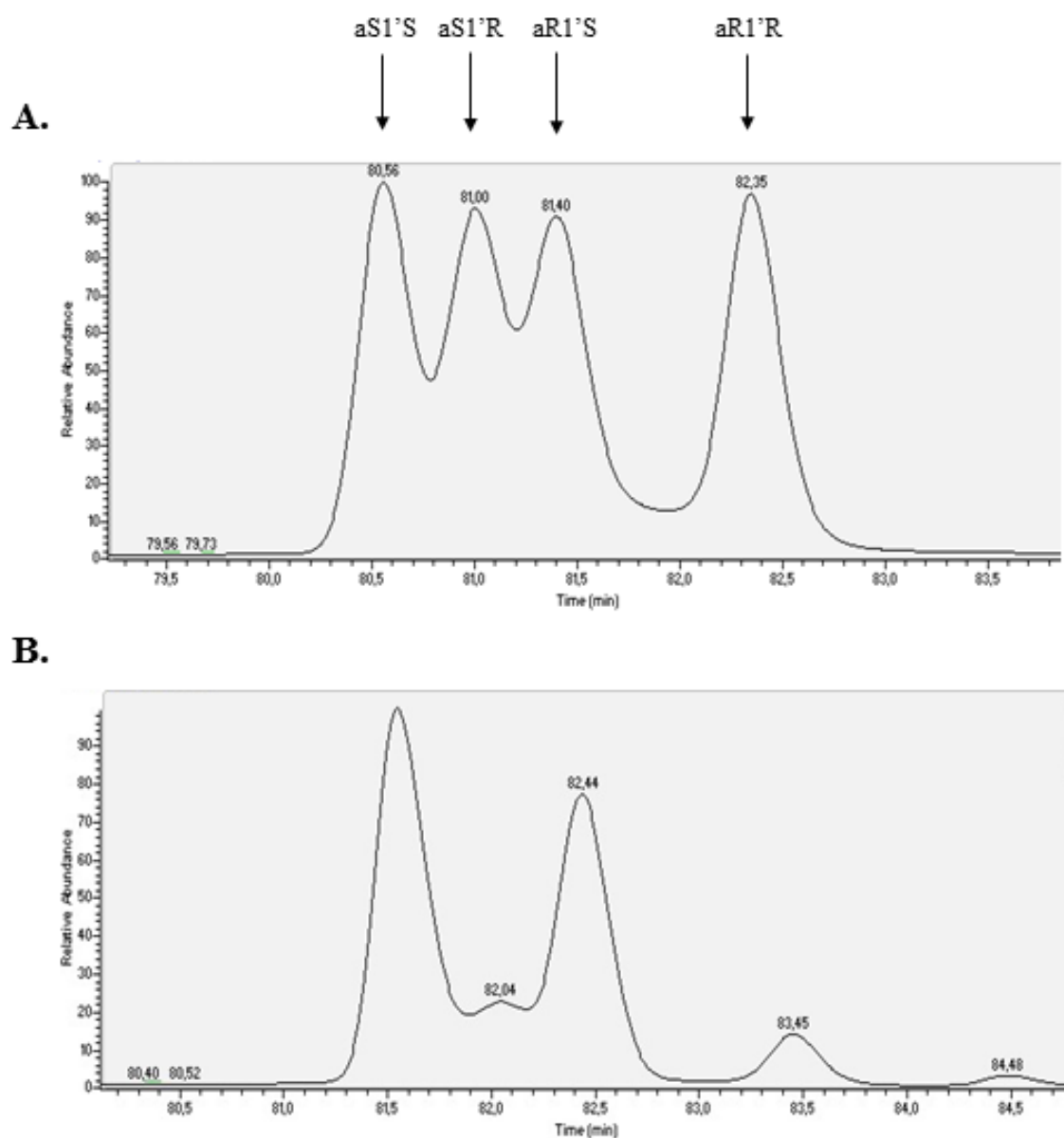


Figure VII-3. Examples of GC-MS/MS chromatograms showing the enantiomeric separation for racemic metolachlor (A) and S-metolachlor (B). The stereoisomer elution was aS1'S; aS1'R; aR1'S; aR1'R.

Table VII-10. Methods and standards for soil hydrodynamic properties analysis.

Variables	Methods in brief	Norms and/or procedure
Soil water content	Drying sample in an oven set at 110°C	NF ISO 11465
pH	KCl at 0.1 mol/L	NF ISO 10390
CaCO <sub>3</sub>	CO <sub>2</sub> gas with hydrochloric acid	NF ISO 10693
CEC	Cobalt hexamine method	NF X 31-130
Exchangeable ions	Ammonium acetate method	AFNOR NF X 31-10
Phosphorus	Joret Herbert method	AFNOR NF X 31-161
Organic matter	Mass loss by ignition at 375°C during 16 h	See Ertlen <i>et al.</i> (2010)
Organic matter	Walkley and Black method	See Ertlen <i>et al.</i> (2010)
Granulometry	Laser granulometer	See Ertlen <i>et al.</i> (2010)
Elementary composition	ICP-AES* after lithium tetraborate fusion	See Chabaux <i>et al.</i> (2013)
Permeability	Head constant permeameter	See Amoozegar <i>et al.</i> (1989)
Water retention curve	Sand/kaolin box	See Madsen <i>et al.</i> (1986)

\* Inductively coupled plasma atomic emission spectroscopy

Table VII-11. Analytical data of the GC-MS/MS quantification of metolachlor and acetochlor and the LC-MS/MS quantification of their degradation products metolachlor ESA (MESA), metolachlor OXA (MOXA), acetochlor ESA (AcESA) and acetochlor OXA (AcOXA).

			Quantification	Identification	Retention time	Recovery	Uncertainties
					[min]	[%]	[%]
			daughter ion 1 [m/z]	daughter ion 2 [m/z]			
GC-MS/MS	Chloroacetanilide herbicides	Acetochlor	146	131	15.3	43	8
		Metolachlor	162	133	16.78	96	8
	Internal standard	Alachlor- <i>d</i> <sub>13</sub>	172		15.3	-	-
		Metolachlor- <i>d</i> <sub>6</sub>	134		16.71	-	-
			Transition SRM1	Transition SRM2			
LC-MS/MS	Degradation products	AcOXA	146	144	10	0.6	59.0
		AcESA	144	162	10.5	10.69	28.0
		MOXA	206	172	11.36	3.28	37.6
		MESA	121	192	9.9	0.58	27.5
	Internal standard	Alachlor- <i>d</i> <sub>13</sub>	251	175	18.3	-	-

Table VII-12. Hydrochemical comparison of water outflowing from the drain, the plot and the catchment using the Wilcoxon Signed Rank test.

	Parameter	Unit	p-value plot/drain	p-value catchement/drain	p-value plot/catchment
Erosion	Total suspended solids (> 0.7µm)	[mg L-1]	n.s	**	***
	Volatile organic carbon (> 0.7µm)	[%]	*	n.s	n.s
Hydrochemistry	Nitrite (NO <sub>2</sub> -)	[mg L-1]	n.s	**	**
	Nitrate (NO <sub>3</sub> -)	[mg L-1]	n.s	n.s	n.s
	Ammonium (NH <sub>4</sub> <sup>+</sup> )	[mg L-1]	n.s	***	**
	Ion phosphate (PO <sub>4</sub> <sup>3-</sup> )	[mg P L-1]	n.s	*	n.s
	Total inorganic carbon (TIC)	[mg C L-1]	**	*	*
	Total organic carbon (TOC)	[mg C L-1]	*	***	***
	Dissolved inorganic carbon (DIC)	[mg C L-1]	*	**	***
	Dissolved organic carbon (DOC)	[mg C L-1]	n.s	***	***
	Total phosphorus (P)	[mg L-1]	n.s	**	***
S-metolachlor	Water concentration (< 0.7 µm)	[µg L-1]	***	***	n.s
	Enantiomeric excess (< 0.7 µm)	[ - ]	**	n.s	n.s
	SS concentration (> 0.7 µm)	[mg kg-1]	n.s	*	n.s
	Enantiomeric excess (> 0.7 µm)	[ - ]	n.s	n.s	n.s
Acetochlor	Water concentration (< 0.7 µm)	[µg L-1]	n.s	n.s	n.s
	SS concentration (> 0.7 µm)	[µg kg-1]			

<sup>1</sup> n.s. = not significant ( $p \geq 0.05$ ); \*  $p \leq 0.05$ ; \*\*  $p \leq 0.01$ ; \*\*\*  $p \leq 0.001$

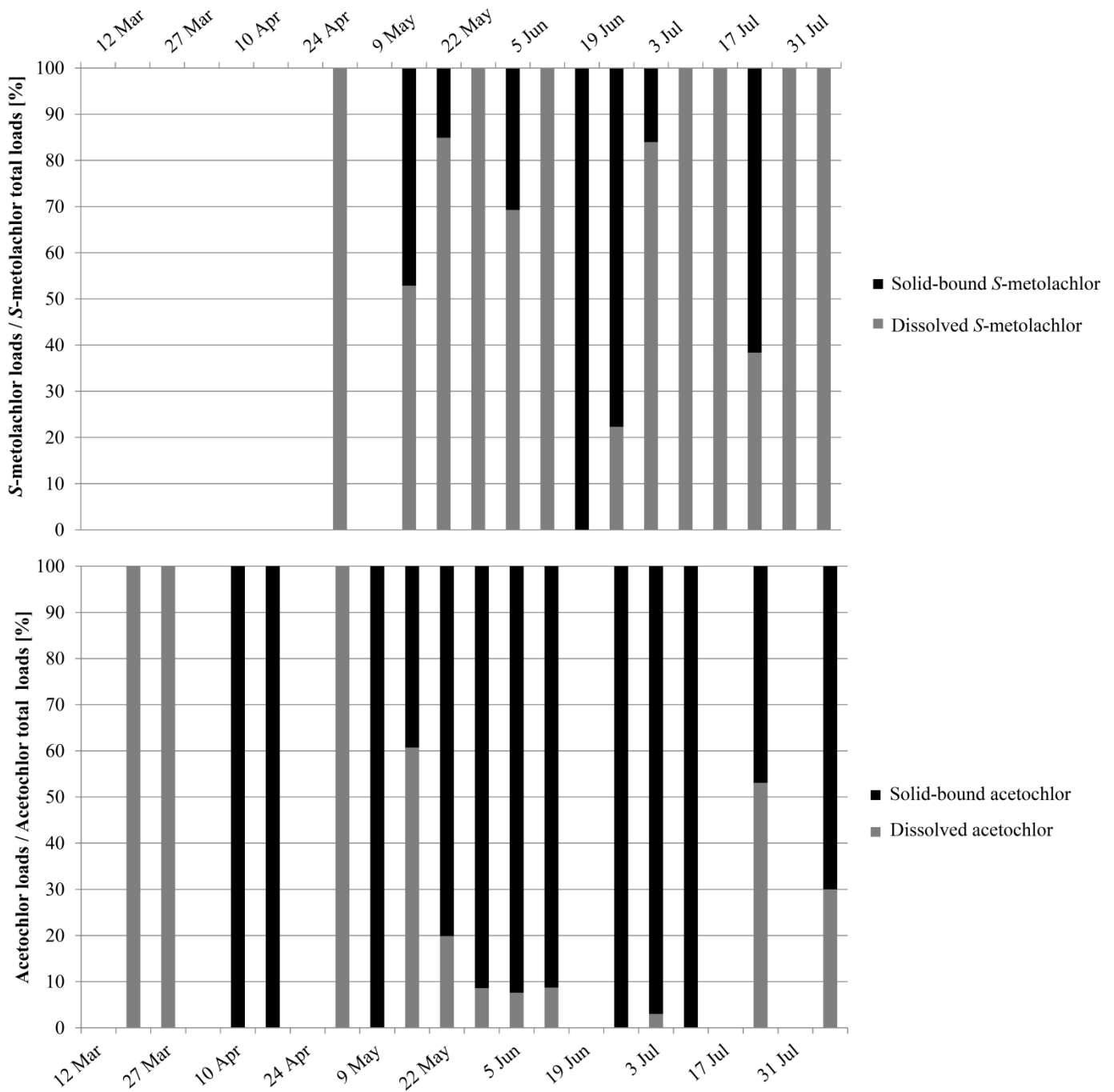


Figure VII-4. Relative loads of solid-bound (> 0.7  $\mu\text{m}$ ) and dissolved (< 0.7  $\mu\text{m}$ ) pesticide for S-metolachlor and acetochlor at the catchment outlet from March 12 and August 14.

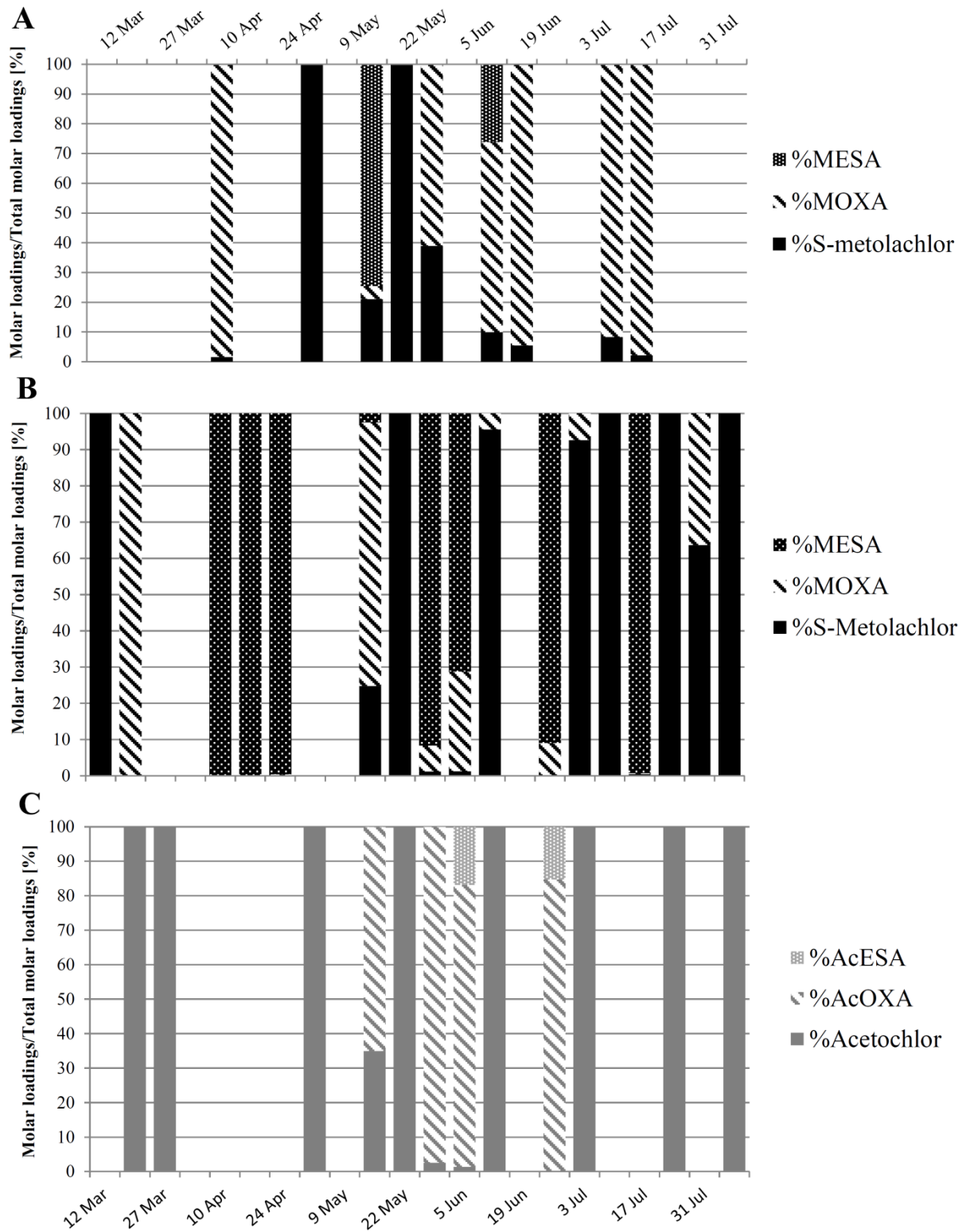


Figure VII-5. Temporal changes of the percentage of total loads of chloroacetanilides and their metabolites expressed in molar load equivalent for *S*-metolachlor at the plot (A) and catchment outlet (B) and for acetochlor at the catchment outlet (C) from March 12 to July 10 2012.

### References

- Amoozegar, A., 1989. A Compact Constant-Head Permeameter for Measuring Saturated Hydraulic Conductivity of the Vadose Zone. *Soil Science Society of America Journal*. 53, 1356-1361.
- Chabaux, F., Blaes, E., Stille, P., Roupert, R.D., Pelt, E., Dosseto, A., Ma, L., Buss, H.L., Brantley, S.L., 2013. Regolith formation rate from U-series nuclides: Implications from the study of a spheroidal weathering profile in the Rio Icacos watershed (Puerto Rico). *Geochimica Et Cosmochimica Acta*. 100, 73-95.
- Ertlen, D., Schwartz, D., Trautmann, M., Webster, R., Brunet, D., 2010. Discriminating between organic matter in soil from grass and forest by near-infrared spectroscopy. *European Journal of Soil Science*. 61, 207-216.
- Kabler, A.K., Chen, S.M., 2006. Determination of the 1 ' S and 1 ' R diastereomers of metolachlor and S-metolachlor in water by chiral liquid chromatography - Mass spectrometry/mass spectrometry (LC/MS/MS). *Journal of Agricultural and Food Chemistry*. 54, 6153-6158.
- Madsen, H.B., Jensen, C.R., Boysen, T., 1986. A Comparison of the Thermocouple Psychrometer and the Pressure Plate Methods for Determination of Soil-Water Characteristic Curves. *Journal of Soil Science*. 37, 357-362.

## Appendices for Chapter V

### Detailed calculations of IDR

Dynamic soil surface and vegetation characteristics, including vegetation and crop residue cover, random roughness and saturated hydraulic conductivity were determined for each landuse in the catchment using a continuous field scale model: indicator of runoff dynamics ( $I_{DR}$ ) developed by the ARAA-INRA (Van Dijk et al., in prep.).  $I_{DR}$  predicts these parameters as a function of the cropping system (crop rotation, tillage practices, crop residue management, etc), climate and soil type.

$I_{DR}$  aims to evaluate the runoff potential during a crop rotation, while accounting for local conditions. The main purpose of  $I_{DR}$  is to predict high risk periods for runoff and to find local solutions for the farmer, e.g. by introducing cover crops, modifying tillage practices and/or crop rotation. Only methods for the parameters that are used in this study are detailed here: i.e. for saturated hydraulic conductivity ( $K_{sat}$ ), initial water content ( $\theta_i$ ), vegetation cover ( $per$ ) and random roughness ( $RR$ ). Additional information is provided in Van Dijk et al. (in prep.).

### Saturated hydraulic conductivity ( $K_{sat}$ )

$K_{sat}$  is determined in two steps: first a matrix saturated conductivity hydraulic ( $K_{s\_matr}$  [ $\text{mm h}^{-1}$ ]) is estimated based on the pedotransfer function of (Cosby et al., 1984) (Eq. 1) which depends only of the soil texture. The second step consists in taking into account the soil tillage and the progressive soil clogging under the influence of the rainfall ( $K_{s,t}$  [ $\text{mm h}^{-1}$ ]) (Eq. 2).

$$K_{s\_matr} = 25.4 \cdot 10^{-0.6+0.012 \times S - 0.0064 \times Si} \quad (\text{Eq. 1})$$

Where  $S$  is the sand content [%] and  $Si$  the silt content [%]. Then the dynamics of the permeability is estimated based on the invariable consolidated bulk density of the matrix ( $DA_{matr}$ ) and time-dependent bulk density ( $DA_t$ ) accounting for tillage-induced macropores and progressive clogging due to rainfall:

$$K_{s,t} = K_{s\_matr} + 100(DA_{matr} - DA_t) \quad (\text{Eq. 2})$$

Where the consolidated bulk density ( $DA_{matr}$  [ $\text{g cm}^{-3}$ ]) is estimated using the pedotransfer function of (Riley, 1996) (Eq. 3):

$$DA_{matr} = 1.522 - 0.06 \times OM + 0.0064 \times CC + 0.0026 \times D - 0.0015 \times Si + 0.0022 \times Cl \quad (\text{Eq. 3})$$

Where  $OM$  is the organic matter [%],  $CC$  the gravel content [%],  $D$  the considered soil depth [cm] and  $Cl$  the clay content [%]. The two effects impacting the time-dependent bulk density will be now considered: the rainfall impact and the soil tillage. For days with tillage,  $DA_t$  is estimated as follows (Eq. 4):

$$DA_t = DA_{t-1} - F_p DA_{t-1} + \frac{2}{1 + f_{soil}} F_p \frac{2}{3} DA_{matr} \quad (\text{Eq. 4})$$

Where  $DA_{t-1}$  is the bulk density of the previous day [ $\text{g cm}^{-3}$ ],  $F_p$  the soil fraction which is impacted by the tillage operation [ ],  $f_{soil}$  a soil roughness factor ( $> 1$  for clay soils,  $1$  for silty soils,  $< 1$  for sandy soils) (USDA, 2003). If the entire soil surface is impacted ( $F_p=1$ ), we obtain equation 5:

$$DA_t = \frac{2}{1 + f_{sol}} \frac{2}{3} DA_{matr} \quad (\text{Eq. 5})$$

For days without tillage, the bulk density for a bare soil without residue cover is estimated by the following equation:

$$DA_{bare\ soil,t} = DA_{bare\ soil,t-1} + (DA_{matr} - DA_{bare\ soil,t-1}) \left(1 - e^{-\frac{P_j}{S_{stab}}}\right) \quad (\text{Eq. 6})$$

Where  $P_j$  is the daily rainfall [mm] and  $S_{stab}$  is a soil structural stability parameter.  $S_{stab}$  is estimated based on the French slaking index ( $I_B$ ) (Rémy and Marin-Lafèche, 1974) (Eq. 7)

$$S_{stab} = 1000/I_B \quad (\text{Eq. 7})$$

For arable land covered by plant residues, the rainfall impact is reduced by 67%:

$$DA_{resi,t} = DA_{resi,t-1} + (DA_{matr} - DA_{resi,t-1}) \left(1 - \frac{2 + e^{-\frac{P_j}{S_{stab}}}}{3}\right)$$

For arable land covered only by crops, it is assumed to be an intermediate case between bare soil and soil covered by crop residue (Eq. 9).

$$DA_{cult,t} = \frac{DA_{sol\ nu,t} + DA_{resi,t}}{2} \quad (\text{Eq. 9})$$

**Initial water content ( $\theta_i$ )**

The approach for estimating humidity in the topsoil layer is based on the soil moisture depletion model from (Kohler and Linsley, 1951).  $API$ , the humidity index is calculated as follow:

$$API_t = P_t + API_{t-1}k_t \quad (\text{Eq. 10})$$

With  $API_t$  the humidity index for day t [mm],  $P_t$  the effective rainfall for day t,  $k_t$  the depletion factor which depends on time, soil depth for which water content is estimated and meteorological conditions.

The depletion factor is estimated with an inverse temperature function:

$$k_t = k_{max} - \frac{T_t - T_0}{T_{mm} - T_0} (k_{max} - k_{min}) \quad \text{for } T_t \geq T_0 \quad (\text{Eq. 11})$$

$$k_t = k_{max} \quad \text{for } T_t < T_0$$

With  $k_t$ ,  $k_{max}$  and  $k_{min}$  the depletion factor for day t, maximal and minimal respectively [-],  $T_t$  the average temperature for day t [°C],  $T_0$  the temperature for which  $k_t = k_{max}$  [°C], here 0°C and  $T_{mm}$  the maximal average temperature on 10 days [°C], here 25°C. For this study,  $k_{min}$  and  $k_{max}$  were fixed to 0.91 and 0.994 respectively (Blanchard et al., 1981). Water content in the 15 cm soil surface was estimated with (Blanchard et al., 1981):

$$sm_t = 1.992 + 0.992 \left( \frac{API_t}{10} \right)^{0.61} \quad (\text{Eq. 12})$$

With  $sm_t$  the water content [cm] in the 0-15 cm soil surface depth. This method gives only an indicator of the humidity in the soil surface.

**Vegetation cover ( $per$ )**

The vegetation cover is calculated according to a sigmoidal curve based on the growth equation of (Hunt, 1982). This equation has been adapted for calculating vegetation cover with mean daily temperature ( $T_t$ ) and a base temperature ( $T_{base}$ ) for the related crop (Eq. 13):

$$C_v(t) = \frac{C_{max}}{1 + \frac{C_{max} - C_{ini}}{C_{ini}} e^{-C_{max} f \frac{\sum DJ_t}{\sum DJ_{C_{max}}}}} \quad (\text{Eq. 13})$$

$$DJ_t = T_t - T_{base} \quad (T_t \geq T_{base})$$

$$DJ_t = 0 \quad (T_t < T_{base})$$

Where  $C_v(t)$  is the crop cover for day  $t$  [%],  $C_{max}$  the maximal crop cover [%],  $C_{ini}$  the initial cover ( $0 < C_{ini} < 100$ ),  $f$  a form parameter ( $\approx 0.07$ ) and  $DJ_t$  = daily temperature [ $^{\circ}\text{C}$ ].

### Random roughness

Random roughness (RR) is calculated based on the equations of Potter (1990). Initial random roughness ( $RR_i$  [cm]), i.e., just after tillage, is calculated according to the following equation:

$$RR_i = f_{soil} RR_{i-tool} \frac{100 + 0.5C_{resi}}{100} \quad (\text{Eq. 14})$$

Where  $RR_{i-tool}$  is the random roughness before the tillage operation in question. Then the dynamics of RR over time for a bare soil is calculated as follows:

$$RR_{bare\ soil,t} = RR_i e^{-\frac{P_{cum}}{S_{stab}}} \quad (\text{Eq. 15})$$

Where  $P_{cum}$  is the cumulated rainfall since the last agricultural practice [mm]. We assumed here that RR for the surface covered by plant residues is not impacted by the rainfall.

$$RR_{resi} = RR_i \quad (\text{Eq. 16})$$

A final random roughness ( $RR_t$ ) can be calculated by a weighted average between  $RR_{res}$  and  $RR_{bare\ soil,t}$  according to the cover fraction of plant residues ( $C_{resi}$ ):

$$RR_t = \frac{(100 - C_{resi})RR_{sol\ nu,t} + C_{resi}RR_{resi}}{100} \quad (\text{Eq. 16})$$

Finally, we assumed that RR remains always larger than 0.5 cm.

### References

- Blanchard, B.J., McFarland, M.J., Schmutge, T.J., Rhoades, E., 1981. Estimation of soil moisture with API algorithms and microwave emission. JAWRA Journal of the American Water Resources Association. 17, 767-774.
- Cosby, B.J., Hornberger, G.M., Clapp, R.B., Ginn, T.R., 1984. A Statistical Exploration of the Relationships of Soil-Moisture Characteristics to the Physical-Properties of Soils. Water Resources Research. 20, 682-690.
- Hunt, R., 1982. Plant growth curves. Edward Arnold, London, 248.
- Kohler, M.A., Linsley, R.K., 1951. Predicting the runoff from storm rainfall. US weather Bureau Res.
- Potter, K.N., 1990. Soil Properties Effect on Random Roughness Decay by Rainfall. Transactions of the Asae. 33, 1889-1892.

- Riley, H., 1996. Estimation of physical properties of cultivated soils in southeast Norway from readily available soil information. Norwegian Journal of Agricultural Sciences. supplement n°25, 1-51.
- Rémy, J.C., Marin-Laflèche, A. 1974. L'analyse de terre : réalisation d'un programme d'interprétation automatique. Annales Agronomiques, 25(4), 607-632.
- USDA, 2003. Revisited Universal Soil Loss Equation. Version 2. RUSLE2.
- Van Dijk, P., Bockstaller, C., Villerd, J. et Koller, R. (in prep). An indicator for overland flow potential of cropping systems: accounting for farmers' control on key variables

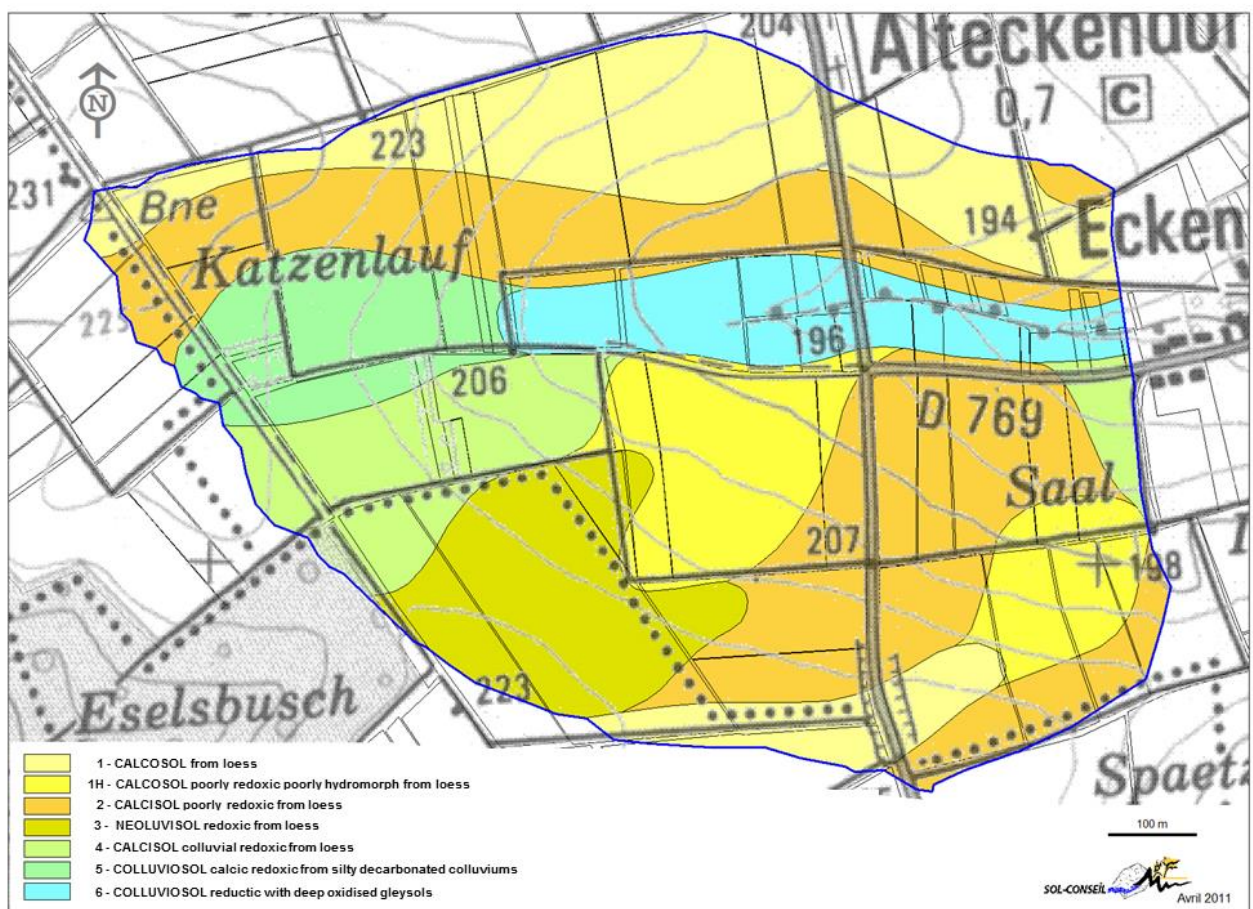


Figure VII- 6. Soil map of the catchment



**A**



**B**



**C**



**C**



**D**



Figure VII- 7. Example of deposition pattern with topography change (A), in headlands (B), behind a vegetal barrier (C) and example of rills erosion (D) and diffusive erosion (E).

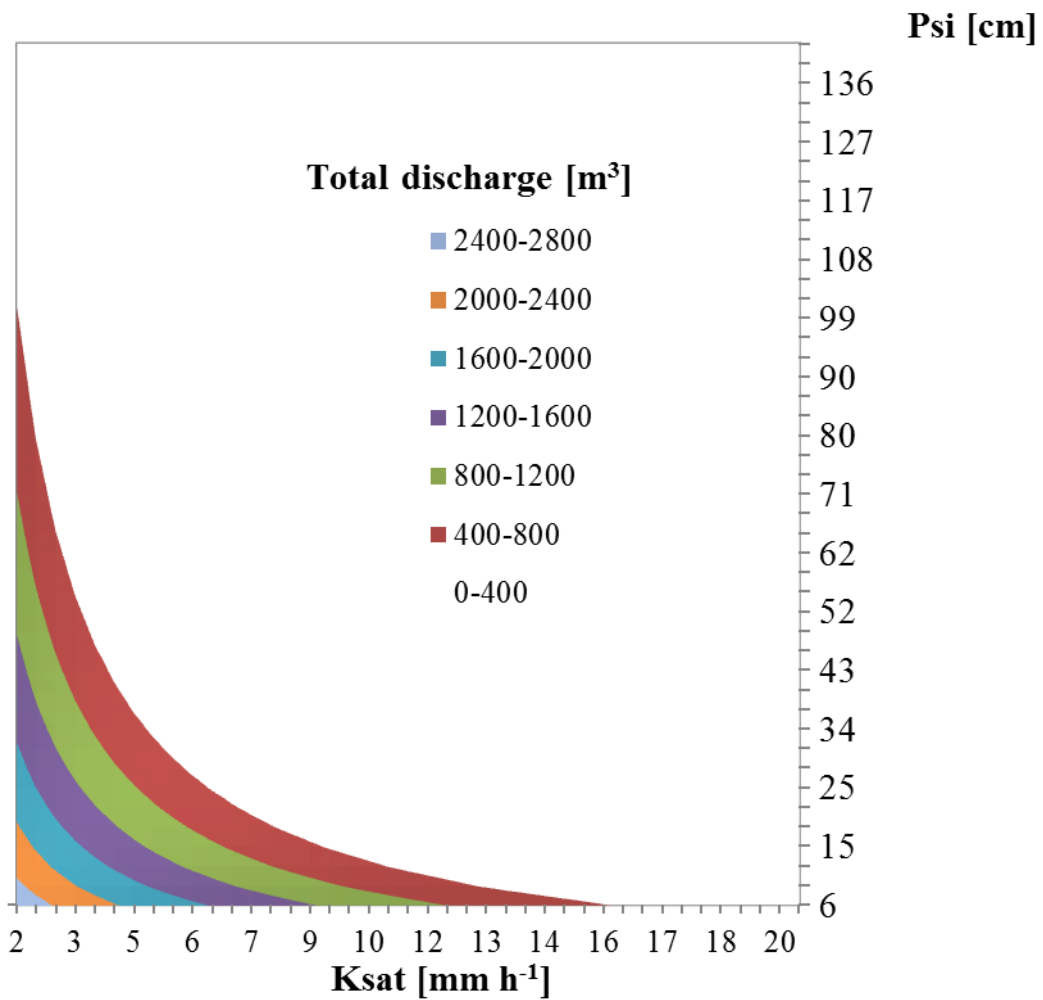


Figure VII-8. Total discharge as a function of  $K_{sat}$  and  $\Psi$  for the event June 7 2012.

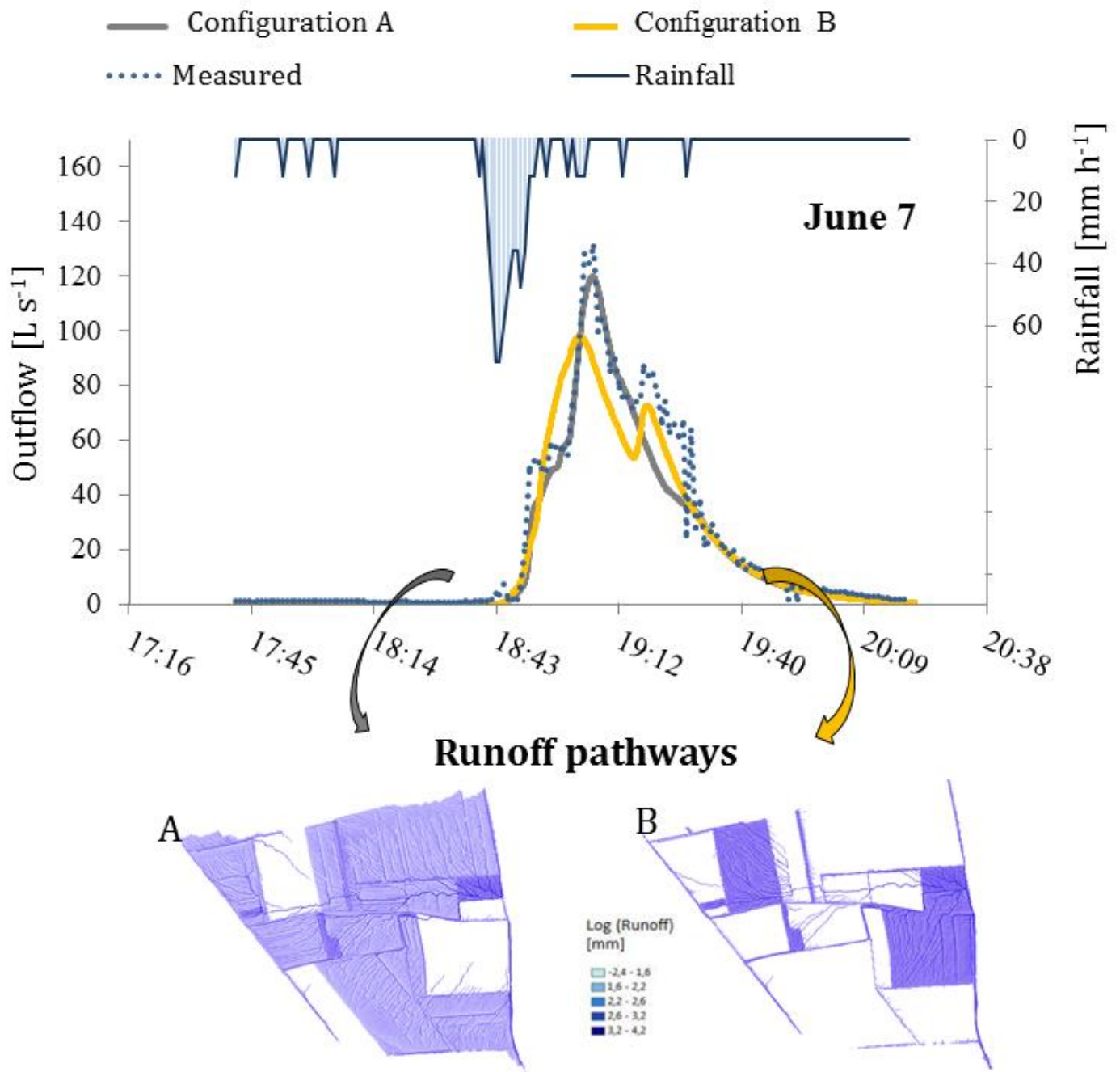
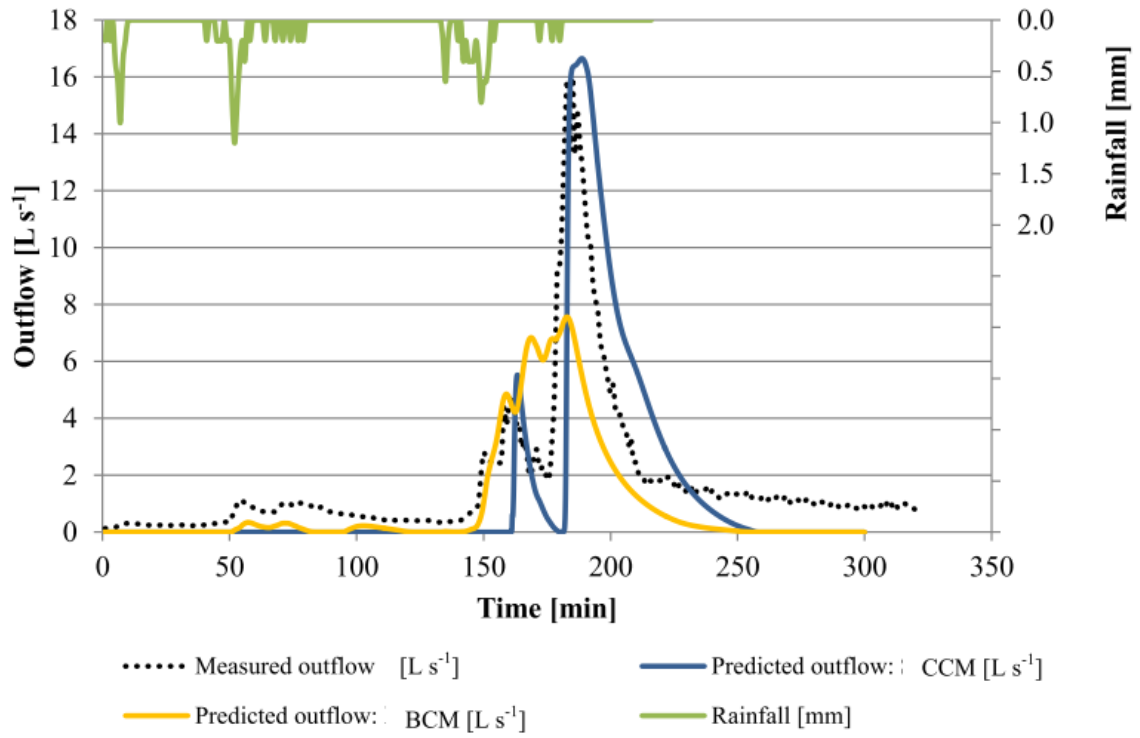
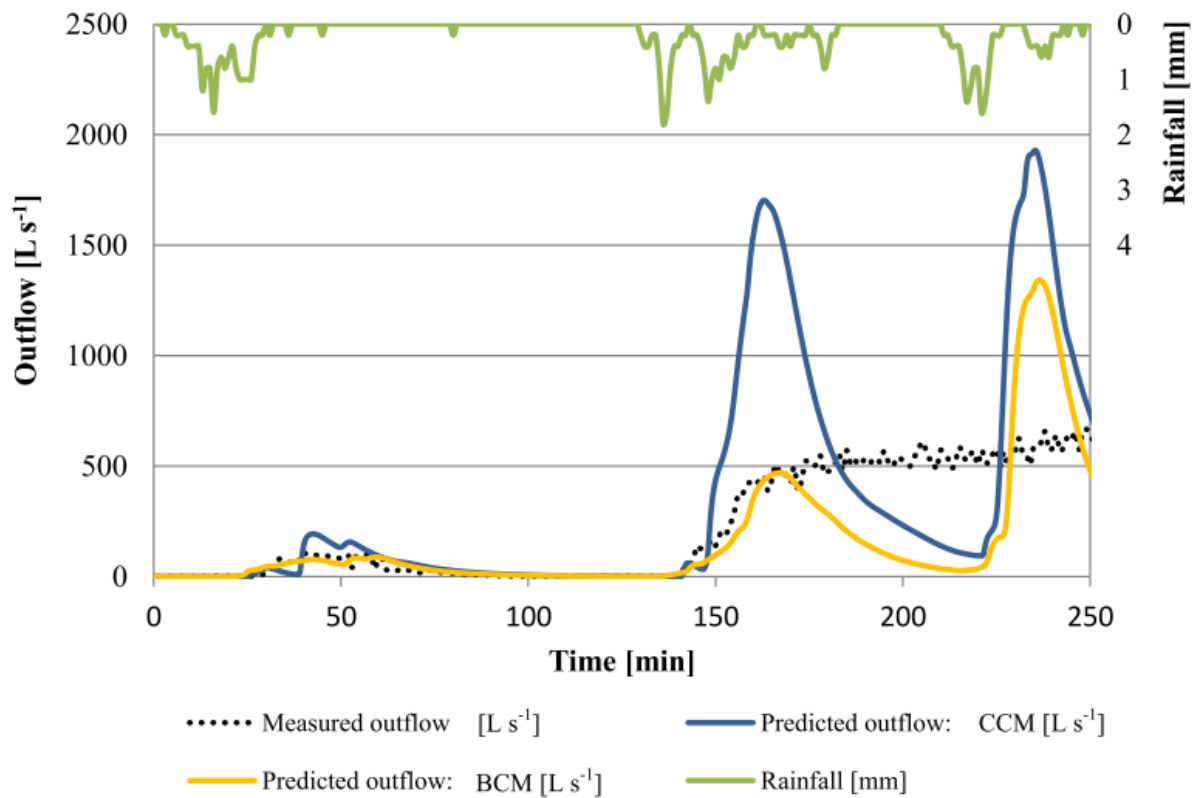


Figure VII-9. Accumulated runoff pathways and predicted hydrograph for two different parameters set for the event June 7 2012. For configuration A,  $K_{sat\ corn}$  and  $K_{sat\ wheat}$  were set to 18 and 60  $\text{mm h}^{-1}$  respectively and for configuration B, 55 and 7  $\text{mm h}^{-1}$ .

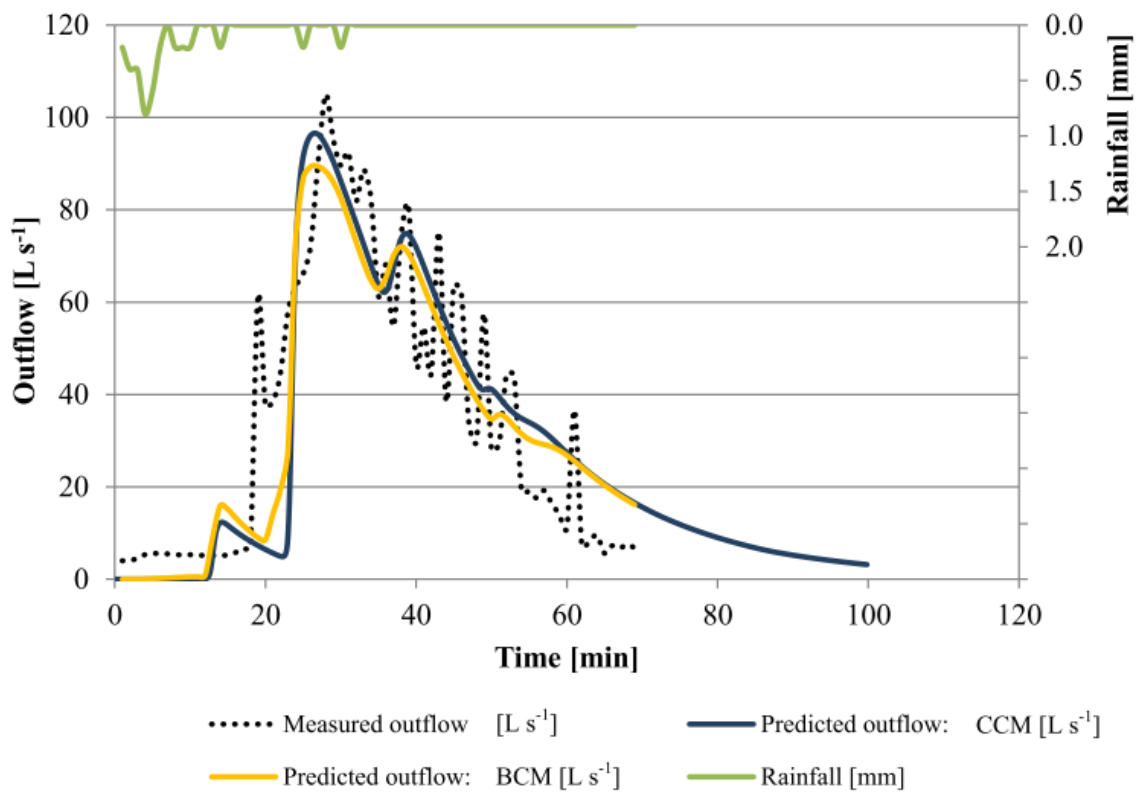
May 2.



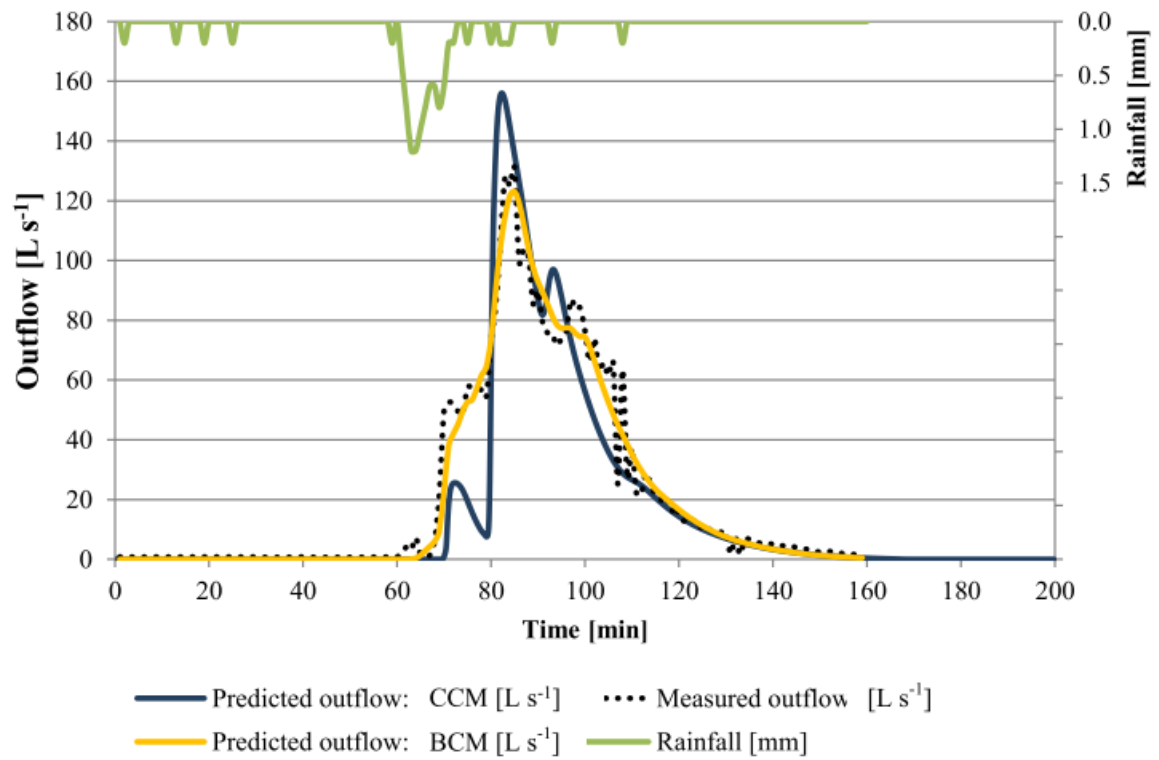
May 21.



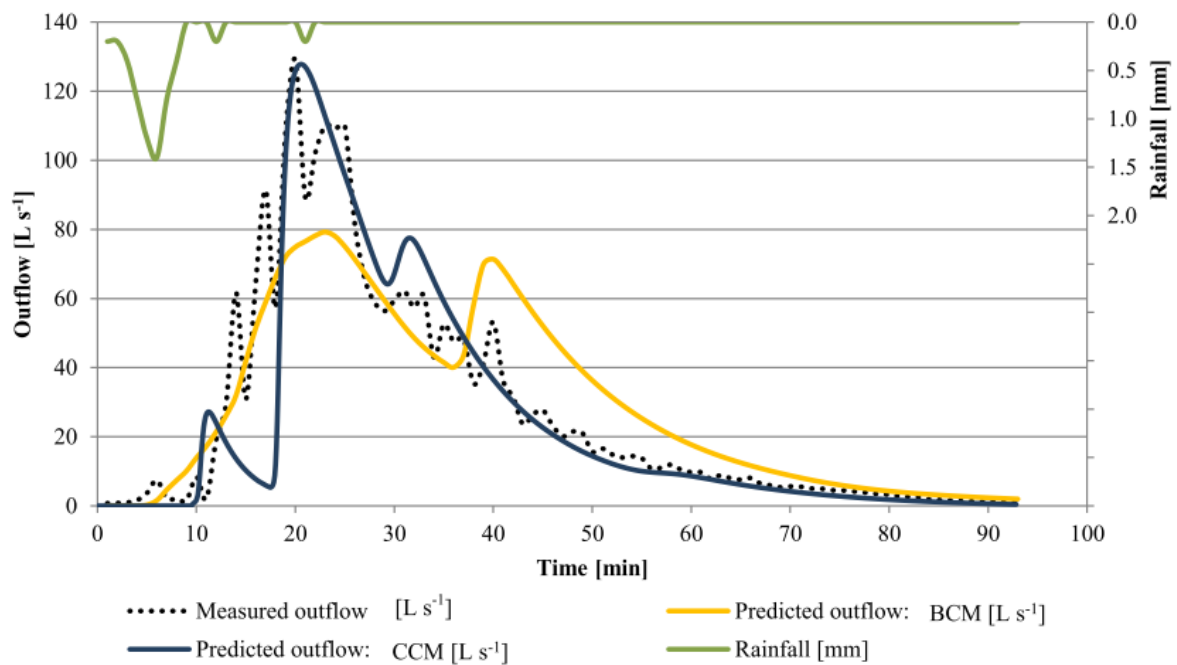
May 23



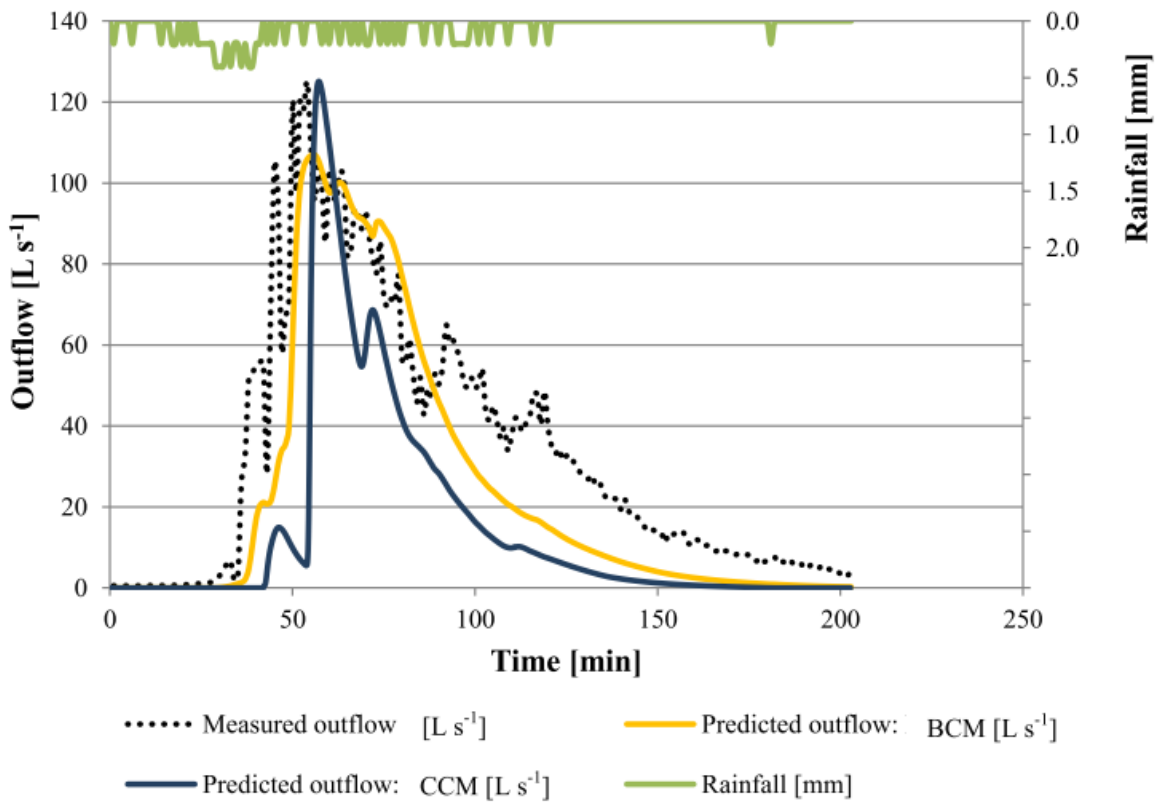
## June 7



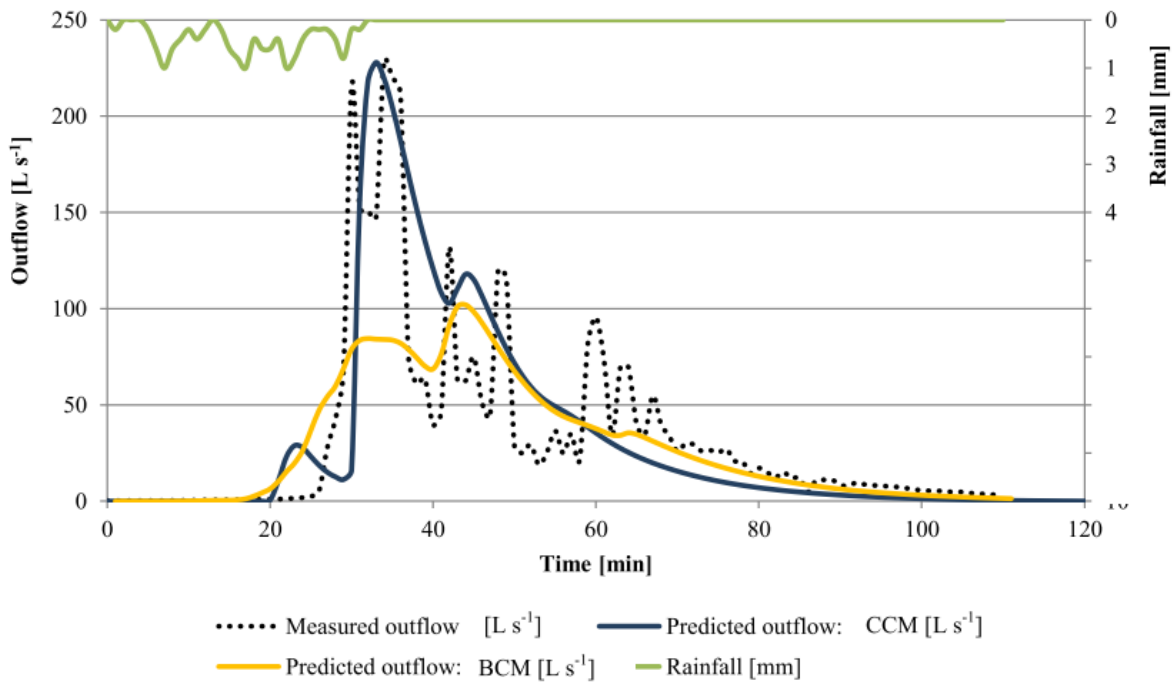
## June 11



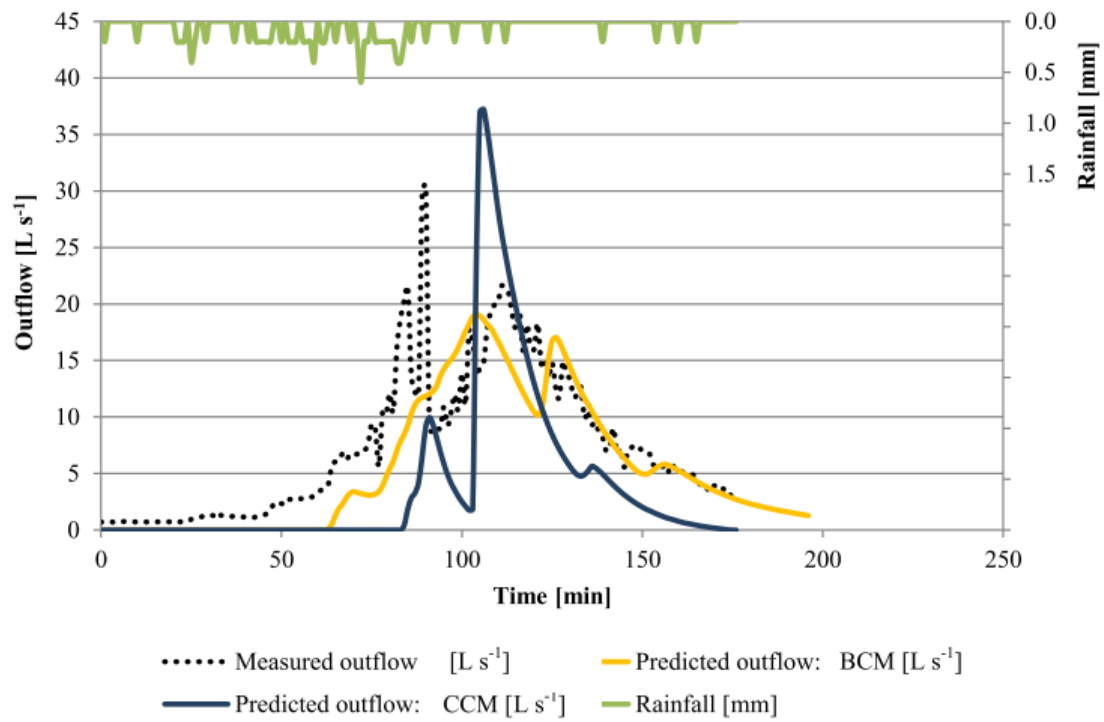
June 12



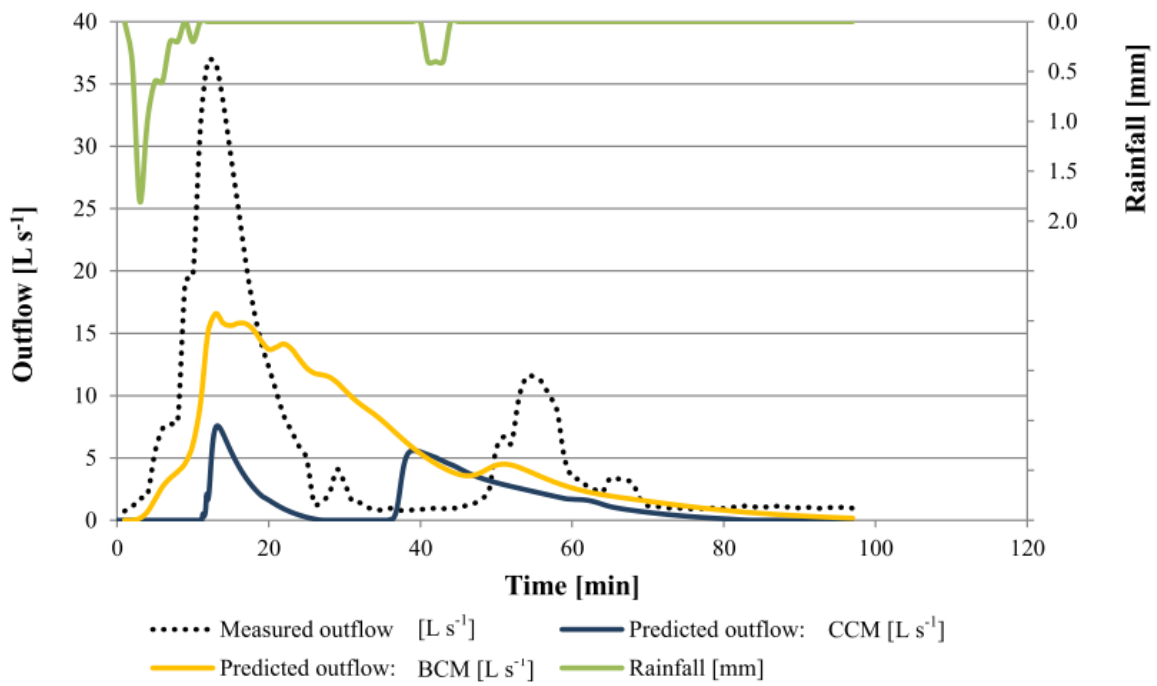
July 7



July 8



July 10



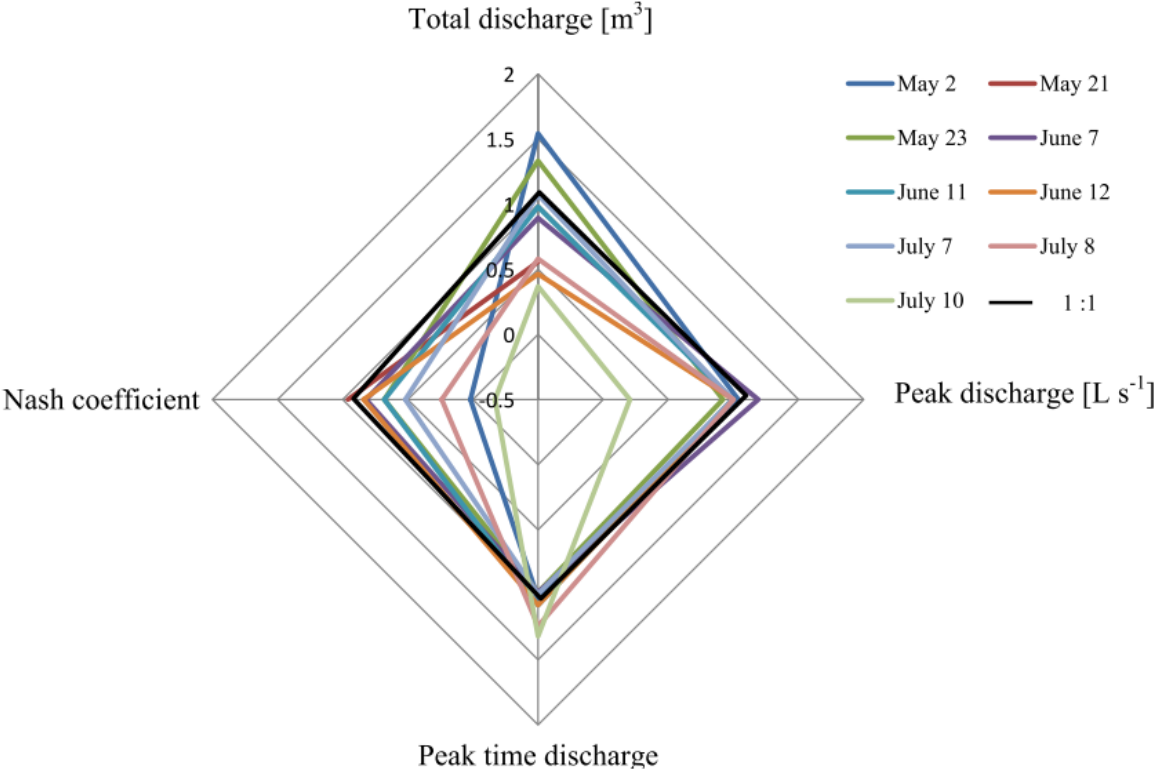


Figure VII-10. Rainfall, discharge and drain water height together with predicted discharge according to the both calibration methods for the nine runoff events within the headwater catchment.

May 21

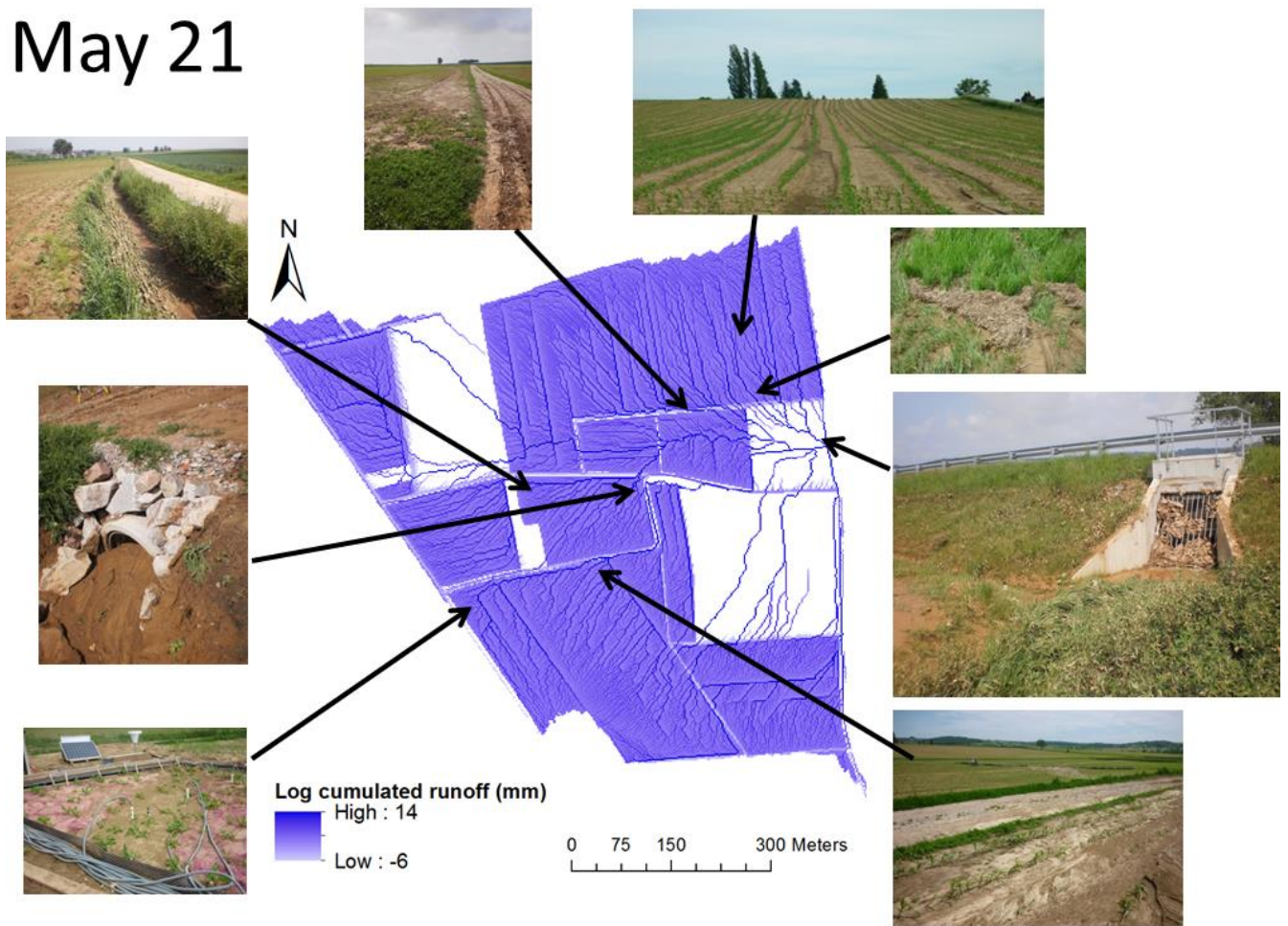


Figure VII-11. Comparison of the predicted runoff pathways for May 21 with the pictures of that day within the headwater catchment.

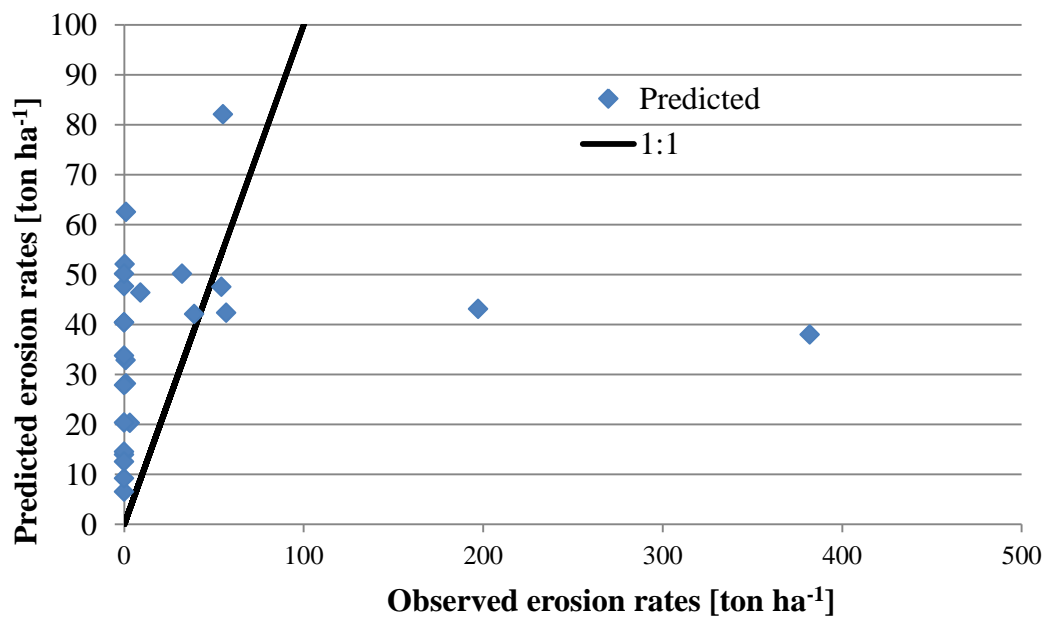


Figure VII-12. Predicted and observed erosion rates for each plot within the agricultural catchment.

### References

- Amoozegar, A., 1989. A Compact Constant-Head Permeameter for Measuring Saturated Hydraulic Conductivity of the Vadose Zone. *Soil Science Society of America Journal*. 53, 1356-1361.
- Blanchard, B.J., McFarland, M.J., Schmugge, T.J., Rhoades, E., 1981. Estimation of soil moisture with API algorithms and microwave emission. *JAWRA Journal of the American Water Resources Association*. 17, 767-774.
- Chabaux, F., Blaes, E., Stille, P., Roupert, R.D., Pelt, E., Dosseto, A., Ma, L., Buss, H.L., Brantley, S.L., 2013. Regolith formation rate from U-series nuclides: Implications from the study of a spheroidal weathering profile in the Rio Icacos watershed (Puerto Rico). *Geochimica Et Cosmochimica Acta*. 100, 73-95.
- Cosby, B.J., Hornberger, G.M., Clapp, R.B., Ginn, T.R., 1984. A Statistical Exploration of the Relationships of Soil-Moisture Characteristics to the Physical-Properties of Soils. *Water Resources Research*. 20, 682-690.
- Ertlen, D., Schwartz, D., Trautmann, M., Webster, R., Brunet, D., 2010. Discriminating between organic matter in soil from grass and forest by near-infrared spectroscopy. *European Journal of Soil Science*. 61, 207-216.
- Hunt, R., 1982. *Plant growth curves*. Edward Arnold, London, 248.
- Kohler, M.A., Linsley, R.K., 1951. Predicting the runoff from storm rainfall. *US weather Bureau Res.*
- Madsen, H.B., Jensen, C.R., Boysen, T., 1986. A Comparison of the Thermocouple Psychrometer and the Pressure Plate Methods for Determination of Soil-Water Characteristic Curves. *Journal of Soil Science*. 37, 357-362.
- Potter, K.N., 1990. Soil Properties Effect on Random Roughness Decay by Rainfall. *Transactions of the Asae*. 33, 1889-1892.
- Rémy, J.C., Marin-Laflèche, A., 1974. L'analyse de terre : réalisation d'un programme d'interprétation automatique. *Annales Agronomiques*. 25(4), 607-632.
- Riley, H., 1996. Estimation of physical properties of cultivated soils in southeast Norway from readily available soil information. *Norwegian Journal of Agricultural Sciences*. supplement n°25, 1-51.
- USDA, 2003. Revisited Universal Soil Loss Equation. Version 2. RUSLE2.
- Van Dijk, P., Bockstaller, C., Villerd, J., Koller, R., In prep. An indicator for overland flow potential of cropping systems: accounting for farmers' control on key variables.

**Annex 1. General solutions of the system for the case  $\Delta = 0$**

For the case  $\Delta = 0$ , if the polynomial has only one real root  $\lambda_0$  with a multiplicity 3, the general solution form depends on the number of independent associate eigenvectors. If  $\lambda_0$  has three linearly independent eigenvectors  $\vec{v}_{p_1}, \vec{v}_{p_2}$  and  $\vec{v}_{p_3}$  then the general solution is:

$$x(t) = (C_1 \vec{v}_{p_1} + C_2 \vec{v}_{p_2} + C_3 \vec{v}_{p_3}) e^{\lambda_0 t} + x_p(t) \quad (1)$$

If  $\lambda_0$  has two linearly independent eigenvectors  $\vec{v}_{p_1}$  and  $\vec{v}_{p_2}$  then the general solution is:

$$x(t) = (C_1 \vec{v}_{p_1} + C_2 \vec{v}_{p_2} + C_3 (t \vec{v}_{p_2} + \vec{v}_{p_3})) e^{\lambda_0 t} + x_p(t) \quad (2)$$

where  $\vec{v}_{p_3}$  is a solution of  $(\lambda_0 I - A) \vec{v}_{p_3} = \vec{v}_{p_2}$

If  $\lambda_0$  has only one linearly independent eigenvectors  $\vec{v}_{p_1}$  then the general solution is:

$$x(t) = (C_1 \vec{v}_{p_1} + C_2 (t \vec{v}_{p_1} + \vec{v}_{p_2}) + C_3 (t^2 \vec{v}_{p_1} + t \vec{v}_{p_2} + \vec{v}_{p_3})) e^{\lambda_0 t} + x_p(t) \quad (3)$$

where  $\vec{v}_{p_2}$  is a solution of  $(\lambda_0 I - A) \vec{v}_{p_2} = \vec{v}_{p_1}$  and  $\vec{v}_{p_3}$  of  $(\lambda_0 I - A) \vec{v}_{p_3} = \vec{v}_{p_2}$

If the polynomial has only two real roots  $\lambda_0$  with a multiplicity 2 and  $\lambda_1$  then the general solution is similarly expressed as previously.

Annex 2. Analytical expressions for  $C_S$  and  $C_M$  computed with Maple 17©

•  $C_S$

$$\begin{aligned} a &= -(K_{film}+Q_{inf}+\epsilon*\rho_b*k_r*K_D)/(n*\epsilon); \\ b &= \rho_b*k_r/n; \\ c &= k_r*K_D; \\ d &= -k_r; \\ e &= (K_{film}+Q_{inf})*C^n/(n*\epsilon); \end{aligned}$$

$$\begin{aligned} c1 &= (2.0*a*b*d*CS0+2.0*pow(b,2.0)*c*CS0+(d*(a*sqrt(pow(d,2.0))- \\ &2.0*a*d+4.0*b*c+pow(a,2.0))-b*c-pow(a,2.0))+b*c*(a-sqrt(pow(d,2.0))- \\ &2.0*a*d+4.0*b*c+pow(a,2.0)))+a*pow(d,2.0))*CM0+(d*(sqrt(pow(d,2.0))- \\ &2.0*a*d+4.0*b*c+pow(a,2.0))- \\ &a)+pow(d,2.0)+2.0*b*c)*e)/(2.0*a*d*sqrt(pow(d,2.0))- \\ &2.0*a*d+4.0*b*c+pow(a,2.0))-2.0*b*c*sqrt(pow(d,2.0))- \\ &2.0*a*d+4.0*b*c+pow(a,2.0)); \end{aligned}$$

$$\begin{aligned} c2 &= -(-2.0*a*b*d*CS0+2.0*pow(b,2.0)*c*CS0+(d*(-a*sqrt(pow(d,2.0))- \\ &2.0*a*d+4.0*b*c+pow(a,2.0))-b*c-pow(a,2.0))+b*c*(sqrt(pow(d,2.0))- \\ &2.0*a*d+4.0*b*c+pow(a,2.0))+a)+a*pow(d,2.0))*CM0+(d*(-sqrt(pow(d,2.0))- \\ &2.0*a*d+4.0*b*c+pow(a,2.0))- \\ &a)+pow(d,2.0)+2.0*b*c)*e)/(2.0*a*d*sqrt(pow(d,2.0))- \\ &2.0*a*d+4.0*b*c+pow(a,2.0))-2.0*b*c*sqrt(pow(d,2.0))- \\ &2.0*a*d+4.0*b*c+pow(a,2.0)); \end{aligned}$$

$$\begin{aligned} C_S(K_{film}, Q_{inf}, \epsilon, \rho_b, k_r, K_D, n, C^n) &= \exp(-(\sqrt{\text{pow}(d, 2.0) - \\ &2.0*a*d+4.0*b*c+pow(a, 2.0)})*t/2.0))*(\sqrt{\text{pow}(d, 2.0) - \\ &2.0*a*d+4.0*b*c+pow(a, 2.0)})*((a*c2*d-b*c*c2)*\exp(\sqrt{\text{pow}(d, 2.0) - \\ &2.0*a*d+4.0*b*c+pow(a, 2.0)})*t+d*t/2.0+a*t/2.0)+(b*c*c1- \\ &a*c1*d)*\exp(d*t/2.0+a*t/2.0))+ (a*c2*pow(d, 2.0)+(-b*c- \\ &pow(a, 2.0))*c2*d+a*b*c*c2)*\exp(\sqrt{\text{pow}(d, 2.0) - \\ &2.0*a*d+4.0*b*c+pow(a, 2.0)})*t+d*t/2.0+a*t/2.0)+(a*c1*pow(d, 2.0)+(-b*c- \\ &pow(a, 2.0))*c1*d+a*b*c*c1)*\exp(d*t/2.0+a*t/2.0)+2.0*b*c*e*\exp(\sqrt{\text{pow}(d, 2.0) - \\ &2.0*a*d+4.0*b*c+pow(a, 2.0)})*t/2.0))/(2.0*a*b*d-2.0*pow(b, 2.0)*c); \end{aligned}$$

•  $C_M$

$$\begin{aligned} a &= -(K_{film}+Q_{inf}+\epsilon*\rho_b*k_r*K_D)/(n*\epsilon); \\ b &= \rho_b*k_r/n; \\ c &= k_r*K_D; \\ d &= -k_r; \\ e &= (K_{film}+Q_{inf})*C^n/(n*\epsilon); \end{aligned}$$

$$\begin{aligned} c1 &= (-2.0*a*b*d*CS0+2.0*pow(b,2.0)*c*CS0+(d*(a*sqrt(pow(d,2.0))- \\ &2.0*a*d+4.0*b*c+pow(a,2.0))-b*c-pow(a,2.0))+b*c*(a-sqrt(pow(d,2.0))- \\ &2.0*a*d+4.0*b*c+pow(a,2.0)))+a*pow(d,2.0))*CM0+(d*(sqrt(pow(d,2.0))- \\ &2.0*a*d+4.0*b*c+pow(a,2.0))- \\ &a)+pow(d,2.0)+2.0*b*c)*e)/(2.0*a*d*sqrt(pow(d,2.0))- \\ &2.0*a*d+4.0*b*c+pow(a,2.0))-2.0*b*c*sqrt(pow(d,2.0))- \\ &2.0*a*d+4.0*b*c+pow(a,2.0)); \end{aligned}$$

$$\begin{aligned} c2 &= -(-2.0*a*b*d*CS0+2.0*pow(b,2.0)*c*CS0+(d*(-a*sqrt(pow(d,2.0))- \\ &2.0*a*d+4.0*b*c+pow(a,2.0))-b*c-pow(a,2.0))+b*c*(sqrt(pow(d,2.0))- \\ &2.0*a*d+4.0*b*c+pow(a,2.0))+a)+a*pow(d,2.0))*CM0+(d*(-sqrt(pow(d,2.0))- \\ &2.0*a*d+4.0*b*c+pow(a,2.0))- \\ &a)+pow(d,2.0)+2.0*b*c)*e)/(2.0*a*d*sqrt(pow(d,2.0))- \\ &2.0*a*d+4.0*b*c+pow(a,2.0))-2.0*b*c*sqrt(pow(d,2.0))- \\ &2.0*a*d+4.0*b*c+pow(a,2.0)); \end{aligned}$$

```
2.0*a*d+4.0*b*c+pow(a,2.0))-2.0*b*c*sqrt(pow(d,2.0)-
2.0*a*d+4.0*b*c+pow(a,2.0)));
```

```
Cm(Kfilm, Qinf, ε, ρb, kr, KD, n, Cn) = exp(-(sqrt(pow(d,2.0)-
2.0*a*d+4.0*b*c+pow(a,2.0))*t/2.0))*((a*c2*d-b*c*c2)*exp(sqrt(pow(d,2.0)-
2.0*a*d+4.0*b*c+pow(a,2.0))*t+d*t/2.0+a*t/2.0)+(a*c1*d-
b*c*c1)*exp(d*t/2.0+a*t/2.0)-d*e*exp(sqrt(pow(d,2.0)-
2.0*a*d+4.0*b*c+pow(a,2.0))*t/2.0))/(a*d-b*c);
```

# Curriculum Vitae

Marie Lefrancq

Born: May 15, 1986 in Périgueux, France

French nationality

marie.lefrancq@etu.unistra.fr

## Educational Background

---

- 2009-10** Master's degree in Earth and Environmental Sciences in Joseph Fourier's university (Grenoble): physical and urban hydrology, water quality, river transport, geostatistics.
- 2006-09** Engineering school of mathematics and mechanical modelling: ENSEIRB-MATMECA <http://www.enseirb-matmeca.fr/> (Bordeaux) specialised in fluids mechanics: numerical simulation of flow, porous media, complex fluid, diphasic flow, geofluid. Masters degree in applied mathematics.
- 2004-06** Preparation for the competitive entrance examination to French engineering schools: mathematics and physics in Faidherbe (Lille).

## Research Experience

---

- Dec.10 – Apr. 14**  
**3 years** PhD student on pesticides transport in runoff at headwater catchment scale: from characterisation to modelling in LHyGeS (Laboratory of hydrology and geochemistry of Strasbourg): field campaigns, chemical analysis, statistical study and modelling.  
Hydrological teaching in ENGEES (engineering school of environmental hydraulics)
- Feb.– Jun.10**  
**6 months** Internship in UNAM (National Autonomous University of Mexico) and in LTHE (Laboratory of transfer in hydrology and environment study) in Grenoble. Study of preferential transport in Mexican volcanic soil: field, laboratory and modelling.
- Feb. – Aug.09**  
**6 months** Internship in Irstea, agricultural and environmental engineering research, in Lyon, France. Development of a model for dimensioning buffer strip to limit pollution transfer in water.
- Jun. – Sept.08**  
**4 months** Internship in INRS-ETE (National Institute of scientific research in Water, Soil and environment) in Québec, Canada. Hydrological modelling at catchment scale.

---

## Scientific contribution

---

### Publication

- **Lefrancq M**, Payraudeau S., García Verdú A. J., Maillard E., Millet M., Imfeld G (2013): Fungicides transport in runoff from vineyard plot and catchment: contribution of non-target areas. *Environ Sci Pollut Res*. Doi: 10.1007/s11356-013-1866-8.
- **Lefrancq M**, Imfeld G, Payraudeau S, Millet M (2013): Kresoxim methyl deposition, drift and runoff in a vineyard catchment. *Science of The Total Environment* 442, 503-508. Doi: 10.1016/j.scitotenv.2012.09.082.
- Imfeld G, **Lefrancq M**, Maillard E, Payraudeau S (2012): Transport and attenuation of dissolved glyphosate and AMPA in a stormwater wetland *Chemosphere* 90, 1333-1339. Doi: 10.1016/j.chemosphere.2012.04.054.

### Oral presentation

- **Lefrancq M.**, Imfeld G., Guyot B., Payraudeau S. Transport and attenuation of chloroacetanilides at the catchment scale. Pesticide behaviour in soils, water and air, York, UK, 2-4/09/2013. Best platform presentation: Enviresearch Young Scientist Awards
- **Lefrancq M.**, García Verdú A. J., Maillard E., Imfeld G., Payraudeau S. Transport of cyazofamid and kresoxim-methyl in runoff at the plot and catchment scales. European Geoscience Union, Vienna, Austria, 7-12/04/2013
- **Lefrancq M.**, Imfeld G., Payraudeau S., Millet M. Kresoxim methyl deposition, drift and runoff in a vineyard catchment. 244th American Chemical Society National Meeting & Exposition, Philadelphia, United States, 19-23/08/12
- **Lefrancq M.**, Imfeld G., García Verdú A. J., Maillard E., Payraudeau S. Devenir et transfert de deux fongicides de la parcelle viticole au bassin versant. 42ème congrès du groupe français des pesticides (GFP), Poitiers, 30/05- 01/06/12

### Poster

- **Lefrancq M.**, Jetten V., Van Dijk P., Payraudeau S. Adapting Lisem to improve modelling of pesticide transfer by runoff and erosion. Pesticide behaviour in soils, water and air, York, UK, 2-4/09/2013
- **Lefrancq M.**, Jetten V., Van Dijk P., Payraudeau S. Adapting Lisem to improve modelling of pesticide transfer by runoff and erosion. European Geoscience Union, Vienna, Austria, 7-12/04/2013
- **Lefrancq M.**, Imfeld G., Millet M., Jetten V., Van Dijk P., Payraudeau S. Hydrological and erosion processes modelling to improve pesticide loads assessment at the catchment scale. XIV Symposium in Pesticide Chemistry, Piacenza, Italy, 30/08-1/09/11
- **Lefrancq M.**, Payraudeau S., Mc Grath G. S., Grégoire C., Hinz C. Using high resolution rainfall data to identify critical source areas for runoff-related pesticides: Luxury or necessity? European Geoscience Union, Vienna, Austria, 3-8/04/2011
- Lauvernet C., **Lefrancq M.**, Carluer N., Development of an operational tool to simulate pesticide transfer through vegetated strips: the 2D runoff part. Pesticide behaviour in soils, water and air, York, UK, 14-16/09/2009
- Gastelum A., Delmas P., **Lefrancq M.**, Duwig C., Marquez J., Prado B., Gimel'farb G., Charrier P. Visualising 3D porous media fluid interaction using X-ray CT data and Smooth Particles Hydrodynamics modelling. Image and Vision Computing New Zealand - IVCNZ. , pp. 1-8, 2010

**Résumé**

Comprendre le transport des pesticides est crucial pour évaluer leur impact écologique. Les connaissances sur la variabilité spatiale des dépôts de pesticides, l'impact de l'érosion sur leur export et leur dégradation *in situ* restent très limitées à l'échelle des bassins versants. La caractérisation expérimentale et la modélisation ont donc été combinées à deux échelles, parcelle et bassin versant, dans deux contextes agricoles. Un formalisme a été développé pour prédire le transport des pesticides par ruissellement et a été intégré dans le modèle LISEM (Limbourg Soil Erosion Model). Les résultats montrent que les surfaces imperméables contribuent significativement à la masse exportée par ruissellement du vignoble. La partition des pesticides entre phase dissoute et particulaire diffère considérablement selon les molécules et le forçage hydrologique, et la présence de produits de dégradation et un enrichissement en *R*-métolachlore ont été observés ce qui souligne le potentiel des analyses énantiomériques pour évaluer la biodégradation des pesticides. Globalement, cette étude a démontré que la combinaison des échelles et des approches permet une meilleure compréhension du transport des pesticides.

**Abstract**

Understanding pesticide transport is crucial to evaluate their ecological impact on ecosystems. Current knowledge on the spatial variability of pesticide deposition, the impact of erosion on pesticides export and the *in situ* pesticide degradation is very limited at the catchment scale. In this thesis, characterisation and modeling at two scales, the plot and catchment, were combined in two agricultural contexts. A formalism was developed to predict pesticide transport in runoff and was integrated in LISEM (Limbourg Soil Erosion Model). The results show that impermeable roads contributed to more than 40% to the overall load of fungicides exported via runoff from the vineyard. Pesticide partitioning between suspended solids and runoff water differed largely according to the molecules and the hydrological dynamics. The occurrence of degradation products and the enrichment of one enantiomer were observed suggesting the potential of chiral analyses for assessing biodegradation of chiral pesticides at such scale. Overall, the investigation demonstrated that combining different approaches enable a better understanding of pesticide transport.